

Three new species of *Macrostomum* (Platyhelminthes, Macrostomorpha) from China and Australia, with notes on taxonomy and phylogenetics

Yongshi Shi¹, Zhiyu Zeng¹, Jia Wang¹, Siyu Zhang¹, Li Deng¹, Antai Wang¹

¹ Shenzhen Key Laboratory of Marine Bioresource and Eco-environmental Science, College of Life Sciences and Oceanography, Shenzhen University, Shenzhen 518055, China

Corresponding authors: Li Deng (lideng03@szu.edu.cn), Antai Wang (wang118@szu.edu.cn)

Academic editor: Tom Artois | Received 16 August 2021 | Accepted 31 March 2022 | Published 3 May 2022

<http://zoobank.org/E008EE26-5871-4957-96FC-F2ACB2D073D9>

Citation: Shi Y, Zeng Z, Wang J, Zhang S, Deng L, Wang A (2022) Three new species of *Macrostomum* (Platyhelminthes, Macrostomorpha) from China and Australia, with notes on taxonomy and phylogenetics. ZooKeys 1099: 1–28. <https://doi.org/10.3897/zookeys.1099.72964>

Abstract

In this paper, three species of the macrostomid free-living flatworm genus *Macrostomum* are described. Two species, *Macrostomum littorale* Wang & Shi, **sp. nov.** and *M. shekouense* Wang & Shi, **sp. nov.**, were collected from coastal water at Shenzhen, Guangdong Province, China. One species, *M. brandi* Wang & Shi, **sp. nov.**, was collected from Perth, Western Australia and Queenscliff, Victoria, Australia. *Macrostomum littorale* **sp. nov.** differs from congeneric species within the genus in the length of the stylet, diameter of stylet opening, and the bend of the stylet. *Macrostomum shekouense* **sp. nov.** and *M. brandi* **sp. nov.** differ from similar species within the genus in the stylet morphology, position of the female antrum and developing eggs, or presence or absence of the false seminal vesicle. Phylogenetic analysis based on cytochrome c oxidase subunit I (COI) gene shows that *M. littorale* **sp. nov.** and *M. hystrix* are sister clades on two well-separated branch, *M. shekouense* **sp. nov.** and *M. brandi* **sp. nov.** are sister clades on two well-separated branches. Accordingly, both morphological and molecular evidence support *M. littorale* **sp. nov.**, *M. shekouense* **sp. nov.**, and *M. brandi* **sp. nov.** as three new species.

Keywords

COI, flatworm, taxonomy, 18S rDNA, 28S rDNA

Introduction

Macrostomum Schmidt, 1848 is a genus of the family Macrostomidae (Platyhelminthes; Macrostomorpha), with more than 160 species described to date from around the world (Tyler et al. 2006–2021; Zhang et al. 2021). These free-living flatworms are transparent, hermaphroditic, mostly 1–2 mm in body length, and have a relatively simple general anatomy. *Macrostomum* is attracting interest because it contains *Macrostomum lignano* Ladurner, Schärer, Salvenmoser & Rieger, 2005, a versatile model organism increasingly used in evolutionary, developmental, and molecular biology (Ladurner et al. 2005; Ladurner et al. 2008; Mouton et al. 2009; Vizoso et al. 2010; Wasik et al. 2015; Wudarski et al. 2020). A recent study revealed that the unusual karyotype of *M. lignano* hinders it from becoming a full-fledged genomic model organism, and *M. cliftonense* Schärer & Brand, 2020 was suggested as the potential primary *Macrostomum* model to replace *M. lignano* (Schärer et al. 2020). To explore and describe new species of *Macrostomum* will obviously be of benefit to these research fields by providing more biological and genetic resources since *Macrostomum* is a species-rich genus (Tyler et al. 2006–2021; Brand et al. 2022a).

Taxonomy of the genus *Macrostomum* is particularly challenging, due to the difficulty of their study. In addition, there is considerable convergent evolution of the copulatory organ morphology, particularly in the morphology of penis stylet (Schärer et al. 2011; Brand et al. 2022b). The penis stylet for *Macrostomum* species is considered as the most typical and significant taxonomic feature for identification (Ferguson 1954; Rieger 1977; Rieger et al. 1994). According to morphology of the genital organs and mating behavior, species can be divided into two groups showing a hypodermic mating syndrome (HMS) or reciprocal mating syndrome (RMS) (Schärer et al. 2011). HMS species have extremely similar stylet morphologies, showing a clear case of convergent evolution, which means that those species are hard to distinguish based on stylet morphology only (Schärer et al. 2011). Some molecular markers, such as nuclear ribosomal RNA genes (18S rDNA and 28S rDNA), were used to determine the molecular phylogenetic placement or help identify *Macrostomum* species. However, the rDNA regions are too conserved to successfully resolve interrelationships between some *Macrostomum* species, such as *M. lignano* and *M. janickei* Schärer, 2020 (Schärer et al. 2020). We therefore also used a partial (mitochondrial) cytochrome c oxidase I (COI) gene sequence, a more rapidly evolving marker that was suggested to be used as potential molecular marker resolving interrelationships between species in the Macrostomorpha by several authors (Janssen et al. 2015; Xin et al. 2019; Schärer et al. 2020; Zhang et al. 2021). However, the sequence of COI gene is available for approximately only ten *Macrostomum* species. To understand the evolutionary relationships within *Macrostomum*, much greater species representation would be required.

The first species of *Macrostomum* described from China was *Macrostomum intermedium* Tu, 1934 (Tu 1934). Seventy years later, our laboratory reported a second *Macrostomum* species, *Macrostomum xiamense* Wang & Luo, 2004. Since then, 22 species of *Macrostomum* have been reported from China, of which 21 species were newly described, 13 from freshwater and eight from brackish environments (Lin et al.

2017a; Xin et al. 2019; Zhang et al. 2021). China is likely to have a high richness and diversity of *Macrostomum* species, since 14 new species were reported in the last five years from south China alone, mainly in Guangdong Province.

In this paper, we describe three new species of *Macrostomum*, two species from China and one from Australia. Twenty COI gene sequences of seven species are provided, and phylogenetic analyses inferred from partial 18S rDNA, 28S rDNA, and COI gene sequences of *Macrostomum* taxa are presented.

Materials and methods

Sample collection and rearing

Specimens of *Macrostomum littorale* sp. nov. and *M. shekouense* sp. nov. were collected in 2018 from Waterlands Resort located at the estuary of Pearl River in the west of Shenzhen (22°43.32'N, 113°45.88'E) and from the seashore at Shekou peninsula (22°28.77'N, 113°55.12'E), Guangdong Province, China, respectively.

Samples were collected by washing off sediment and organisms from floating plants or underwater stones and using 750-, 125-, and 75- μ m mesh nets sequentially. The material retained by the 125- μ m and 75- μ m mesh nets was transported to the laboratory. All living flatworms were maintained in the water of the original location with a 12:12 h light/dark period at room temperature (25 ± 1 °C). The flatworms were fed with *Paramecium* sp. every two days.

In addition to our own specimens, we also analyzed specimens of *M. brandi* sp. nov. that were previously deposited by Brand et al. (2022a) under the name *Macrostomum* sp. 81 (also called *M. sp. 81* or Mac081), since it was found to be a close relative of *M. shekouense* sp. nov. These specimens of *M. brandi* sp. nov. were collected in 2017 from Perth, Western Australia (31°59.22'S, 115°49.72'E) (Suppl. material 4: Fig. S1C) and Queenscliff, Victoria (38°16.20'S, 144°38.34'E) (Suppl. material 4: Fig. S1D), Australia (see below for more details).

Specimen preparation, observations, and data processing

The procedures of specimen preparation followed the method described by Zhang et al. (2021). In brief, the specimens were fixed in Bouin's solution after being anesthetized successively with 5% (for 1–2 min) and 7% (for 1–2 min) ethanol in habitat water. The dehydrated specimens were embedded in paraffin and serially sectioned along the sagittal plane (thickness 6 μ m) using a manual rotary microtome (Leica RM2235, Leica Biosystems, Germany). After being stained with either hematoxylin-eosin (H&E) or modified Cason's Mallory–Heidenhain stain and hematoxylin (Yang et al. 2020), the specimens were mounted in neutral balsam for histological observation. Lactic acid phenol liquid (lactic acid: phenol = 1:1 in volume) was used for penis stylet dissection.

All the specimens were observed by stereomicroscope (Leica EZ4, Leica Microsystems, Germany) and differential interference microscopy (Olympus BX51, PA, USA).

Images were captured and measured with Olympus DP 2-BSW and Image-Pro Plus software v. 6.0. Type material has been deposited in the Institute of Zoology, Chinese Academy of Sciences, Beijing (IZCAS), with the abbreviation PLA–Ma (*Platyhelminthes–Macrostomum*) followed by catalog numbers.

DNA extraction, amplification, and sequencing

After being deprived of food for three days, three individuals of each species (non-types) were placed into liquid nitrogen for 15 s for the following DNA extraction. An E.Z.N.A.™ Mollusk DNA Isolation Kit (Omega, Norcross, GA, USA) was used to extract DNA. PCR reactions were performed using KOD One™ PCR Master Mix (TOYOBO Co. LTD, Japan) with a Thermal Cycler (Applied Biosystems 2720, Thermo Fisher Scientific, USA). The primers for 18S rDNA, 28S rDNA and COI sequences and PCR amplification procedures are listed in Table 1. The amplified 18S rDNA, 28S rDNA, and COI fragments were approximately 1250, 1200, and 610 bp long, respectively. PCR products were separated on a 1.2% agarose gel and purified using a Gel DNA Extraction Kit (Chinatopbio, Shenzhen, China), and were inserted into the pESI-Blunt vector (Hieff Clone™ Zero TOPO-Blunt Cloning Kit, Yeasen, Shanghai, China), respectively. The amplified DNA fragments were sequenced by Sanger sequencing by Beijing Genomics Institute (BGI, Shenzhen, China) or Beijing TsingKe Biotech Co., Ltd (Beijing, China).

Molecular phylogenetic analyses

Newly obtained sequences have been deposited in the GenBank database at NCBI. Sequences used for phylogenetic analyses in this study were obtained from GenBank under accession numbers shown in Suppl. material 1, 2: Tables S1, S2. In total, 43 18S rDNA sequences, 54 28S rDNA sequences, and 46 COI sequences from 42 *Macrostomum* species were included. The 18S rDNA and 28S rDNA of five species of *Psammomacrostomum* and one COI sequence of *Psammomacrostomum* sp. 5 were selected as outgroups for rDNA and COI trees, respectively.

Alignments were performed with the online version of the software MAFFT v. 7 (Kuraku et al. 2013; Katoh et al. 2017), applying the E-INS-i interactive refinement method. Surprisingly, a single-base deletion was found in the COI

Table 1. Primer sequences and PCR procedures used for amplification and sequencing.

Gene	Primers	Direction	Sequence(5'-3')	PCR procedures	References
18S rDNA	Macro_18S_200F	forward	GGCGCAITTTATTAGATCAAACCA	94 °C (2 min); 40× [94 °C (30 s), 54 °C (30 s), 72 °C (2 min)]; 72 °C (7 min)	Schärer et al. (2011)
	Macro_18S_1640R	reverse	GCAAGCCCCGATCCCTGTGTC		
28S rDNA	ZX-1	forward	ACCCGCTGAATTTAAGCATAT	95 °C (5 min); 40× [95 °C (30 s), 55 °C (30 s), 72 °C (2 min)]; 72 °C (7 min)	
	1500R	reverse	GCTATCCTGAGGGAAACTTCG		
COI	Mac_COIF	forward	GTCTACAATCATAAGGATATTGG	94 °C (1 min); 5× [94 °C (30 s), 45 °C (90 s), 72 °C (60 s)]; 35× [94 °C (30 s), 51 °C (90 s), 72 °C (60 s)]; 72 °C (5 min)	Janssen et al. (2015)
	Mac_COIR	reverse	TAAACYTCWGGGTGACCAAAAAACCA		
F-MS-COI		forward	GGATATTGGWACHTTDTAITTT	98 °C (3 min); 20× [98 °C (15 s), 52–42 °C (5 s), 72 °C (10 s)]; 30× [98 °C (15 s), 42 °C (5 s), 72 °C (10 s)]; 72 °C (5 min)	this study
	R-MS-COI	reverse	TTHCGATCWGTTAAHAACAT		

sequences of *Macrostomum littorale* sp. nov., *M. hystrix* Örsted, 1843, *M. sp.* 34, *M. taurinum* Wang & Zhang, 2021, and *M. zhujiangense* Wang & Fang, 2016 when it was translated by ORFfinder in NCBI with the genetic code 9, and we discuss this observation in more detail below. For alignment and analysis, the missing bases were filled with N. Ambiguous sites (e.g., containing gaps and poorly aligned sites) were removed by Gblocks v. 0.91b (Castresana 2000) with default settings. The final length of the aligned 18S rDNA, 28S rDNA, and COI sequences were 1195, 776, and 406 bp, respectively. Uncorrected pairwise distances between species were calculated in MEGA v. 6.06 (Tamura et al. 2013). Uncorrected genetic distances (GDs) for COI were calculated based on all sequences obtained from *M. littorale* sp. nov., *M. shekouense* sp. nov., and *M. brandi* sp. nov. together with those used for phylogenetic tree calculation (alignment length: 406 bp). A concatenated dataset (18S–28S rDNA) was combined using MEGA v. 6.06 (Tamura et al. 2013); missing sequences are denoted as Ns in the concatenated alignment. A substitution saturation test was carried out in DAMBE v. 5 (Xia and Lemey 2009; Xia 2017) to assess the nucleotide substitution saturation.

Based on the Akaike information criterion (AIC), we used ModelFinder (Kalyaanamoorthy et al. 2017) to find the best evolution model for maximum likelihood (ML) method; the GTR+F+I+G4 model was selected for all datasets. Meanwhile, to find the best-fit model for Bayesian inference (BI) analyses, MrModelTest v. 2.3 (Nylander 2004) was used applying the AIC; GTR+I+G model was chosen for all datasets. The gene partitions in the concatenated dataset were defined as 18S rDNA/28S rDNA. PartitionFinder v. 2.1.1 (Lanfear et al. 2017) was used to select the best-fit models for each partition based on AIC; for ML and BI methods, the models for both 18S rDNA and 28S rDNA were GTR+I+G. After that, phylogenetic trees were constructed by both ML and BI. For ML, analyses were performed in IQ-TREE v. 1.6.2 (Nguyen et al. 2015) with 1000 bootstrap replicates. Model parameters were calculated independently for each gene partition of the concatenated dataset. For BI, analyses were performed in MrBayes v. 3.2.6 (Ronquist et al. 2012) with two simultaneous runs of one cold and three heated chains. Partitioned analysis was performed on the concatenated dataset. The Markov Chain Monte Carlo (MCMC) algorithm was run for 1,500,000 generations for all datasets in four simultaneous chains. Every 1000th generation was sampled. Burn-in was chosen as 25% of the results. Effective sample size (ESS) values of each parameter in the .p files were checked by TRACER v. 1.7.1 (Rambaut et al. 2018) to ensure good convergence. All trees were visualized using FigTree v. 1.4.3 (Rambaut 2009) and Adobe Photoshop CC 2017.

Results

Molecular phylogeny

Twenty fragments of sequences of COI were amplified and sequenced from two specimens of *Macrostomum littorale* sp. nov., and 18 specimens of the other six

Macrostomum species, *M. baoanense* Wang & Fang, 2016, *M. pseudosinense* Wang & Zhang, 2021, *M. shenda* Wang & Xin, 2019, *M. shekouense* sp. nov., *M. taurinum*, *M. zhujiangense*, using three specimens of each species. Three fragments of sequences of COI were obtained from deposited transcriptome assemblies obtained from individual specimens of *M. brandi* sp. nov. (MTP LS 3136, SAMN15061113; MTP LS 2864, SAMN15061091) and *M. sp.* 34 (MTP LS 2041, SAMN15061043), respectively (Brand et al. 2022a). The results of phylogenetic analyses are shown in Figs 1, 2, and Suppl. material 5, 6: Figs S2, S3. The values of the posterior probability from the BI analyses were added to ML consensus trees, since the topology of phylogenetic trees from the BI analyses and the ML analyses are congruent, both

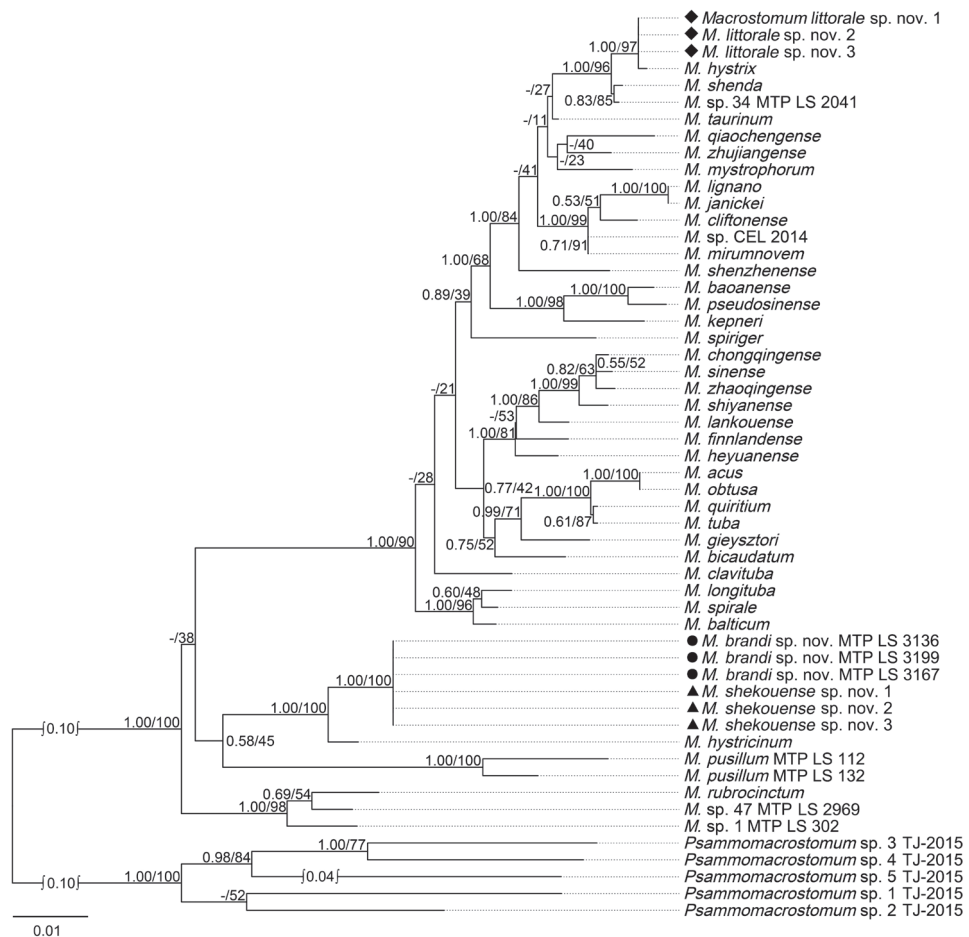


Figure 1. Maximum likelihood phylogenetic tree topology based on the 18S–28S rDNA dataset. Numbers on branches indicate support values (posterior probability/bootstrap). Scale bar: substitutions per nucleotide position.

Systematic account

Macrostomorpha Doe, 1986

Family Macrostomidae Beneden E, 1870

Genus *Macrostomum* Schmidt, 1848

Macrostomum littorale Wang & Shi, sp. nov.

<http://zoobank.org/B06653BF-4D32-4C53-AB47-659F0CBC6655>

Figs 3–5

Type material. Two specimens: holotype IZCAS PLA–Ma0140, collected by Fan Xin from Waterlands Resort located at the estuary of pearl River in the west of Shenzhen, Guangdong, China (22°43.32'N, 113°45.88'E) in April 2018, unsectioned whole-body mounted in neutral balsam. The paratype (collection date and locality same as the holotype), is one serially-sectioned specimen mounted in neutral balsam (IZCAS PLA–Ma0141). Digital photomicrographs of the holotype specimen and the sectioned paratype specimen, as well as photomicrographs of five non-type specimens (IZCAS PLA–Ma0140a–e) imaged in vivo, were deposited on the Macrostomorpha Taxonomy and Phylogeny website (at <https://macrostomorpha.myspecies.info>) and can also be accessed at <https://doi.org/10.5281/zenodo.4585492>.

Habitat. Specimens were collected from Waterlands Resort at the estuary of the Pearl River at Shenzhen, Guangdong Province, China (Suppl. material 4: Fig. S1A). The animals were collected from floating plants. Salinities of the water in habitat were 9‰–11‰.

Diagnosis. A *Macrostomum* species with dorsoventrally flattened body, two almost round eyes, and rounded rostrum (Fig. 3A). Body length and width of mature worms are $920 \pm 109 \mu\text{m}$ and $192 \pm 49 \mu\text{m}$, respectively. Testes clearly larger than ovaries. Stylet ($62 \pm 7.9 \mu\text{m}$) is a hook-like and gradually narrowing funnel with an 105° bend in the 66% position (when measured from the proximal to the distal part). The stylet opening is $6 \pm 0.9 \mu\text{m}$ in diameter, willow leaf-shaped, located on the concave side of the subterminal region of the stylet (Fig. 3F, G, H). Muscular walls of vesicula seminalis and vesicula granulorum thickened. No bristles and brush on sperm ($35 \pm 1.1 \mu\text{m}$) (Fig. 3E).

Etymology. The name of this new species is derived from its habitat.

Description. Body dorsoventrally flattened, colorless. Mature individual $920 \pm 109 \mu\text{m}$ in length and $192 \pm 49 \mu\text{m}$ in width ($n = 6$) (Fig. 3A). Entire body covered with cilia ($6 \pm 1.3 \mu\text{m}$ in length, $n = 6$). Tufts of sensory hairs, $7 \pm 1.1 \mu\text{m}$ ($n = 6$) long, sparsely distributed along body edges. Anterior and posterior edges of body equipped with rigid cilia, $6 \pm 1.0 \mu\text{m}$ ($n = 6$) long. The rhabdite rods scattered in groups (mostly 5–7 rhabdites in each group) on the body surface, most abundant on the dorsal side. Two round eyes, separated from each other by a distance of $37 \pm 6.1 \mu\text{m}$ ($n = 6$) (Fig. 3A). Pharynx surrounded by abundant gland cells on both sides, mouth $73 \pm 16 \mu\text{m}$ ($n = 6$) in length (Fig. 3A).

Paired elliptic testes, $154 \pm 7.9 \mu\text{m}$ ($n = 5$) in length and $40 \pm 13 \mu\text{m}$ ($n = 5$) in width (Figs 3B, 4A, 5A). Male copulatory apparatus consisting of false vesicula seminalis, vesicula seminalis, vesicula granulorum and stylet (Figs 3C, 4B–E, 5A–C). False vesicula

seminalis oval-shaped, located behind female antrum, connecting to vesicula seminalis at its left side from ventral view. Vesicula granulorum connecting to oval-shaped vesicula seminalis on the right rear part from ventral view, while extending into proximal opening of penis stylet on the other side. Both vesicula seminalis and vesicula granulorum have a thickened muscular wall (Figs 3C, 4B–E, 5A–C). Stylet $35 \pm 6.3 \mu\text{m}$ ($n = 5$) in diameter at its proximal opening; curved length from proximal to distal ends (dotted line 'cl' in Fig. 5C) $64 \pm 7.4 \mu\text{m}$ ($n = 5$); direct distance between proximal and distal ends (dotted line 'dd' in Fig. 5C) $62 \pm 7.9 \mu\text{m}$ ($n = 5$). Stylet hook-like, gradually narrowing from the proximal end, curved at 66% position from proximal end with bending angle of 105° ($n = 5$) (Figs 3F–H, 5D); The stylet opening $6 \pm 0.9 \mu\text{m}$ ($n = 5$) in diameter, willow leaf-shaped, located at the concave side of the subterminal region of stylet (Figs 3F–H, 5D). Mature sperm $35 \pm 1.1 \mu\text{m}$ ($n = 5$) in length, having neither bristle nor brush. The boundary between feeler, sperm body and sperm shaft not clear (Figs 3E, 5E).

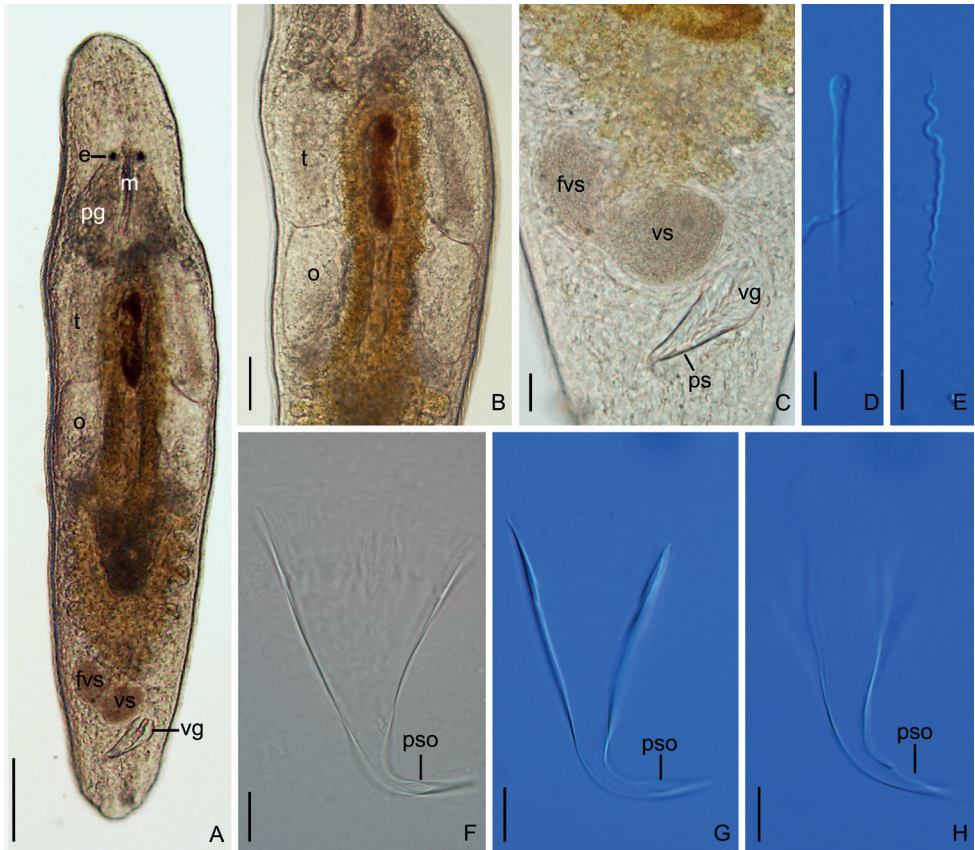


Figure 3. *Macrostomum littorale* Wang & Shi, sp. nov. **A** whole animal, ventral view **B** testes and ovaries **C** male copulatory apparatus, ventral view **D** immature sperm **E** mature sperm **F–H** penis stylet. Abbreviations: e: eye; fvs: false vesicula seminalis; m: mouth; o: ovary; pg: pharyngeal glands; ps: penis stylet; pso: penis stylet opening; t: testis; vg: vesicula granulorum; vs: vesicula seminalis. Scale bars: 100 μm (**A**); 50 μm (**B**); 20 μm (**C**); 5 μm (**D, E**); 10 μm (**F–H**).

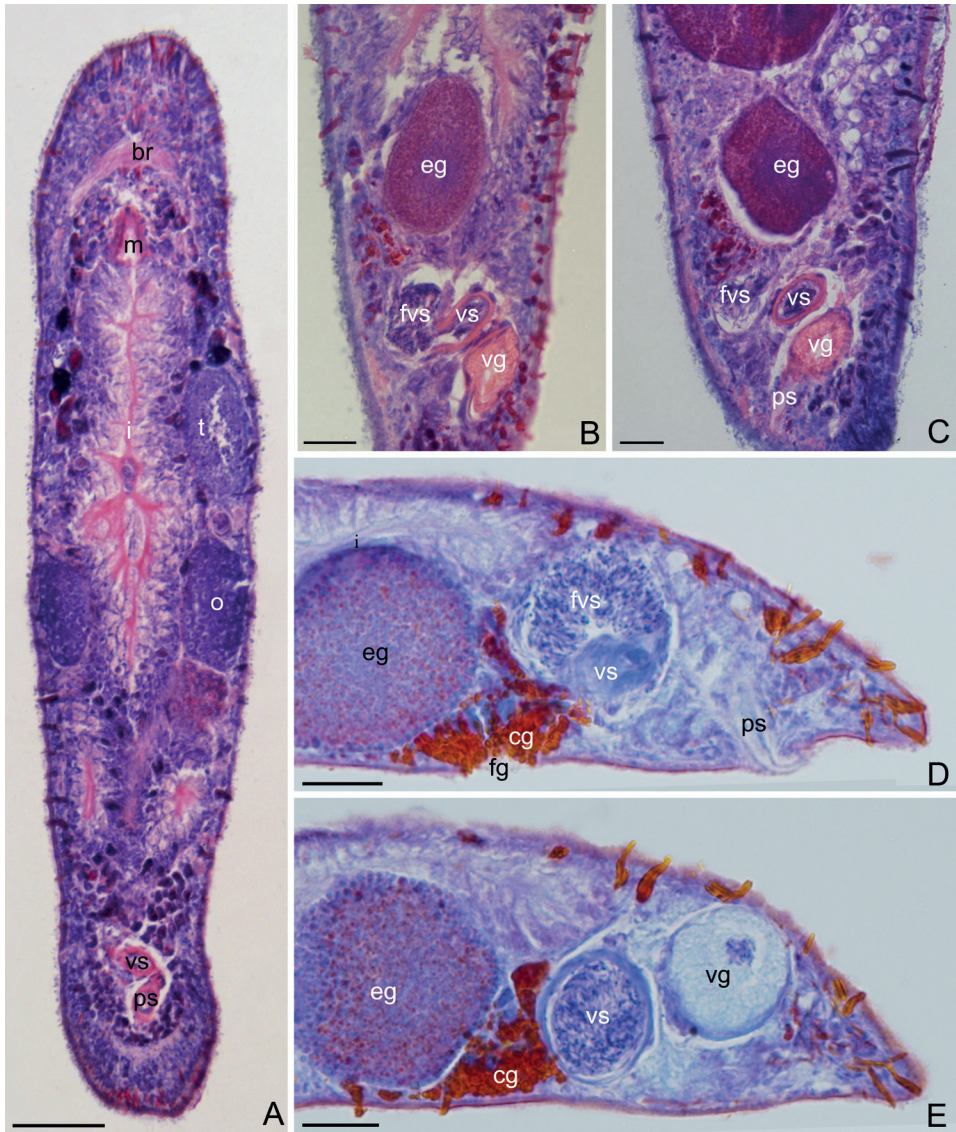


Figure 4. *Macrostomum littorale* Wang & Shi, sp. nov. **A–C** horizontal whole-body sections, ventral view (stained by H&E) **D, E** longitudinal sections, showing male copulatory apparatus (stained by modified Mallory-Heidenhain/Cason stain and hematoxylin). Abbreviations: br: brain; cg: cement glands; eg: egg; fg: female gonopore; fvs: false vesicula seminalis; i: intestine; m: mouth; o: ovary; ps: penis stylet; t: testis; vg: vesicula granulorum; vs: vesicula seminalis. Scale bars: 50 μm (**A**); 20 μm (**B–E**).

Pair of oval ovaries, $115 \pm 9.9 \mu\text{m}$ ($n = 6$) in length and $44 \pm 8.9 \mu\text{m}$ ($n = 6$) in width, located on both sides of intestine (Figs 3B, 5A). Female gonopore opening ventrally at female antrum, surrounded by numerous cement glands.

Remarks. A comparison between *Macrostomum littorale* sp. nov. in this study and eleven similar species (stylet hook-like) within the genus is shown in Table 2.

The main difference between *M. littorale* sp. nov. and *M. astericis* Schmidt & Soppott-Ehlers, 1976, *M. qiaochengense* Wang & Fang, 2017, and *M. sp. 1* is the location of penis stylet opening (ps), which is at the concave side of the curved tube in *M. littorale* sp. nov., while it is located at the convex side of the curved tube in the other species. Moreover, the length of the stylet in *M. hystricinum* and *M. astericis* is shorter than that in *M. littorale* sp. nov. The distal opening of *M. qiaochengense* (diameter $20 \pm 1.6 \mu\text{m}$) is much larger than that of *M. littorale* sp. nov. (diameter $6 \pm 0.9 \mu\text{m}$).

The length of the stylet in *M. peteraxi* Mack-Fira, 1971 ($27\text{--}30 \mu\text{m}$) and *M. pusillum* ($24\text{--}26 \mu\text{m}$) is smaller than that in *M. littorale* sp. nov. ($64 \pm 7.4 \mu\text{m}$). Furthermore, the stylet proximal opening in *M. peteraxi* (diameter $12.5 \mu\text{m}$) and *M. pusillum* (diameter $9\text{--}12 \mu\text{m}$) is much smaller than that in *M. littorale* sp. nov. (diameter $35 \pm 6.3 \mu\text{m}$).

The bending angle of the stylet in *M. rubrocinctum* Ax, 1951 (90°) is smaller than that in *M. littorale* sp. nov. (105°). The body length of *M. rubrocinctum* ($1,500\text{--}2,000 \mu\text{m}$) is

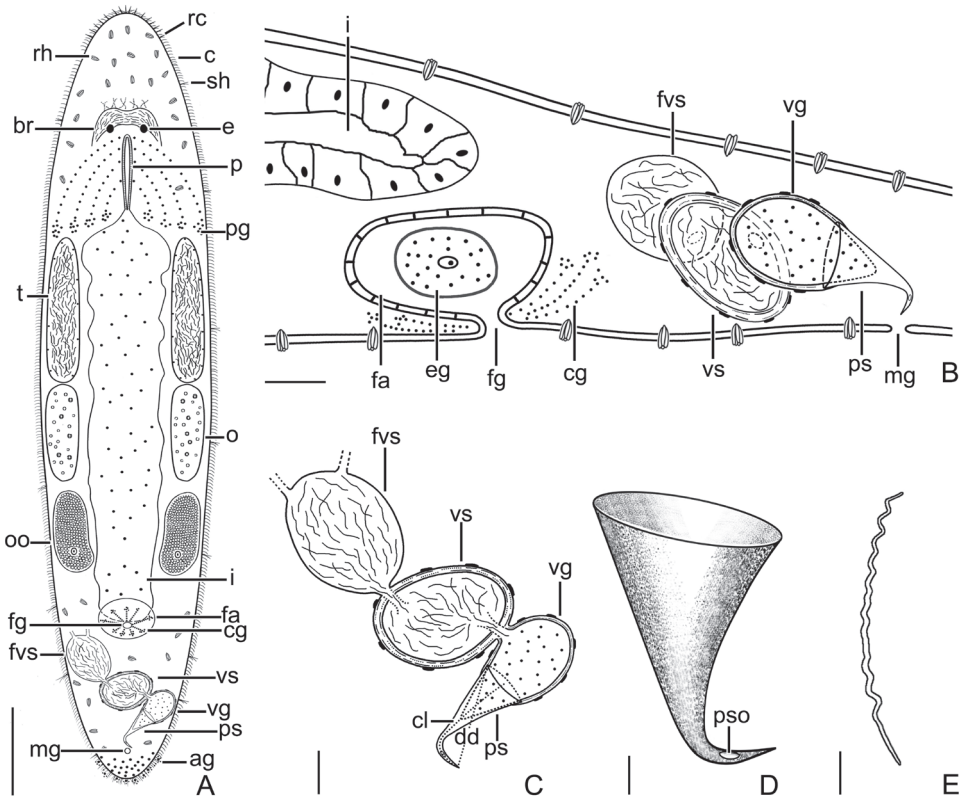


Figure 5. *Macrostomum littorale* Wang & Shi, sp. nov. **A** whole body, ventral view **B** sagittal section of the tail **C** male copulatory apparatus **D** penis stylet **E** mature sperm. Abbreviations: ag: adhesive glands; br: brain; c: cilia; cl: curved length from proximal to distal ends; cg: cement glands; dd: direct distance between proximal and distal ends; e: eye; eg: egg; fa: female antrum; fg: female gonopore; fvs: false vesicula seminalis; i: intestine; mg: male gonopore; o: ovary; oo: oocyte; p: pharynx; pg: pharyngeal glands; ps: penis stylet; pso: penis stylet opening; rc: rigid cilia; rh: rhabdites; sh: sensory hair; t: testis; vg: vesicula granulorum; vs: vesicula seminalis. Scale bars: $100 \mu\text{m}$ (**A**); $20 \mu\text{m}$ (**B**, **C**); $10 \mu\text{m}$ (**D**); $5 \mu\text{m}$ (**E**).

Table 2. Comparison between the new species and the similar species with hook-like stylets within the genus.

Species	Body Length (µm)	Female antrum position	Stylet length ^a (µm)	Diameter of stylet opening (proximal / distal µm)	Penis stylet opening (µm) position ^a	Bending angle (°) and position of curve in stylet ^a	Habitat	Distribution	Reference
<i>M. aseritici</i>	800	posterior	25–32	13–16/2.7*	65%/convex	93°/50%	Marine	Galapagos, Ecuador	Schmidt and Sopot-Ehlers (1976)
<i>M. hystricinum</i>	NA	posterior	32	22/4–6	81%/convex	85°/81%	Brackish	Widely distributed	Beklemischev (1951) and Wang et al. (2017)
<i>M. hystrix</i> ^a	NA	posterior	44	20/5	78%/convex	85°/75%	Brackish	Italy	Schärer et al. (2011) and Brand et al. (2022a)
<i>M. litonale</i> sp. nov.	920 ± 109	posterior	64 ± 7.4	35 ± 6.3/6 ± 0.9	85%/concave	105°/66%	Brackish	China	this study
<i>M. shenkouense</i> sp. nov.	978 ± 143	50% of body length	46 ± 3.5	22 ± 2.7/3 ± 0.3	73%/convex	90°/65%	Brackish	China	this study
<i>M. brandi</i> sp. nov.	1147 ± 151	50% of body length	55 ± 5.0	37 ± 9/2.4 ± 0.05	70%/convex	90°/70%	Marine	Australia	<i>M. sp. 81</i> in Brand et al. (2022a)
<i>M. abalici</i>	1,000–2,000	50% of body length	35–50	16–25/NA	77%/convex	90°/69%	Marine	Galapagos, Ecuador	Schmidt and Sopot-Ehlers (1976)
<i>M. petenxi</i>	1,500	posterior	27–30	12.5/NA	NA	90°/NA	Marine	Romania	Mack-Fira (1971)
<i>M. pusillum</i>	500–800	posterior	24–26	9–12/NA	NA	90°/42%	Marine	Germany	Ax (1951)
<i>M. quiochengense</i>	1,147 ± 52	posterior	51 ± 3.5	21 ± 1.2/20 ± 1.6	63%/convex	90°/63%	Brackish	China	Wang et al. (2017)
<i>M. rubroinctum</i>	1,500–2,000	posterior	55	30/NA	NA	90°/67%	Marine	Germany	Ax (1951)
<i>M. sp 1 MTP LS 302</i> ^a	NA	posterior	42	23/4.4	73%/convex	105°/60%	NA	Italy	Schärer et al. (2011)

^aMeasurement based on images and scales given in the references. The procedures of measuring the angle refer to Ferguson (1940). NA: Not available, information cannot be obtained from the literature. a: Stylet length refers to curved length (cl) from proximal to distal ends.

much larger than that in *M. littorale* sp. nov. ($920 \pm 109 \mu\text{m}$). Moreover, *M. rubrocinctum* has a red pigmented ring on its head, which is absent in *M. littorale* sp. nov.

Accordingly, it is evident that *M. littorale* sp. nov. is a new species within the genus *Macrostomum* based on morphology in combination with phylogenetic analyses.

***Macrostomum shekouense* Wang & Shi, sp. nov.**

<http://zoobank.org/190A7664-768C-4D1F-BBE8-A1CA316D26D4>

Figs 6–8

Type material. Three specimens: holotype (stained by H&E) IZCAS PLA–Ma0150, collected by Linhong Zhong in October 2018 from the seashore at Shekou peninsula,

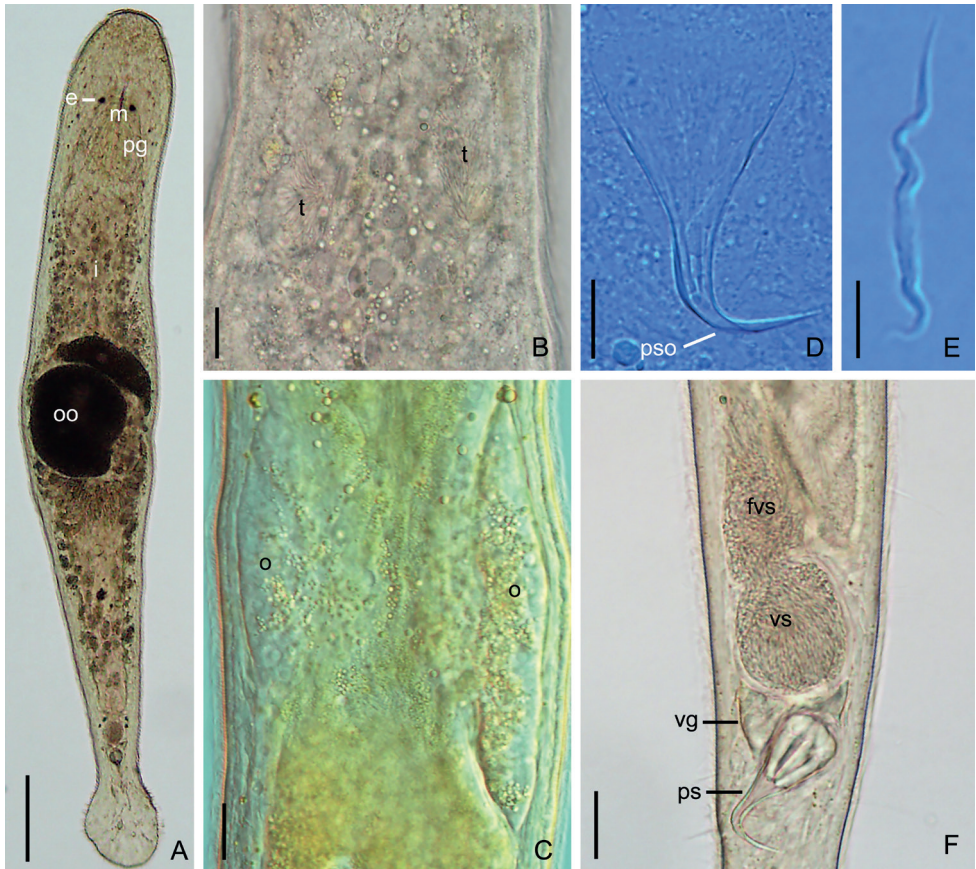


Figure 6. *Macrostomum shekouense* Wang & Shi, sp. nov. **A** whole animal, ventral view **B** testes **C** ovaries **D** penis stylet **E** mature sperm **F** male copulatory apparatus, ventral view. Abbreviations: e: eye; fvs: false vesicula seminalis; i: intestine; m: mouth; o: ovary; oo: oocyte; pg: pharyngeal glands; ps: penis stylet; pso: penis stylet opening; t: testis; vg: vesicula granulorum; vs: vesicula seminalis. Scale bars: 100 μm (**A**); 20 μm (**B, C, F**); 5 μm (**D, E**).

Guangdong, China (22°28.77'N, 113°55.12'E), the unsectioned whole body mounted in neutral balsam. The paratypes (collection date and locality same as holotype), comprising two serially-sectioned specimens mounted in neutral balsam (IZCAS PLA–Ma0151–152). Digital photomicrographs of the holotype specimen and the sectioned paratype specimens, as well as photomicrographs of four non-type specimens (IZCAS

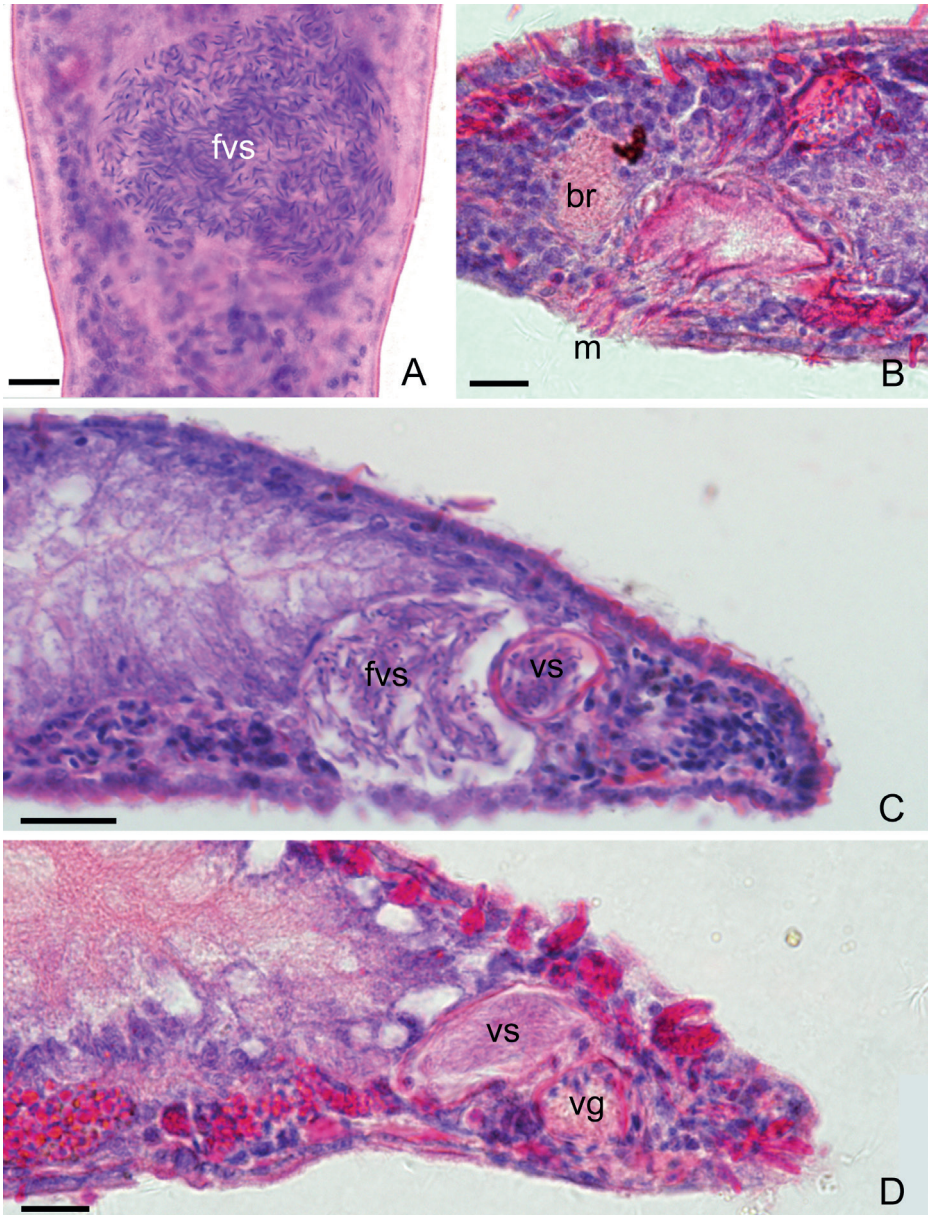


Figure 7. *Macrostromum shekouense* Wang & Shi, sp. nov. **A** mounted specimen, ventral view **B–D** longitudinal whole-body sections **A–D** stained by H&E. Abbreviations: br: brain; fvs: false vesicula seminalis; m: mouth; vg: vesicula granulorum; vs: vesicula seminalis. Scale bars: 10 μ m (**A–C**); 20 μ m (**D**).

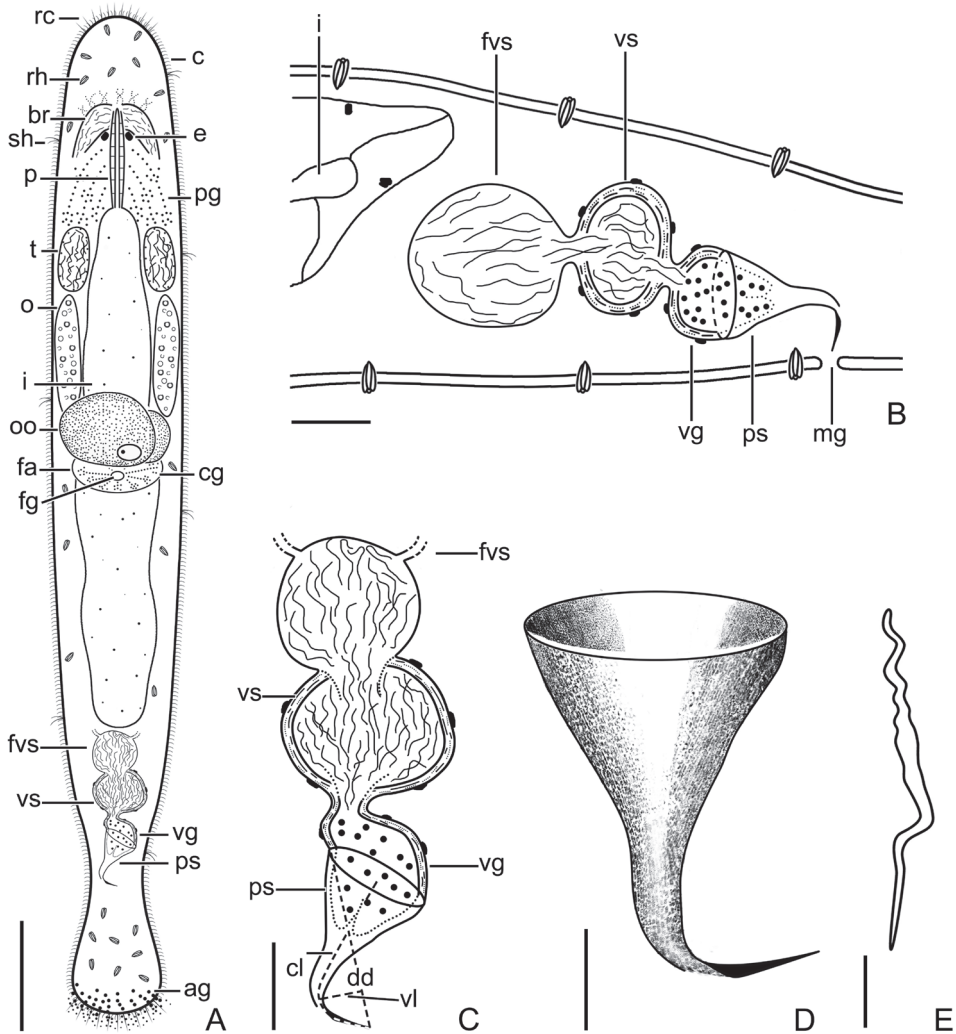


Figure 8. *Macrostomum shekouense* Wang & Shi, sp. nov.: **A** whole body, ventral view **B** sagittal section of the tail **C** male copulatory apparatus **D** penis stylet **E** mature sperm. Abbreviations: ag: adhesive glands; br: brain; c: cilia; cl: curved length from proximal to distal ends; cg: cement glands; dd: direct distance between proximal and distal ends; e: eye; fa: female antrum; fg: female gonopore; fvs: false vesicula seminalis; i: intestine; mg: male gonopore; o: ovary; oo: oocyte; p: pharynx; pg: pharyngeal glands; ps: penis stylet; rc: rigid cilia; rh: rhabdites; sh: sensory hair; t: testis; vl: vertical line from line “dd” to curve vertex of line “cl”; vg: vesicula granulorum; vs: vesicula seminalis. Scale bars: 100 μm (**A**); 20 μm (**B, C**); 10 μm (**D**); 5 μm (**E**).

PLA–Ma0150a–d) imaged *in vivo*, were further deposited on the Macrostomorpha Taxonomy and Phylogeny website (at <https://macrostomorpha.myspecies.info>) and can also be accessed at <https://doi.org/10.5281/zenodo.4585492>.

Habitat. Specimens were collected from the seashore at Shekou peninsula (Suppl. material 4: Fig. S1B). The animals were collected from underwater stones. Salinities of the water in habitat were 16‰–21‰.

Diagnosis. *Macrostomum* with slightly dorsoventrally flattened body and wider arc-shaped tail (Fig. 6A). Muscular wall of both vesicula seminalis and vesicula granulorum thickened. The stylet, hook-like in shape, is a gradually narrowing funnel, including a 90° bending at the 65% position from proximal end (Fig. 6D). No bristles and brush on sperm (Fig. 6E).

Etymology. The specific epithet refers to the locality where the species was found, which is the Shekou peninsula, Guangdong, China.

Description. Mature worms $978 \pm 143 \mu\text{m}$ in length and $115 \pm 18 \mu\text{m}$ in width, covered with dense cilia $4 \pm 0.7 \mu\text{m}$ in length ($n = 7$) (Fig. 6A). Two eyes appear cup-shaped in most individuals, kidney-shaped in some individuals. Rigid cilia, $9 \pm 0.8 \mu\text{m}$ ($n = 7$) and $14 \pm 1.2 \mu\text{m}$ ($n = 5$) in length, at anterior and posterior body end, respectively. Sensory hairs, $13 \pm 0.8 \mu\text{m}$ ($n = 7$) in length, sparsely distributed on body edges. Rhabdite rods mainly distributed on the dorsal side of the body. Distance between the two eyes $23 \pm 1.5 \mu\text{m}$ ($n = 5$) (Fig. 6A). Mouth $83 \pm 3.8 \mu\text{m}$ ($n = 5$) in length (Figs 6A, 7B).

Testes oval in shape, $70 \pm 9.0 \mu\text{m}$ ($n = 7$) in length and $23 \pm 5.2 \mu\text{m}$ ($n = 7$) in width, located on the ventral side of the intestine and situated closely behind the pharynx (Figs 6B, 7A). Male copulatory apparatus consisting of false vesicula seminalis, vesicula seminalis, vesicula granulorum, and penis stylet. False vesicula seminalis oval-shaped, located at the posterior of the body. Vesicula seminalis oval-shaped, connecting to false vesicula seminalis on one side, while connecting to vesicula granulorum on the other side. Muscular wall of both vesicula seminalis and vesicula granulorum thickened. Vesicula granulorum extended into proximal end of penis stylet (Figs 6F, 7C, D, 8B, C). The stylet, hook-like in shape, is a gradually narrowing funnel, including a 90° bending in the 65% position (Fig. 6D); proximal opening $22 \pm 2.7 \mu\text{m}$ ($n = 6$) in diameter; curved length from proximal to distal ends (dotted line ‘cl’ in Fig. 8C) $46 \pm 3.5 \mu\text{m}$ ($n = 6$); direct distance between the proximal and distal ends (dotted line ‘dd’ in Fig. 8C) $39 \pm 2.9 \mu\text{m}$ ($n = 6$); vertical line from line “dd” to the curve vertex of line “cl” (dotted line ‘vl’ in Fig. 8C) $12.7 \pm 0.94 \mu\text{m}$ ($n = 5$). Stylet has an opening (diameter $3 \pm 0.3 \mu\text{m}$ ($n = 4$)) located at the convex side of the subterminal region of stylet and a pointed distal thickening (Figs 6D, 8D). Sperm, $27 \pm 0.8 \mu\text{m}$ in length, having neither bristles nor brush. The boundary between feeler, sperm body, and sperm shaft is not clear (Figs 6E, 8E).

Pair of short elliptic ovaries, $101 \pm 16 \mu\text{m}$ ($n = 7$) in length and $19 \pm 4.7 \mu\text{m}$ ($n = 7$) in width, located on both sides of intestine (Figs 6B, 8A). Female antrum located at the ventral side at 50% of body length. Female gonopore surrounded by numerous cement glands.

***Macrostomum brandi* Wang & Shi, sp. nov.**

<http://zoobank.org/53CB59EA-8C1F-4B5D-B9CC-2F2D1FBC1535>

Figs 9, 10

Type material. *Macrostomum brandi* sp. nov. was first collected in 2017 by Brand et al. (2022a) and therein referred to as *Macrostomum* sp. 81 (as well as *M.* sp. 81 and Mac081). The present description of the species is based on photomicrographs and videos that

Brand et al. (2022a) deposited with multiple specimens of the species. As the holotype we designate their transcriptome-sequenced specimen MTP LS 2864 (transcriptome accession SAMN15061091). The digital type materials of the specimen are available on Zenodo (<https://zenodo.org/record/5656981>) (for details see Brand et al. 2022a).

Habitat. The type specimen was collected from shallow subtidal sediment in Perth (Suppl. material 4: Fig. S1C). The longitude and latitude of the sampling site was described in part *Sample collection and rearing*. Salinities of the water in the habitat was 30‰.

Diagnosis. A *Macrostomum* species with slightly dorsoventrally flattened body and wider arc-shaped tail (Figs 9A, 10A). Both vesicula seminalis and vesicula granulorum have a thickened muscular wall. The stylet, hook-like in shape, is a gradually narrowing funnel, including a 90° bending at the 70% position (Figs 9D, 10C). No bristles and brush on sperm (Figs 9E, 10D).

Etymology. Species name in honor of Lukas Schärer's former PhD student Jeremias Brand, with whom Lukas Schärer collected this species in both Perth, Western Australia and Queenscliff, Victoria, Australia.

Description. Mature individuals $1147 \pm 151 \mu\text{m}$ in length and $229 \pm 48 \mu\text{m}$ in width. Two eyes appear kidney-shaped in most individuals, circular in some individuals. Distance between two eyes $37 \pm 10 \mu\text{m}$ ($n = 15$) (Fig. 9A). Mouth $55 \pm 18 \mu\text{m}$ ($n = 9$) in length (Fig. 9A). The body is covered homogeneously with cilia, $8 \pm 1.7 \mu\text{m}$ in length ($n = 12$). Rigid cilia are $12 \pm 2.1 \mu\text{m}$ ($n = 15$) and $9 \pm 2.0 \mu\text{m}$ ($n = 16$)

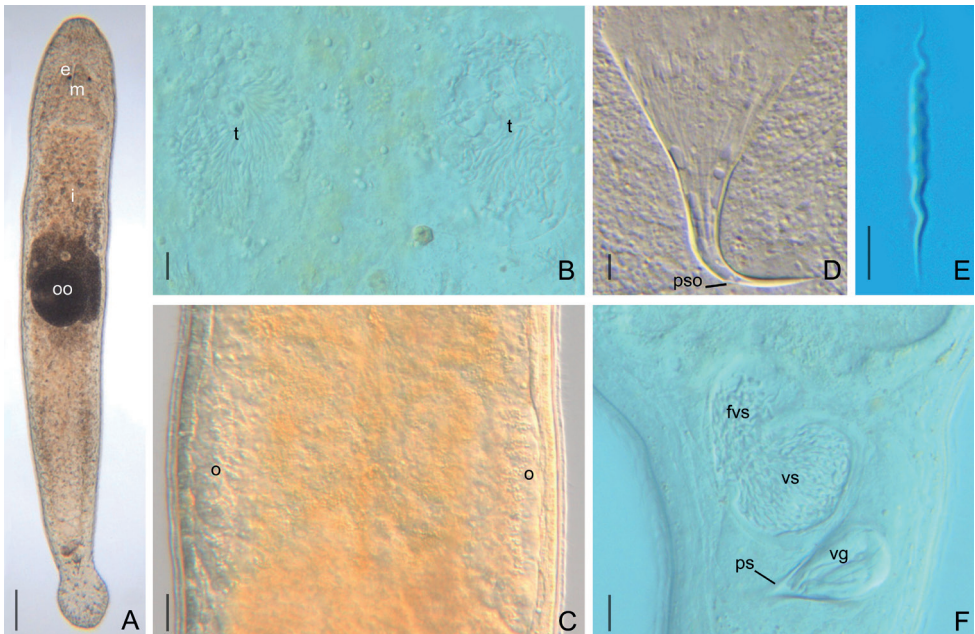


Figure 9. *Macrostomum brandi* Wang & Shi, sp. nov. **A** whole animal, ventral view **B** testes **C** ovaries **D** penis stylet **E** mature sperm **F** male copulatory apparatus, ventral view. Abbreviations: e: eye; fvs: false vesicula seminalis; m: mouth; o: ovary; oo: oocyte; ps: penis stylet; pso: penis stylet opening; t: testis; vg: vesicula granulorum; vs: vesicula seminalis. Scale bars: 100 μm (**A**); 10 μm (**B, D**); 20 μm (**C, F**); 5 μm (**E**).

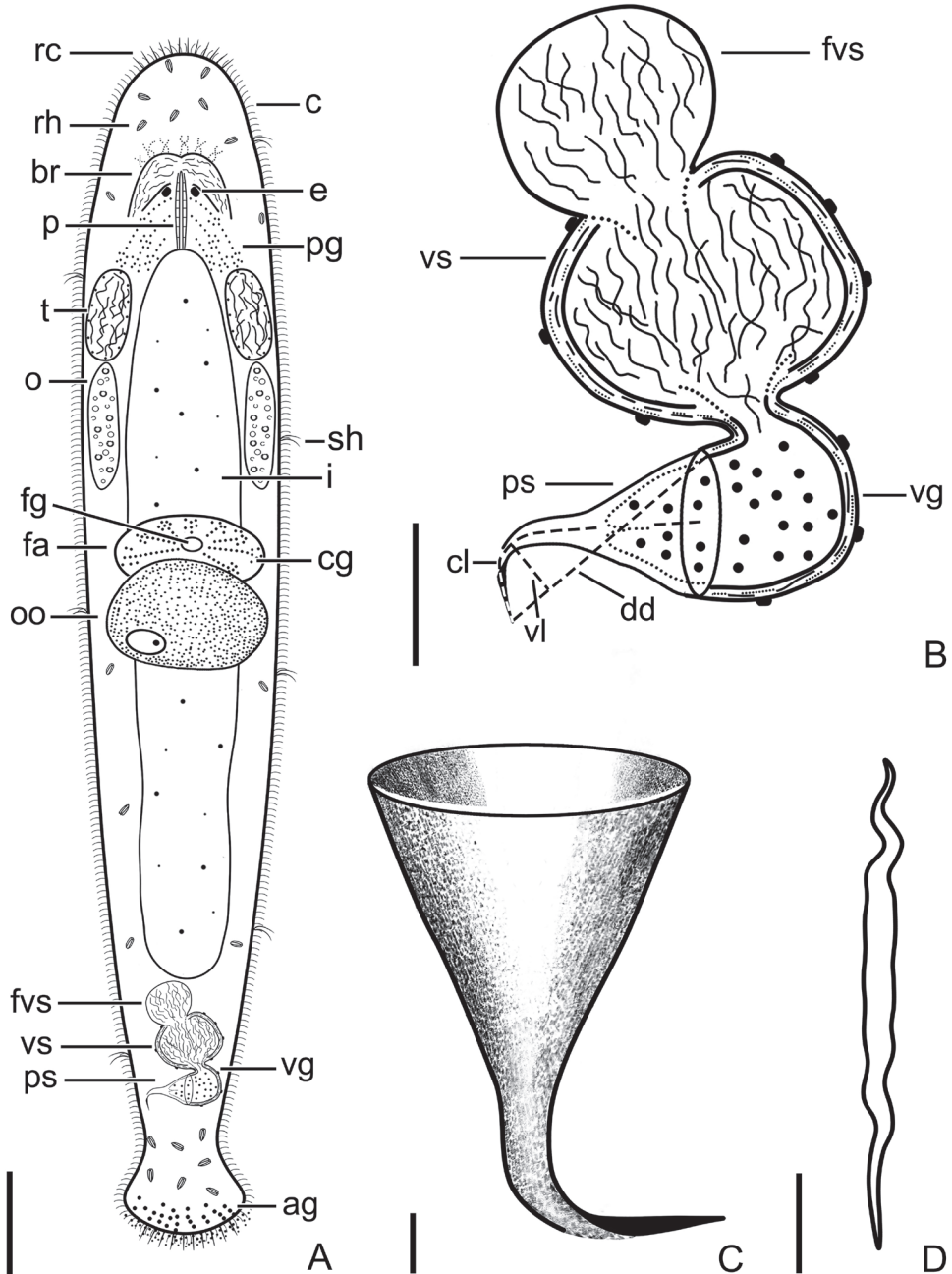


Figure 10. *Macrostomum brandi* Wang & Shi, sp. nov. **A** whole body, ventral view **B** sagittal section of the tail **C** male copulatory apparatus **D** penis stylet **E** mature sperm. Abbreviations: ag: adhesive glands; br: brain; c: cilia; cl: curved length from proximal to distal ends; cg: cement glands; dd: direct distance between proximal and distal ends; e: eye; fa: female antrum; fg: female gonopore; fvs: false vesicula seminalis; i: intestine; mg: male gonopore; o: ovary; oo: oocyte; p: pharynx; pg: pharyngeal glands; ps: penis stylet; rc: rigid cilia; rh: rhabdites; sh: sensory hair; t: testis; vl: vertical line from line “dd” to curve vertex of line “cl”; vg: vesicula granulorum; vs: vesicula seminalis. Scale bars: 100 μm (**A**); 20 μm (**B**); 5 μm (**C, D**).

in length at the anterior and posterior body end, respectively. Tufts of sensory hairs sparsely distributed along the body edges. Rhabdite rods mainly distributed on the dorsal side of the body (Fig. 9A).

Paired elliptic testes, $89 \pm 22 \mu\text{m}$ ($n = 5$) in length and $53 \pm 30 \mu\text{m}$ ($n = 5$) in width, located on the ventral side of the intestine and situated closely behind the pharynx (Figs 9B, 10A). Male copulatory apparatus consisting of false vesicula seminalis, vesicula seminalis, vesicula granulorum, and penis stylet. False vesicula seminalis oval-shaped, located at the posterior of the body. It connects on the rear part to an oval-shaped muscular vesicula seminalis. The vesicula seminalis is connected anterolaterally to the muscular vesicula granulorum. Muscular wall of both vesicula seminalis and vesicula granulorum thickened. Vesicula granulorum extended into proximal end of penis stylet (Figs 9E, 10B). The stylet is a hook-like and gradually-narrowing funnel with a 90° bending at the 70% position (Figs 9D, 10C); proximal opening $37 \pm 9 \mu\text{m}$ ($n = 7$) in diameter; curved length from proximal to distal ends (dotted line 'cl' in Fig. 10B) $55 \pm 5.0 \mu\text{m}$ ($n = 7$); direct distance between proximal and distal ends (dotted line 'dd' in Fig. 10B) $49 \pm 5 \mu\text{m}$ ($n = 7$); vertical line from line "dd" to curve vertex of line "cl" (dotted line 'vl' in Fig. 10B) $9 \pm 1 \mu\text{m}$ ($n = 7$). The stylet opening $2.5 \pm 0.05 \mu\text{m}$ ($n = 6$) in diameter, located at the convex side of the subterminal region of stylet and it has a pointed distal thickening (Figs 9D, 10C). Mature sperm without bristles and brush, $24 \pm 2 \mu\text{m}$ in length. The boundary between feeler, sperm body, and sperm shaft is not clear (Figs 9E, 10D).

Pair of ovaries lie directly behind the testes and show the short elliptic shape, $124 \pm 31 \mu\text{m}$ ($n = 8$) in length and $30 \pm 7 \mu\text{m}$ ($n = 8$) in width (Figs 9C, 10A). Female gonopore opening ventrally at female antrum, surrounded by numerous cement glands. Female antrum lies at the ventral side at 50% of body length.

Remarks. A comparison between *Macrostomum shekouense* sp. nov., *M. brandi* sp. nov., and ten similar species with hook-like stylets within the genus is shown in Table 2. For the 12 listed species, the female antrum of only three species (*M. shekouense* sp. nov., *M. brandi* sp. nov., and *M. obeliscis*) lies at the ventral side at 50% of body length, while that of the other nine species lies considerably further towards the posterior.

Based on the 28S rDNA phylogenetic tree in Brand et al. (2022a) it seems clear that there currently are no other known species that are very close to *Macrostomum brandi* sp. nov. *M. shekouense* sp. nov., *M. brandi* sp. nov., and *M. obeliscis* are very similar in stylet morphology, particularly with respect to the position of the stylet opening, as well as the bending angle and position of the curve in the stylet, although the stylet is a little larger in *M. brandi* sp. nov. than that in *M. shekouense* sp. nov. and in *M. obeliscis*. In terms of overall morphology of the flatworms, *M. shekouense* sp. nov. is much more similar to *M. brandi* sp. nov. This includes a central position of the developing eggs at ~ 50% (rather than an even more anterior position at ~ 40% in *M. obeliscis*), and the linear anterior-posterior arrangement of the false seminal vesicle, the true seminal vesicle, and a posteriorly pointing stylet (while the *M. obeliscis* lacks a false seminal vesicle, and has a seminal vesicle and stylet that are oriented laterally in an opposite direction). In agreement with this, the molecular phylogenetic analyses based on 18S–28S rDNA show that *M. shekouense* sp. nov. is a very close relative of *M. brandi* sp. nov.

However, in the COI gene tree, *M. shekouense* sp. nov. occupied a separate branch by 0.99 PP, 93% BP, supporting a separation between *M. shekouense* sp. nov. and *M. brandi* sp. nov. (Fig. 2). GDs based on the COI sequence within the genus *Macrostomum* were also calculated, showing that GDs between individuals of *M. shekouense* sp. nov. and *M. brandi* sp. nov. were between 10.1% and 10.9% (Suppl. material 3: Table S3), while the two specimens from Perth and Queenscliff differed by only 0.2%. Hebert et al. (2003) found that GDs between species are ordinarily greater than 3% for a range of invertebrates. Moreover, we note that *M. littorale* sp. nov. and *M. hystrix* show a clearly different stylet morphology, while the GD between these two species (8.9%) is less than that between *M. shekouense* sp. nov. and *M. brandi* sp. nov.

In addition, we calculated and compared the ratio of the length of two lines of the stylet as shown in Fig. 8 and Fig. 10, dd and vl. This suggests that the dd-to-vl ratio in *M. brandi* sp. nov. (5.2 ± 0.62 , $n = 7$) is significantly higher than that in *M. shekouense* sp. nov. (3.1 ± 0.26 , $n = 5$) (2-tail $p < 0.001$, Independent Sample Test) (Suppl. material 7: Fig. S4).

Accordingly, both morphological and molecular evidence supports that *M. shekouense* sp. nov. and *M. brandi* sp. nov. are two new species.

Discussion

It is a challenging task to identify *Macrostomum* species for various reasons. Firstly, these small, fragile microturbellarians are difficult to study. Secondly, there is considerable convergent evolution of the copulatory organ morphology in *Macrostomum* species, particularly the morphology of the penis stylet (e.g., Schärer et al. 2011; Brand et al. 2022b). Brand et al. (2022a) suggested that investigations of species within the hypodermic clade without support from molecular data thus require considerable caution due to the striking cases of convergent evolution found in HMS species. Molecular markers such as the mitochondrial COI, showing a more rapid evolutionary rate than nuclear 18S and 28S rDNA, was suggested to better resolve species-level relationships (Schärer et al. 2020). However, mitochondrial COI are currently not available in most species of *Macrostomum* to date. The present study has now identified a primer pair, which was used to amplify and sequence eight new mitochondrial COI sequences of three *Macrostomum* species, as well as extracting three COI sequences from previously deposited transcriptomes (Suppl. material 2: Table S2). The COI gene tree supported a separation between *M. janickei* and *M. lignano* (see also Schärer et al. 2020), and it supported separation between *M. littorale* sp. nov. and *M. hystrix*, as well as between *M. shekouense* sp. nov. and *M. brandi* sp. nov., although in all these cases these species pairs could not be separated by 18S and 28S rDNA trees (Figs 1, 2). Accordingly, with an increase in the number of COI sequences provided for *Macrostomum* species, molecular phylogenetic analyses based on mitochondrial COI gene could be a useful tool for helping to identify *Macrostomum* species in combination with morphological characters. In addition, it is suggested that mitochondrial COI sequences of *Macrostomum* species could be amplified using primer pair provided either by Janssen et al. (2015) or by this study showing in Table 1.

In this study, a significant difference was found in dd-to-vl ratio of stylet in *M. shekouense* sp. nov. and *M. brandi* sp. nov. We propose that the dd-to-vl ratio of stylet could serve as an additional character for the delimitation of the hypodermic species with hook-like stylets, considering that the values of dd and vl vary with the change of stylet length, the bending angle and position of the curve in the stylet, and the diameter of proximal opening of stylet.

It is interesting to note that the COI gene sequences of both *M. littorale* sp. nov. and *M. sp. 34* show single-base deletions at two positions, position 336 and position 434 when counting from the ATT start codon of the 1,548 bp COI gene of *M. lignano* (Egger et al. 2017, GenBank: MF078637), leading to a frameshift mutation and a TAG stop codon only ten bases (and three more stop codons in the sequenced fragment alone). Furthermore, two species, *M. taurinum* and *M. zhujiangense*, show a single-base deletion at position 434, resulting in the frameshift mutation of ten amino acid residues followed by a stop codon (Fig. 11). A similar phenomenon was previously reported in *M. hystrix* (Schärer et al. 2020), for which the COI gene sequence shows a single-base deletion at position 336, leading to a frameshift mutation and a TAG stop codon only ten bases on (and eight more stop codons in the sequenced fragment alone). The single-base deletion at position 336 or at position 434 would be expected to lead to a truncation of the resulting COI protein.

Given the importance of the COI protein in the electron transport chain of mitochondrial oxidative phosphorylation, this finding is surprising and requires further examination and validation, as already noted by Schärer et al. (2020). Further studies are needed to elucidate the phenomenon of single-base deletion in the COI gene of *Macrostomum* species. It will be interesting to further explore the mechanism of gene expression of the COI gene in the *Macrostomum* species, particularly the post-transcriptional processing of precursor-messenger RNA, since at least in *M. hystrix* the frameshifted transcript seems to be abundantly expressed (Schärer et al. 2020).

Acknowledgements

The authors would like to thank Yaohang Xie, Linhong Zhong, and Fan Xin for assisting with sample collection. We also thank Zicheng Zeng, Shuxin Huang, Jiajie Huang, and Yuanyuan Liao for their kind support in the experiments. We sincerely thank the reviewer Dr. Lukas Schärer who provided valuable feedback on earlier versions of the manuscript and helped us navigate the available material that allowed us to describe the species from Australia. We also sincerely thank reviewers Dr. Marco Curini-Galletti and the subject editor Dr. Tom Artois for their valuable and insightful comments which improved the quality of the paper. This work was supported by the National Key R&D Program of China (2020YFA0908700), Basic Research Program (JCYJ20190808121811243) funded by Shenzhen Municipal Government, and the Guangdong Provincial Undergraduate Training Program for Innovation and Entrepreneurship (S202110590033).

References

- Ax P (1951) Die Turbellarien des Eulitorals der Kieler Bucht. *Zoologische Jahrbucher. Abteilung für Systematik, Ökologie und Geographie der Tiere* 80: 277–378.
- Beklemischev VN (1951) Species of the genus *Macrostomum* (Turbellaria, Rhabdocoela) of the USSR. *Zeitschrift der Moskauer Naturwissenschaftlichen Gesellschaft* 56: 31–40. [English Translation]
- Brand JN, Viktorin G, Wiberg R, Beisel C, Schärer L (2022a) Large-scale phylogenomics of the genus *Macrostomum* (Platyhelminthes) reveals cryptic diversity and novel sexual traits. *Molecular Phylogenetics and Evolution* 166: e107296. <https://doi.org/10.1016/j.ympev.2021.107296>
- Brand JN, Harmon LJ, Schärer L (2022b) Frequent origins of traumatic insemination involve convergent shifts in sperm and genital morphology. *Evolution Letters* 6(1): 63–82. <https://doi.org/10.1002/evl3.268>
- Castresana J (2000) Selection of conserved blocks from multiple alignments for their use in phylogenetic analysis. *Molecular Biology and Evolution* 17(4): 540–552. <https://doi.org/10.1093/oxfordjournals.molbev.a026334>
- Egger B, Bachmann L, Fromm B (2017) Atp8 is in the ground pattern of flatworm mitochondrial genomes. *BMC Genomics* 18(1): e414. <https://doi.org/10.1186/s12864-017-3807-2>
- Fang CY, Wang L, Zhang Y, Wang AT (2016) Two new species of brackish-water *Macrostomum* (Platyhelminthes, Macrostomida) from southern China. *Zootaxa* 4170(2): 298–310. <https://doi.org/10.11646/zootaxa.4170.2.4>
- Ferguson FF (1940) A monograph of the genus *Macrostomum* O. Schmidt 1848. Part VII. *Zoologischer Anzeiger* 129: 120–146.
- Ferguson FF (1954) Monograph of the Macrostomine worms of Turbellaria. *Transactions of the American Microscopical Society* 73(2): 137–164. <https://doi.org/10.2307/3223751>
- Hebert PDN, Cywinska A, Ball SL, deWaard JR (2003) Biological identifications through DNA barcodes. *Proceedings of the Royal Society B: Biological Sciences* 270(1512): 313–321. <https://doi.org/10.1098/rspb.2002.2218>
- Janssen T, Vizoso DB, Schulte G, Littlewood DTJ, Waeschenbach A, Schärer L (2015) The first multi-gene phylogeny of the Macrostomorpha sheds light on the evolution of sexual and asexual reproduction in basal Platyhelminthes. *Molecular Phylogenetics and Evolution* 92: 82–107. <https://doi.org/10.1016/j.ympev.2015.06.004>
- Kalyaanamoorthy S, Minh BQ, Wong TKF, von Haeseler A, Jermiin LS (2017) ModelFinder: Fast model selection for accurate phylogenetic estimates. *Nature Methods* 14(6): 587–589. <https://doi.org/10.1038/nmeth.4285>
- Katoh K, Rozewicki J, Yamada KD (2017) MAFFT online service: Multiple sequence alignment, interactive sequence choice and visualization. *Briefings in Bioinformatics* 20(4): 1160–1166. <https://doi.org/10.1093/bib/bbx108>
- Kuraku S, Zmasek CM, Nishimura O, Katoh K (2013) ALeaves facilitates on-demand exploration of metazoan gene family trees on MAFFT sequence alignment server with enhanced interactivity. *Nucleic Acids Research* 41(W1): W22–W28. <https://doi.org/10.1093/nar/gkt389>

- Ladurner P, Schärer L, Salvenmoser W, Rieger RM (2005) A new model organism among the lower Bilateria and the use of digital microscopy in taxonomy of meiobenthic Platyhelminthes: *Macrostomum lignano*, n. sp. (Rhabditophora, Macrostomorpha). *Journal of Zoological Systematics and Evolutionary Research* 43(2): 114–126. <https://doi.org/10.1111/j.1439-0469.2005.00299.x>
- Ladurner P, Egger B, De Mulder K, Pfister D, Kualess G, Salvenmoser W, Schärer L (2008) The Stem Cell System of the Basal Flatworm *Macrostomum lignano*. In: Bosch TCG (Ed.) *Stem Cells*. Springer, Dordrecht, 75–94. https://doi.org/10.1007/978-1-4020-8274-0_5
- Lanfear R, Frandsen PB, Wright AM, Senfeld T, Calcott B (2017) PartitionFinder 2: New methods for selecting partitioned models of evolution for molecular and morphological phylogenetic analyses. *Molecular Biology and Evolution* 34(3): 772–773. <https://doi.org/10.1093/molbev/msw260>
- Laumer CE, Giribet G (2014) Inclusive taxon sampling suggests a single, stepwise origin of ectolecithality in Platyhelminthes. *Biological Journal of the Linnean Society. Linnean Society of London* 111(3): 570–588. <https://doi.org/10.1111/bij.12236>
- Lin YT, Feng WT, Xin F, Zhang L, Zhang Y, Wang AT (2017a) Two new species and the molecular phylogeny of eight species of *Macrostomum* (Platyhelminthes: Macrostomorpha) from southern China. *Zootaxa* 4337(3): 423–435. <https://doi.org/10.11646/zootaxa.4337.3.7>
- Lin YT, Zhou WW, Xiao P, Zheng YH, Lu J, Li JC, Wang AT (2017b) Two new species of freshwater *Macrostomum* (Rhabditophora: Macrostomorpha) found in China. *Zootaxa* 4329(3): 267–280. <https://doi.org/10.11646/zootaxa.4329.3.5>
- Mack-Fira V (1971) Deux turbellariés nouveaux de la mer noire. *Revue Roumaine de Biologie, série Zoologie* 16(4): 233–240.
- Mouton S, Willems M, Braeckman BP, Egger B, Ladurner P, Schärer L, Borgonie G (2009) The free-living flatworm *Macrostomum lignano*: A new model organism for ageing research. *Experimental Gerontology* 44(4): 243–249. <https://doi.org/10.1016/j.exger.2008.11.007>
- Nguyen LT, Schmidt HA, von Haeseler A, Minh BQ (2015) IQ-TREE: A fast and effective stochastic algorithm for estimating maximum-likelihood phylogenies. *Molecular Biology and Evolution* 32(1): 268–274. <https://doi.org/10.1093/molbev/msu300>
- Nylander JAA (2004) MrModeltest v2. Program distributed by the author. Evolutionary Biology Centre, Uppsala University. <https://github.com/nylander/MrModeltest2> [accessed 13 Nov 2019]
- Örsted AS (1843) Forsøg til en ny Classification of Planarierne (Planariae Dugés) grundet paa mikroskopisk-anatomiske Undersøgelser. *Kroyer's Naturhistorisk Tidsskrift* 4(I): 519–581.
- Rambaut A (2009) FigTree: tree figure drawing tool. Version 1.3.1. Institute of Evolutionary Biology, University of Edinburgh, UK. <http://tree.bio.ed.ac.uk/software/figtree/> [accessed 4 Jan 2020]
- Rambaut A, Drummond AJ, Xie D, Baele G, Suchard MA (2018) Posterior summarisation in Bayesian phylogenetics using Tracer 1.7. *Systematic Biology* 67(5): 901–904. <https://doi.org/10.1093/sysbio/syy032>
- Rieger RM (1977) The relationship of character variability and morphological complexity in copulatory structures of Turbellaria-Macrostomida and Haplopharyngida. *Mikrofauna. Meeresboden* 61: 197–216.

- Rieger RM, Salvenmoser W, Legniti A, Tyler S (1994) Phalloidin-rhodamine preparations of *Macrostomum hystricinum marinum* (Plathelminthes): Morphology and postembryonic development of the musculature. *Zoomorphology* 114(3): 133–147. <https://doi.org/10.1007/BF00403261>
- Ronquist F, Teslenko M, van der Mark P, Ayres DL, Darling A, Höhna S, Larget B, Liu L, Suchard MA, Huelsenbeck JP (2012) MrBayes 3.2: Efficient Bayesian phylogenetic inference and model choice across a large model space. *Systematic Biology* 61(3): 539–542. <https://doi.org/10.1093/sysbio/sys029>
- Schärer L, Littlewood DT, Waeschenbach A, Yoshida W, Vizoso DB (2011) Mating behavior and the evolution of sperm design. *Proceedings of the National Academy of Sciences of the United States of America* 108(4): 1490–1495. <https://doi.org/10.1073/pnas.1013892108>
- Schärer L, Brand JN, Singh P, Zadesenets KS, Stelzer PC, Viktorin G (2020) A phylogenetically informed search for an alternative *Macrostomum* model species, with notes on taxonomy, mating behavior, karyology, and genome size. *Journal of Zoological Systematics and Evolutionary Research* 58(1): 41–65. <https://doi.org/10.1111/jzs.12344>
- Schmidt P, Sopott-Ehlers B (1976) Interstitielle Fauna von Galapagos XV. *Macrostomum* O. Schmidt, 1948 und *Siccomacrostomum triviale* nov. gen. nov. spec. (Turbellaria, Macrostomida). *Mikrofauna des Meeresbodens* 57: 1–45.
- Tamura K, Stecher G, Peterson D, Filipski A, Kumar S (2013) MEGA6: Molecular evolutionary genetics analysis version 6.0. *Molecular Biology and Evolution* 30(12): 2725–2729. <https://doi.org/10.1093/molbev/mst197>
- Tu TJ (1934) Notes on some turbellarians from the Tsing Hua campus. *The Science Reports of National Tsing Hua University. Series B Biological and Psychological Science* 1: 191–206.
- Tyler S, Schilling S, Hooge M, Bush LF [comp.] (2006–2021) Turbellarian taxonomic database. Version 1.8. <http://turbellaria.umaine.edu>
- Vizoso DB, Rieger G, Schärer L (2010) Goings-on inside a worm: Functional hypotheses derived from sexual conflict thinking. *Biological Journal of the Linnean Society. Linnean Society of London* 99(2): 370–383. <https://doi.org/10.1111/j.1095-8312.2009.01363.x>
- Wang AT, Luo ZG (2004) A new species of the genus *Macrostomum* from China (Turbellaria: Macrostomida). *Dong Wu Fen Lei Xue Bao* 29(4): 700–703. [in Chinese]
- Wang L, Xin F, Fang CY, Zhang Y, Wang AT (2017) Two new brackish-water species of *Macrostomum* (Platyhelminthes: Macrostomorpha) from mangrove wetland in southern China. *Zootaxa* 4276(1): 107–124. <https://doi.org/10.11646/zootaxa.4276.1.5>
- Wasik K, Gurtowski J, Zhou X, Ramos OM, Delás MJ, Battistoni GEI, Demerdash O, Falcatori I, Vizoso DB, Smith AD, Ladurner P, Schärer L, McCombie WR, Hannon GJ, Schatz M (2015) Genome and transcriptome of the regeneration-competent flatworm, *Macrostomum lignano*. *Proceedings of the National Academy of Sciences of the United States of America* 112(40): 12462–12467. <https://doi.org/10.1073/pnas.1516718112>
- Wudarski J, Egger B, Ramm SA, Schärer L, Ladurner P, Zadesenets KS, Rubtsov NB, Mouton S, Berezikov E (2020) The free-living flatworm *Macrostomum lignano*. *EvoDevo* 11(1): e5. <https://doi.org/10.1186/s13227-020-00150-1>
- Xia X (2017) DAMBE6: New tools for microbial genomics, phylogenetics and molecular evolution. *The Journal of Heredity* 108(4): 431–437. <https://doi.org/10.1093/jhered/esx033>

- Xia X, Lemey P (2009) Assessing substitution saturation with DAMBE. In: Lemey P, Salemi M, Vandamme MA (Eds) *The Phylogenetic Handbook: A Practical Approach to Phylogenetic Analysis and Hypothesis Testing*. Cambridge University Press, Cambridge, 615–630. <https://doi.org/10.1017/cbo9780511819049.022>
- Xin F, Zhang SY, Shi YS, Wang L, Zhang Y, Wang AT (2019) *Macrostomum shenda* and *M. spiriger*, two new brackish-water species of *Macrostomum* (Platyhelminthes: Macrostomorpha) from China. *Zootaxa* 4603(1): 105–124. <https://doi.org/10.11646/zootaxa.4603.1.5>
- Yang Y, Li JY, Sluys R, Li WX, Li SF, Wang AT (2020) Unique mating behavior, and reproductive biology of a simultaneous hermaphroditic marine flatworm (Platyhelminthes, Tricladida, Maricola). *Invertebrate Biology* 139(1): e12282. <https://doi.org/10.1111/ivb.12282>
- Zhang SY, Shi YS, Zeng ZC, Xin F, Deng L, Wang AT (2021) Two New Brackish-water Species of *Macrostomum* (Platyhelminthes: Macrostomorpha) from China and Their Phylogenetic Positions. *Zoological Science* 38(3): 273–286. <https://doi.org/10.2108/zs200121>

Supplementary material 1

Table S1

Authors: Yongshi Shi, Zhiyu Zeng, Jia Wang, Siyu Zhang, Li Deng, Antai Wang

Data type: docx file

Explanation note: GenBank accession numbers of 18S and 28S rDNA sequences for species taxa used in the phylogenetic analyses.

Copyright notice: This dataset is made available under the Open Database License (<http://opendatacommons.org/licenses/odbl/1.0/>). The Open Database License (ODbL) is a license agreement intended to allow users to freely share, modify, and use this Dataset while maintaining this same freedom for others, provided that the original source and author(s) are credited.

Link: <https://doi.org/10.3897/zookeys.1099.72964.suppl1>

Supplementary material 2

Table S2

Authors: Yongshi Shi, Zhiyu Zeng, Jia Wang, Siyu Zhang, Li Deng, Antai Wang

Data type: docx file

Explanation note: GenBank accession numbers of COI sequences for species taxa used in the phylogenetic analyses.

Copyright notice: This dataset is made available under the Open Database License (<http://opendatacommons.org/licenses/odbl/1.0/>). The Open Database License (ODbL) is a license agreement intended to allow users to freely share, modify, and use this Dataset while maintaining this same freedom for others, provided that the original source and author(s) are credited.

Link: <https://doi.org/10.3897/zookeys.1099.72964.suppl2>

Supplementary material 3

Table S3

Authors: Yongshi Shi, Zhiyu Zeng, Jia Wang, Siyu Zhang, Li Deng, Antai Wang

Data type: xls file

Explanation note: The genetic distances (GDs) among *Macrostomum* species calculated from COI sequences.

Copyright notice: This dataset is made available under the Open Database License (<http://opendatacommons.org/licenses/odbl/1.0/>). The Open Database License (ODbL) is a license agreement intended to allow users to freely share, modify, and use this Dataset while maintaining this same freedom for others, provided that the original source and author(s) are credited.

Link: <https://doi.org/10.3897/zookeys.1099.72964.suppl3>

Supplementary material 4

Figure S1

Authors: Yongshi Shi, Zhiyu Zeng, Jia Wang, Siyu Zhang, Li Deng, Antai Wang

Data type: jpg file

Explanation note: Locality and habitat of the different species.

Copyright notice: This dataset is made available under the Open Database License (<http://opendatacommons.org/licenses/odbl/1.0/>). The Open Database License (ODbL) is a license agreement intended to allow users to freely share, modify, and use this Dataset while maintaining this same freedom for others, provided that the original source and author(s) are credited.

Link: <https://doi.org/10.3897/zookeys.1099.72964.suppl4>

Supplementary material 5

Figure S2

Authors: Yongshi Shi, Zhiyu Zeng, Jia Wang, Siyu Zhang, Li Deng, Antai Wang

Data type: jpg file

Explanation note: Maximum-likelihood phylogenetic tree topology based on 18S rDNA dataset.

Copyright notice: This dataset is made available under the Open Database License (<http://opendatacommons.org/licenses/odbl/1.0/>). The Open Database License (ODbL) is a license agreement intended to allow users to freely share, modify, and use this Dataset while maintaining this same freedom for others, provided that the original source and author(s) are credited.

Link: <https://doi.org/10.3897/zookeys.1099.72964.suppl5>

Supplementary material 6

Figure S3

Authors: Yongshi Shi, Zhiyu Zeng, Jia Wang, Siyu Zhang, Li Deng, Antai Wang

Data type: jpg file

Explanation note: Maximum-likelihood phylogenetic tree topology based on 28S rDNA dataset.

Copyright notice: This dataset is made available under the Open Database License (<http://opendatacommons.org/licenses/odbl/1.0/>). The Open Database License (ODbL) is a license agreement intended to allow users to freely share, modify, and use this Dataset while maintaining this same freedom for others, provided that the original source and author(s) are credited.

Link: <https://doi.org/10.3897/zookeys.1099.72964.suppl6>

Supplementary material 7

Figure S4

Authors: Yongshi Shi, Zhiyu Zeng, Jia Wang, Siyu Zhang, Li Deng, Antai Wang

Data type: jpg file

Explanation note: Comparison of value dd/vl between *M. shekouense* sp. nov. and *M. brandi* sp. nov. (2-tail $p < 0.001$, Independent Sample Test).

Copyright notice: This dataset is made available under the Open Database License (<http://opendatacommons.org/licenses/odbl/1.0/>). The Open Database License (ODbL) is a license agreement intended to allow users to freely share, modify, and use this Dataset while maintaining this same freedom for others, provided that the original source and author(s) are credited.

Link: <https://doi.org/10.3897/zookeys.1099.72964.suppl7>

Molecular analysis of *Lepidopleurus cajetanus* (Poli, 1791) (Polyplacophora, Leptochitonidae) from the Mediterranean and near Atlantic

Mariastella Colomba¹, Julia D. Sigwart², Walter Renda³,
Armando Gregorini¹, Maurizio Sosso⁴, Bruno Dell'Angelo⁵

1 University of Urbino, Dept. of Biomolecular Sciences, via I. Maggetti 22, 61029 Urbino (PU), Italy **2** Senckenberg Research Institute and Museum, Senckenberganlage 25, 60325 Frankfurt, Germany **3** Via Bologna 18/A, 87032 Amantea (CS), Italy **4** Via Bengasi 4, 16153 Genova (GE), Italy **5** Via Briscata 16, 16154 Genova (GE), Italy

Corresponding author: Mariastella Colomba (mariastella.colomba@uniurb.it)

Academic editor: Frank Köhler | Received 27 September 2021 | Accepted 28 March 2022 | Published 3 May 2022

<http://zoobank.org/AD593D6B-D21F-4576-A8A2-EF8E12D3A840>

Citation: Colomba M, Sigwart JD, Renda W, Gregorini A, Sosso M, Dell'Angelo B (2022) Molecular analysis of *Lepidopleurus cajetanus* (Poli, 1791) (Polyplacophora, Leptochitonidae) from the Mediterranean and near Atlantic. ZooKeys 1099: 29–40. <https://doi.org/10.3897/zookeys.1099.75837>

Abstract

In the present paper we used a molecular data set (including mitochondrial partial 16S rRNA and COI gene sequences) to examine the genetic structure of *Lepidopleurus cajetanus* (Poli, 1791) (Polyplacophora, Leptochitonidae) - a distinctive shallow water chiton and member of the basal branching Lepidopleurida, which is widespread in and adjacent to the Mediterranean. The analyses of the two mt-standard marker fragments resolved two main discrete clusters reported as *L. cajetanus* s.s. and *L. aff. cajetanus*, respectively. *Lepidopleurus cajetanus* s.s. is widespread throughout the area under study, while the second distinct lineage apparently co-occurs on the eastern Spanish mainland coast of the Balearic Sea. This result is discussed comparing our data with those reported, in 2014, by Fernández and colleagues who described *L. cajetanus* as exhibiting “a ‘chaotic patchiness’ pattern defined by a high genetic variability with locality-exclusive haplotypes, high genetic divergence, and a lack of geographic structure”. Although genetic data alone are not sufficient to draw any definitive conclusions, nevertheless we believe that present results shed new light on *L. cajetanus* which apparently shows more geographically patterned genetic structure than supposed so far.

Keywords

16S rRNA, chitons, COI, phylogeny, standard mitochondrial markers

Introduction

Chitons (class Polyplacophora) are the third-largest class in the phylum Mollusca by species richness of living taxa (Ponder et al. 2020). The superficial similarity of the living species, with a distinctive eight-part shell armour covering a soft foot that adheres to the substratum, has created some long-term confusion in the ecological identification of species. Yet *Lepidopleurus cajetanus* (Poli, 1791) (Polyplacophora, Leptochitonidae) was recognised as a distinct form in the Mediterranean very early in the history of formal modern taxonomy. Although it is phylogenetically nested within the genus *Leptochiton* s.s. with other species in this clade from the Mediterranean and North Atlantic (Sigwart et al. 2011), taxonomists have maintained the genus *Lepidopleurus* in acknowledgement of its unique morphology. WoRMS (World Register of Marine Species) reports two living species of *Lepidopleurus*, *L. cajetanus* (Poli, 1791) and *L. cullierti* Roch, 1891 (<https://www.marinespecies.org/aphia.php?p=taxdetails&id=138116>). Actually, Castellanos (1988) cites *L. cullierti* showing also a figure of it (later taken up by Forcellini 2000), without taking into account that this species was already considered by Pilsbry (1893: 111) a *nomen dubium* (certainly not a *Lepidopleurus*, but belonging probably to the genus *Chaetopleura*). The species is not reported in recent papers dealing with Leptochitonidae from Chile (Sirenko 2006; Schwabe 2009; Schwabe and Sellanes 2010; Sirenko 2015; Sirenko and Sellanes 2016), but it is still (erroneously) reported in various lists. Recently, Aldea et al. (2020) reported *L. cullierti* as a dubious species. In conclusion, at least as far as concerns living species, *Lepidopleurus* is presently a monotypic genus. Notably, nomenclature is still confusing and a clear distinction between *Lepidopleurus* and *Leptochiton* has not been fully achieved.

Lepidopleurus was the first genus name proposed for lepidopleuran chitons, including only the species *L. cajetanus*. In 1847, Gray established the genus name *Leptochiton*. Both genera were included in the family Leptochitonidae Dall, 1889 with *Leptochiton asellus* as the type species. A few years later, Pilsbry (1892) listed *Leptochiton* as a junior subjective synonym of *Lepidopleurus*, and changed the family name to Lepidopleuridae. Since then, *Lepidopleurus* and *Leptochiton* (and family names) have been used more or less interchangeably (Sigwart et al. 2011). To date, there is insufficient evidence to separate *Lepidopleurus* and *Leptochiton* s.s. as distinct genera, even if they are often distinguished on the basis of shell thickness and sculpture [i.e., distinctive shell morphology with pronounced concentric ridges on the lateral areas and terminal valves (*Lepidopleurus*), or flat and plain shells generally lacking strong raised sculpture (*Leptochiton*)].

Lepidopleurus cajetanus is widespread throughout the Mediterranean (where, even if quite discontinuously, it can be very common locally) and more rarely in the Atlantic, from the Iberian Peninsula (Spain and Portugal) to Morocco and to the Canary Islands (Spain) and Berlengas Archipelago (Portugal) (Kaas and Van Belle 1985; Dell'Angelo and Smriglio 2001). The species is known as fossils in the European Neogene: from the lower Miocene (Burdigalian) of the Aquitaine Basin to the middle Miocene of the Aquitaine Basin and Paratethys and the French and Italian upper Miocene, to the

Pliocene of Italy, Spain and Greece, to the Pleistocene of Italy and Greece (Dell'Angelo et al. 2018a, 2018b and references therein). As has been widely described (see for example, Dell'Angelo et al. 2013, 2015, 2018a, 2018b), fossils of *L. cajetanus* show great variability in the morphological characters of the plates (sculpture, shape, etc.), which is much less evident in the living specimens.

Living chitons are broadly divided into two main clades, the orders Lepidopleurida and Chitonida. The former group retains plesiomorphic shell forms and is therefore particularly interesting for studies of molluscan phylogeny (Sigwart et al. 2011). Most members of Lepidopleurida inhabit deep sea environments, but as *Lepidopleurus cajetanus* can be found intertidally it has been widely used in genetic studies including molecular phylogenetic studies of molluscs (see for example, Giribet and Wheeler 2002).

In addition to data on the impact of strong biogeographical barriers on gene flow (Ayre et al. 2009), other studies on chiton population genetics have recovered well-mixed populations in spite of geographic barriers (e.g., Doonan et al. 2012), including some species in the Mediterranean such as *Rhyssoplax olivacea* (Spengler, 1797) (Fernández et al. 2014). One study described a cryptic species on the basis of differential haplotype structures which were attributed to potentially different dispersal capacity of two species of *Leptochiton* s.l. (Sigwart and Chen 2018): *L. rugatus* (Carpenter in Pilsbry, 1892) and *L. cascadiensis* Sigwart & Chen, 2018. In contrast to previous results for chitons, a focussed study on the population genetic structure of *Lepidopleurus cajetanus* from the Atlantic and Mediterranean coasts found 'chaotic patchiness' defined by unique haplotypes, high genetic divergence, and yet no apparent geographic partitioning (Fernández et al. 2014). In particular, the authors found two major clades, one of which was divided into two subclades. The possibility that some of these lineages represented multiple cryptic species in *L. cajetanus* was raised but, eventually, dismissed "because of the unique morphology of *L. cajetanus*". Starting from that paper, in the present study, we collected genetic samples from additional locations, expanding the geographical coverage examined for *Lepidopleurus cajetanus*, in order to test whether increasing the number of samples and adding new collection sites could confirm the pattern already described as suggesting old and stable populations with, however, limited distinguishable geographical structure. Alternatively, by filling in more of the geographic range of this species, new results could help resolve a broader structure of distinctive co-occurring but separate clades.

Materials and methods

Thirteen (13) *Lepidopleurus cajetanus* specimens were sampled from the Atlantic and Mediterranean coasts of Spain, Italy, Croatia and the Canary Islands by two of the authors (BDA and WR) and other collectors (Table 1).

Total genomic DNA was isolated from a small piece of tissue taken from the foot of ethanol-preserved specimens. The extractions were carried out using the Wizard Genomic DNA Purification Kit (Promega). All the DNA extractions were kept at

Table 1. GenBank accession numbers of 16S rRNA and COI partial sequences of the specimens used in the study and reported in the phylogenetic tree.

Species / sample nr	COI	16S rRNA	Collection site (CS)	CS nr	Reference
<i>L. cajetanus</i> s.s.					
1	KF052983	KF052732	Cadaques (Girona, Spain)	2	b
3	KF052981	KF052735	Cadaques (Girona, Spain)	2	b
4	KF052980	KF052737	Cadaques (Girona, Spain)	2	b
5	KF052979	KF052713	Tossa de Mar (Girona, Spain)	3	b
6	KF052978	KF052724	Tossa de Mar (Girona, Spain)	3	b
7	KF052977	KF052715	Tossa de Mar (Girona, Spain)	3	b
8	KF052976	KF052723	Tossa de Mar (Girona, Spain)	3	b
9	KF052975	KF052725	Tossa de Mar (Girona, Spain)	3	b
10	KF052974	KF052729	Tossa de Mar (Girona, Spain)	3	b
12	KF052972	KF052728	Calafat (Tarragona, Spain)	9	b
13	KF052971	KF052711	Calafat (Tarragona, Spain)	9	b
14	KF052970	KF052733	Cabo de Palos (Murcia, Spain)	1	b
15	KF052969	KF052714	Cabo de Palos (Murcia, Spain)	1	b
16	KF052968	KF052731	Mar Menuda, Tossa de Mar (Girona, Spain)	10	b
17	KF052967	KF052738	Mar Menuda, Tossa de Mar (Girona, Spain)	10	b
18	KF052966	KF052730	Mar Menuda, Tossa de Mar (Girona, Spain)	10	b
19	KF052965	KF052734	Mar Menuda, Tossa de Mar (Girona, Spain)	10	b
23	KF052960	KF052727	Mar Menuda, Tossa de Mar (Girona, Spain)	10	b
24	KF052959	KF052726	Mar Menuda, Tossa de Mar (Girona, Spain)	10	b
26	KF052957	KF052721	Cadaques (Girona, Spain)	2	b
27	KF052956	KF052722	Xabia (Alicante, Spain)	5	b
28	KF052954	KF052736	Xabia (Alicante, Spain)	5	b
30	KF052952	KF052712	NA	NA	b
31	KF052951	KF052719	Rhodes (Greece)	7	b
32	KF052950	KF052720	Rhodes (Greece)	7	b
33	KF052948	KF052718	Rhodes (Greece)	7	b
34	KF052947	KF052717	Rhodes (Greece)	7	b
35	KJ500166	KJ500177	Santa Maria Navarrese (Sardinia, Italy)	23	b
36	AF120626	AY377585	NA	NA	a
37	KF052961		Mar Menuda, Tossa de Mar (Girona, Spain)	10	b
38	KF052955		Xabia (Alicante, Spain)	5	b
39	KF052949		Rhodes (Greece)	7	b
40	KF052944		Cabrera (Balearic Islands, Spain)	8	b
41	KF052945		Cabrera (Balearic Islands, Spain)	8	b
42	KF052946		Cabrera (Balearic Islands, Spain)	8	b
44		KF052709	Tossa de Mar (Girona, Spain)	3	b
46		KF052710	Rhodes (Greece)	7	b
47		KF052716	Rhodes (Greece)	7	b
A		MW748076	Torre Ovo (Taranto, Italy)	24	c
B	MW751980	MW748077	Chia, Cagliari (Sardinia, Italy)	23A	c
C		MW748078	Aguilas (Murcia, Spain)	1A	c
D	MW751981		Playa de Las Heras (Tenerife, Canary Is.)	26	c
E		MW748079	Arzachena, Sassari (Sardinia, Italy)	23A	c
F		MW748080	Tertenia, Nuoro (Sardinia, Italy)	23A	c
G	MW751982		Tertenia, Nuoro (Sardinia, Italy)	23A	c
H	MW751983	MW748081	Poetto, Cagliari (Sardinia, Italy)	23A	c
I	MW751984	MW748082	San Lucido (Cosenza, Italy)	24	c
J	MW751985	MW748083	Aguilas (Murcia, Spain)	1A	c
K	MW751986	MW748084	Umago (Croatia)	25	c
L		MW748085	Lussino Is. (Croatia)	25	c
M	MW751987		Vrsar, Orsera (Croatia)	25	c

Species / sample nr	COI	16S rRNA	Collection site (CS)	CS nr	Reference
<i>L. aff. cajetanus</i>					
2	KF052982	KF052702	Cadaques (Girona, Spain)	2	b
11	KF052973	KF052707	Tossa de Mar (Girona, Spain)	3	b
20	KF052964	KF052708	Mar Menuda, Tossa de Mar (Girona, Spain)	10	b
21	KF052963	KF052706	Mar Menuda, Tossa de Mar (Girona, Spain)	10	b
22	KF052962	KF052703	Mar Menuda, Tossa de Mar (Girona, Spain)	10	b
25	KF052958	KF052700	Cadaques (Girona, Spain)	2	b
29	KF052953	KF052705	Xabia (Alicante, Spain)	5	b
43		KF052701	Tossa de Mar (Girona, Spain)	3	b
45		KF052699	Cabo de Palos (Murcia, Spain)	1	b
<i>Rhysoplax olivaceus</i>					
1–16	KJ500158 – KJ500165, KF052941 – KF052942, KF052875 – KF052877, KF052885 – KF052887, KF052889	KJ500168 – KJ500174, KJ500176, KF052739 – KF052740, KF052778, KF052800 – KF052802, KF052791 – KF052792			
<i>Ischnochiton</i> spp.					
	AY377704 – AY377709	AY377593 – AY377596			

Lepidopleurus cajetanus specimens are indicated by numbers (available data) or letters (present study) along with collection sites, collection site numbers and reference: a: Giribet and Wheeler (2002); b: Fernández et al. (2014); c: present study.

4 °C for short-time use. Undiluted or different dilutions (from 1:10 to 1:50, based on the DNA concentration) of each DNA extraction were used as templates for PCR amplification of a portion of each of the two loci: the mitochondrial large subunit ribosomal DNA (mt-16S rRNA) and the cytochrome oxidase subunit I (mt-COI) genes. For the COI gene the primers used were LCO1490 (5'-GGTCAACAAATCATAAA-GATATTGG-3') and HCO2198 (5'-TAAACTTCAGGGTGACCAAAAAATCA-3') (Folmer et al. 1994). PCR conditions involved an initial denaturation step at 95 °C for 5 min; then 35 cycles of denaturation at 95 °C for 1 min, annealing at 42 °C for 1 min and extension at 72 °C for 1 min; followed by a final extension step at 72 °C for 5 min. For the 16S rRNA gene, the primers used were 16sF (5'-CGGCCGCCTGTT-TATCAAAAACAT-3') and 16sR (5'-GGAGCTCCGGTTTGAAGCTCAGATC-3') (Palumbi et al. 1991). The PCR conditions involved an initial denaturation step at 95 °C for 5 min; then 35 cycles of denaturation at 95 °C for 1 min, annealing at 50 °C for 1 min and extension at 72 °C for 1 min; followed by a final extension at 72 °C for 5 min. Amplified products were purified using the Wizard SV Gel and PCR CleanUp System (Promega).

Pinna muricata Linnaeus, 1758 (Bivalvia) and *Haliotis discus* Reeve, 1846 (Gastropoda) were selected as outgroup for molecular analysis following the prior study by Fernández et al. (2014). *Pinna muricata* and *H. discus* 16S rRNA and COI partial sequences (AB076929, GQ166570, AM049335 and AY146392), retrieved from GenBank, were added to homologous sequences of *Lepidopleurus cajetanus* previously studied (Giribet and Wheeler 2002; Fernández et al. 2014) and of *L. cajetanus* examined in the present study for the first time, with a total of 60 *L. cajetanus* ingroup terminals. Sixteen *Rhysoplax olivacea* (Spengler, 1797) and four *Ischnochiton* spp., were also added to the analysis (Table 1). All the sequences for each gene were aligned with BioEdit

ClustalW. The substitution model for each partition was determined via the CIPRES Science Gateway (<http://www.phylo.org/>) (Miller et al. 2010) by the tool jModelTest of XSEDE. MrBayes analysis of multiple sequence alignment (COI+16S rRNA genes, in nexus format) was run on CIPRES by MrBayes on XSEDE, with the parameters for the consensus tree (50% majority rule, excluding 25% of trees as burnin) specified on the MrBayes block. All sequences generated in the present study were deposited in NCBI GenBank (Table 1).

Automatic Barcode Gap Discovery (ABGD) was also used on all available *L. cajetanus* COI sequence data (Puillandre et al. 2012) in order to tentatively delimit potential genetic lineages. Finally, Population Analysis with Reticulate Trees (PopART; Leigh and Bryant 2015) was employed to infer the *L. cajetanus* haplotype networks by the TCS (Templeton, Crandall and Sing) method.

Results and discussion

Results from the ABGD based on the COI fragments recovered two distinct groups, plus a separate group represented by only one specimen (specimen 35, KJ500166). These two main groups correspond exactly to the two major clades of *Lepidopleurus cajetanus* recovered in the combined phylogenetic analysis (Fig. 1). The COI haplotype network reconstruction (Fig. 2) also resulted in two groups that also correspond to those identified by the barcode gap and phylogenetic analysis. By comparison of the outputs obtained from these analyses (ABGD and TCS haplotype networks) and considering the phylogenetic tree topology, it appears that the two groups form well resolved and distinct populations. As far as concerns specimen 35 (from Fernández et al. 2014) it nests within the primary *Lepidopleurus cajetanus* clade but is quite different from the others. The phylogenetic reconstruction for *L. cajetanus* shows a deep split, with two major clades supported by high (100%) posterior probability values. One of the clades is composed of individuals drawn from all the sampled populations, which we refer to as *Lepidopleurus cajetanus* s.s. The other clade, which we refer to as *Lepidopleurus* aff. *cajetanus* is formed by specimens from the eastern Iberian Peninsula (i.e., various localities of Girona, Alicante and Murcia including Cadaqués, Tossa del Mar, Xabia and Cabo de Palos), thus suggesting the presence of two genetically divergent lineages on the eastern Spanish coast. Fernández et al. (2014) sampled three specimens from the Balearic Islands (COI marker only, GenBank accession numbers KF052944–KF052946) which are part of the broader *Lepidopleurus cajetanus* s.s. lineage. Since both clades co-occur on the eastern Spanish mainland coast, hypothetically, we cannot exclude the possibility that *L. aff. cajetanus* may be present also in the Balearic Islands.

Comparing these two clades nominally comprising *Lepidopleurus cajetanus*, it appears that the *L. aff. cajetanus* clade has a much more limited genetic variability compared to the larger, more broadly distributed clade. The pairwise distances of COI fragments for the larger clade had a maximum separation of 8.3% (or up to 20% including specimen 35) and an average distance of 3.6%; the maximum distance

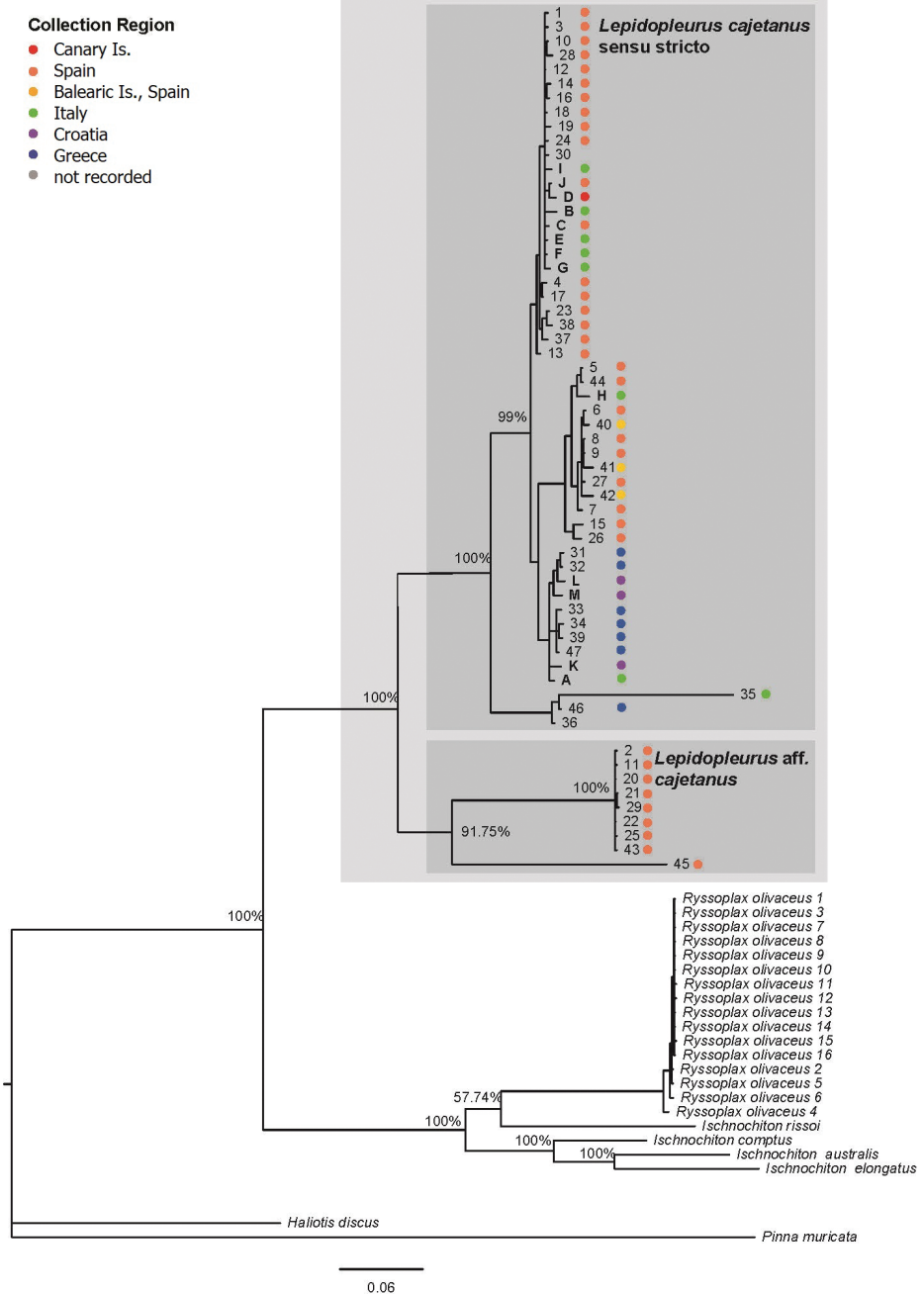


Figure 1. Bayesian phylogenetic tree obtained with MrBayes on the basis of a multiple sequence alignment (COI+16S rRNA genes) analysis. Nodal supports are Bayesian inference posterior probability (expressed in percentage). Scale bar represents units of length in expected substitutions per site. *Lepidopleurus cajetanus* specimens previously analysed (Giribet and Wheeler 2002; Fernández et al. 2014) are indicated by numbers, *L. cajetanus* specimens added in the present study are indicated by letters in bold. Colours correspond to the geographic distribution (see also Table 1).

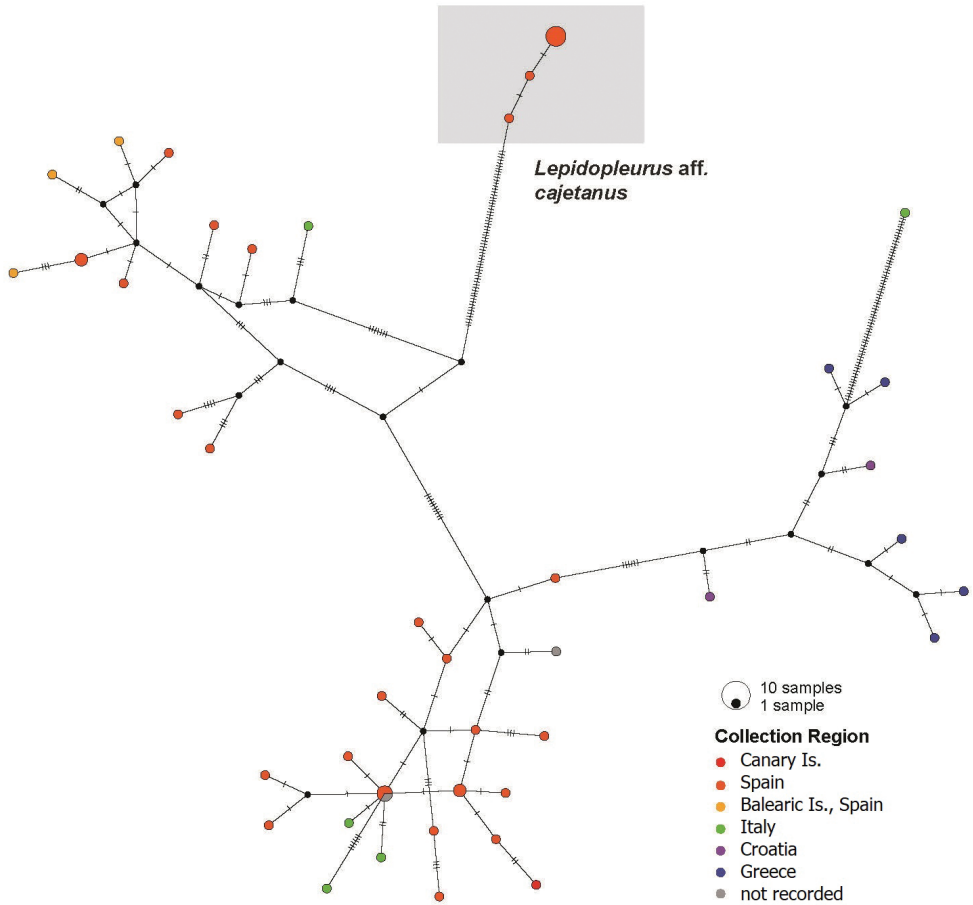


Figure 2. COI haplotype (TCS) network showing the relationships of *L. cajetanus* specimens. Circle size is proportional to the observed haplotype frequencies. Colours correspond to the geographic distribution as in Fig. 1 (see also Table 1).

between members of the *L. aff. cajetanus* clade was 0.49% with an average of 0.22%. This is reflected in the smaller distances and smaller number of haplotypes among the *L. aff. cajetanus* clade specimens (Fig. 2). It may be an artefact of comparative sample numbers for the COI fragment, with only seven specimens of the *L. aff. cajetanus* clade compared to 43 from *Lepidopleurus cajetanus* s.s., but the observed differences might indicate biological separation of the two lineages. The two clades are separated by a mean distance of 17.8%, which is similar to the value of 15.7% used as part of the description to separate *Leptochiton cascadiensis* from *Leptochiton rugatus* (Sigwart and Chen 2018).

Our results confirm that the population genetic structure of *Lepidopleurus cajetanus* based on the COI barcode marker is characterized by a high number of private haplotypes, and high genetic divergence between haplotypes and between clades, extending the

pattern first identified by Fernández et al. (2014). However, with the addition of a broader geographical sampling, it seems that the “chaotic patchiness” nonetheless divides into two discrete clades, and further to some larger biogeographic patterns. The combined phylogenetic reconstruction shows one clade of specimens from Greece and Croatia, and two groupings of specimens from Italy and Spain, within the *Lepidopleurus cajetanus* s.s. clade. We suspect that the *Lepidopleurus cajetanus* s.s. clade and the *L. aff. cajetanus* clade might represent two distinct lineages, where *Lepidopleurus cajetanus* s.s. contains substantially more genetic diversity, at least in the COI marker, and the *L. aff. cajetanus* clade is more constrained. Whether *L. aff. cajetanus* could be interpreted as a possible (cryptic?) species is impossible to say, as genetic data alone are not sufficient to draw any definitive conclusions. In fact, further morphological examination of Spanish specimens is certainly required to re-examine potential diagnostic characters, and to obtain additional independent sources of comparative data. Unfortunately, all of the sequence data corresponding to the *L. aff. cajetanus* clade came from prior work; we have not examined specimens known to be from the *L. aff. cajetanus* clade in the present work. In fact, new materials that we sequenced from Aguilas, Murcia, Spain, are also part of the *Lepidopleurus cajetanus* s.s. clade.

The fossil valves of *Lepidopleurus cajetanus* sensu lato show remarkable variations, e.g. in the sculpture of the lateral areas of the intermediate valves (with the starting point of the concentric ribs neighbouring the lateral margin and not near the apex, as in normal valves, and consequently with a different frontal view; compare Dell’Angelo et al. 2013: pl. 1 figs B-C and D-E), in the position of the mucro in the tail valves [almost central in juvenile specimens but moves posterior (even to the end of the valve) as individuals grew older, as well described and illustrated by Laghi (1977: fig. 3a-b) and Dell’Angelo et al. (2013: pl. 1, figs F-G)], and in the sculpture of the central area of the intermediate valves and the antemucronal area of the tail valve [normally with longitudinal and parallel chains of granules, somewhat branching or anastomosing, very irregular, transversally intersected by thinner cords that give a pitted appearance (see Dell’Angelo et al. 2015: pl. 1, figs 4–11)]. Future studies of material of living *Lepidopleurus cajetanus* s.l. from the eastern Spanish mainland coast (and Balearic Is.) should focus on these shell characteristics, to determine whether the two lineages can be diagnosed morphologically, and also how they compare to the extensive fossil record.

It is now well known that standard barcode markers such as COI show some variability within and among species (e.g., Sigwart and Garbett 2018), and it is not appropriate to use an a priori distance cut-off to distinguish species. Taking into account the limitations of the current study (reliance of mt-DNA only) and that species status is best assessed in light of an integrative, total evidence approach, caution is required in interpreting the *L. aff. cajetanus* clade until a morphological diagnosis is available. However, our results seem to suggest the presence of (at least) two genetic lineages within *L. cajetanus* that will need to be adequately investigated in future studies including also additional (nuclear) markers and/or anatomy to arrive at systematically more robust conclusions. Importantly, this is a species (or species complex) with a very good fossil record and representing greater disparity than the living lineages (Dell’Angelo et al. 2013, 2015, 2018a, 2018b). Although

Lepidopleurus cajetanus s.s. has apparently high variability in these mitochondrial markers, we are cautious about making any inferences about phylogeographic patterns or potential for cryptic species or incipient speciation. These issues do require integrated evidence from the morphology of living and fossil populations, nonetheless this study indicates a novel genetic pattern in a common and phylogenetically important species.

Acknowledgements

Special thanks are due to Diego Viola (Muggia, Italy), Michele Pisanu (Quartu S. Elena, Italy), Iván Mulero Méndez and Brian Cunningham Aparicio (Murcia, Spain) for the valuable material collected.

This work was supported by MIUR (PRIN 2009, prot. 2009LFSNAN_003) funds to A. Gregorini. Moreover, A. Gregorini wishes to thank the Ilaria Giacomini Association (Cantiano, PU, Italy) for financial support.

The authors are grateful to the referees for careful reading of the paper and valuable suggestions and comments that improved the manuscript.

References

- Aldea C, Novoa L, Alcaino S, Rosenfeld S (2020) Diversity of benthic marine mollusks of the Strait of Magellan, Chile (Polyplacophora, Gastropoda, Bivalvia): A historical review of natural history. *ZooKeys* 963: 1–36. <https://doi.org/10.3897/zookeys.963.52234>
- Ayre DJ, Minchinton TE, Perrin C (2009) Does life history predict past and current connectivity for rocky intertidal invertebrates across a marine biogeographic barrier? *Molecular Ecology* 18(9): 1887–1903. <https://doi.org/10.1111/j.1365-294X.2009.04127.x>
- Castellanos ZA (1988) Catálogo Descriptivo de la Malacofauna Marina Magallánica 1. Placóforos. Comisión de Investigaciones Científicas, Buenos Aires, 41 pp.
- Dell'Angelo B, Smriglio C (2001) Book – Living Chitons of the Mediterranean Edizioni Evolver, Rome, 256 pp.
- Dell'Angelo B, Sosso M, Prudenza M, Bonfitto A (2013) Notes on Fossil Chitons. 5. Polyplacophora from the Pliocene of Western Liguria, Northwest Italy. *Rivista Italiana di Paleontologia e Stratigrafia* 119: 65–107.
- Dell'Angelo B, Giuntelli P, Sosso M, Zunino M (2015) Polyplacophora from the Miocene of North Italy. Part 1: Leptochitonidae, Hanleyidae, Ischnochitonidae and Callistoplacidae. *Rivista Italiana di Paleontologia e Stratigrafia* 121: 217–242.
- Dell'Angelo B, Landau B, Van Dingenen F, Ceulemans L (2018a) The upper Miocene chitons of northwest France (Mollusca: Polyplacophora). *Zootaxa* 4447: 1–62. <https://doi.org/10.11646/zootaxa.4447.1.1>
- Dell'Angelo B, Lesport JF, Cluzaud A, Sosso M (2018b) The Oligocene to Miocene chitons (Mollusca: Polyplacophora) of the Aquitaine Basin, southwestern France, and Ligerian Basin, western France. Part 1: Leptochitonidae, Hanleyidae, Ischnochitonidae,

- Chitonidae, Spinochitonidae fam. nov. and Schizochitonidae. *Bollettino Malacologico* 54: 1–47.
- Doonan J, Beatty GE, Sigwart JD, Provan J (2012) Extensive local-scale gene flow and long-term population stability in the intertidal mollusc *Katharina tunicata* (Mollusca: Polyplacophora). *Biological Journal of the Linnean Society* 106(3): 589–597. <https://doi.org/10.1111/j.1095-8312.2012.01892.x>
- Fernández R, Lemer S, McIntyre E, Giribet G (2014) Comparative phylogeography and population genetic structure of three widespread mollusc species in the Mediterranean and near Atlantic. *Marine Ecology* 36 (2015): 701–715. <https://doi.org/10.1111/maec.12178>.
- Folmer O, Black M, Hoeh W, Lutz R, Vrijenhoek R (1994) DNA primers for amplification of mitochondrial cytochrome c oxidase subunit I from diverse metazoan invertebrates. *Molecular Marine Biology and Biotechnology* 3: 294–299. [PMID: 7881515]
- Forcelli DO (2000). *Moluscos Magallánicos. Guía de los Moluscos de la Patagonia y del Sur de Chile*. Buenos Aires, Vazquez Mazzini Editores, 200 pp.
- Giribet G, Wheeler W (2002) On bivalve phylogeny: a high-level analysis of the Bivalvia (Mollusca) based on combined morphology and DNA sequence data. *Invertebrate Biology* 121(4): 271–324. <https://doi.org/10.1111/j.1744-7410.2002.tb00132.x>
- Gray JE (1847) Additional observations on Chitons. *Proceedings of the Zoological Society of London* 15: 126–127.
- Kaas P, Van Belle RA (1985) *Monograph of Living Chitones (Mollusca: Polyplacophora)*. Vol. 1. Order Neoloricata: Lepidopleurina. In: Brill EJ, Backuys W (Eds) Leiden, 240 pp.
- Laghi GF (1977) Polyplacophora (Mollusca) neogenici dell'Appennino settentrionale. *Bollettino della Società Paleontologica Italiana* 16: 87–115. [pls 1–4]
- Leigh JW, Bryant D (2015) PopART: Full-feature software for haplotype network construction. *Methods in Ecology and Evolution* 6(9): 1110–1116. <https://doi.org/10.1111/2041-210X.12410>
- Miller MA, Pfeiffer W, Schwartz T (2010) Creating the CIPRES Science Gateway for inference of large phylogenetic trees. In: *Proceedings of the Gateway Computing Environments Workshop (GCE)*, 14 Nov. 2010, New Orleans, LA, 1–8. <https://doi.org/10.1109/GCE.2010.5676129>
- Palumbi S, Martin A, Romano S, McMillan W, Stine O, Grabowski G (1991) *The simple fool's guide to PCR*. Ver. 2. University of Hawaii, Honolulu.
- Pilsbry HA (1892–1894) *Monograph of Polyplacophora*. In: Tryon GW (Ed.) *Manual of Conchology*. Academy of Natural Sciences, Philadelphia, 14: 1–128, pls 1–30 (1892); i–xxxiv, 129–350, pls 31–68 (1893); 15: 1–64, pls 1–10 (1893); 65–133, pls 11–17 (1894).
- Ponder W, Lindberg DJ, Ponder J (2020) *Biology and Evolution of the Mollusca, Volume 1*. CRC Press, Boca Raton, 924 pp. <https://doi.org/10.1201/9781351115667>
- Puillandre N, Lambert A, Brouillet S, Achaz G (2012) ABGD, Automatic Barcode Gap Discovery for primary species delimitation. *Molecular Ecology* 21(8): 1864–1877. <https://doi.org/10.1111/j.1365-294X.2011.05239.x>
- Schwabe E (2009). Polyplacophora - chitons. In: Häussermann V, Försterra G (Eds) *Marine benthic Fauna of Chilean Patagonia. An illustrated identification guide*. Puerto Montt, Chile: Nature in Focus. 1st edn., 1000 pp. [pp. 389–424]

- Schwabe E, Sellanes J (2010) Revision of Chilean bathyal chitons Mollusca: Polyplacophora associated with cold-seeps, including description of a new species of *Leptochiton* (Lep-tochitonidae). *Organisms, Diversity & Evolution* 10(1): 31–55. <https://doi.org/10.1007/s13127-009-0002-6>
- Sigwart JD, Chen C (2018) Life history, patchy distribution, and patchy taxonomy in a shallow- water invertebrate (Mollusca: Polyplacophora: Lepidopleurida). *Marine Biodiversity* 48(4): 1867–1877. <https://doi.org/10.1007/s12526-017-0688-1>
- Sigwart JD, Garbett A (2018) Biodiversity assessment, DNA barcoding, and the minority majority. *Integrative and Comparative Biology* 58(6): 1146–1156. <https://doi.org/10.1093/icb/icy076>
- Sigwart JD, Schwabe E, Saito H, Samadi S, Giribet G (2011) Evolution in the deep sea: a combined analysis of the earliest diverging living chitons (Mollusca: Polyplacophora: Lepidopleurida). *Invertebrate Systematics* 24(6): 560–572. <https://doi.org/10.1071/IS10028>
- Sirenko BI (2006) Report on present state of our knowledge with regard to the chitons of the Magellan Strait and Falkland Islands. *Venus (Tokyo)* 65: 81–89. https://doi.org/10.18941/venus.65.1-2_81
- Sirenko BI (2015) Shallow and deep-sea chitons of the genus *Leptochiton* Gray, 1847 (Mollusca: Polyplacophora: Lepidopleurida) from Peruvian and Chilean waters. *Zootaxa* 4033(2): 151–202. <https://doi.org/10.11646/zootaxa.4033.2.1>
- Sirenko BI, Sellanes J (2016) Update of the genus *Leptochiton* (Mollusca: Polyplacophora) in Chilean deep waters: three new reports and description of two new species. *Zootaxa* 4173(3): 259–279. <https://doi.org/10.11646/zootaxa.4173.3.5>

Two new *Drawida* (Oligochaeta, Moniligastridae) earthworms from Vietnam

Tung T. Nguyen¹, Dang H. Lam¹, Binh T.T. Tran², Anh D. Nguyen^{3,4}

1 Department of Biology, School of Education, Can Tho University, Can Tho City, Vietnam **2** Faculty of Biology, Hanoi University of Education, Xuan Thuy Str., Cau Giay, Hanoi, Vietnam **3** Department of Soil Ecology, Institute of Ecology and Biological Resources, Vietnam Academy of Science and Technology, 18, Hoangquocviet, Cau Giay, Hanoi, Vietnam **4** Graduate University of Science and Technology, Vietnam Academy of Science and Technology, 18, Hoangquocviet, Cau Giay, Hanoi, Vietnam

Corresponding author: Anh D. Nguyen (ducanh410@yahoo.com)

Academic editor: Samuel James | Received 25 July 2021 | Accepted 19 April 2022 | Published 3 May 2022

<http://zoobank.org/7326D563-3CD1-45DB-96DC-3AB5CAB640A1>

Citation: Nguyen TT, Lam DH, Tran BTT, Nguyen AD (2022) Two new *Drawida* (Oligochaeta, Moniligastridae) earthworms from Vietnam. ZooKeys 1099: 41–56. <https://doi.org/10.3897/zookeys.1099.72112>

Abstract

Two new earthworm species are described, namely *Drawida angiang* **sp. nov.** and *Drawida cochinchina* **sp. nov.** The former can be recognized by having male pores on spiniform penises in intersegment 10/11, an erect and sac-shaped spermathecal atrium, glandular prostate, the capsule coiled one round, the vas deferens strongly coiled but small, two large, round, genital markings on segments ix–x, and three gizzards in xiii–xv. The latter species is distinguished in having the male pores placed on highly elevated, backwardly directed, conical penises in 10/11, a slender spermathecal atrium, a glandular prostate, a somewhat folded capsule, the vas deferens strongly coiled as a bunch and equal size to the testis sacs, a pair of genital markings located closely anterior to the penises with 1–3 additional ones in xi–xii, and three or four gizzards in xiii–xvi. The DNA barcode fragment of the COI gene was extracted for each species, and the COI genetic distances and phylogenetic analysis also supported two new species..

Keywords

Biodiversity, bio-investigation, COI, new species, taxonomy

Introduction

To date, the earthworms of Vietnam are well known with 245 species and subspecies described (Nguyen TT et al. 2016a, 2016b, 2018; Nguyen QN et al. 2020; Lam et al. 2021), of which 232 belong to the species-rich family Megascolecidae; the family Moniligastridae has been reported with only five species, although Vietnam is located in the region of origin of this family (Sims and Easton 1972). Five *Drawida* Michaelsen, 1900 species are *Drawida annamensis* Michaelsen, 1934, *D. beddardi* (Rosa, 1890), *D. delicata* Gates, 1962, *D. chapaensis* Do & Huynh, 1993, and *D. langsonensis* Do, 1993 in Do & Huynh, 1993. Three species are only known from Vietnam: *D. annamensis*, *D. chapaensis*, and *D. langsonensis* (Nguyen TT et al. 2016b).

Most recent research on earthworms in Vietnam focuses mainly on the family Megascolecidae, especially the pheretimoid group. There are no works on the family Moniligastridae or the genus *Drawida* in Vietnam. This work, therefore, aims to contribute to a better knowledge of the genus *Drawida* through descriptions of two new species.

Materials and methods

Specimen collecting and preservation

Earthworms were manually searched for and collected in Vietnam for a decade during the rainy season, September to November, in 2010–2020. After collection, specimens were cleaned with tap water, killed in 2% formalin, temporarily fixed in 4% formalin for 12 hours, then transferred to fresh 4% formalin for long-term preservation. Specimens for molecular study were preserved in 95% ethanol. Specimens including holotypes and paratypes were deposited in Laboratory of Zoology, Department of Biology, Can Tho University (CTU). Some were shared with the Department of Soil Ecology, Institute of Ecology and Biological Resources (IEBR), Hanoi, Vietnam.

Morphological examination

Material was examined under a Motic Digital microscope (model: DM143-FBGG-C) and dissected from the dorsal side for internal observations. Transverse body sections were processed using the classical method of Hematoxylin & Eosin. Selected segments were cleaned and dehydrated using graded ethanol concentrations. Segments were imbedded with paraffin, then cut using a microtome Sakura Accu SRM 200CW. The cut sections were stained using Hematoxylin & Eosin Y (Feldman and Wolfe 2014) and transferred onto glass slides and mounted.

Color images were taken using a camera attached directly to the microscope. Line drawings and color images were improved and grouped into plates using Photoshop CS6.

DNA extractions, PCR, and sequencing

Total genomic DNA was extracted from several body segments using a DNeasy Blood & Tissue Kit (Qiagen TM). A fragment of the mitochondrial gene, cytochrome c oxidase subunit I (COI), was amplified using polymerase chain reaction (PCR). Universal primers LCO-1490 and HCO-2198 (Folmer et al. 1994) were used to amplify a 680 bp fragment of the COI region. PCR conditions for amplification of the COI gene were as follows: an initial denaturation at 95 °C for 2 minutes followed by 36 cycles of 95 °C for 20 seconds, 42 °C for 45 seconds, and 72 °C for 1 minute, and a final extension at 72° for 5 minutes. Successfully amplified samples were sent for purifying and sequencing at the FirstBase Company (Malaysia). The same primers for the initial PCR were also used as sequencing primers.

Each sequence chromatogram was manually checked using BioEdit v.7.1 (Hall 1999), and the identity confirmed by a BLAST search (Zhang et al. 2000). All confirmed sequences were aligned using multiple sequence alignment with the program ClustalX v. 2.0 (Larkin et al. 2007).

After trimming, the final COI dataset consists of 580 bp from 47 samples of 19 species including the outgroup, *Pontoscolex corethrurus* (Table 1). The nucleotide frequencies of A, T, G, and C were 25.6%, 34.2%, 18.4%, and 21.8%, respectively. The GC content was 41.5%. The dataset contained 242 (41.7%) parsimony informative and 252 (43.4%) variable sites.

The K2P (Kimura 2 parameters) genetic distance was calculated in MEGA 7.0 (Kumar et al. 2016). The phylogenetic tree was reconstructed using a maximum-likelihood analysis with the best model chosen using ModelFinder (Kalyaanamoorthy et al. 2017) performed in IQTREE v.1.6.2 for Windows (Nguyen LT et al. 2015). The best model was GTR + F + I + G4 with BIC score = 12628.239 and $-\ln L = 6005.512$.

Abbreviations

ag	accessory gland;	gm	genital markings;	prg	prostate gland;
amp	ampulla;	mp	male pore;	sp	spermathecal pore;
atr	atrium;	os	ovi sac;	ts	testis sac;
cl	clitellum;	pc	penial chamber;	vd	vas deferens.
CTU	Can Tho University;	pn	penis;		

Results

Molecular analysis

The genetic distance between new species and other *Drawida* ranges from 21.5% (*D. cochinchina* and *D. japonica*) to 29.3% (*D. angiang* and *D. scandens*).

Table 1. Species vouchers and GenBank accession numbers of species used for analyses.

Species	Locality / species voucher	Accession number	Source
<i>Drawida angiang</i> sp. nov.	Vietnam/CTU-EW.181.018EW	ON303834	
<i>Drawida cochinchina</i> sp. nov.	Vietnam/ CTU-EW.032.019EW	ON303833	
<i>Drawida cochinchina</i> sp. nov.	Vietnam/ CTU-EW.032.19a	ON303831	
<i>Drawida cochinchina</i> sp. nov.	Vietnam/ CTU-EW.032.19b	ON303832	This study
<i>Drawida nepalensis</i> Michaelsen, 1907	Vietnam/ CTU-EW.031.06	ON303830	
<i>Drawida nepalensis</i> Michaelsen, 1907	Vietnam/ CTU-EW.031.07	ON303828	
<i>Drawida nepalensis</i> Michaelsen, 1907	Vietnam/ CTU-EW.031.08	ON303829	
<i>Drawida nepalensis</i> Michaelsen, 1907		MT472588	
<i>Drawida nepalensis</i> Michaelsen, 1907		MT570063	
<i>Drawida nepalensis</i> Michaelsen, 1907		MT570064	
<i>Drawida nepalensis</i> Michaelsen, 1907		MH845467	
<i>Drawida japonica</i> Michaelsen, 1892		EF077597	Huang et al. (2007)
<i>Drawida hattamimizu</i> Hatai, 1930		AB543219	
<i>Drawida hattamimizu</i> Hatai, 1930		AB543220	
<i>Drawida hattamimizu</i> Hatai, 1930		AB543224	
<i>Drawida ghatensis</i> Michaelsen, 1910	India/ IEW386-17		
<i>Drawida ghatensis</i> Michaelsen, 1910	India/ IEW432-17		
<i>Drawida ghatensis</i> Michaelsen, 1910	India/ IEW433-17		
<i>Drawida ghatensis</i> Michaelsen, 1910	India/ IEW434-17		
<i>Drawida ghatensis</i> Michaelsen, 1910	India/ IEW435-17		
<i>Drawida ghatensis</i> Michaelsen, 1910	India/ IEW436-17		
<i>Drawida brunnea</i> Stephenson, 1915	India/ IEW388-17		
<i>Drawida impertusa</i> Stephenson, 1920	India/ IEW391-17		
<i>Drawida impertusa</i> Stephenson, 1920	India/ IEW393-17		
<i>Drawida impertusa</i> Stephenson, 1920	India/ IEW447-17		Thakur et al. (2021)
<i>Drawida impertusa</i> Stephenson, 1920	India/ IEW448-17		
<i>Drawida impertusa</i> Stephenson, 1920	India/ IEW424-17		
<i>Drawida circumpapillata</i> Aiyer, 1929	India/ IEW420-17		
<i>Drawida travancorensis</i> Michaelsen, 1910	India/ IEW425-17		
<i>Drawida robusta</i> (Bourne, 1887)	India/ IEW444-17		
<i>Drawida robusta</i> (Bourne, 1887)	India/ IEW445-17		
<i>Drawida scandens</i> Rao, 1921	India/ IEW451-17		
<i>Drawida nilamburensis</i> (Bourne, 1887)	India/ IEW459-17		
<i>Drawida gracilis</i> Gates, 1925		JN793516	
<i>Drawida gracilis</i> Gates, 1925		JN887887	
<i>Drawida bullata</i> Gates, 1933		JN793527	
<i>Drawida bullata</i> Gates, 1933		JN887894	
<i>Drawida gisti gisti</i> Michaelsen, 1931		JQ405262	
<i>Drawida ghilarovi</i> Gates, 1969		KY711477	
<i>Drawida ghilarovi</i> Gates, 1969		KY711499	Ganin and Atopkin (2018)
<i>Drawida ghilarovi</i> Gates, 1969		KY711501	
<i>Drawida ghilarovi</i> Gates, 1969		KY711517	
<i>Drawida koreana</i> Kobayashi 1936		KR047039	Shen et al. (2015)
<i>Drawida koreana</i> Kobayashi 1936		MH845538	
<i>Drawida koreana</i> Kobayashi 1936		MH882566	Yuan et al. (2019)
<i>Drawida koreana</i> Kobayashi 1936		MH882855	
<i>Pontosclex corethrusus</i> (Müller, 1856)		JN260736	

The interspecific divergence among *Drawida* species ranges from 16.3% (*D. impertusa* and *D. robusta*) to 31.1% (*D. nilamburensis* and *D. japonica*). The average interspecific distance in the genus *Drawida* was previously reported as 22%, and the maximum one was 34.3% between *D. impertusa* and *D. deshayesi* (Thakur et al. 2021). The *p*-genetic distance was also known to range from 18% between *D. koreana* and *D. japonica japonica* to 24.82% between *D. koreana* and *D. gracilis* (Zhang et al. 2020).

In the maximum-likelihood tree (Fig. 1), *Drawida angiang* sp. nov. is closely related to both East Asian species, *D. japonica* and *D. koreana*. The relationship is moderately supported with a bootstrap value of 72%. On the contrary, *D. cochinchina* sp. nov. is clustered as a

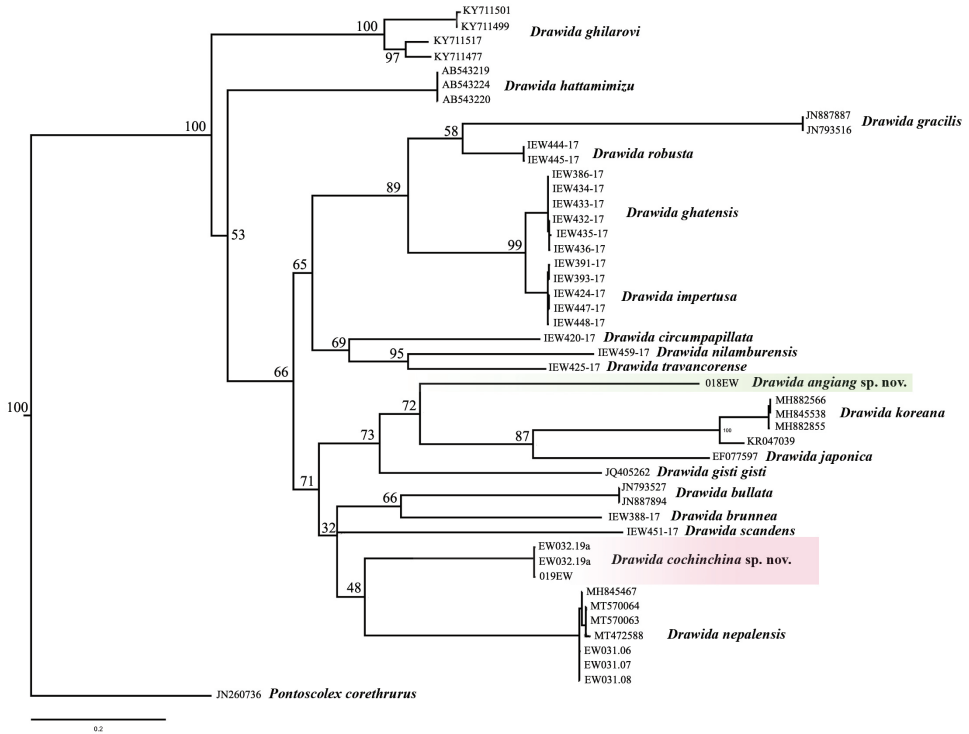


Figure 1. Phylogenetic diagram inferred from 580 bp COI dataset using maximum likelihood analysis. Numbers at node show the bootstrap values.

sister species to the South Asian *D. nepalensis*, but the relationship is poorly supported by bootstrap and Bayesian values (48%). In other words, two species, *D. cochinchina* and *D. nepalensis* are distantly related; there must be intermediate species, which are still unknown and need to be discovered. The presence of *D. cochinchina* in Vietnam also indicates that the genus has a long presence in Asia, with some dispersal within Asia.

Taxonomic part

Family Moniligastridae Claus, 1880

Genus *Drawida* Michaelsen, 1900

Drawida Michaelsen, 1900: 114; Stephenson 1930: 814; Gates 1972: 244.

Type species. *Moniligaster barwelli* Beddard, 1886.

Distribution. India, Myanmar, Malay Peninsula, Thailand, Cambodia, Laos, Vietnam, China, Korea, Japan, Philippines, Malaysia, Indonesia, Borneo, Sumatra, Java, Sri Lanka, Taiwan, Far East of Russia, Caribbean, Australia, and various Pacific islands (Gates 1972; Blakemore 2002; Chang et al. 2009; Zhang et al. 2020).

***Drawida angiang* sp. nov.**

<http://zoobank.org/CBBB4135-C65E-459C-A874-93CF63728135>

Fig. 2

Drawida sp. 1. — Nguyen TT 2013: 100; 2014: 113.

Material examined. Holotype. VIETNAM • clitellate; An Giang Province, Tinh Bien District, Nhon Mountain; 10.5882°N, 104.9506°E; 56 m a.s.l.; 07 Nov. 2010; Nguyen Thanh Tung leg.; natural forest; CTU-EW.181.h01.

Paratypes. VIETNAM • 2 clitellates, 12 acitellates; An Giang Province, Tinh Bien District, Nhon Mountain; 10.5882°N, 104.9506°E; 56 m a.s.l.; 07 Nov. 2010, coll. Nguyen Thanh Tung leg.; natural forest; CTU-EW.181.p02.

Other material. VIETNAM • 8 juveniles; An Giang Province, Tinh Bien District, Tinh Bien town; 10.5895°N, 104.9501°E; 24 m a.s.l.; 19 Oct. 2020; Nguyen Thanh Tung leg.; near a pond inside a *Citrus grandis* garden; CTU-EW.181.03.

Diagnosis. Body cylindrical, small-medium size, length 72–116 mm, diameter 3.6–4.0 mm, 170–221 segments. Setal formula aa: ab: bc: cd: dd = 6.5–7.0: 1: 6.5–7.0: 1: 35–37. No dorsal pores. Clitellum within ix–xiv. Male pores located on tip of spiniform penis in 10/11. Spermathecal pores located median to c. Genital markings, present, two, circular, on ix and x. Spermathecal atrium erect in vii, sac-like. Testis sacs in 10, much larger than the coils of vas deferens. Prostate glandular, glandularity reduced; prostatic capsule cylindrical, somewhat folded. Gizzards 3, in xiii–xv.

Description. External: body cylindrical, gradually tapering towards tail, small-medium-sized, length 72–116 mm, diameter 3.6–4.0 mm, 170–221 segments (holotype: length 80 mm, diameter 3.9 mm, 199 segments).

Coloration: body general darkish grey on both dorsum and ventrum, but greener toward telson. Setae lumbricine, with eight setae more concentrated on ventrum; setal formula: aa: ab: bc: cd: dd = 6.5–7.0: 1: 6.5–7.0: 1: 35–37. Prostomium prolobous. Dorsal pores absent. Clitellum annular, within ix–xiv, reddish brown. Spermathecal pores located in intersegmental furrow 7/8, median to c. Female pore hardly visible, paired in intersegment 11/12. Male pores located in intersegment 10/11, between setae b and c, somewhat spiniform penis exposed or not. Genital marking present, two, large circular markings, highly elevated from body surface, located on setal line b on segment ix and medio-ventral segment x, respectively. Nephridiopores anterior margin of segments iv onwards, in d lines, especially clear from vi to xii.

Internal: no pigmentation. Septa 4/5/6/7/8/9/10 thick, 10/11 thin. Gizzards 3, in xiii–xv. Nephridia holoic, from segment iv onwards. Intestinal origin at xvii; intestinal caeca absent. Last hearts in ix. Typhlosole absent. Spermathecae paired in viii, spermathecal ampulla oval, without diverticulum; spermathecal ducts strongly twisted and coiled, going through the septum 7/8 and joinomg atrium in vii subventrally; spermathecal atrium erect, sac-like. No accessory glands in spermathecal region. Prostate glandular, glandularity strongly reduced; prostatic capsule cylindrical, somewhat folded.

Testis sacs, paired, large, located on posterior side of septum 9/10, much larger than coils of vas deferens; vas deferens twisted and strongly coiled, ending at ental ends of prostate capsule which basally connect to penial pouch. Ovaries on septum 10/11; ovisacs sac-shaped in xiii and xiv. Accessory glands in ix and x in correspondence with genital markings outside.

DNA characters. The COI fragment was uploaded to GenBank with an accession number ON303834. The new species has a close COI identity of 81.5% with *D. koreana* (KR047039)

Distribution. The species was previously recorded from Kien Giang Province (Da Dung Mountain), An Giang Province (Ba Doi Mountain, Cam Mountain, Nhon Mountain, Phu Tan, Cho Moi), Vinh Long Province (Vung Liem), Dong Thap Province (Lai Vung, Long Thuan Island, Tan Long Island), Can Tho, Hau Giang (Phung Hiep) (Nguyen T.T. 2014 as *Dr. sp. 1*).

Etymology. A noun in apposition, *angiang*, is used to emphasize the province where type specimens were collected.

Remarks. The species is very similar to *D. angchiniana* Chen, 1933 from northern China (Anhui and Kiangsu) and South Korea (Jeju Island) (Michaelsen 1931; Chen 1933; Kobayashi 1937) by the presence of genital markings in the male region and

Table 2. Character comparison between *Drawida angiang* sp. nov., *D. cochinchina* sp. nov., *D. longatria* Gates, 1925, *D. ofunatoensis* (Ohfuchi, 1938), and *D. angchiniana* Chen, 1933.

Species	<i>D. angiang</i>	<i>D. cochinchina</i>	<i>D. longatria</i> ¹	<i>D. ofunatoensis</i> ²	<i>D. angchiniana</i> ³	<i>D. nepalensis</i> ⁴	<i>D. koreana</i> ⁵	<i>D. japonica</i> ⁶
Length (mm)	72–116	84–123	153	228–283	62–80	129–180	63–100	28
Diameter (mm)	3.6–4.0	3.3–4.9	6	≤6.5	3–5	4–5	3–4	3
Segments	170–221	101–294	208	189–242	134–145	78–130	80–90	95
Clitellum	ix–xiv	ix–xiv	x–xiii	x–xiii	x–xiii	ix–xiv	x–xiii	ix–xiii or xiv
Genital markings in	two, in ix and x	many, vary in viii, 10/11, x–xiii	paired, viii, 10/11, xii	many, vary in vii–xii	two, in x and xi	paired, vii, x, 10/11, xi	unpaired, vii–x	unpaired, vii–xiii
Gizzards	3, within xiii–xv	3 or 4 within xiii–xvi	4 within xv–xviii	4 within xii–xvii	3, sometimes 2	2–4, within xii–xx	2 or 3, xii–xiv	2, xii and xiii
Spermathecal pores	in c-line	median to c	in c-line or median to c	median to c	median to c	median to c	in c-line or median to c	In c-line or median to c
Spermathecal atrium	vii	vii	viii	absent	vii	vii	vii,	Vii
Shape of Spermathecal atrium	erect, sac-like	slender and strongly coiled as a bunch	Slender and strongly coiled as a bunch	n/a	short, cylindrical	song, sac-like	short, sac-like	small
Testis sacs	9/10	10/11	9/10	10/11	10/11	n/a	9/10	9/10
Vas deferens	strongly coiled as a bunch	strongly coiled as a bunch	strongly coiled as a bunch	coiled and twisted, but not a bunch	coiled and twisted, but not a bunch	strongly coiled as a bunch	Loosely twisted, small	coiled and twisted, but not a bunch
Prostate	glandular, but strongly reduced; cylindrical, somewhat folded	glandular, but strongly reduced; cylindrical, somewhat folded	glandular?; coiled or curve, digitiform	glandular?; roundish-shaped	muscular; cylindrical, slender	glandular, club-shaped, slender	glandular?; thumb-shaped	glandular; club-shaped and erect
Ovisacs	xii–xiii	xii–xv, sometimes xviii	n/a	xii	from xii	n/a	xii–xviii, seldom xxii or xxiii	xii–xvi
Accessory glands	ix and x	not visible	present	present	present	present	present	present

Data extracted from: ¹ Gates (1925), ² Blakemore et al. (2014), ³ Chen (1933), ⁴ Kobayashi (1938), ⁵ Michaelsen (1892), and Blakemore and Kupriyanova (2010)

absence in the spermathecal region. However, the two species can be distinguished by the location of genital markings (ix and x vs x and xi), number of segments (170–221 vs 134–145), location of clitellum (x–xiv vs ix–xiv), and shape of the spermathecal atrium (long, enlarged distally vs short or cylindrical) (Table 2).

The new species, *D. japonica* (Michaelsen, 1892) and *D. koreana* Kobayashi, 1938 share several common characters, such as the presence of genital markings and accessory glands. However, the new species differs from those two species in having three gizzards from xiii, the spermathecal atrium erect, the vas deferens strongly coiled as a bunch, and the prostate cylindrical and somewhat folded, while *D. japonica* and *D. koreana* have two to three gizzards from xii, the spermathecal atrium short and small, the vas deferens not into a bunch (coiled or loosely twisted), and the club-shaped or thumb-shaped prostate (Table 2).

Compared to other *Drawida* species recorded in Vietnam, *D. annamensis*, *D. chapaensis*, *D. delicata*, *D. langsonensis*, and *D. beddardi*, the new species is clearly distinguished by having genital markings in ix and x, and the spermathecal atrium and spermathecal ducts strongly twisted and coiled, while all other species have no genital markings, and the spermathecal atrium and spermathecal ducts simply undulated.

***Drawida cochinchina* sp. nov.**

<http://zoobank.org/02322457-3AC4-4E1A-BABC-1994958EE562>

Fig. 3

Drawida sp. 2. – Nguyen TT 2013: 100; 2014: 113.

Material examined. Holotype. VIETNAM • clitellate; Dong Nai Province, Xuan Loc District, Xuan Hoa Commune; 10.7931°N, 107.5257°E; 88 m a.s.l.; 12 Sep. 2012; Nguyen Van Thang leg. (long-term tree plantation CTU-EW.032.h01),

Paratypes. VIETNAM • 8 clitellates; same data as for the holotype; CTU-EW.032.p02 • 3 clitellates; same data as for the holotype; CTU-EW.DNA.032.p02 • 8 clitellates; Tay Ninh Province, Ba Den Mountain; 11.3901°N, 106.1553°E; 149 m a.s.l.; 26 Sep. 2019, coll. Nguyen Quoc Nam leg.; *Mangifera* plantations; CTU-EW.032.p03.

Other material. VIETNAM • 50 clitellates; same data as for the holotype; CTU-EW.032.04 • 5 clitellates; same data as for the sample CTU-EW.032.p03; CTU-EW.032.09 • 2 clitellates, 8 acitellates; An Giang Province, Tinh Bien District, Nhon Mountain; 10.5882°N, 104.9506°E; 56 m a.s.l.; 07 Nov. 2010; Nguyen Thanh Tung leg.; *Mangifera* plantations; CTU-EW.032.05 • 2 clitellates; An Giang Province, Tinh Bien District, Tinh Bien town; 10.5895°N, 104.9501°E; 24 m a.s.l.; 19 Oct. 2020; Nguyen Thanh Tung leg.; orange garden; CTU-EW.032.19 • 3 clitellates; same data as for the sample CTU-EW.032.19; IEBR-EW.032.19 • 2 clitellates, 17 acitellates; Kien Giang Province, Kien Hai District, Hon Tre Island; 9.9538°N, 104.8359°E; 187 m a.s.l.; 13 Nov. 2013; Trinh Thi Kim Binh leg.; *Acacia* plantation; CTU-EW.032.18 • 3 clitellates, 10 acitellates; Tay Ninh Province, Ba Den Mountain; 11.3944°N, 106.1499°E; 46 m a.s.l.; Oct. 2012, Nguyen Thi Anh Ngoc leg.; *Mangifera* plantations; CTU-EW.032.06 • 5 clitellates; Ho Chi Minh City, Hoc Mon District, Tan Hiep Commune; 10.9142°N,

106.5662°E; 2 m a.s.l.; 24 Sep. 2019; Nguyen Quoc Nam leg.; bushes; CTU-EW.032.07 • 1 clitellate; Tay Ninh Province, Tan Chau District, Tan Hiep Commune; 11.6024°N, 106.1144°E; 44 m a.s.l.; 25 Sep. 2019; Nguyen Quoc Nam leg.; rubber plantation; IEBR-EW. 032.10 • 35 clitellates; Tay Ninh Province, Trang Bang District, Loc Hung Commune; 11.0775°N, 106.4000°E; 24 Sep. 2019; Nguyen Quoc Nam leg.; rice field; CTU-EW.032.08 • 3 clitellates; same data as for the sample CTU-EW.032.08; IEBR-EW.032.08 • 2 matures, 19 acitellates; Ba Ria – Vung Tau Province, Con Son Island,

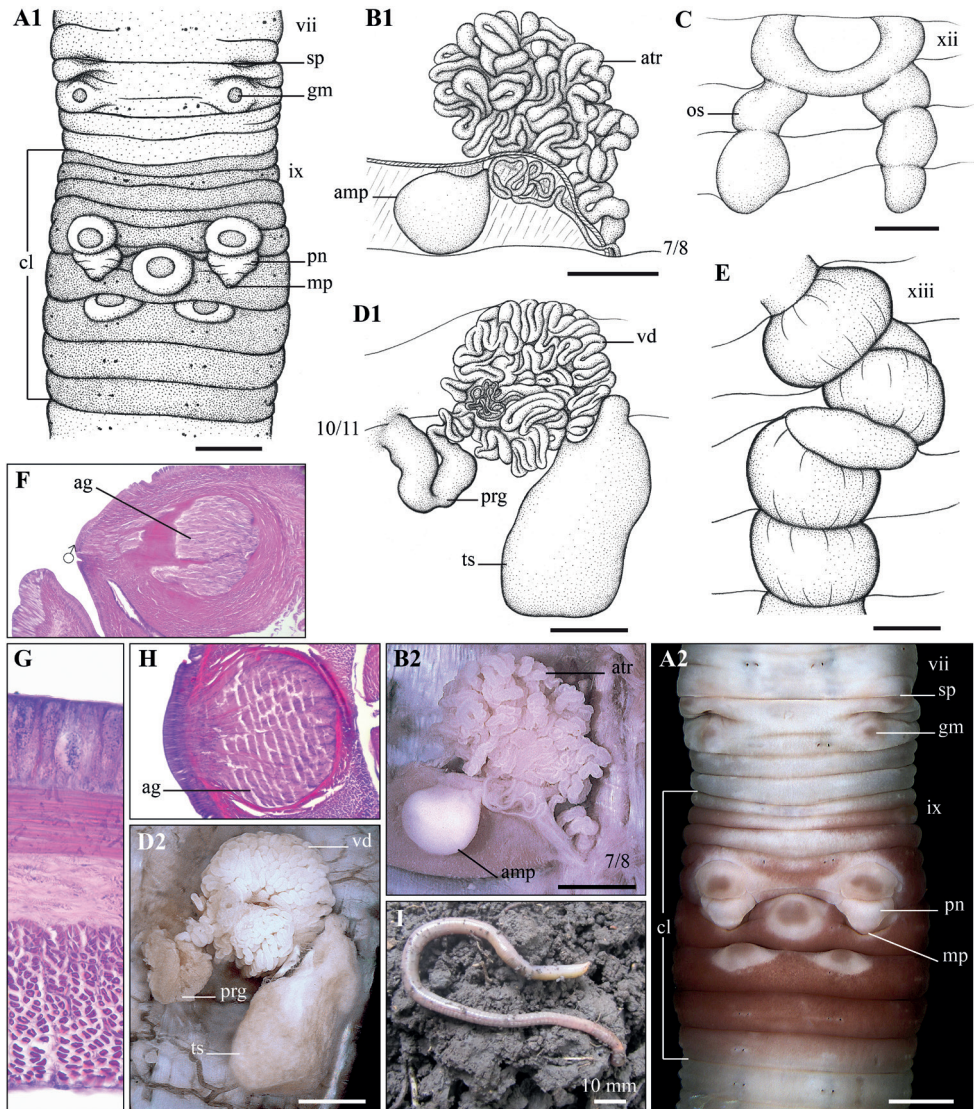


Figure 3. *Drawida cochinchina* sp. nov. Holotype (CTU-EW.032.h01) **A1, A2** clitellum region, ventral view **B1, B2** left spermatheca **C** ovisacs **D1, D2** right male sexual system **E** oesophagous gizzards **F** longitudinal section of clitellum region **G** transverse section of body wall **H** transverse section of genital marking **I** living specimen. Scale bars: 1 mm.

8.7008°N, 106.6175°E; 10 m a.s.l.; 19 Nov. 2019; Nguyen Thanh Tung & Nguyen Thi Bao Ngoc leg.; bushes; CTU-EW.032.11 • 3 clitellates; same data as for the sample CTU-EW.032.11; IEBR-EW.032.11 • 14 clitellates; Ba Ria – Vung Tau Province, Dinh Mountain; 10.51111 N, 107.12694 E; 27 Oct. 2016; Nguyen Quoc Nam leg.; natural forest; CTU-EW.032.13 • 3 clitellates; Dong Nai Province, Cam My District, Lam Son Commune; 10.83944 N, 107.26508 E; 16 Oct. 2019; Nguyen Quoc Nam leg.; rubber plantation; IEBR-EW.032.12 • 12 clitellates, 18 acitellates; Binh Duong Province, Dau Tieng District, Dinh An Commune; 11.3765°N, 106.4234°E; 27 Oct. 2017; Nguyen Quoc Nam leg.; rubber plantation; CTU-EW.032.14 • 2 clitellates, 19 acitellates; Binh Duong Province, Dau Tieng District, Minh Thanh Commune; 11.3811°N, 106.5159°E; 37 m a.s.l.; 27 Oct. 2017; Nguyen Quoc Nam leg.; cashew plantation; CTU-EW.032.15. CTU-EW.032.16 • 12 clitellates; Dong Nai Province, Long Thanh District, Long Phuoc Commune; 10.7018°N, 107.0040°E; 10 m a.s.l.; 12 Oct. 2012; Le Van Nhan leg.; long-term tree plantation; CTU-EW.032.17.

Diagnosis. Body cylindrical, small-medium in size, length 84–123 mm, diameter 3.3–4.9 mm, 101–294 segments. Setal formula aa: ab: bc: cd: dd = 6.2–7.0: 1: 7.0–8.5: 1: 33–35. A pair of spermathecal pores in ventro-lateral intersegment 7/8, close to seta c. Genital markings, variable, one or two pairs, in viii and ix, located between seta b and c, (sometimes with additional one or two genital markings in medio-ventral viii and ix), one pair closely anterior to penises, and additional 1–3 ones in xi–xii. Male pores located on the top of highly elevated, posteriorly directed, conical penises in 10/11. Spermathecal atrium tubular, strongly coiled in vii. Testis sacs in x, large, in equal size to the coils of vas deferens. Prostate glandular, glandularity reduced; prostatic capsule cylindrical-shaped, somewhat folded. Gizzards 3–4, in xiii–xvi.

Description. External: body cylindrical, small-medium size, length 84–123 mm, diameter 3.3–4.9 mm, 101–294 segments (holotype: length 95, diameter 5.1, 198 segments).

Coloration: body light grey, uniformly color in both ventrum and dorsum. Prostomium undeveloped. No dorsal pores. Setae lumbricine, with eight setae distributed round body, setal formula aa: ab: bc: cd: dd = 6.2–7.0: 1: 7.0–8.5: 1: 33–35. Clitellum annular, within ix–xiv, reddish brown. Spermathecal pores paired, in ventro-lateral intersegmental furrow 7/8, close to seta c. Genital markings present, variable, one or two pairs in viii and ix, located between setae b and c, sometimes with an additional one or two in medio-ventral viii and ix, one pair anterior to penis in x, and additional 1–3 in xi–xii. Female pore hardly visible. Male pores located in intersegmental furrow 10/11, between setae b and c, closed to seta c, on the top of highly elevated, backwardly directed, conical penises in 10/11. Nephridiopores anterior margin of segments iv onwards, in d lines, especially clear from vii to xv.

Internal: Septa 5/6/7/8/9 thick, 9/10 and subsequence septa thin. Gizzards three or four in xiii–xvi. Last hearts in ix. Intestinal origin at xvi or xvii. Spermathecae paired, on viii, spermathecal ampulla oval; spermathecal ducts coiled and twisted, passing through septum 7/8, and ending at ectal end of atrium; Spermathecal atrium tubular, strongly coiled as a bunch in vii, mass larger than spermathecal ampulla. Prostate glandular, glandularity strongly reduced; prostatic capsule cylindrical, somewhat folded. Testis sacs paired, in x, large, sac-shaped; vas deferens strongly

coiled as a bunch, equal in size to testis sacs, and entering testis sac at its ental end. Ovarian chamber complete, ovisacs well developed, in xii–xviii. Accessory glands present, but invisible.

DNA character. The COI fragment was uploaded to GenBank with accession numbers ON303831, ON303832, ON303833. The new species has a close COI identity of 81% with *D. ghilarovi* (KY711506)

Distribution. The species was also found in Kien Giang (Da Do, Da Dung, and Ta Bang Mountains), An Giang (Tinh Bien District), Vinh Long (Vung Liem District), Ho Chi Minh City (Hoc Mon, Binh Chanh, and Cu Chi Districts), Tay Ninh (Ba Den Mountain, Trang Bang District), Binh Duong (Dau Tieng and Bau Bang Districts), Dong Nai (Xuan Loc, Long Thanh, and Cam My Districts), Ba Ria Vung Tau (Dat Do Districts, Ba Ria City, and Con Son Island) (Nguyen T.T. 2014 as *Dr.* sp. 2).

Etymology. The noun *cochinchina* (= southern Vietnam) is used in apposition to accentuate its wide distribution in southern Vietnam.

Remarks. The new species is very similar to *D. longatria* Gates, 1925 in having genital markings in 10/11, the presence of a spermathecal atrium, and the spermathecal ducts being twisted and strongly coiled. However, it differs from *D. longatria* in having prostate capsule cylindrical, somewhat folded, three or four esophageal gizzards in xiii–xvi, the spermathecal atrium in vii, testis sacs in 10/11, ovisacs well developed in xii–xvii, and having hidden accessory glands. On the contrary, *D. longatria* has the prostate capsule digitiform, four esophageal gizzards in xv–xviii, the spermathecal atrium in viii, testis sacs in 9/10, ovisacs in xi–xiv, and obvious accessory glands.

The new species is also similar to *D. ofunatoensis* (Ofuchi, 1938) in having paired genital markings and testis sacs in septum 10/11. However, it differs in having the clitellum within ix–xi, the spermathecal atrium and seminal ducts twisted and strongly coiled, and the prostate cylindrical and strongly folded. *Drawida ofunatoensis* has the clitellum located in x–xiii, the spermatheca lacking an atrium, and the male atrium globular.

The new species is somewhat similar to *D. nepalensis* in having the clitellum within ix–xiv, the presence of genital markings, spermathecal pores located median to c, and the vas deferens strongly coiled as a bunch. However, it differs from *D. nepalensis* in having the spermathecal atrium slender and strongly coiled as a bunch, one gizzard per segment (three to four within xiii–xvi), a folded cylindrical prostate, and hidden accessory glands. On the contrary, *D. nepalensis* has each gizzard pass through several segments (two to four within xii–xx), the spermathecal atrium stouter and sac-like, the prostate club-shaped, and obvious accessory glands.

Compared to the other five *Drawida* species recorded in Vietnam, *D. annamensis*, *D. chapaensis*, *D. delicata*, *D. langsonensis*, and *D. beddardi*, this new species is clearly distinguished by having paired genital markings and the spermathecal atrium and spermathecal ducts strongly twisted and coiled, while all other species have no genital markings and the spermathecal atrium and spermathecal ducts are simply undulated.

Conclusions

The discovery of two new species of *Drawida* brings the number of species in Vietnam to seven. However, due to the placement of Vietnam in region of origin of the genus *Drawida*, this number of species does not reflect the true biodiversity in this country. It is, therefore, suggested that additional intensive surveys are needed to reveal more new species awaiting discovery.

Acknowledgements

This research was funded by Ministry of Education and Training of Vietnam under the grant B2021-TCT-08. Our research activities were also supported by the Tokyo Metropolitan University Fund for TMU Strategic Research (leader: Noriaki Murakami; FY2020-FY2022).

References

- Aiyer KS (1929) An account of the Oligochaeta of Travancore. Records of the Indian Museum 31: 14–75. <http://faunaofindia.nic.in/PDFVolumes/records/031/01/0013-0076.pdf>
- Beddard FE (1886) Notes on some earthworms from Ceylon and the Philippine Islands, including a description of two new species. Annals and Magazine of Natural History (Series 5) 17: 89–98. <https://doi.org/10.1080/00222938609460120>
- Blakemore RJ (2002) Cosmopolitan Earthworms—an Eco-Taxonomic Guide to the Peregrine Species of the World. VermEcology, Kippax, Australia, 506 pp.
- Blakemore RJ, Kupriyanova EK (2010) Unravelling some Kinki worms (Annelida: Oligochaeta: Megadrili: Moniligastridae) Part I. Opuscula Zoologica 40: 3–18.
- Blakemore RJ, Lee S, Seo HY (2014) Reports of *Drawida* (Oligochaeta: Moniligastridae) from far East Asia. Journal of Species Research 3(2): 127–166. <https://doi.org/10.12651/JSR.2014.3.2.127>
- Bourne AG (1887) On Indian earthworms.— Part I. Preliminary notice of earthworms from the Nilgiris and Shevaroy. Proceedings of the Zoological Society of London 1886: 652–672.
- Chang CH, Shen HP, Chen JH (2009) Earthworm Fauna of Taiwan. Biota Tawanica. National Taiwan University Press, Taipei, 174 pp.
- Chen Y (1933) The preliminary survey of the earthworms of the lower Yangtze valley. Contributions from the Biological Laboratory of the Science Society of China, Zoological Series 9(4): 177–294.
- Claus C (1880) Grundzüge der Zoologie, zum wissenschaftlichen Gebrauche [fourth edition]. N.G. Elwert'sche Verlagsbuchhandlung, Marburg, 822 pp. <https://doi.org/10.5962/bhl.title.1113>
- Do VN, Huynh TKH (1993) New species of earthworms of genus *Drawida* Michaelsen, 1900 (Moniligastridae, Oligochaeta) from mountain of Lang Son and Cha Pa (Lao Cai Province). Tạp chí Sinh Học 15(4): 36–38.

- Feldman AT, Wolfe D (2014) Tissue processing and hematoxylin and eosin staining. In: Day C (Ed.) *Histopathology. Methods in Molecular Biology. Methods and Protocols*. 1180. Humana Press, New York, 31–43. https://doi.org/10.1007/978-1-4939-1050-2_3
- Folmer O, Black M, Hoeh W, Lutz R, Vrijenhoek R (1994) DNA primers for amplification of mitochondrial cytochrome oxidase subunit I from diverse metazoan invertebrates. *Molecular Marine Biology and Biotechnology* 3: 294–299.
- Ganin GN, Atopkin DM (2018) Molecular differentiation of epigeic and anecic forms of *Drawida ghilarovi* Gates, 1969 (Moniligastridae, Clitellata) in the Russian Far East: Sequence data of two mitochondrial genes. *European Journal of Soil Biology* 86: 1–7. <https://doi.org/10.1016/j.ejsobi.2018.02.004>
- Gates GE (1925) Some new earthworms from Rangoon, Burma.—II. *Annals and Magazine of Natural History (Series 9)* 16: 49–64. <https://doi.org/10.1080/00222932508633274>
- Gates GE (1933) The earthworms of Burma. IV. Records of the Indian Museum 35: 413–606.
- Gates GE (1962) On some Burmese earthworms of the moniligastrid genus *Drawida*. *Bulletin of the Museum of Comparative Zoology* 127: 297–373. <https://www.biodiversitylibrary.org/part/25697>
- Gates GE (1969) On a new species of the moniligastrid earthworm genus *Drawida* Michaelsen, 1900. *Zoologicheskij Zhurnal* 48(5): 674–676.
- Gates GE (1972) Burmese earthworms: An introduction to the systematics and biology of megadrile oligochaetes with special reference to Southeast Asia. *Transactions of the American Philosophical Society* 62(7): 1–326. <https://doi.org/10.2307/1006214> [New Series]
- Hall TA (1999) BioEdit: A user-friendly biological sequence alignment editor and analysis program for Windows 95/98/NT. *Nucleic Acids Symposium Series* 41: 95–98.
- Hatai S (1930) On *Drawida hattamimizu*, sp. nov. *Science Reports of the Tohoku Imperial University. 4th Series. Biology (Basel)* 5(3): 485–508.
- Huang J, Xu Q, Sun ZJ, Tang GL, Su ZY (2007) Identifying earthworms through DNA barcodes. *Pedobiologia* 51(4): 301–309. <https://doi.org/10.1016/j.pedobi.2007.05.003>
- Kalyaanamoorthy S, Minh BQ, Wong TKF, von Haeseler A, Jermiin LS (2017) ModelFinder: Fast model selection for accurate phylogenetic estimates. *Nature Methods* 14(6): 587–589. <https://doi.org/10.1038/nmeth.4285>
- Kobayashi S (1937) Preliminary survey of the earthworms of Quelpart Island. *Science Report of the Tohoku Imperial University (B)* 11(3): 333–351.
- Kobayashi S (1938) Earthworms of Korea I. *Science Report of the Tohoku Imperial University* 13(2): 89–170.
- Kumar S, Stecher G, Tamura K (2016) MEGA7: Molecular Evolutionary Genetics Analysis version 7.0 for bigger datasets. *Molecular Biology and Evolution* 33(7): 1870–1874. <https://doi.org/10.1093/molbev/msw054>
- Lam DH, Nguyen NQ, Nguyen AD, Nguyen TT (2021) A checklist of earthworms (Annelida: Oligochaeta) in southeastern Vietnam. *Journal of Threatened Taxa* 13(2): 17693–17711. <https://doi.org/10.11609/jott.6535.13.2.17693-17711>
- Larkin MA, Blackshields G, Brown NP, Chenna R, McGettigan PA, McWilliam H, Valentin F, Wallace IM, Wilm A, Lopez R, Thompson JD, Gibson TJ, Higgins DG (2007) Clustal W and Clustal X version 2.0. *Bioinformatics (Oxford, England)* 23(21): 2947–2948. <https://doi.org/10.1093/bioinformatics/btm404>

- Michaelsen W (1892) Terricolen der Berliner Zoologischen Sammlung, II. Archiv für Naturgeschichte 58: 209–261. <https://doi.org/10.5962/bhl.part.8321>
- Michaelsen W (1900) Oligochaeta. Das Tierreich 10: 1–575. <https://doi.org/10.5962/bhl.title.11605>
- Michaelsen W (1907) Neue Oligochäten von Vorder-Indien, Ceylon, Birma und den Andaman-Inseln. Mitteilungen aus dem Naturhistorischen Museum in Hamburg 24: 143–193.
- Michaelsen W (1910) Oligochäten von verschiedenen Gebieten. Jahrbuch der Hamburgischen Wissenschaftlichen Anstalten 27: 47–169.
- Michaelsen W (1931) Ausländische opisthopore Oligochäten. Zoologische Jahrbücher. Abteilung für Systematik 61: 523–578.
- Michaelsen W (1934) Oligochäten von Französisch-Indochina. Archives de Zoologie Expérimentale et Générale 76: 493–546.
- Müller W (1856) *Lumbricus corethrurus*, Burstenschwanz. Archiv für Naturgeschichte 23(1) 38: 113–116.
- Nguyen TT (2013) The earthworm fauna of the Cuu Long delta. PhD dissertation in Zoology. Hanoi National University of Education, Hanoi, 169 pp.
- Nguyen TT (2014) Checklist and some remarks on faunistic characteristics of earthworms in the Mekong Delta, Vietnam. Journal of Science, Cantho University, Section A: Science. Technology and Environment 32: 106–119.
- Nguyen L-T, Schmidt HA, von Haeseler A, Minh BQ (2015) IQ-TREE: A fast and effective stochastic algorithm for estimating maximum likelihood phylogenies. Molecular Biology and Evolution 32(1): 268–274. <https://doi.org/10.1093/molbev/msu300>
- Nguyen TT, Lam DH, Nguyen AD (2016a) On the giant pheretimoid earthworms from Vietnam (Clitellata: Megascolecidae), with descriptions of three new species. Zoological Studies (Taipei, Taiwan) 55: e52. <https://doi.org/10.6620/ZS.2016.55-52>
- Nguyen TT, Nguyen AD, Tran BTT, Blakemore RJ (2016b) A comprehensive checklist of earthworm species and subspecies from Vietnam (Annelida: Clitellata: Oligochaeta: Almididae, Eudrilidae, Glossoscolecidae, Lumbricidae, Megascolecidae, Moniligastridae, Ocnerodrillidae, Octochaetidae). Zootaxa 4140(1): 1–92. <https://doi.org/10.11646/zootaxa.4140.1.1>
- Nguyen TT, Nguyen NQ, Nguyen AD (2018) First record of the earthworm genus *Pheretima* Kinberg, 1867 sensu stricto in Vietnam, with description of a new species (Annelida: Clitellata: Megascolecidae). Zootaxa 4496(1): 251–258. <https://doi.org/10.11646/zootaxa.4496.1.20>
- Nguyen QN, Nguyen AD, Phan TQ, Nguyen TT (2020) Diversity and phylogenetic relationship of earthworm species in Binh Duong and Binh Phuoc Provinces. Journal of Science of Can Tho University, Section A: Natural Science. Technology and Environment 56(2A): 11–20. <https://doi.org/10.22144/ctu.jvn.2020.025>
- Ohfuchi S (1938) New species of earthworms from northeastern Honshu, Japan. Research Bulletin of Saito Ho-on Kai Museum 15: 33–52.
- Rao CRN (1921) On the anatomy of some new species of *Drawida*. Annals and Magazine of Natural History (Series 9) 8: 496–535. <https://doi.org/10.1080/00222932108632613>
- Rosa D (1890) Moniligastridi, Geoscolecidi ed Eudrilidi. Annali del Museo Civico di Storia Naturale di Genova 29(2): 365–398.
- Shen HP, Chang CH, Chih WJ (2015) Earthworms from Matsu, Taiwan with descriptions of new species of the genera *Amyntas* (Oligochaeta: Megascolecidae) and *Drawida*

- (Oligochaeta: Moniligastridae. *Zootaxa* 3973(3): 425–450. <https://doi.org/10.11646/zootaxa.3973.3.2>
- Sims RW, Easton EG (1972) A numerical revision of the earthworm genus *Pheretima* auct. (Megascolecidae: Oligochaeta) with the recognition of new genera and an appendix on the earthworms collected by the Royal Society North Borneo Expedition. *Biological Journal of the Linnean Society*. Linnean Society of London 4(3): 169–268. <https://doi.org/10.1111/j.1095-8312.1972.tb00694.x>
- Stephenson J (1915) On some Indian Oligochaeta, mainly from Southern India and Ceylon. *Memoirs of the Indian Museum* 6: 35–108.
- Stephenson J (1920) On a collection of oligochaeta from the lesser known parts of India and from eastern Persia. *Memoirs of the Indian Museum* 7: 191–261.
- Stephenson J (1930) *The Oligochaeta*. Clarendon Press, Oxford, 978 pp.
- Thakur SS, Lone AR, Tiwari N, Jain SK, James SW, Yadav S (2021) A contribution to the earthworm diversity (Clitellata, Moniligastridae) of Kerala, a component of the Western Ghats biodiversity hotspot, India, using integrated taxonomy. *Animal Biodiversity and Conservation* 44(1): 117–137. <https://doi.org/10.32800/abc.2021.44.0117>
- Yuan Z, Jiang J, Dong Y, Zhao Q, Gao X, Qiu J-P (2019) The dispersal and diversification of earthworms (Annelida: Oligochaeta) related to paleogeographical events in the Hengduan Mountains. *European Journal of Soil Biology* 94: e103118. <https://doi.org/10.1016/j.ejsobi.2019.103118>
- Zhang Z, Schwartz S, Wagner L, Miller W (2000) A greedy algorithm for aligning DNA sequences. *Journal of Computational Biology* 7(1–2): 203–214. <https://doi.org/10.1089/10665270050081478>
- Zhang YF, Ganin GN, Atopkin DM, Wu DH (2020) Earthworm *Drawida* (Moniligastridae) Molecular phylogeny and diversity in Far East Russia and Northeast China. *The European Zoological Journal* 87(1): 180–191. <https://doi.org/10.1080/24750263.2020.1741705>

Supplementary material I

COI dataset

Authors: Tung T. Nguyen, Dang H. Lam, Binh T.T. Tran, Anh D. Nguyen

Data type: fas file

Explanation note: COI dataset.

Copyright notice: This dataset is made available under the Open Database License (<http://opendatacommons.org/licenses/odbl/1.0/>). The Open Database License (ODbL) is a license agreement intended to allow users to freely share, modify, and use this Dataset while maintaining this same freedom for others, provided that the original source and author(s) are credited.

Link: <https://doi.org/10.3897/zookeys.1099.72112.suppl1>

Description of *Chilearinus* Sharkey gen. nov. and status of Nearctic *Earinus* Wesmael, 1837 (Braconidae, Agathidinae) with the description of new species

Michael J. Sharkey¹, Austin Baker², Ramya Manjunath³, Paul D. N. Hebert³

1 *The Hymenoptera Institute, 116 Franklin Ave., Redlands, CA, 92373, USA* **2** *Department of Biological Sciences and Center for Biodiversity Research, University of Memphis, TN, USA* **3** *Centre for Biodiversity Genomics, University of Guelph, Guelph, ON, Canada*

Corresponding author: Michael J. Sharkey (msharkey@uky.edu)

Academic editor: Jose Fernandez-Triana | Received 31 January 2022 | Accepted 14 March 2022 | Published 3 May 2022

<http://zoobank.org/B08A029E-7272-4C35-B0BE-62AE9411979E>

Citation: Sharkey MJ, Baker A, Manjunath R, Hebert PDN (2022) Description of *Chilearinus* Sharkey gen. nov. and status of Nearctic *Earinus* Wesmael, 1837 (Braconidae, Agathidinae) with the description of new species. ZooKeys 1099: 57–86. <https://doi.org/10.3897/zookeys.1099.81473>

Abstract

The Neotropical members formerly included in *Earinus* Wesmael, 1837 are transferred to a new genus, *Chilearinus* Sharkey **gen. nov.** Presently three Nearctic species of *Earinus* are recognized, i.e., *Earinus erythropoda* Cameron, 1887, *Earinus limitaris* Say, 1835, and *Earinus zeirapherae* Walley, 1935, and these are retained in *Earinus*. *Earinus chubuquensis* Berta, 2000 and *Earinus scitus* Enderlein, 1920 are transferred to *Chilearinus*, i.e., *C. chubuquensis*, and *C. scitus*, **comb. nov.** One other species is transferred to *Chilearinus*, i.e., *Microgaster rubricollis* Spinola, 1851, *Chilearinus rubricollis*, **comb. nov.** Two other Neotropical species, *Earinus hubrechtiae* Braet, 2002 and *Earinus bourguignoni* Braet, 2002 were described under the genus *Earinus* but are here transferred to *Lytopylus*, *L. hubrechtiae*, and *L. bourguignoni* **comb. nov.** Two new species of *Chilearinus* are described, *C. covidchronos* and *C. janbert* **spp. nov.** The status of *Agathis laevithorax* Spinola, 1851, *Agathis rubricata* Spinola, 1851, and *Agathis areolata* Spinola, 1851 is discussed. A neotype is designated for *Earinus limitaris* (Say, 1835) and diagnosed with a COI barcode. *Earinus austinbakeri* and *Earinus walleyi* **spp. nov.** are described. The status of both *Earinus* and *Chilearinus* in the Americas is discussed. A revised key to the genera of Agathidinae of the Americas is presented.

Keywords

Accelerated taxonomy, BIN code, COI barcode Hymenoptera, COI DNA barcode, conservation, Ichneumonoidea

Introduction

Neotropical species formerly included in *Earinus* Wesmael, 1837 are transferred to a new genus, *Chilearinus* Sharkey gen. nov. Presently three Nearctic species of *Earinus* are recognized, i.e., *Earinus erythropoda* Cameron, 1887, *Earinus limitaris* Say, 1835, and *Earinus zeirapherae* Walley, 1935, and these are retained in *Earinus*. *Earinus chubuquensis* Berta, 2000 and *Earinus scitus* Enderlein, 1920 are transferred to *Chilearinus*, i.e., *C. chubuquensis* and *C. scitus*, comb. nov. One other species is transferred to *Chilearinus*, i.e., *Microgaster rubricollis* Spinola, 1851, *Chilearinus rubricollis*, comb. nov. Two other Neotropical species, *Earinus hubrechtiae* Braet, 2002, and *Earinus bourguignoni* Braet, 2002 were described under the genus *Earinus* but are here transferred to *Lytopylus*, *L. hubrechtiae*, and *L. bourguignoni* comb. nov. Two new species of *Chilearinus* are described, *C. covidchronos* and *C. jamberi* spp. nov. The status of *Agathis laevithorax* Spinola, 1851, *Agathis rubricata* Spinola, 1851, and *Agathis areolata* Spinola, 1851 is discussed. A neotype is designated for *Earinus limitaris* (Say, 1835) and diagnosed with a COI barcode. *Earinus austinbakeri* and *Earinus walleyi* spp. nov. are described. The status of both *Earinus* and *Chilearinus* in the Americas is discussed. A revised key to the genera of Agathidinae of the Americas is presented.

Methods

DNA extraction and sequencing

Molecular work was carried out at the CBG using standard protocols. A leg from each frozen-then-oven-dried specimen was destructively sampled for DNA extraction using a glass fiber protocol (Ivanova et al. 2006). Extracted DNA was amplified for a 658 bp region near the 5' terminus of the cytochrome *c* oxidase subunit I (COI) gene using standard insect primers LepF1 (5'-ATTCAACCAATCATAAAGATATTGG-3') and LepR1 (5'-TAAACTTCTGGATGTCCAAAAAATCA-3') (Ivanova and Grainger 2007). If initial amplification failed, additional PCRs were conducted following established protocols using internal primer pairs: LepF1–C113R (130 bp) or LepF1–C_ANTMR1D (307 bp) and MLepF1–LepR1 (407 bp) to generate shorter overlapping sequences. Most amplicons were Sanger sequenced, but some recent specimens were analyzed on SEQUEL.

The BOLD database can be used to identify specimens using the following steps: (1) navigate to the identification tab of the BOLD Systems database (http://www.boldsystems.org/index.php/IDS_OpenIdEngine); (2) paste the COI sequence of the query organism (in forward orientation) into the query box and search against the appropriate library (e.g., All Barcode Records on BOLD, Species Level Barcode Records, etc.); (3) the search results page shows the top hits based on percentage similarity starting with the closest matches (This page also provides additional information to help verify the identity of a match, such as links to the BIN where specimen data, including images, can be found, a distribution map, and a tree-based identification tool); (4) use the Tree-Based Identification button to generate a neighbor-joining tree and find the query taxon (name in red). This allows you to visualize how distant the query sequence is from the closest matches.

Taxonomic account

Chilearinus Sharkey, gen. nov.

<http://zoobank.org//82CEAEE1-8CDB-48DD-B79F-1B59F8CF74A1>

Type species. *Chilearinus janbert* Sharkey, sp. nov.

Etymology. A conjunction of Chile, where 90% of the species are likely to be found, and *Earinus*, a reference to the probable sister group of the species, based on preliminary analyses. The genus is masculine.

Diagnosis. Notauli absent; hind coxal cavities open; tarsal claws with basal lobes; second submarginal cell quadrate, never petiolate; foretibia lacking sclerotized spines/pegs; hind wing Cub strong and emanating from an angle on the basal cell. Most similar morphologically to *Earinus* and *Lytopylus*. *Earinus* and *Chilearinus* do not have overlapping distributions. The former is restricted to the Nearctic and the latter to the Neotropics; therefore, there is little chance of confusing the two. Nonetheless, the lack of pegs on the foretibia of members of *Chilearinus* and the morphological characters given in the key (below) can also be employed to differentiate them. Members of *Lytopylus* differ most significantly in that they lack vein Cub in the hind wing. See couplet 25 in the key below.

Description. Head. Lateral carina on frons (as found in members of *Alabagrus*) absent; interantennal space slightly raised above antennal sockets; gena not extended ventroposteriorly into sharp prominence; mandible dorsoventrally flattened (twisted); labial palpus with 4 segments, third segment slightly more than ½ length of apical segment. **Mesosoma.** Propleuron lacking a sharp bump; notauli absent; mesoscutum smooth with a median pit (presumably a remnant of notauli), postscutellar depression absent; propodeum mostly smooth, sometimes with weak smooth sculpture medially; sclerite between hind coxal cavities and metasomal foramen absent. Precoxal groove absent or smooth and weakly impressed. **Legs.** Foretibia lacking dull pegs (unlike *Earinus*); mid- and hind tibia with blunt apical or preapical pegs; all tarsal claws with a rounded basal lobe. **Wings.** Forewing RS+Ma vein mostly present but not usually completely tubular; second submarginal cell large, quadrate and usually (perhaps always) higher than long; RS of forewing complete to wing margin; hind wing r and r-m cross veins absent; hind wing vein Cub strong and emanating from an angle on the basal cell. **Metasoma.** First median tergite smooth, longer than apical width, lateral longitudinal carina absent or weak and short; remaining terga smooth; ovipositor ranging from as long as the body to twice the length of the body, but this is based on small sample of a few dozen species.

Biology. Unknown.

Diversity and distribution. This is a species-rich genus with hundreds of species, based on specimens identified by MS. It is widespread in Chile and southern Argentina. A few species are found at high altitudes as far north as Ecuador and Colombia.

Notes. Sharkey (1997) included members of what are now *Chilearinus* in a broader concept of *Earinus*. Spinola (1851) described three species of Agathidinae from Chile. Since members of *Chilearinus* are by far the most species-rich of Chilean agathidines, and since his descriptions do not contradict membership in the genus, these species are probably members of *Chilearinus*, i.e., *Agathis laevithorax*, *Agathis rubricata*, and *Agathis areolata*. They certainly

are not members of *Agathis* since this genus does not extend into the southern regions of South America. These specimens should be in the Hymenoptera collection of Maximilian Spinola whose collection is housed in the Museo Regionale di Scienze Naturali (MRSN) in Turin (Torino). One of us (MS) could not locate these specimens during a visit to MRSN in 1985, but a specimen of *Chilearinus*, *Microgaster rubricollis* Spinola, 1851, was present. *Microgaster* may seem an odd place for placement of what we now consider an agathidine, but such was the classification at the time. It is clear from the following that Spinola knew the species was closely related to *Earinus*, “Este *Microgastro* habria pertenecido á [sic] la primera seccion del *G. Microdus*, N. V. Es., y al sub-género *Earinus* Wesm.” (Spinola 1851: 34).

It is almost pointless to present a morphological key to the five recognized species of *Chilearinus* as they represent just five species out of hundreds. Many undescribed species will undoubtedly key to these named species. The only way to handle species-rich undocumented genera such as *Chilearinus* is to include COI barcode data in the diagnoses. We know this diagnostic is sufficient to differentiate all but a few species of Agathidinae (Sharkey et al. 2018). Nonetheless, despite the absurdity, a key is presented below to mollify critics (e.g., Zamani et al. 2020).

Key to the few described species of *Chilearinus*

- 1 Forewing with two yellow bands *C. scitus*
- Forewing evenly colored, weakly infusate 2
- 2 Mesonotum orange *C. rubricollis*
- Mesonotum black 3
- 3 Hind femur entirely yellow except extreme apex dorsally *C. janbert*
- Hind femur mostly or entirely black 4
- 4 Hind femur black except extreme apex yellow *C. chubuquensis*
- Hind femur entirely black *C. covidchronos*

***Chilearinus covidchronos* Sharkey, sp. nov.**

<http://zoobank.org/67B17FE2-0DD1-4E44-A862-A5E3275E3D8D>

Fig. 1

Holotype. ♀, Chile, Región IX, PN Nahualbuta, 37.809°S, 73.016°W, 3680' [1122 m], 9–12.i.2000, Malaise trap, Webb and Yeates (Canadian National Collection).

Diagnosis. COI barcode. BOLD sample ID H1145. BOLD BIN code BOLD:AAV0870. GenBank Accession Code OL702761.

AATTTTATATTTTATATTTGGAATTTGATCGGGAATTTTAGGTT-TATCAATAAGTTTAATTATTCGAATAGAATTAAGAGTAGGGGGTAATTT-TATTGGTAATGATCAAATTTATAATAGAATTGTNGCTGCTCATGCTTT-TATTATAATTTTTTTATAGTTATAACCAATTATAAATTGGAGGATTTG-GAAATTGATTAATTCATTAATATTTGGGGGGCCAGATATAGCTTTCC-CTCGAATAAATAATAAGATTTTGATTATTAATTCCTTCATTATTATTAT-

TAATTTTAAGGTCTTTAATTAATGTTGGGGTAGGTAAGTACTGGATGAACTGTT-
 TATCCTCCTTTATCATTAATATAAGTCATAGTGGTATATCTGTAGATT-
 TAGCTATTTTTTCTTTACATATTGCTGGAATTTCTTCAATTATAGGTGC-
 TATAAATTTTATTACAACCTATTTTAAATATGTGAATAATTAATATAAAATTGA-
 TAAAATACCTTTATTAGTTTGATCAATTTTAAATTACGGCAATTTTATTATT-
 ATTATCTTTGCCAGTTTTAGCTGGAGCTATTACTATATATTAAACAGATCG-
 TAATTTAAATACTAGATTTTTTGATCCTTCTGGAGGAGGAGATCCAATTT-
 TATATCAACATTTATTT

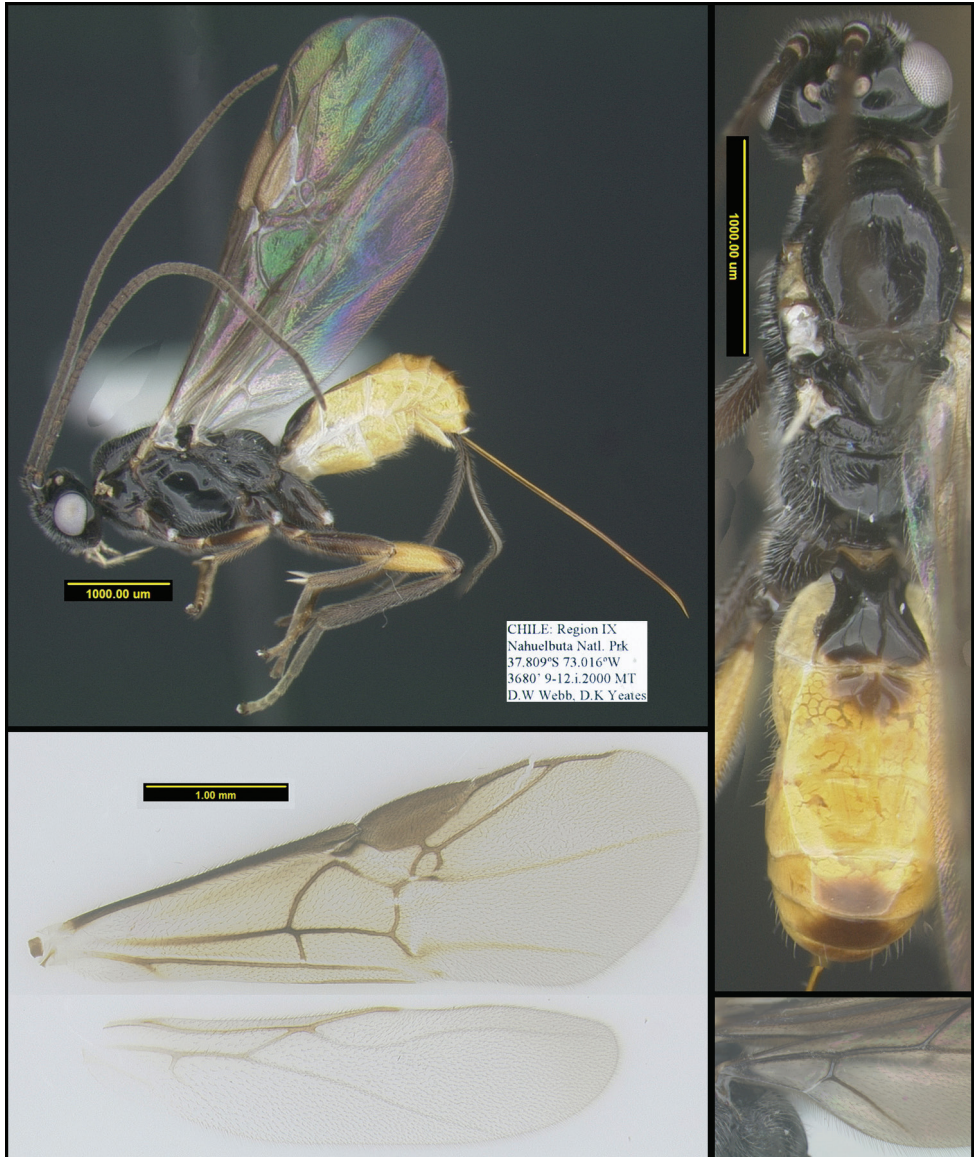


Figure 1. *Chilearinus covidchronos* Sharkey, sp. nov., holotype.

Morphological diagnosis. See key.

Paratypes. None.

Etymology. Named in acknowledgment of the covid pandemic occurring during the production of this manuscript.

***Chilearinus janbert* Sharkey, sp. nov.**

<http://zoobank.org/AF4C4A3B-EBD8-4305-AF39-DC9176C868A8>

Fig. 2

Holotype. ♀, Chile, Región IX, PN Nahualbuta, 37.493°S, 72.582°W, 1168 m, 8.ii.2005, Heraty, (Canadian National Collection).

Diagnosis. COI barcode. BOLD sample ID H12114. BOLD BIN: BOLD:AEM7846. GenBank Accession Code OL702760.

TTT TAGGATTATCAATAAGTTTAATTATTCGAATAGAATTAAGAGTAGGTGGTAATTTTATTGGTAATGATCAAATTTATAATAGGATTGTNACTGCTCATGCTTTTATTATAATTTT TTTTATAGTTATAACCAATTATAATTGGAGGATTTGGAAATTGATTAATTCATTAAATATTAGGGGGTCCAGATATAGCCTTCCCTCGAATAAATAATATAAGATTTTGATTATTAATTCCTTCATTATTATTATTAATTTTAAGATCTTTAATTAATGTTGGAGTAGGTACTGGATGAAGTGTATCCTCCTTTATCATTAAATATAAGTCATAGTGGTATATCTGTAGATTTGGCTATTTT TCTTTACATATTGCTGGAATTTCTTCAATTATAGGGGCTATAAATTTTATACAAC TATTTTAAATATATGAATAATTAATATTAATAATGATAAAATACCTTTATTAGTTTGATCAATTTTGATTACAGCAATTTTATTATTATTATCTTTACCAGTTT TAGCTGGGGCTATTACTATATTAAACAGATCGTAATTTAAATACTAGATTTTTTGATCCTTCTGGAGGGGGAGATCCAATTTTATATCAACATTTATTTTGATTTTT

Morphological diagnosis. See key.

Paratypes. None.

Etymology. A conjunction of Paul Hebert and Dan Janzen in recognition of their enormous contributions towards the conservation of nature.

***Earinus* Wesmael, 1837**

Note. In the Americas, there are three previously recognized species of *Earinus*, i.e., *E. erythropoda* Cameron, 1887, *E. limitaris* (Say, 1835), and *E. zeirapherae* Walley, 1935, and here we describe two more, *Earinus austinbakeri* sp. nov. and *Earinus walleyi* sp. nov. In the Nearctic, *Earinus* is common and widespread with the southernmost record being the sole recognized specimen of *E. erythropoda* from northern Sonora state, Mexico. *Earinus* differs from *Chilearinus* in the possession of pegs/spines in the foretibia and the characters given in the key.

Based on the collection in the Hymenoptera Institute (MS's personal collection, which will eventually be deposited in the CNC) and borrowed specimens, there are

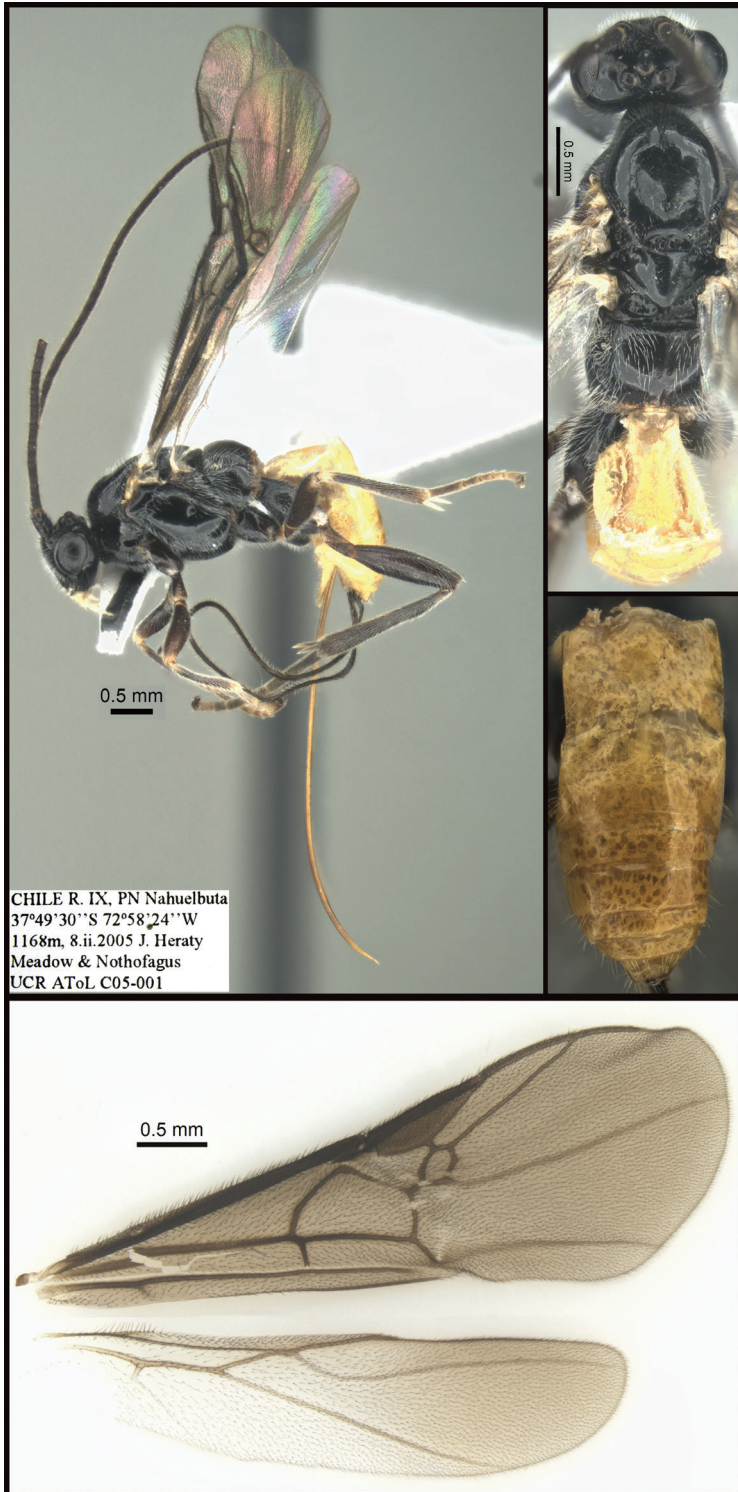


Figure 2. *Chilearinus janbert* Sharkey, sp. nov., holotype.

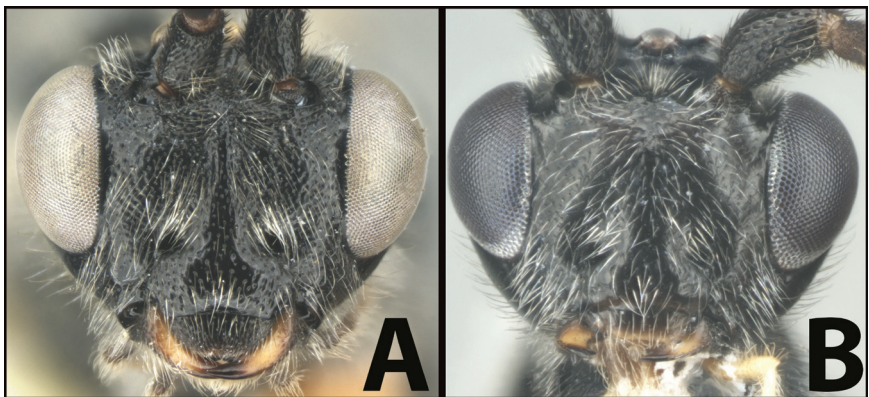
probably between eight and 12 species in the Nearctic region. They are extremely similar in color, but there are obvious differences among specimens in body dimensions, degree of punctation, color of the hind coxae, ocellar configuration, ovipositor length, length and density of setae on the ovipositor sheath, and dimensions of the first metasomal tergum. Unfortunately, these are not sufficient to allow confident delineation of species limits. For example, the differences in the key between *E. limitaris* and *E. erythropoda* are trivial. There are numerous specimens scattered over the Nearctic region that will key to *E. erythropoda*, but they might all be *E. limitaris*, or the two nominal species may be conspecific, or there may be multiple cryptic species. Likewise, there are probably a number of undescribed Nearctic species that will key to either *E. zeirapherae* or *E. austinbakeri*. In other words, the key is sufficient to discriminate among the barcoded species and *E. zeirapherae* but not among these and the undescribed species. The key is presented in part to satisfy the code of Zoological Nomenclature to act as a diagnosis for *E. austinbakeri* and *E. walleyi*. Only dense sampling of COI barcodes and perhaps other genes will supply the information necessary to delimit Nearctic *Earinus* species.

Key to the species of *Earinus* of North America

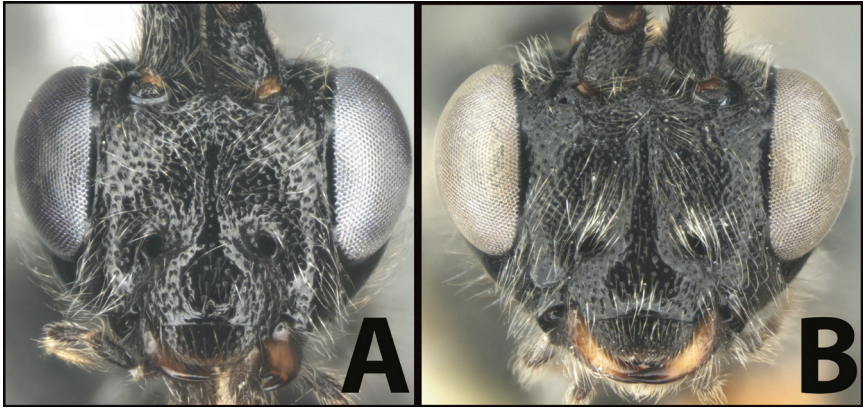
- 1 **A** Mid- and hind coxae slightly (**A**) to distinctly (**AA**) melanic, darker than their respective femora*E. zeirapherae*
- **B** Mid- and hind coxae mostly or entirely pale (yellow to orange) concolorous with their respective femora 2



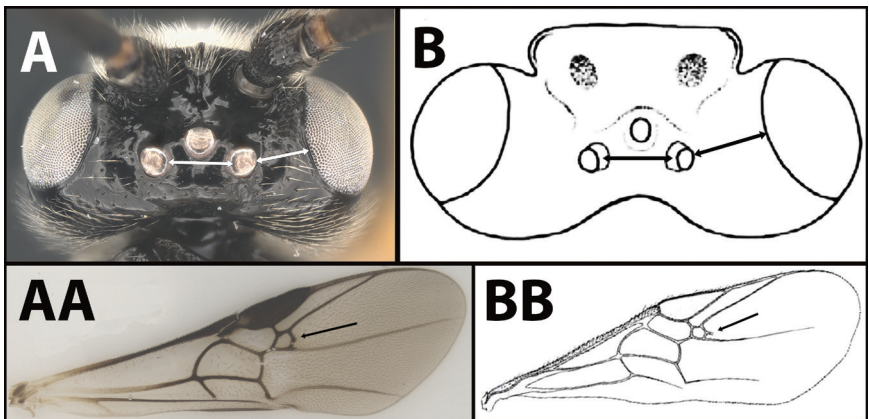
- 2(1) **A** Face distinctly punctate. Body length > 6 mm (average = 6.8 mm.)..... 3
- **B** Face mostly smooth with shallow punctation. Body length < 6 mm (average = 5.3 mm) 5



- 3(2) A Facial punctures deeper and wider
 *E. limitaris* variation, or perhaps *E. sp. nov.*
- B Facial punctures shallower and narrower 4



- 4(3) A Distance between lateral ocelli longer than distance between lateral ocellus and eye. AA Second submarginal cell lacking distinct 2RS2 vein
 *E. limitaris*
- B Distance between lateral ocelli equidistant or shorter than distance between lateral ocellus and eye. BB Second submarginal cell with distinct 2RS2 vein.
 *E. erythropoda*. [Line drawings modified from Berta (2000)]



- 5(2) **A** First metasomal tergum relatively longer and slimmer, distinctly longer than wide..... *E. austinbakeri*
- **B** First metasomal tergum relatively shorter and broader, about as long as wide..... *E. walleyi*

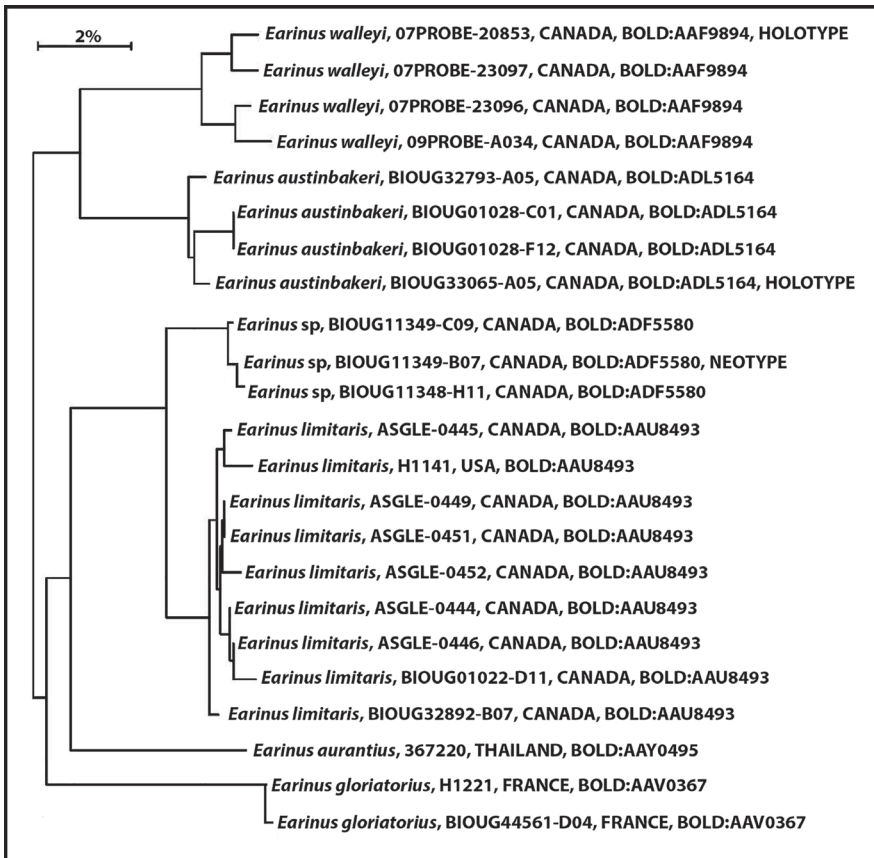
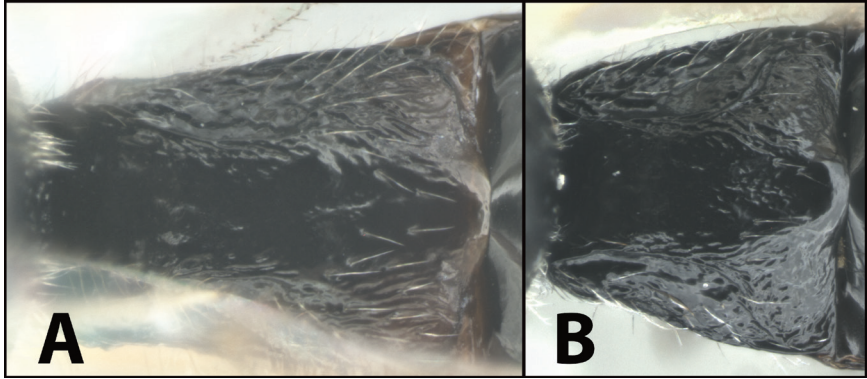


Figure 3. Neighbor joining tree of specimens of *Earinus* on BOLD with unique barcodes over 400 base pairs long (BOLD accessed 2022-1-20).

***Earinus austinbakeri* Sharkey, sp. nov.**

<http://zoobank.org/D169A981-8A48-4E53-B1D1-CB072D898147>

Figs 4, 5

Holotype. ♀, Canada, Ontario, Ferris Provincial Park, 44.2829°N, 77.7963°W, 131 m, 05–20.Jun.2014 (Canadian National Collection). BOLD sample ID BIOUG33065-A05, BOLD BIN code BOLD:ADL5164. GenBank Accession Code OM158425.

Diagnosis. Consensus barcode based on four specimens.

ATTTTATATTTTATATTTGGGATTTGATCYGGAATTGTGGGKT-TATCAATAAGTTTAATTATTCGTATGGARTTAAGAGTAGGGGGBAATT-

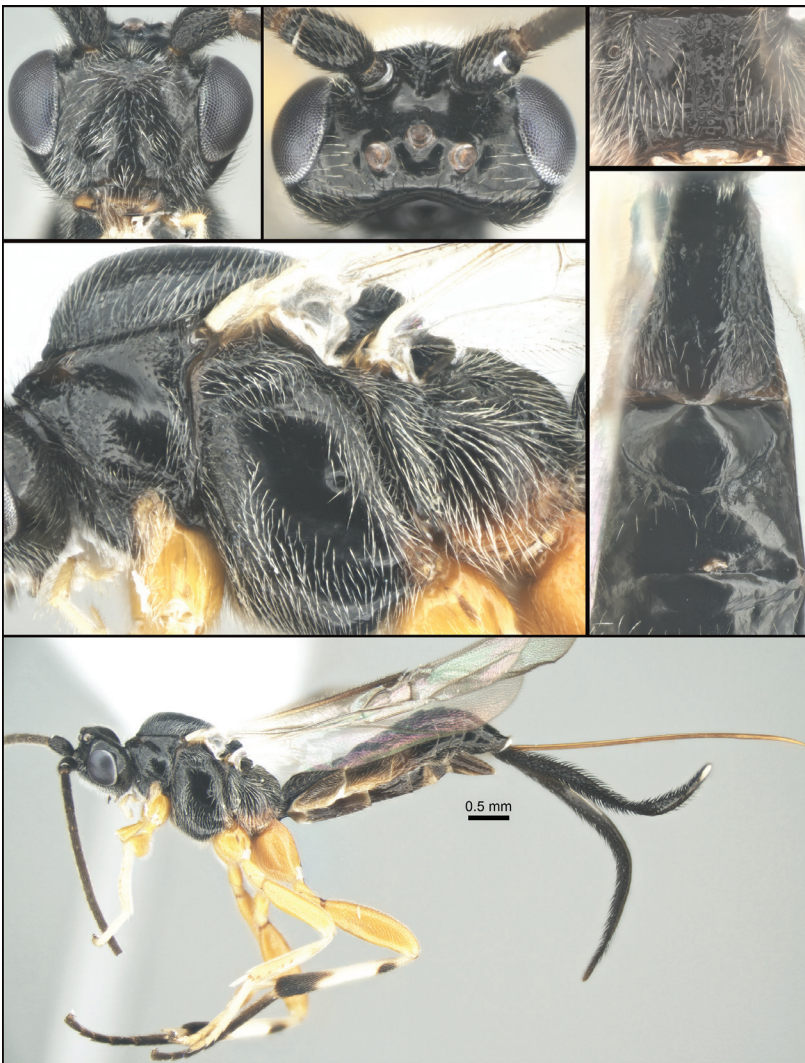


Figure 4. *Earinus austinbakeri* Sharkey, sp. nov., holotype.

TAATTGGKAATGATCAAATTTATAATAGTATTGTTACTGCTCATGCATT-TATTATAATTTTTTTTATAGTTATRCCAATTATAAATTGGTGGGTTTG-GTAATTGGTTAATTCCTTTAATATTAGGRGGTCCCGATATRGCTTTC-CCTCGAATGAAYAATATAAGRTTTTGATTATTAATTCCTTCTTTATT-ATTATTAATTTAAGATCTTTAATTAATATTGGGGTTGGAAGTGGTT-GAACGGTYTATCCTCCTTTATCATTRAATATAAGTCATAGTGGTATATCT-GTTGATTTGGCIATTTTTYTCTTTACATATTGCGGGGRATTTCTTCTAT-TATAGGGGCAATAAATTTTATTACTACTATTTTAAATATATGAATAATAAAT-ATTAAGTTGATAAAATGTCTTTATTRATTTGATCAATTTTAATTACTGC-TATTTTATTATATTATCTTTACCTGTTTTAGCRGGRGCAATTACTATAT-TATTAACAGATCGTAATTTAAATACAAGATTTTTTGATCCTTCTGGAG-GTGGGGATCCAATTTTATATCAACATTTATTT

Morphological diagnosis. Very similar to *E. austinbakeri* but differing by the characters given in the key as well as having the ovipositor sheath more setose. The COI barcodes of the two species differ by 6.29% (*p*-distance), reinforcing the conclusion that they are different species.

Paratypes. BIOUG01028-C01, BIOUG01028-F12, BIOUG32793-A05. These are sample IDs; the data for these specimens can be found by searching for these codes on BOLD (<http://www.boldsystems.org>).

Distribution. The holotype and paratypes were found at two localities just north and northeast of Lake Ontario. This species may be widespread throughout the eastern USA as far south as the Carolinas.

Etymology. Named in honor Austin Baker, hymenopterist extraordinaire.

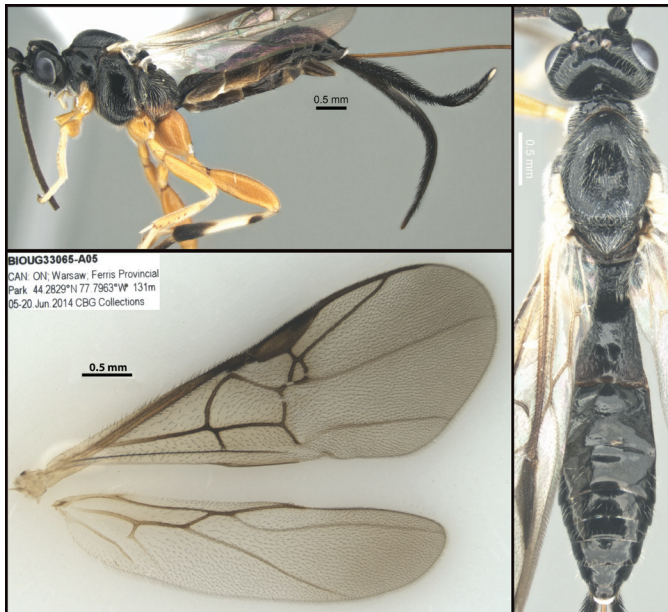


Figure 5. *Earinus austinbakeri* Sharkey, sp. nov., holotype.

***Earinus erythropoda* Cameron, 1887**

Holotype. ♀, “N. Sonora, Mexico, Morrison” (British Museum Natural BM3c893, viewed).

Notes. The sole identified specimen is the holotype. It differs little from many specimens that are widespread in the United States. It could be that they all belong to *E. limitaris*, or several more species may have similar morphologies. COI barcode data are needed. Several line drawings, modified from Berta (2000), are included in the key and others are in Berta’s (2000) treatment.

***Earinus limitaris* (Say, 1835)**

Figs 6, 7

Bassus limitaris Say, 1835.

Neotype. ♂, USA, West Virginia, Hardy County, 3 mi. NE Mathias, 38°55'N, 78°49'W, 30.viii–19.ix.2005 (Canadian National Collection). BOLD sample ID H1141. BOLD BIN code BOLD:AAU8493. GenBank Accession Code OM237775.

Diagnosis. Consensus COI barcode based on 9 specimens.

AATTTTATATTTTATATTTGGAATTTGATCAGGAATTTTAG-GTTTATCAATAAGATTAATTATTCGAATAGAATTAAGDATAGGTGG-TAATTTTRATTGGTAATGATCAAATTTATAATAGTGTTGTTYCTGCT-CATGCTTTTATTATAATTTTTTTTATAGTTATAACCAATTATGATTG-GRGGRTTTGGRAATTGATTAGTTCCTTTAATATTGGGRGGTCCTGA-TATAGCTTTYCCTCGAATAAATAATATAAGATTTTGATTATTAATTC-CTTCTTTATTATTATTAATTTTGAGTTCCTTTAATTAATATTGGGGTRGG-GACTGGKTGAACAGTTTATCCTCCRTTATCTTTAAATATAAGRCAT-AGTGGAATATCAGTTGATTTAGCTATTTTTTTCATTACATATYGCAG-GAATTTCTTCAATTATAGGGGCAATAAATTTTATTACTACTATYATAAATA-TATGAATAAATAATTTAAATTTGATAAAATACCTTTATTAGTTTGAT-CAATTTAATTACTGCTATTTTATTATTATTATCATTRCCAGTTTGTAGCTG-GRGCAATTACTATATTATTAACAGATCGAAATTTTRAATACAAGATTTTTT-GATCCTTCTGGAGGGGGGATCCAATTTTATATCAACATTTATTT

Morphological diagnosis. See key.

Other specimens with barcode data. ASGLE-0444, ASGLE-0446, ASGLE-0449, ASGLE-0451, ASGLE-0452, ASGLE-0445, BIOUG01022-D11, BIOUG32892-B07. These are sample IDs; data on them can be found by searching for these codes on BOLD (<http://www.boldsystems.org>).

Biology. The following are listed as hosts of *E. limitaris* by Yu et al. (2016); all belong to Noctuidae: *Egira dolosa*, *Enargia decolor*, *Homoglaea hircina*, *Ipimorpha pleonectusa*, and *Orthosia hibisci*. Because there are probably a number of cryptic species in *E. limitaris*, these records need confirmation.

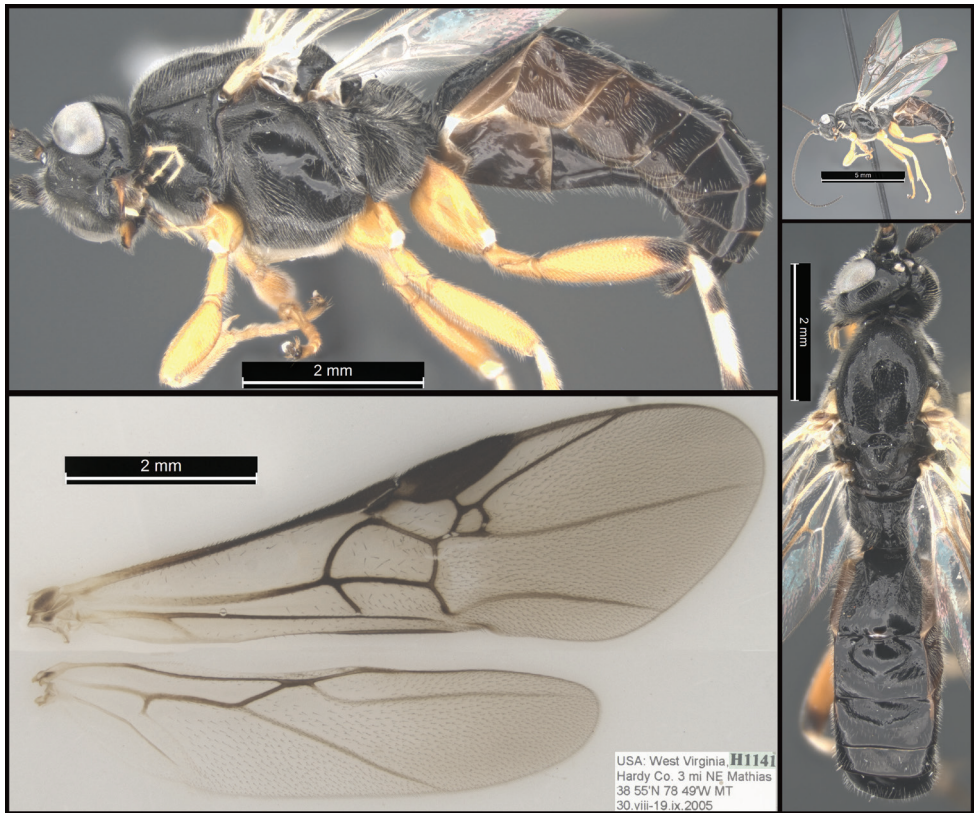


Figure 6. *Earinus limitaris*, neotype.

Notes. There are 15 specimens from one locality in Quebec that are in a different BIN (BOLD:ADF5580) which differs by only 2.54% (p -distance) from *E. limitaris* (*Earinus* sp. in Fig. 3). Because of the small distance between these two BINs, we refrain from describing this BIN as a new species but suggest that it may be a distinct species. Broader geographic sampling is required to clarify the significance of this barcode split.

Like many of Say's types, the type of *B. limitaris* is lost (Muesebeck 1927).

The following is from Say's original description.

"*B[assus] limitaris*. Black; feet honey-yellow.

Inhabits Missouri and Indiana.

Body black: palpi white: thorax longitudinally indented behind the middle: wings nearly hyaline, at base yellowish; nervures fuscous; stigma large; first cubital cell complete; second rather large, quadrangular: radial cellule also rather large: feet honey-yellow; posterior pair of tibiae whitish, their tips and annulus near the base black; posterior pair of tarsi black.

Length seven twentieths of an inch.

Var. a. Maxillary palpi, first joint black.

♀ Oviduct hairy, decurved, somewhat robust.”

Except for the body length, this description is consistent with all of the estimated 8–12 Nearctic species of *Earinus*. We have a number of specimens of what we believe to be *E. limitaris*. The neotype was selected because it is geographically closest to the two specimens included in Say’s (1835) original description, despite the fact that it is a male.

Distribution. Unknown, except for barcoded specimens (West Virginia, southern Ontario), as well as either Missouri or Indiana, or both. It is unknown if Say’s (1835) two specimens are conspecific. Based on specimens that one of us (MS) recently viewed, this species is probably widespread across southern Canada and northern United States, extending south as far as southern New Mexico (presumably at high altitudes) in the west and South Carolina in the east. The holotype of *E. erythropoda* may also belong here, which would extend the distribution into northern Sonora state, Mexico.



Figure 7. *Earinus limitaris*, neotype.

***Earinus walleyi* Sharkey, sp. nov.**

<http://zoobank.org/BDFBEADA-2082-46A5-B648-EB181E09CBB5>

Figs 8, 9

Holotype. ♀, Canada, Manitoba, Churchill pump house, 15 km S Churchill, Goose Creek Road, 58.3734°N, 94.1342°W, 3–7.vii.2007, Malaise trap (Canadian National Collection). BOLD sample ID. 07PROBE-20853, BOLD BIN code BOLD:AAF9894. GenBank Accession Code FJ413805.

Diagnosis. Consensus barcode based on four specimens.

TATTTTATATTTTATATTTGGAATTTGATCAGGTATTGTAGGTT-
TATCAATAAGATTAATTATTCGAATGGAATTAAGAGTGGGRGGTAATT-
TAATTGGRAATGATCAAATTTATAATAGTATTGTTACTGCTCATGCTTT-
TATTATAATTTTTTTTATAGTTATAACCTATTATAATTGGGGGRTTTGG-
TAATTGATTARTCCCATTAATATTGGGAGGTCCTGATATAGCTTTCC-
CTCGTATAAATAATATGAGATTTTGATTATTAATCCCYTCTTTATTAAT-
ATTAATTTTAAGATCTTTAATTAATATTGGAGTAGGGACTGGTTGGA-
CAGTTTATCCTCCKTTATCATTAAATATAAGTCATAGTGGAAATATCT-
GTTGATTTGGCTATTTTTTCTTTACATATTGCGGGRGTTCCTTC-
TATTATAGGGGCAATAAATTTTATTACTACTATTTTAAATATRT-

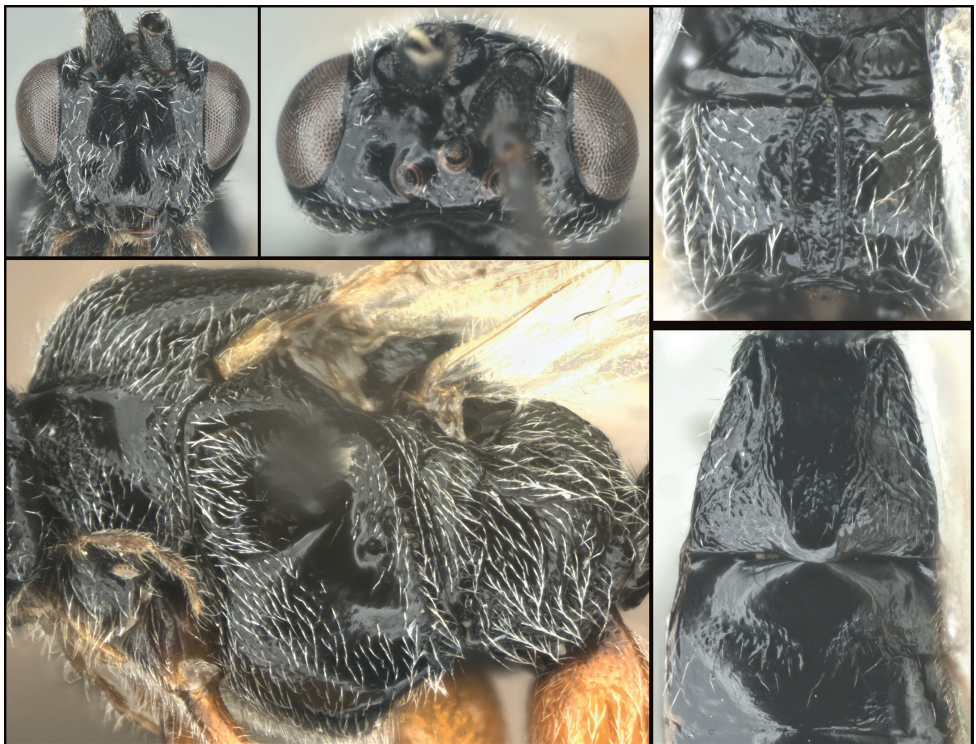


Figure 8. *Earinus walleyi* Sharkey, sp. nov., holotype.

GAATAATAAATATTTAAAATTGATAAAATGTCTTTATTAATTTGAT-
CAATTTTAATTACTGCTATTTTATTATTATTRTCTTTACCAGTTT-
TAGCAGGAGCTATTACTATATTATTAACAGATCGTAATTTAAATA-
CAAGATTTTTTGATCCTTCYGGAGGGGGTGACCCAATTTTATAT-
CAACATTTATTT

Morphological diagnosis. Very similar to *E. zeirapherae*, differing by the characters given in the key as well as having the ovipositor sheath less setose. The COI barcodes of the two species differ by 6.29% (p -distance) all but ensuring that they are different species.

Paratypes. All are from the same locality as the holotype, 07PROBE-23096, 07PROBE-23097, 09PROBE-A0304. These are specimen IDs; more data on the specimens can be found by searching for these codes on BOLD (<http://www.boldsystems.org>).

Distribution. Unknown but likely widespread in Alaska and northern and mid-latitudinal areas of Canada. Some or all records in Yu et al. (2016) for *E. zeirapherae* occurring from Alaska, Nunavut, and the Yukon may belong to this species.

Etymology. Named in honor Stuart Walley (RIP), former research scientist at the Canadian National Collection and author of *E. zeirapherae*.

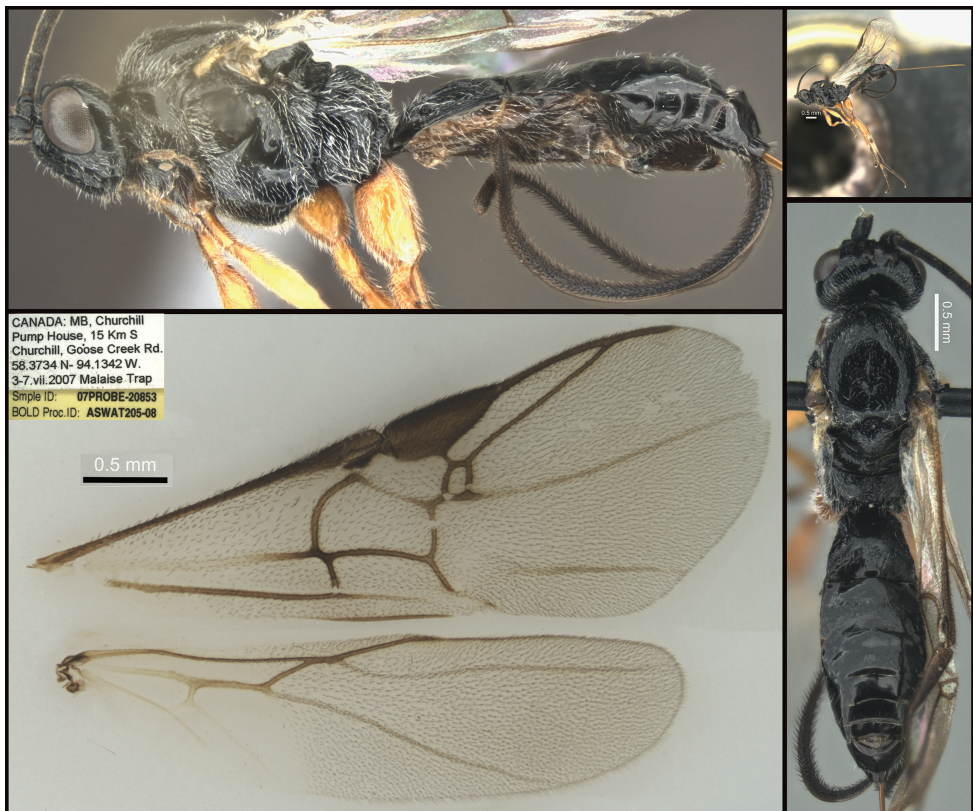


Figure 9. *Earinus walleye* Sharkey, sp. nov., holotype.

***Earinus zeirapherae* Walley, 1935**

Figs 10, 11

Holotype. ♀, Grand River, Nova Scotia, 11.May.1932 (M. L. Prebble) No. 3847 (Canadian National Collection, viewed).

Biology. The following are all reported as hosts by Yu et al. (2016). All belong to Tortricidae: *Acleris hudsoniana*, *Choristoneura rosaceana*, *Rhyacionia adana*, *Zeiraphera canadensis*, *Zeiraphera griseana*, and *Zeiraphera ratzeburgiana*. Since there are many species, including *E. austinbakeri* and *E. walleyi*, that are morphologically similar to *E. zeirapherae*, all hosts that do not belong to the genus *Zeiraphera* need confirmation.



Figure 10. *Earinus zeirapherae*, holotype female.

Notes. The holotype (Fig. 10) is from Nova Scotia, as is the male in Figure 11; both were reared from *Zeiraphera ratzburgiana*. Contrary to the image of the holotype in Figure 10, the original description by Walley (1935) states that the fore and mid coxae and hind coxa are basally blackish, “front and middle coxae mostly, all trochanters faintly, hind coxae basally ... blackish.” (Walley 1935: 56). It seems likely that over time the coxae of the holotype have faded. There are other specimens in the Canadian National Collection that have similar coloration but that are not likely to be conspecific based on other characters, e.g., one specimen from New Mexico. This serves as a reminder that the key will only function to separate the described species from each other.



Figure 11. *Earinus zeirapherae*, male.

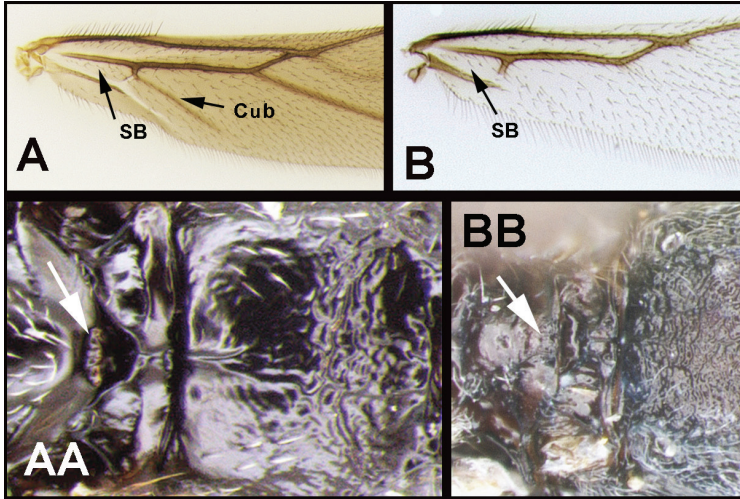
Key to the New World genera of Agathidinae

(Modified from Sharkey et al. 2021)

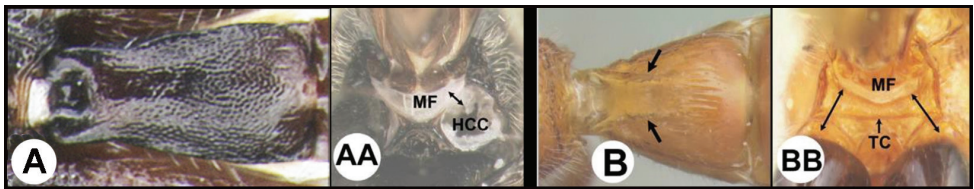
- 1 **A** Forewing venation greatly reduced; RS absent and crossvein r present only as a short stub; Neotropical, rare **Mesocoelus**
- **B** Forewing venation moderately reduced; apical abscissa of RS absent, or mostly so, but crossvein r complete to junction of RS; Neotropical and rare **2**
- **C** Forewing venation not significantly reduced; apical abscissa of RS complete or almost complete to wing margin; widespread, common (99+ % of specimens) **4**



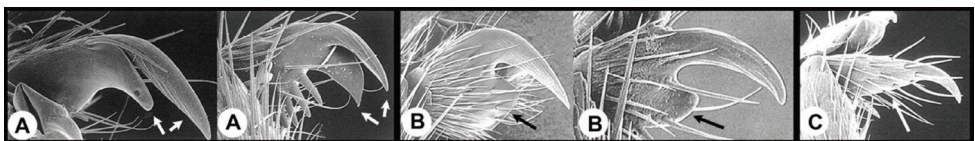
- 2(1) **A** Hind wing subbasal (SB) cell 4-sided with vein Cub emanating from an angle in the cell AND/OR **AA** Posterior surface of scutellum with a semi-circular or arc-shaped depression (post-scutellar depression) *Therophilus* (in part)
- **B** Hind wing subbasal (SB) cell 3-sided. If Cub vein is present, it emanates from a straight vein. **BB** Post scutellar depression absent, but rugose sculpture usually present 3



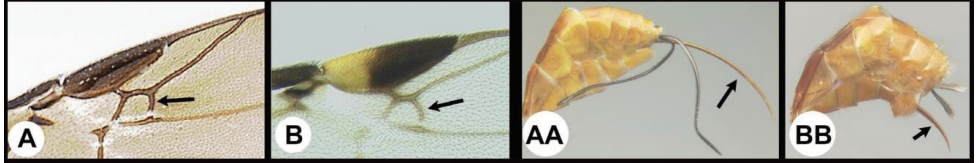
- 3(2) **A** Median area of first tergum not raised above lateral portions and granulate or striogranulate. **AA** Hind coxal cavities (HCC) open to metasomal foramen or narrowly closed and positioned partly above ventral margin of metasomal foramen (MF)..... *Plesiocoelus*
- **B** Median area of first tergum raised above lateral portions, sculpture variable but often smooth or smoothly striate. **BB** Hind coxal cavities closed and positioned completely below the metasomal foramen; ventral margin of metasomal foramen with a strong, relatively straight transverse carina (TC) *Aerophilus* (in part)



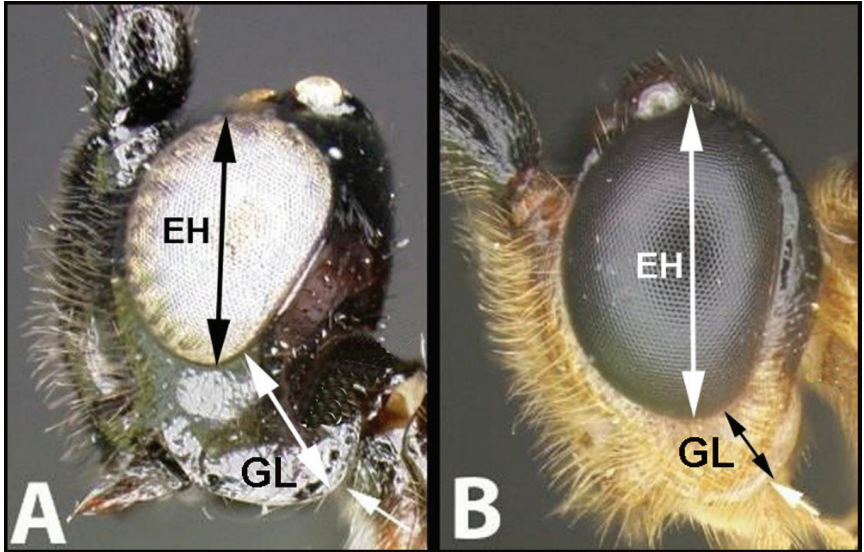
- 4(1) **A** Fore tarsal claws bifid 5
- **B** Fore tarsal claws simple, with distinct basal lobe..... 9
- **C** Fore tarsal claws simple, lacking a distinct basal lobe..... 31



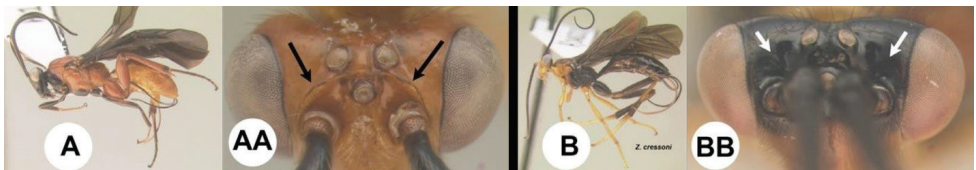
- 5(4) **A** Forewing areolet quadrate, not or only slightly narrower anteriorly. **AA** Ovipositor as long as or longer than half the length of metasoma 7
- **B** Forewing areolet triangular or if quadrate much narrower anteriorly. **BB** Ovipositor shorter than half the length of metasoma 6



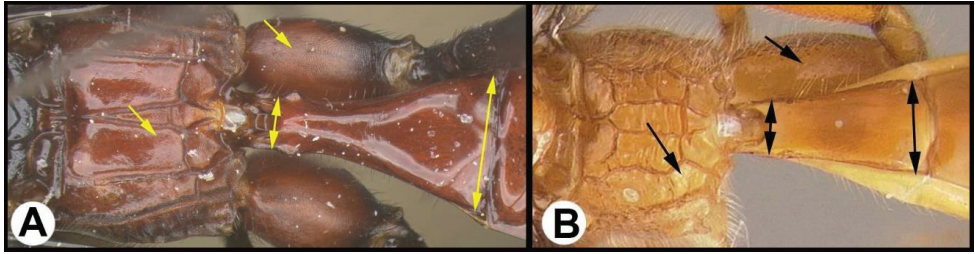
- 6(5) **A** Gena expanded into a flange posteriorly; malar space (MS) >1/2 length of eye height (EH); Neotropical, rare *Hemichoma*
- **B** Gena not modified into a flange posteriorly; malar space (MS) <1/2 length of eye height (EH); widespread, common *Zelomorpha*



- 7(5) **A** Body predominantly orange/yellow. **AA** Frons bordered by a carina posteriorly; widespread, common..... 8
- **B** Body predominantly black. **BB** Frons not bordered by a carina posteriorly; southern USA through the tropical Neotropics..... *Zacremnops*



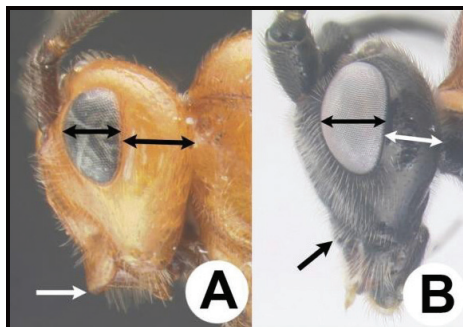
- 8(7) **A** Propodeum and hind coxa with granulate sculpture; first metasomal tergum almost 3× wider at apex than at base; rare; Neotropical, rare *Labagathis*
- **B** Propodeum and hind coxa lacking granulate sculpture; first metasomal tergum not nearly 3× wider at apex than at base; common; widespread, relatively common *Cremonops*



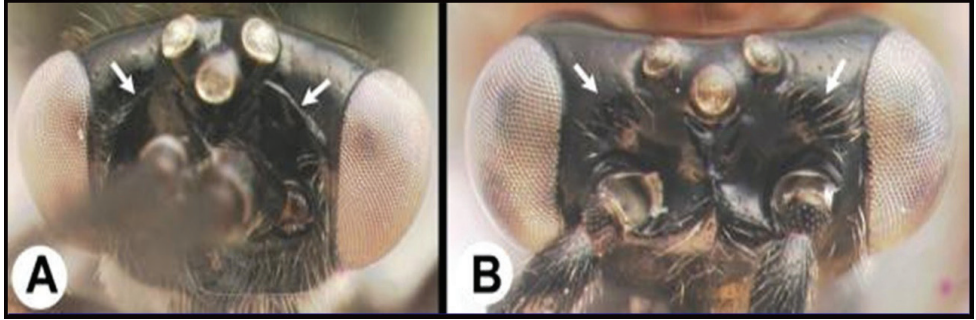
- 9(4) **A** Notauli present, though sometimes weak 10
- **B** Notauli completely absent 25



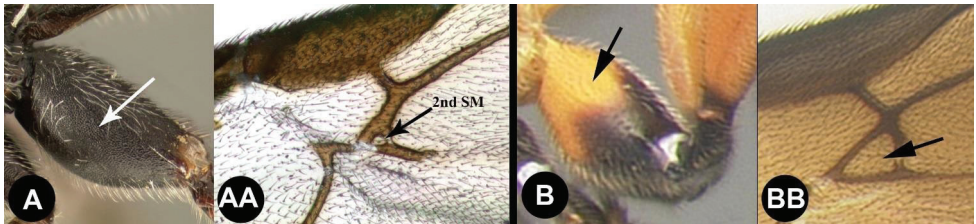
- 10(9) **A** Ventral margin of clypeus projecting; width of temple longer than width of eye in lateral view; Nearctic, rare *Gelastagathis*
- **B** Ventral margin of clypeus not projecting; width of temple shorter than width of eye in lateral view; widespread, common 11



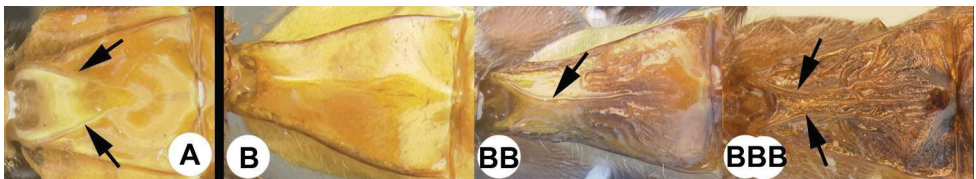
- 11(10) **A** Frons bordered by carinae or grooves posteriorly 12
- **B** Frons not bordered by carinae or grooves posteriorly 14



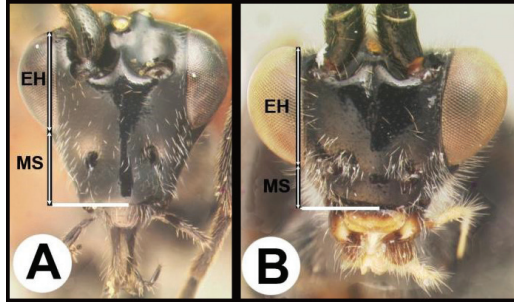
- 12(11) **A** Hind coxa with granulate sculpture. **AA** Second submarginal cell minute or absent; Neotropical, rare *Trachagathis*
- **B** Hind coxa smooth, lacking granulate sculpture. **BB** Second submarginal cell of normal dimensions; widespread, relatively common 13



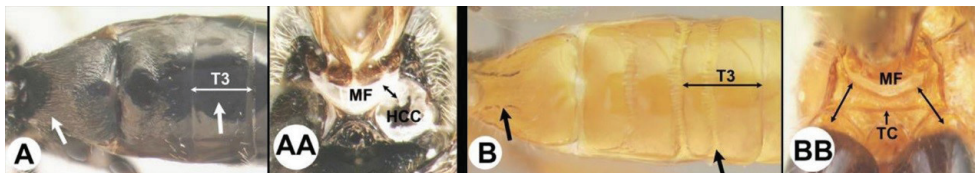
- 13(12) **A** First metasomal tergum smooth with two widely spaced converging carinae forming a tear-shaped basal area; Neotropical, rare *Pharpha*
- **B** First metasomal tergum usually smooth and convex, or **BB** with a median longitudinal carina, or **BBB** rarely with 2 carinae in which case the tergum has more extensive sculpture; widespread, common *Alabagrus*



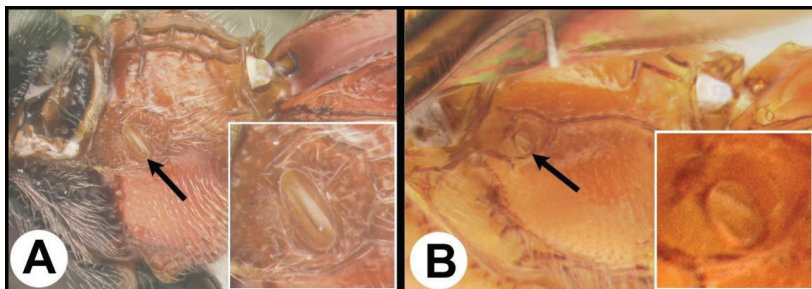
- 14(11) **A** Malar space (MS) distinctly $> \frac{1}{2}$ eye height (EH). Head shape in frontal view elongate, at least as high (measure from ventral margin of clypeus) as wide..... **15**
- **B** Malar distance usually (95%) $\leq \frac{1}{2}$ eye height. Head shape in frontal view wide, wider than high (measure from ventral margin of clypeus) **16**



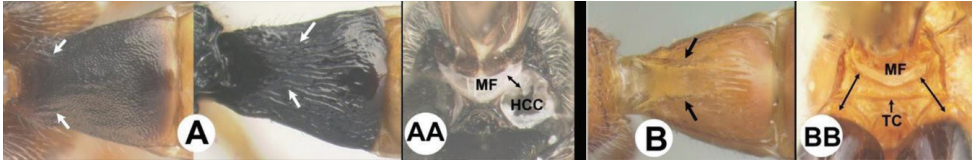
- 15(14) **A** Third tergum completely smooth; pair of carinae on first tergum not prominent. **AA** Hind coxal cavities (HCC) open to metasomal foramen or narrowly closed and positioned partly above ventral margin of metasomal foramen (MF); common in the Nearctic, very rare in the Neotropics *Agathis* (in part)
- **B** Third tergum usually (95%) partly or completely sculptured, often sculpture confined to narrow line along transverse depression; pair of carinae on first tergum prominent. **BB** Hind coxal cavities closed and positioned completely below the metasomal foramen; ventral margin of metasomal foramen with a strong, relatively straight transverse carina (TC); widespread, common..... *Aerophilus* (in part)



- 16(14) **A** Propodeal spiracle elongate, $> 2\times$ longer than wide; widespread, common *Pneumagathis*
- **B** Propodeal spiracle circular or oval, $< 2\times$ longer than wide **17**



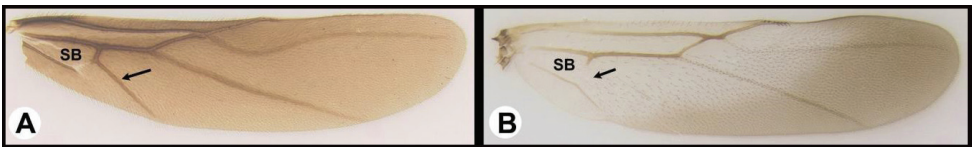
- 17(16) **A** Pair of carinae on first tergum NOT prominent. **AA** Hind coxal cavities (HCC) open to metasomal foramen or narrowly closed and positioned partly above ventral margin of metasomal foramen (MF)..... **18**
- **B** Pair of carinae on first tergum prominent; **BB** Hind coxal cavities closed and positioned below the metasomal foramen; ventral margin of metasomal foramen with a strong, relatively straight transverse carina (TC); widespread, common **Aerophilus (in part)**



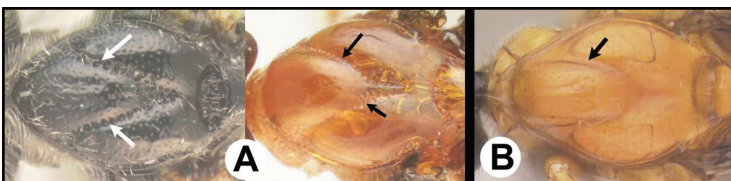
- 18(15) **A** First tergum completely smooth, or rarely with some punctures posterolaterally..... **20**
- **B** First tergum with sculpture **19**



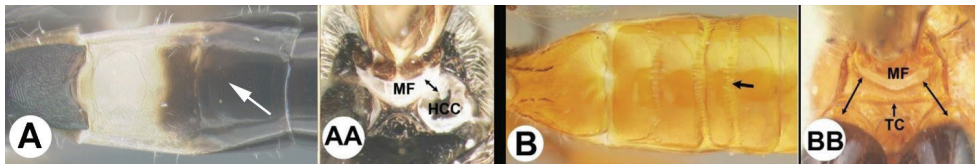
- 19(18) **A** Cub vein of hind wing long and partly tubular, apical margin of subbasal (SB) cell angled; widespread, common..... **Therophilus (in part)**
- **B** Cub vein of hind wing weak or absent and never tubular; apical margin of subbasal cell (SB) straight. Nearctic and northern Neotropics, i.e., Mexico and Central America, rare **Agathirsia (in part)**



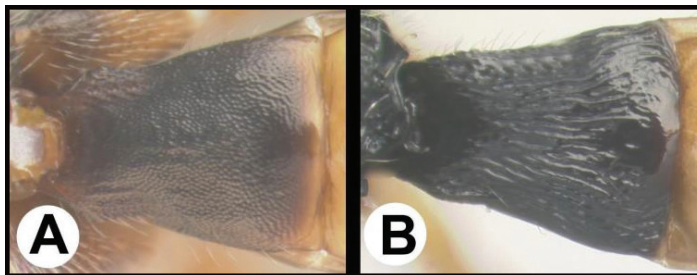
- 20(18) **A** Notauli pitted or crenulate **21**
- **B** Notauli smooth **24**



- 21(17) **A** Third tergum usually entirely smooth or weakly and partly coriarius (leather-like), if with different sculpture (especially in transverse depressions) then pair of longitudinal carinae on first metasomal tergum weaker than in B or absent. **AA** Hind coxal cavities (HCC) open to metasomal foramen or narrowly closed and positioned partly above ventral margin of metasomal foramen (MF) **22**
- **B** Third tergum usually partly or completely sculptured, often sculpture confined to narrow line along transverse depression. **B** Pair of longitudinal carinae on first metasomal tergum present and extending past spiracles. **BB** Hind coxal cavities closed and positioned entirely below the metasomal foramen (MF); ventral margin of metasomal foramen with a strong, relatively straight transverse carina (TC); widespread, common.....*Aerophilus* (in part)



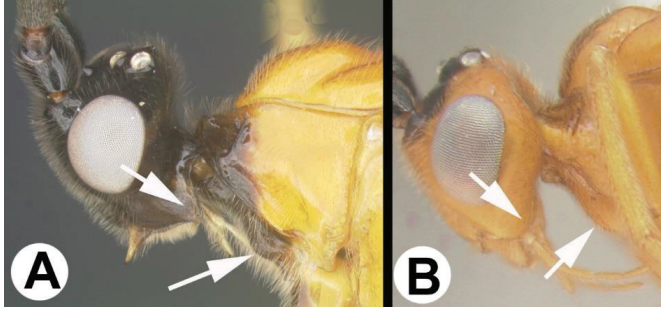
- 22(21) **A** First tergum partly or completely granulate; widespread, common
 *Neothlipsis*
- **B** First tergum otherwise sculptured, usually striate or rugosostriate **23**



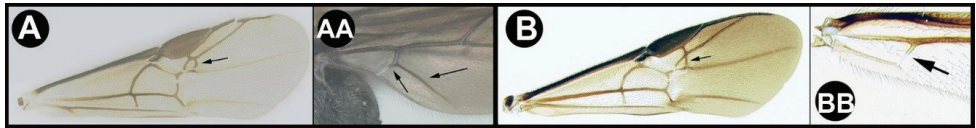
- 23(22) **A** Posterior apex of scutellum with a distinct depression in the form of a semi-circle or two distinct pits; widespread, common..... *Therophilus* (in part)
- **B** Posterior apex of scutellum lacking depression, smooth to rugose; common in the Nearctic, very rare in the Neotropics.....*Agathis* (in part)



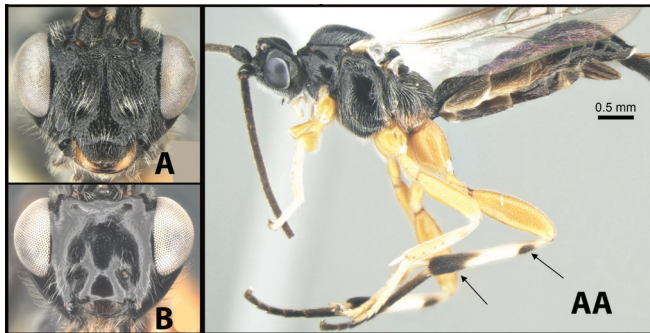
- 24(19) **A** Propleuron with a distinct protuberance; gena expanded into an acute angle posteroventrally; Neotropical, rare*Zamicrodus*
- **B** Propleuron flat or weakly convex, lacking a distinct protuberance; genae not expanded and rounded posteroventrally; Neotropical, rare.....*Aphelagathis*



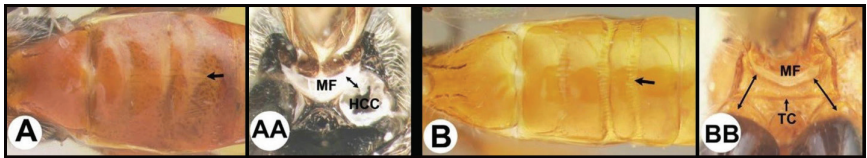
- 25(9) **A** Second submarginal cell of forewing quadrate. **AA** Cub vein of hind wing present and often tubular; subbasal cell angled distally at junction of Cub.....**26**
- **B** Not combining the above character states. **B**. Second submarginal cell usually triangular. **BB** Cub vein of hind wing usually absent or not tubular and subbasal cell not angled distally; widespread, common.....**27**



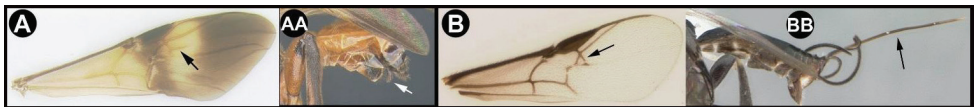
- 26(25) **A** Face distinctly punctate **AA**. Body and antenna black, all femora pale (yellow to orange), hind tibia pale (yellow to orange with a melanic apex and a melanic ring or lateral spot subbasally. **AAA** Holarctic and Oriental (in the Americas from northern Canada and rarely as far south as northern Mexico) *Earinus*
- **B** Face smooth with very tiny punctation **BB** Often brightly colored and otherwise not as above. **BBB** Neotropical: Chile, and southern Argentina, and rarely in high altitudes of the Andes far north as Colombia and Ecuador *Chilearinus*



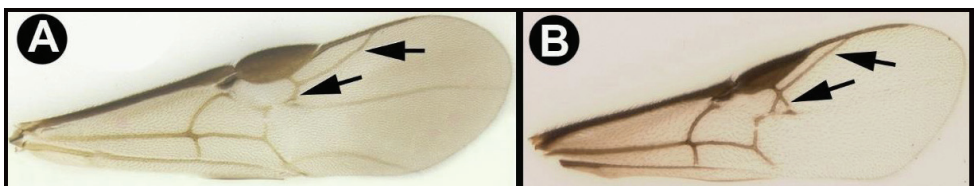
- 27(25) **A** Third tergum completely smooth. **AA** Hind coxal cavities (HCC) open to metasomal foramen (MF), or narrowly closed such that the ventral part of the metasomal foramen is below the dorsal margin of the hind coxal cavities..... 28
- **B** Third tergum usually (95% of specimens encountered) partly or completely sculptured, often sculpture confined to narrow lines along transverse depressions. **BB** Hind coxal cavities closed and positioned completely below the metasomal foramen; ventral margin of metasomal foramen with a strong, relatively straight transverse carina; widespread, common *Aerophilus* (in part)



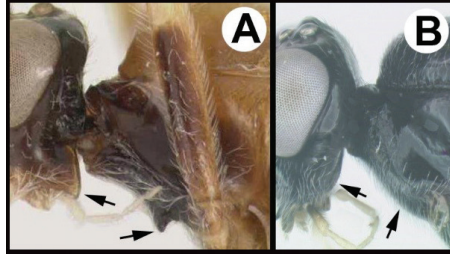
- 28(27) **A** Spurious vein, RS2b, well developed. **AA** Ovipositor barely exerted, much shorter than metasoma; Neotropical, very rare *Marjoriella*
- **B** Spurious vein, RS2b, lacking. **BB** Ovipositor at least as long as metasoma 29



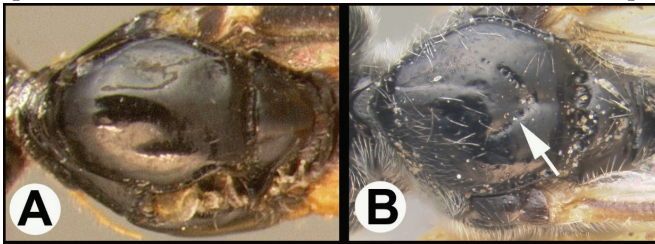
- 29(28) **A** Second submarginal cell smaller than its dorsal stem; apical abscissa of RS curving towards fore margin of wing; Neotropical, very rare *Smithagathis*
- **B** Second submarginal cell larger than its dorsal stem; apical abscissa of RS straight 30



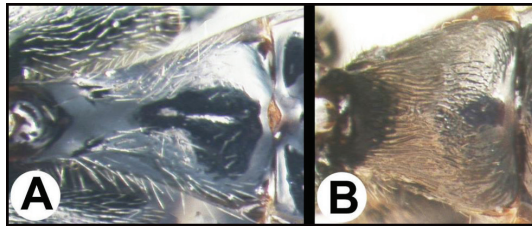
- 30(29) **A** Posterolateral corner of gena sharp; propleuron with a protuberance; Neotropical, rare *Amputoearinus*
- **B** Posterolateral corner of gena rounded; propleuron evenly convex, lacking a protuberance; widespread, common..... *Lytopylus*



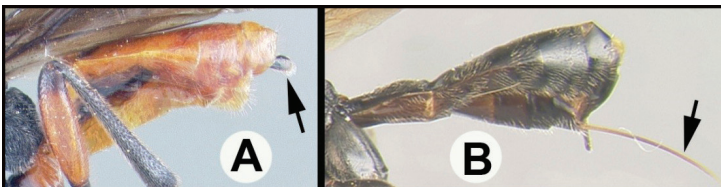
- 31(4) **A** Notauli absent, mesoscutum completely smooth; Neotropical, rare *Sesioctonus*
- **B** Notauli present though sometimes only indicated anteriorly or posteriorly; widespread and common in the Nearctic, rare in the Neotropics 32



- 32(31) **A** First tergum smooth, lacking microsculpture and pair of longitudinal carinae, at most with punctures laterally 33
- **B** First tergum with microsculpture, usually in the form of longitudinal striae or rugae; widespread and common in the Nearctic, extremely rare in the Neotropics *Agathis* (in part)



- 33(32) **A** Ovipositor barely exerted, shorter than half the length of metasoma; Nearctic and Central America, rare *Crassomicrodus*
- **B** Ovipositor at least as long as half the metasoma, often much longer; Nearctic and Central America, rare *Agathirsia* (in part)



References

- Berta DC (2000) Contribución sobre las especies neotropicales del género *Earinus* Wesmael (Himenóptera: Braconidae, Agathidinae). Boletín de la Asociación Española de Entomología 24: 229–241. <https://notablesdelaciencia.conicet.gov.ar/handle/11336/78424>
- Braet Y (2002) Contribution to the knowledge of Agathidinae (Hymenoptera Braconidae) from French Guiana with description of two new species of *Earinus* Wesmael, 1837. Belgian Journal of Entomology 4: 41–51.
- Ivanova NV, Grainger CM (2007) CCDB protocols, COI amplification. http://ccdb.ca/site/wp-content/uploads/2016/09/CCDB_Amplification.pdf [accessed 1 July 2019]
- Ivanova NV, Dewaard JR, Hebert PDN (2006) An inexpensive, automation-friendly protocol for recovering high-quality DNA. Molecular Ecology Resources 6(4): 998–1002. <https://doi.org/10.1111/j.1471-8286.2006.01428.x>
- Muesebeck CFW (1927) A revision of the parasitic wasps of the subfamily Braconinae occurring in America north of Mexico. Proceedings of the United States National Museum 69(2642): 1–73. <https://doi.org/10.5479/si.00963801.69-2642.1>
- Say T (1835) Descriptions of new North American Hymenoptera, and observations on some already described. Boston Journal of Natural History 1(3): 210–305. <https://www.biodiversitylibrary.org/page/32413933>
- Sharkey MJ (1997) Subfamily Agathidinae. In: Wharton RA, Marsh PM, Sharkey MJ (Eds) Manual of the New World genera of Braconidae (Hymenoptera). Special Publication of the International Society of Hymenopterists, Vol. 1., 69–84.
- Sharkey MJ, Meierotto S, Chapman EG, Janzen DJ, Hallwachs W, Dapkey T, Solis MA (2018) *Alabagrus* Enderlein (Hymenoptera, Braconidae, Agathidinae) species of Costa Rica, with an emphasis on specimens reared from caterpillars in Area de Conservación Guanacaste. Contributions in Science 526: 31–180. <https://doi.org/10.5962/p.320146>
- Sharkey MJ, Janzen DH, Hallwachs W, Chapman EG, Smith MA, Dapkey T, Brown A, Ratnasingham S, Naik S, Manjunath R, Perez K, Milton M, Hebert PDN, Shaw SR, Kittel RN, Solis MA, Metz MA, Goldstein PZ, Brown JW, Quicke DLJ, van Achterberg C, Brown BV, Burns JM (2021) Minimalist revision and description of 403 new species in 11 subfamilies of Costa Rican braconid parasitoid wasps, including host records for 219 species. ZooKeys 1013: 1–665. <https://doi.org/10.3897/zookeys.1013.55600>
- Spinola M (1851) *Ichneumonónidos*. In: Gay C (Ed.) Historia física y política de Chile. Zoología 6: 471–550.
- Walley GS (1935) Five new species of Braconidae with host records of additional species. Canadian Entomologist 67(3): 55–61. <https://doi.org/10.4039/Ent6755-3>
- Yu DSK, van Achterberg C, Horstmann K (2016) Taxapad, Ichneumonoidea. Vancouver. <http://www.taxapad.com>
- Zamani A, Vahtera V, Sääksjärvi IE, Scherz MD (2020) The omission of critical data in the pursuit of “revolutionary” methods to accelerate the description of species. Systematic Entomology 46(1): 1–4. <https://doi.org/10.1111/syen.12444>

New species and new records of the genus *Filatima* Busck, 1939 (Lepidoptera, Gelechiidae) from Central Asia

Oleksiy Bidzilya¹, Peter Huemer²

1 Institute for Evolutionary Ecology of the National Academy of Sciences of Ukraine, 37 Academician Lebedev str., 03143, Kiev, Ukraine **2** Tiroler Landesmuseen Betriebsges.m.b.H., Sammlungs- und Forschungszentrum, Naturwissenschaftliche Sammlungen, Krajnc-Str. 1, 6060 Hall in Tirol, Austria

Corresponding author: Oleksiy Bidzilya (olexbid@gmail.com)

Academic editor: Mark Metz | Received 20 February 2022 | Accepted 4 April 2022 | Published 3 May 2022

<http://zoobank.org/76811B37-D047-4F53-8F51-FBED91622021>

Citation: Bidzilya O, Huemer P (2022) New species and new records of the genus *Filatima* Busck, 1939 (Lepidoptera, Gelechiidae) from Central Asia. ZooKeys 1099: 87–110. <https://doi.org/10.3897/zookeys.1099.82530>

Abstract

Four new species of *Filatima* Busck, 1939 are described from Central Asia: *Filatima armata* **sp. nov.** (Iran), *F. subarmata* **sp. nov.** (Pakistan, Iran), *F. afghana* **sp. nov.** (Afghanistan), and *F. karii* **sp. nov.** (Tajikistan). The hitherto unknown female of *Filatima multicornuta* Bidzilya & Nupponen, 2018 is described. Recorded to occur for the first time are *Filatima textorella* (Chrétien, 1908) from North Macedonia and Turkey, *F. pallipalpella* (Snellen, 1884) from Kyrgyzstan, and *Filatima zagulajevi* Anikin & Piskunov, 1996 from Kazakhstan. *Filatima fontisella* Lvovsky & Piskunov, 1989 is removed from the list of Russian Gelechiidae due to re-identification of the only record as *F. multicornuta*. An annotated checklist of Palearctic *Filatima* species is provided.

Keywords

Afghanistan, Gelechiinae, Iran, Pakistan, Palearctic Region, Russia, systematics, taxonomy

Introduction

Filatima Busck, 1939 is a large genus of Holarctic Gelechiidae with the majority of species known from North America (Lee et al. 2009). The systematic position of the genus is still rather unclear. Both male and female genitalia are very peculiar and show no clear relation to other genera in the Gelechiidae. However, species in the genus share

the feature of a deeply separated segment VIII into a free tergum and sternum, which is a putative synapomorphy for Gelechiinae (Hodges 1999). Within this subfamily the genus has been placed in the tribe Gelechiini provisionally near *Aroga* Busck, 1914 and *Athrips* Billberg, 1820 (Huemer and Karsholt 1999). Hodges (1999: 15) proposed and developed the argument that *Chionodes* Hübner, [1825], *Aroga*, and *Filatima* “comprise a closely related, highly speciose group”. Recently obtained results of molecular studies place the genus closest to *Aroga* and *Stegasta* Meyrick, 1904 (Karsholt et al. 2013), and these authors already stressed the need of increased taxon sampling.

Eight species of the European fauna were revised by Huemer and Karsholt (1999). Later two additional species were described, one from Romania (Kovács and Kovács 2001) and one from Spain (Corley 2014). Compared with the European fauna the Asian species remained poorly studied. By the end of the 20th century only nine species had been recorded from Kyrgyzstan eastwards to the Amur region of Russia and Eastern China (Sattler 1968; Ivinskis and Piskunov 1989; Lvovsky and Piskunov 1989; Bidzilya et al. 1998). Recently new species were described from Southern Siberia and two new synonyms have been established (Bidzilya and Nupponen 2018). On the basis of these studies the genus currently comprises 57 Nearctic (Lee et al. 2009) and 19 Palearctic species.

Here we provide descriptions of four new species from Central Asia, and also describe the hitherto unknown female of *F. multicornuta* Bidzilya & Nupponen, 2018. We also provide an annotated list of Palearctic species of *Filatima* updated according to taxonomic changes proposed in the last few decades and new faunistic records.

Materials and methods

Male and female genitalia were dissected and prepared using standard methods for the Gelechiidae (Huemer and Karsholt 2010). Male genitalia were spread implementing the unrolling technique described by Pitkin (1986) and Huemer (1988). The descriptive terminology of the genitalia structures follows Huemer and Karsholt (1999); the order of species in the checklist is alphabetical. Pinned specimens were photographed with a Canon EOS 5DSR DSLR camera attached to an Olympus SZX12 stereomicroscope. Slide-mounted genitalia were photographed with a Canon EOS 600D DSLR camera mounted on an Olympus U-CTR30-2 trinocular head mounted on a Carl Zeiss compound microscope. For each photograph, sets of 10–20 images were taken at different focal planes and focused-stacked using Helicon Focus 6 with the final image edited in Adobe Photoshop CS5.

Abbreviations of collections

- NHMB** Hungarian Natural History Museum, Budapest, Hungary
NHMV Naturhistorisches Museum, Vienna, Austria
NHMUK Natural History Museum, London, U.K.

NUPP	Research Collection of Kari & Timo Nupponen, Espoo, Finland
SMNK	Staatliches Museum für Naturkunde Karlsruhe, Germany
TLMF	Tiroler Landesmuseum Ferdinandeum, Innsbruck, Austria
ZIN	Zoological Institute, Russian Academy of Sciences, Sankt-Petersburg, Russia
ZMKU	Zoological Museum, Kyiv Taras Shevchenko National University, Kyiv, Ukraine
ZMUC	Zoological Museum, Natural History Museum of Denmark, Copenhagen, Denmark

Other abbreviations

HT	holotype
PT	paratype
OB	Oleksiy Bidzilya

Results

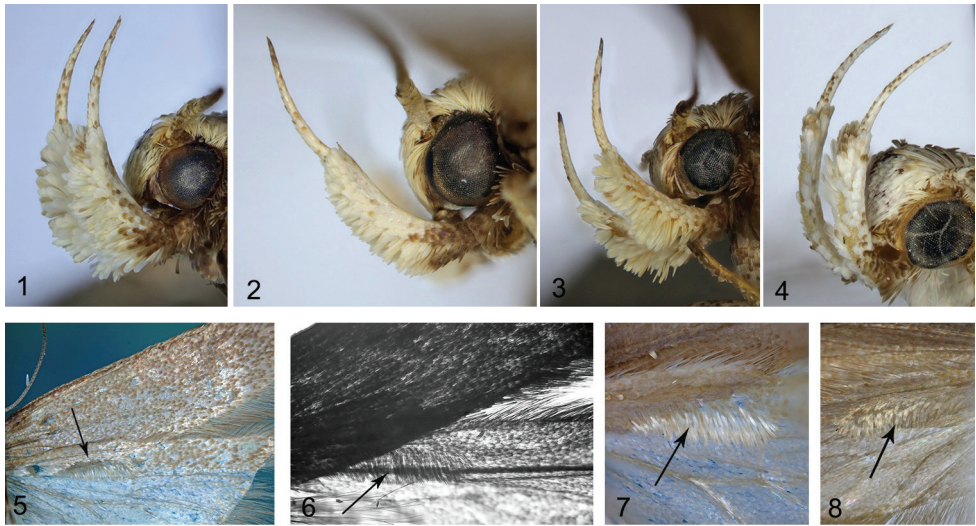
Taxonomic account

Filatima armata sp. nov.

<http://zoobank.org/C0D30913-82AA-471D-ABAE-8C83CAF79538>

Figs 1, 5, 9–21

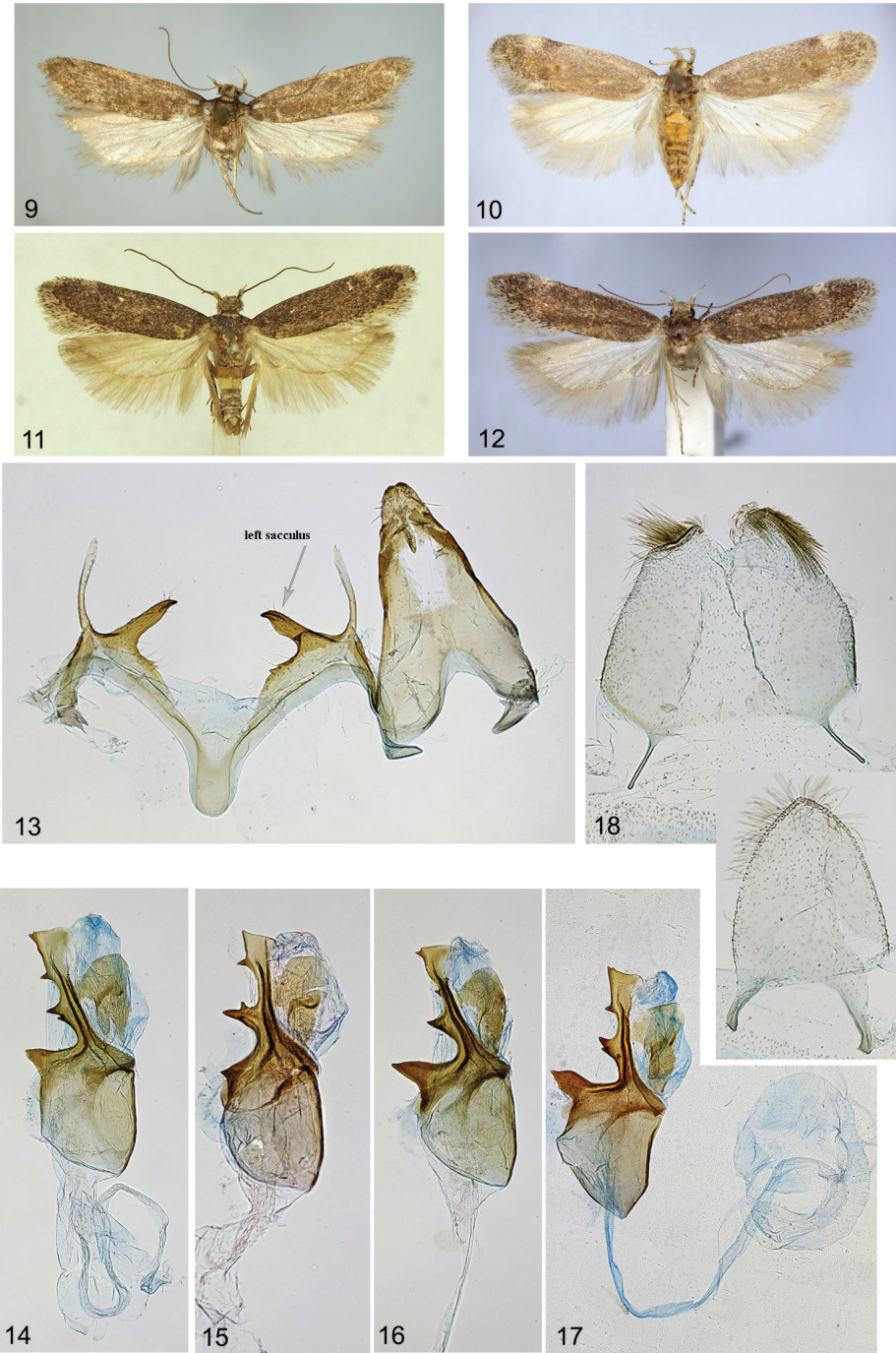
Material examined. *Holotype* [IRAN] • ♂; Khusestan, Yassudi, Sisakht; 2250 m; 13–14 Jun 1972; [genitalia slide number] 73/17, O. Bidzilya; G. Ebert and H. Falkner leg; SMNK. *Paratypes* [IRAN] • 1 ♂, 2 ♀♀; same collection data as for holotype; [genitalia slide number] 74/17♀, O. Bidzilya • 1 ♂; Khusestan, Yassudi, Sisakht; 2250 m; 15–18 Jun 1975; G. Ebert and H. Falkner leg. • 1 ♀; Khusestan, 15 km SE Yassudi; 2050 m; 15 Jun 1972; [genitalia slide number] 6/18, O. Bidzilya; G. Ebert and H. Falkner leg. • 5 ♀♀; Khusestan, 30 km S Yassudi, Kuschk; 2220 m; 12 Jun 1972 [genitalia slide number] 73/17, O. Bidzilya; G. Ebert and H. Falkner leg. • 1 ♂; Fars, 50 km NW Ardekan, Tange Surkh; 2250 m; 16 Jun 1972 [genitalia slide number] 5/18, O. Bidzilya; G. Ebert and H. Falkner leg. • 4 ♀♀; Fars, 50 km NW Ardekan, Tange Surkh; 2250 m; 12–15 Jun 1975; [genitalia slide number] 46/22, O. Bidzilya; G. Ebert and H. Falkner leg. • 1 ♀; Fars, Daschte Ardian, Kotal-Pirehsan; 2000 m; 18 Jun 1972 [genitalia slide number] 77/17, O. Bidzilya; G. Ebert and H. Falkner leg. • 1 ♂, 1 ♀; Strasse Shiraz-Kazeru, Imam Sade; 1200 m; 3 Jun 1969; H. Amsel leg. • 2 ♂♂; Sineh Safid, Fars, FF. 57; c. 6500 ft; 19 May 1950 [genitalia slide number] 78/17; 24/18, O. Bidzilya; E. P. Wiltshire leg. • 1 ♀; Baloutchistan, Kouh i Taftan (Khach); 2500 m; 28 Jun 1938; F. Brandt leg. • 1 ♂; Elburs Gebirge, Keredj; [day? month?] 1936; F. Brandt leg. • 1 ♂; Fars, Strasse Chiraz-Kazeroun, Fort Sine-sefid;



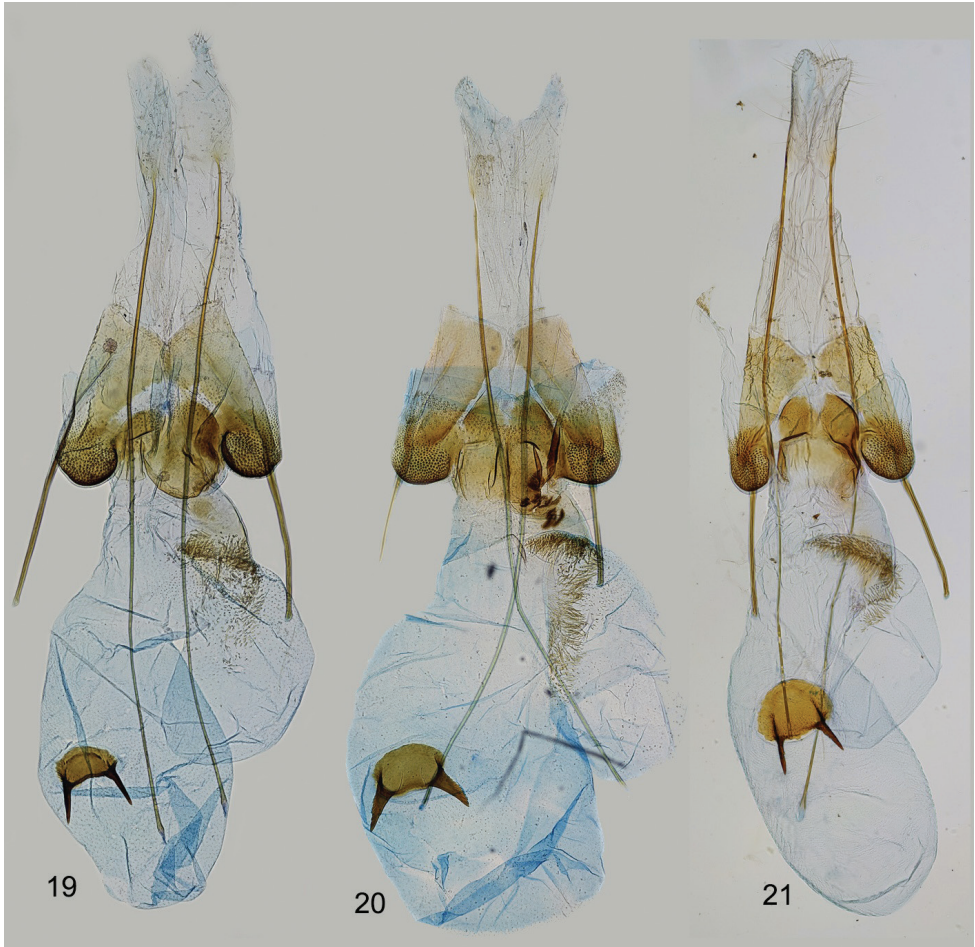
Figures 1–8. *Filatima* spp., details of external morphology **1–4** head, lateral view **1** *F. armata* sp. nov., PT, 50 km NW Ardekan, Tange Surkh **2** *F. subarmata* sp. nov., PT, Quetta **3** *F. afghana* sp. nov., PT, Kabul **4** *F. kariii* sp. nov., HT **5–8** male hindwing, underside (arrow indicates row of caudally directed scales on R5) **5** *F. armata* sp. nov., HT **6, 7** *F. subarmata* sp. nov., PT, 70 km S. v. Teheran **6** in transmitted light **7** in reflected light **8** *F. afghana* sp. nov., PT, Sarobi.

2200 m; 28 Jun 1938; F. Brandt leg. • 1 ♂; Fars, Strasse Ardekan-Talochosroe, Comé; 2600 m; 29 Jul 1937; F. Brandt leg.; all SMNK • 3 ♂; Berge O Kasri Schirin; 24 May 1963; [genitalia slide number] MV 15.338♂, P. Huemer; F. Kasy and E. Vartian leg. • 1 ♂, 1 ♀; 65 km W Shiraz; 16 Apr 1970; [♂ genitalia in glycerin]; Exp. Mus. Vind.; all NHMV • 1 ♂; Khorasan, Qucahn; 19 May 2010; G. Petrányi and P. Hentschel leg. • 1 ♂; Kars, Ardekan, Sepidan; 8–11 May 2010; G. Petrányi and P. Hentschel leg. • 1 ♂; Hamedan, Nehavand, 13 May 2010; G. Petrányi and P. Hentschel leg.; all ZMUC.

Diagnosis. The new species has the elongate uniformly brown forewings usually with markings (Figs 9–12) which are typical for *Filatima*, *Chionodes* and other nearby taxa in Gelechiinae. It is similar externally to *F. textorella* (Chrétien, 1908) and *F. transsilvanella* Kovács & Kovács, 2001, but the first species does not have a row of caudally directed scales to 1/2 of R5 on the underside of the male hindwing, which is present in the male of *F. transsilvanella* and *F. armata* sp. nov. (Fig. 5). There are no reliable external differences for *F. subarmata* sp. nov. The male genitalia (Fig. 13) are distinctive in having weakly asymmetrical sacculi with a small tooth at the base of the left one; despite some variation, the phallus (Figs 14–17) is also very peculiar having a strongly sclerotised longitudinal ribbon with three large and several small lateral thorns and a sclerotised plate in the vesica. *Filatima transsilvanella* differs in the longer uncus, the absence of a tooth on the right sacculus and the phallus having smaller thorns and without a sclerotised plate in the vesica. The female genitalia (Figs 19–21) are identifiable from the ribbon of long, needle-shaped spines in the bulla seminalis in



Figures 9–18. *Filatima armata* sp. nov. **9–12** adults **9** holotype **10** paratype, female, S Iran (gen. slide 46/22, O. Bidzilya) **11** paratype, male, S Iran **12** paratype, female, Pakistan (gen. slide 39/22, O. Bidzilya) **13** male genitalia (gen. slide 24/18, OB) **14–17** phallus, Iran **14** gen. slide 24/18, OB **15** gen. slide 2/18, OB **16** gen. slide 5/18, OB. **17** HT, gen. slide 73/17, OB **18** male segment VIII, gen. slide 24/18, OB.



Figures 19–21. *Filatima armata* sp. nov., female genitalia **19** gen. slide 6/18, OB **20** gen. slide 74/17, OB **21** gen. slide 46/22, OB.

combination with broadly rounded lateral sclerites, and a short sub-rectangular medial sclerite with an emarginated posterior margin. Among Palearctic *Filatima* species the bulla seminalis is known in *F. transilvanella*, *F. pallipalpella* (Snellen, 1884), and *F. afghana* sp. nov. The first species has a rounded and short bulla seminalis (Kovács and Kovács 2001; Junnilainen et al. 2010), whereas *F. pallipalpella* has an elongate one with short spines. *Filatima afghana* sp. nov. like *F. armata* sp. nov. has a ribbon of needle-shaped spines, but differs in the narrower and inwardly curved lateral sclerites.

Description. (Figs 1, 5, 9–12). Wingspan 15.0–22.0 mm. Head light brown, frons paler, greyish white, labial palpus (Fig. 1) recurved, segment 2 greyish white, dark brown at base, upperside brown, underside with brush of modified scales, segment 3 light brown with a few dark scales, antennal scape and flagellum brown; thorax, tegulae and forewing (Figs 9–12) uniformly brown, fold mixed with ochreous,

ochreous brown spot in fold and in cell in some specimens, diffuse white spot at $3/4$ of costal margin, cilia tipped grey-brown; hindwing grey, row of caudally directed scales to $1/2$ of R5 underside in male (Fig. 5); abdominal terga I–IV yellow, remaining terga grey.

Male genitalia (Figs 13–18). Tergum VIII tongue-shaped, with long, narrow anterolateral arms; sternum VIII rounded to sub-trapezoidal, posterior margin with paired patch of hairs and with short medial emargination, anterolateral arms long and narrow (Fig. 18). Uncus sub-trapezoidal, weakly narrowed apically, posterior margin weakly rounded, with short triangular medial incision, laterally covered with strong setae; gnathos slightly longer than uncus, medial sclerite weakly curved, distally weakly serrate on dorsal surface; tegumen sub-triangular, gradually narrowed distally, anteromedial incision reaching to $\sim 1/3$ of its length; valva short and slender, subapex weakly broadened; sacculus inwardly turned, $\sim 2/3$ as long and $3 \times$ as broad as valva, left sacculus broader basally and shorter than left one, with small basal tooth; vinculum with broad and deep sub-triangular medial emargination, weakly serrate posteriorly; saccus $1.5\text{--}2 \times$ longer than broad, sub-rectangular, apex rounded; phallus as long as tegumen, swollen at base, distal $2/3$ with sclerotised ribbon along the left side and four strong lateral thorns: basal one longest, triangular, medial one shortest, paired, subapical thorn very short, and apical one largest, subtriangular, vesica with large irregular sclerotised plate, bulbus ejaculatorius long, coiled.

Variation. Adults vary in size from 15.0 to 22.0 mm in wingspan. Valva, saccus, and thorns of the phallus vary in length.

Female genitalia. (Figs 19–21). Papillae anales sub-ovate, elongated, setose; apophyses posteriores extending the length of corpus bursae, apophyses anteriores shorter than segment VIII, straight; sternum VIII longer than broad, sub-rectangular, weakly narrowed posteriorly, sub-genital plates weakly broadened and joined posteromedially, medial area membranous, mainly covered with fine microtrichia medially and anteriorly, lateral sub-ostial sclerite densely covered with short teeth, broad, rounded, medial sub-ostial sclerite sub-rectangular to rounded with posteromedial emargination; antrum half the length of apophyses anteriores, with strongly sclerotised edge in anterior part; ductus bursae short, broad, with indistinct transition to corpus bursae, with bulla seminalis arising from the right side and extending to $1/2\text{--}2/3$ length of corpus bursae, with ribbon of long and narrow needle-shaped spines extending from ductus bursae to base of bulla seminalis corpus bursae broadly rounded; signum plate sub-ovate with paired long, narrow, acute sclerites directed anteriorly.

Biology. The adults have been collected from mid-April to late July at altitudes between 1200 and 2600 m.

Distribution. Iran.

Etymology. The name of the new species is derived from the Latin *armatus* meaning armed warrior, and refers to the strongly sclerotised phallus armed with strong thorns.

***Filatima subarmata* sp. nov.**

<http://zoobank.org/4804423B-3B9F-4FD9-BE65-7565AA16EE6D>

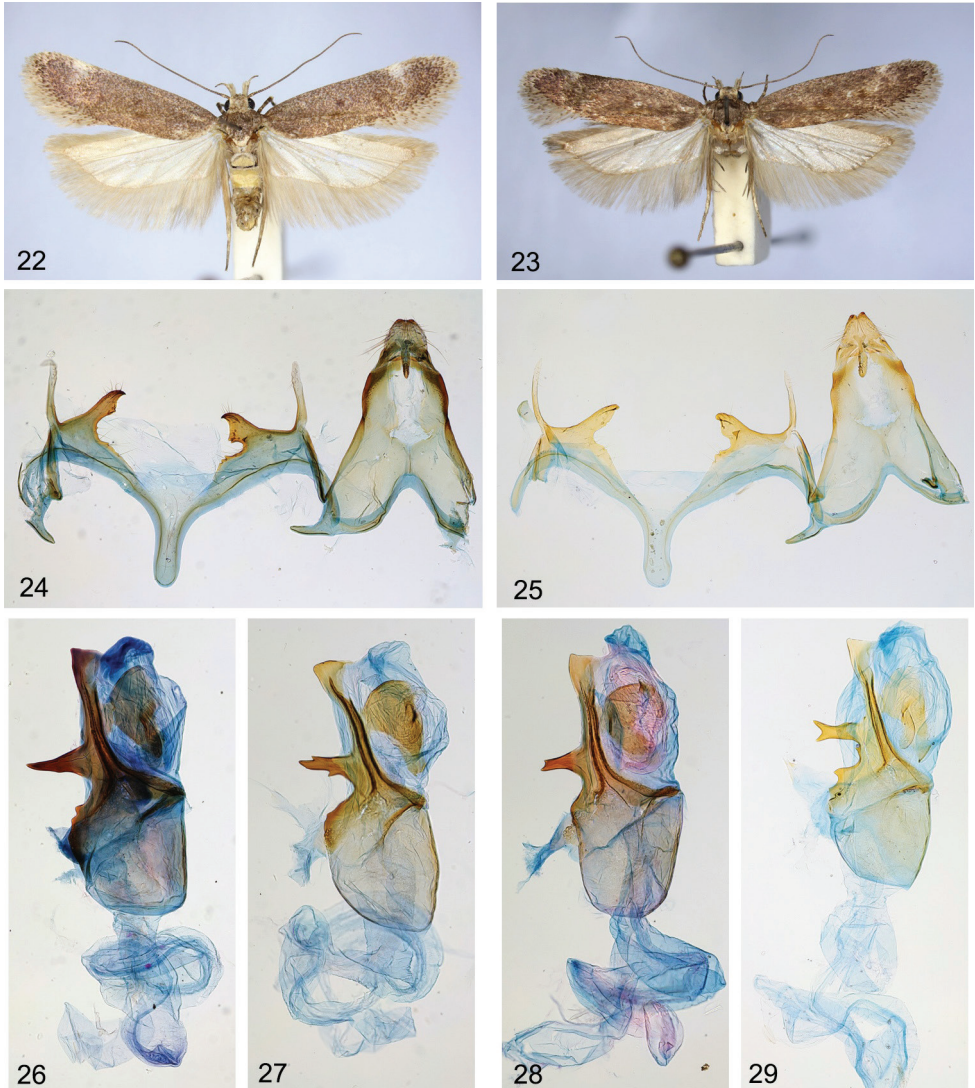
Figs 2, 6, 7, 22–29

Material examined. *Holotype* [PAKISTAN] • ♂; 80 km NW v. Quetta; 2100 m; 15 May 1965; [genitalia slide number] 45/22, O. Bidzilya; F. Kasy and E. Vartian leg.; NHMV. *Paratypes* • 1 ♂; same collection data as for holotype; [genitalia slide number] 34/22, O. Bidzilya; [IRAN] • 2 ♂♂; 70 km S. v. Teheran; 1300 m; 5 May 1965; [genitalia slide number] 54/22, O. Bidzilya; F. Kasy and E. Vartian leg.; all NHMV; • 1 ♂, same data as for proceeding but ex coll. Glaser [genitalia slide number] 91/18, O. Bidzilya; SMNK.

Diagnosis. The new species shows a close relationship with the previous one in respect of the male genitalia and external appearance. However, the male genitalia (Figs 24, 25) of *F. subarmata* sp. nov. differ in the shorter and broader left sacculus and the broader right sacculus. Additionally, the basal thorn of the phallus is shorter, the medial thorn is elongate and apically bifurcate rather than triangular as in *F. armata* sp. nov. and a small subapical thorn is absent in *F. subarmata* sp. nov. (Figs 26–29). We observed also differences in the shape of the saccus which is slightly longer and narrower in *F. subarmata* sp. nov. We did not find reliable differences in the external appearance between *F. subarmata* sp. nov. and *F. armata* sp. nov.

Description. (Figs 2, 6, 7, 22, 23). Wingspan 18.1–19.1 mm. Head covered with grey brown-tipped scales, frons white to pale, labial palpus (Fig. 2) recurved, far protruded over the head, yellowish white, segment 2 with brown base and a few light brown scales on inner surface mainly, on underside with brush of modified scales, segment 3 approximately 2/3 length and 1/3 width of segment 2, mottled with brown; scape brown with a few grey scales at apex, antennal flagellomeres brown with indistinct grey rings; thorax and tegulae brown mixed with grey; forewing (Figs 22, 23) brown rarely mixed with grey, three diffuse indistinct dark, ochreous-brown spots in cell, fold with ochreous brown suffusion, white costal spot at 3/4, subapical pale narrow transverse fascia weakly indicated, cilia tipped grey-brown; hindwing grey, with darkened veins, margins and apex, row of caudally directed scales to 1/2 of R5 underside (Figs 6, 7), cilia grey.

Male genitalia (Figs 24–29). Tergum VIII tongue-shaped, with long, narrow anterolateral arms; sternum VIII rounded to sub-trapezoidal, posterior margin with paired patch of hairs and with short medial emargination, anterolateral arms long and narrow. Uncus sub-trapezoidal, weakly narrowed apically, posterior margin weakly rounded, with short triangular medial incision, laterally covered with strong setae; gnathos slightly longer than uncus, medial sclerite weakly curved, distally weakly serrate on dorsal surface; tegumen sub-triangular, gradually narrowed distally, anteromedial incision reaching to ~ 1/3 of its length; valva short and very slender, bluntly acute; sacculus curved medially, ~ 1/2 length and 4 × as broad as valva, the left sacculus broader and shorter than the right one, with small basal tooth; vinculum with broad and deep sub-triangular medial emargination, weakly serrated posteriorly; saccus 2 × longer than



Figures 22–29. *Filatima subarmata* sp. nov. **22, 23** adult **22** HT **23** PT, Iran (gen. slide 54/22, OB) **24, 25** male genitalia **24** HT **25** PT, Iran (gen. slide 91/18, OB) **26–29** Phallus **26** HT **27** PT, Iran (gen. slide 54/22, OB) **28** PT, Pakistan (gen. slide 34/22, OB) **29** PT, Iran (gen. slide 91/18, OB).

broad, sub-rectangular, apex rounded; phallus as long as tegumen, swollen at base, distal 2/3 with a sclerotised ribbon along the left side with four lateral thorns: two basal thorns are short, triangular, the medial thorn is the longest, slender, bifurcated apically except the HT (Fig. 26), and the apical one is the broadest, subtriangular, vesica with large irregular sclerotised plate, bulbus ejaculatorius long, coiled.

Female genitalia. Unknown.

Biology. Adults have been collected in May at altitudes of 2100 m in Pakistan and 1300 m in Iran.

Distribution. Pakistan, Iran.

Etymology. The specific name reflects the relationship of the species to *F. armata* sp. nov.

***Filatima afghana* sp. nov.**

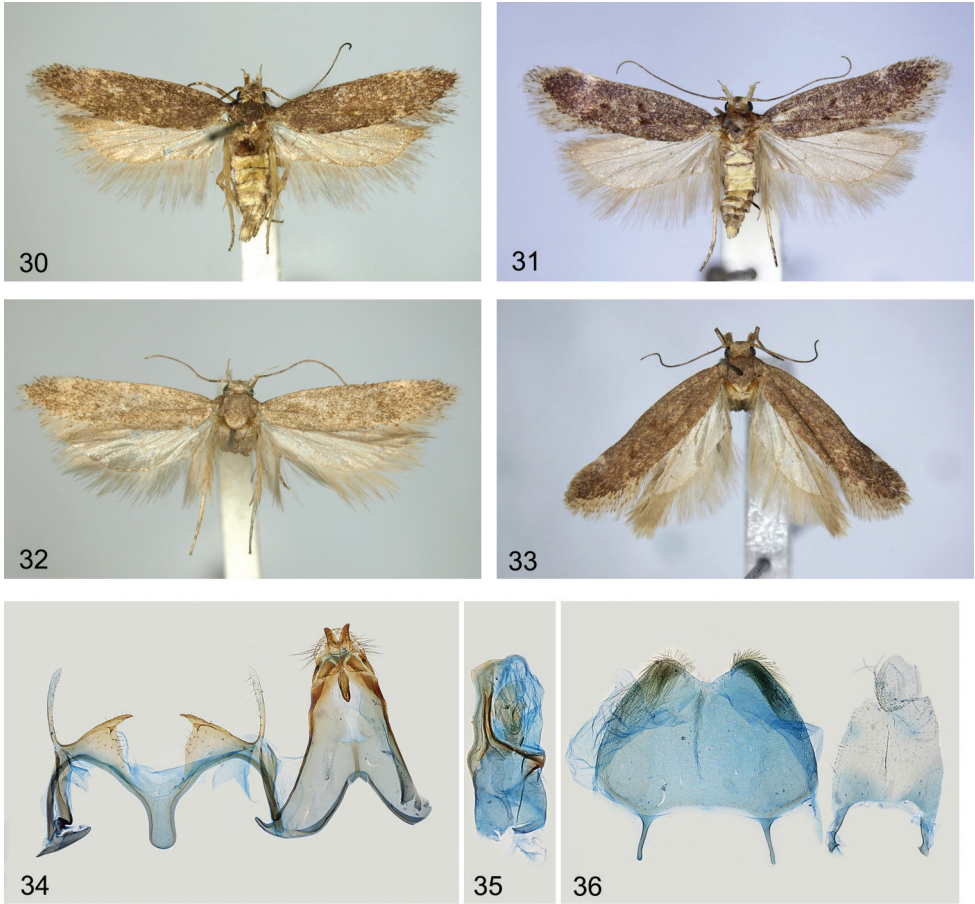
<http://zoobank.org/872CE8C8-EEC4-437D-B3F4-82BFE0B03DD3>

Figs 3, 8, 30–39

Material examined. Holotype [AFGHANISTAN] • ♀; Pol-i-Charchi, 18 km östl. Kabul; 1700 m, 25 Jun –3 Jul 1966; H. Amsel leg.; SMNK. **Paratypes** [AFGHANISTAN] • 1 ♀; Safed Koh, S Seite Kotkai; 2350 m; 19–23 Jun 1966; H. Amsel leg. • 1 ♂; Sarobi, 1100 m; 17 Aug 1961; [genitalia slide number] 47/17, O. Bidzilya; G. Ebert leg. • 1 ♂, 1 ♀; Sarobi, 1100 m; 13 Aug 1961; [genitalia slide number] Am. 1756♂, D. Povolný; 45/17♀, O. Bidzilya; G. Ebert leg. • 2 ♀♀; Arghandab-Damm, 35 km ndl. Kandahar; 1150 m; 23/27 May 1961; [genitalia slide number] Am. 1761♀, D. Povolný; 3/18, O. Bidzilya; G. Ebert leg. • 1 ♂, 2 ♀♀; Herat; 970 m; 5 May 1956; [genitalia slide number] Am. 1720♂, D. Povolný; 25/18♀, O. Bidzilya; H. Amsel leg.; all SMNK • 3 ♂♂, 2 ♀♀; 40 km SW v. Kabul; 2300 m; 29 Jun 1965; [genitalia slide number] MV 16.509♀, MV 15.340♂, MV 16.510♂, MV 16.512♂, P. Huemer; 57/22♀, O. Bidzilya; F. Kasy and E. Vartian leg. • 1 ♀; 80 km NO v. Kandahar; 27 Jun 1963; F. Kasy and E. Vartian leg.; all NHMV; [PAKISTAN] • 1 ♀; 80 km NW v. Quetta; 2100 m; 15 May 1965; [genitalia slide number] 39/22♀, O. Bidzilya; F. Kasy and E. Vartian leg.; all NHMV.

Diagnosis. The new species is rather uniformly dark brown (Figs 30–33), darker than *F. armata* sp. nov. and *F. subarmata* sp. nov., with indistinct markings. It is very similar externally to those two species, but on average it has a smaller wingspan, is darker, and has a paler, white rather than greyish white, head and labial palpus. The apically bifurcate uncus, short and narrow sacculus with a basal tooth (Fig. 34), and phallus with longitudinal sclerotised ribbon and sclerotised plate of the vesica (Fig. 35) are characteristic in the male genitalia. *Filatima transilvanella* differs in the longer uncus that is not divided apically and the longer and broader sacculus without a basal tooth. The female genitalia are recognisable by the ribbon of long needle-shaped spines in the bulla seminalis in combination with narrow inwardly curved lateral sclerites. *Filatima transilvanella* differs in the rounded rather than elongate bulla seminalis, longer apophyses anteriores and the lateral sclerite that is not turned inwards.

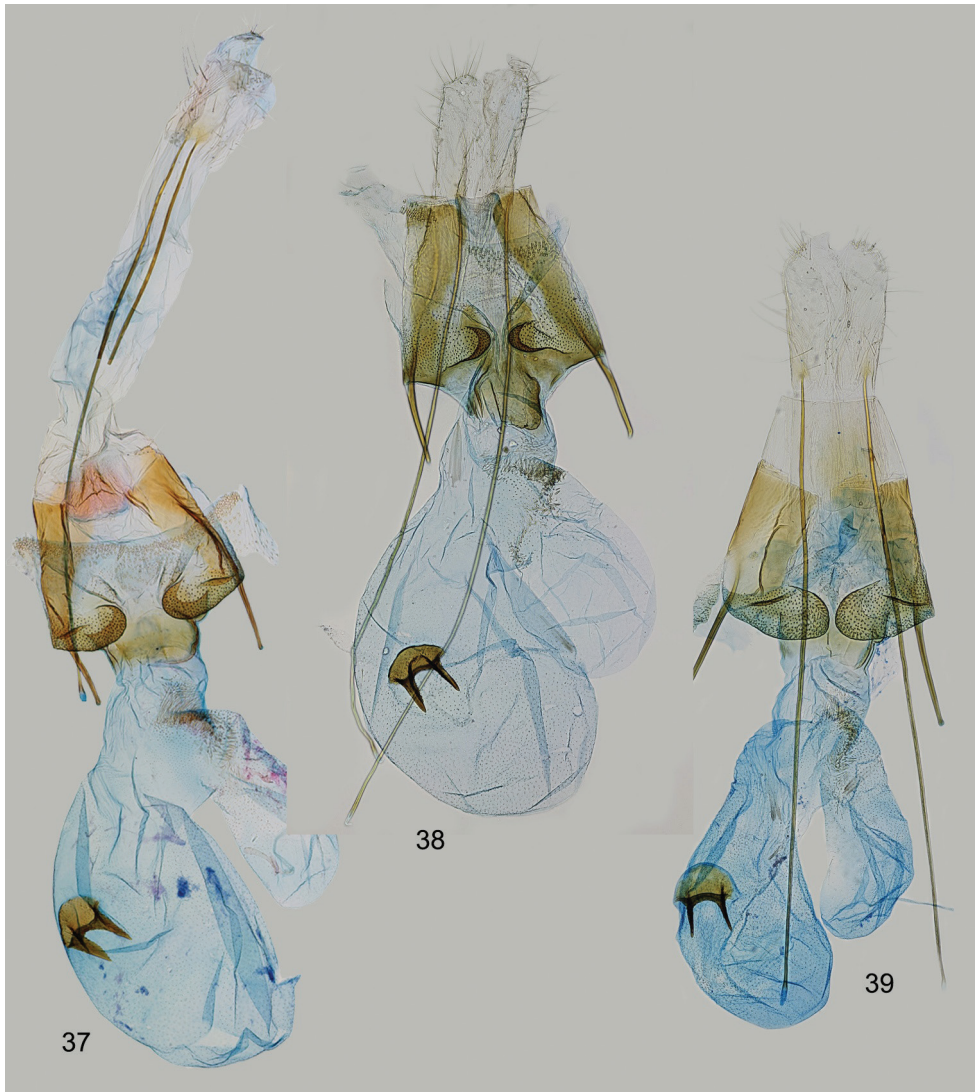
Description. (Figs 3, 8, 30–33). Wingspan 13.0–17.3 mm. Head pale white, neck distinctly mottled with brown, labial palpus recurved, segment 2 creamy white, dark brown at base, underside with brush of modified scales, segment 3 slender, 1/3 width and approx. as long as segment 2, brown, upper side white, antennal scape and flagellum brown (Fig. 3); thorax, tegulae and forewing uniformly brown, fold mixed with



Figures 30–36. *Filatima afghana* sp. nov. **30–33** adults **30** HT **31** PT, female (gen. slide 57/22, OB) **32** PT, female (gen. slide 25/18, OB) **33** PT, female (gen. slide 91/18, OB) **34–36** male genitalia and abdominal segment VIII (gen. slide 47/17, OB) **34** unrolling **35** phallus **36** abdominal segment VIII.

ochreous, ochreous brown spot in fold and in cell in some specimens, diffuse white spot on 3/4 of costal margin, cilia tipped grey-brown; hindwing grey, row of caudally directed scales to 1/2 of R5 underside in male (Fig. 8); abdominal terga I–IV yellow, remaining terga grey.

Male genitalia (Figs 34–36). Tergum VIII tongue-shaped, with long, narrow anterolateral arms; sternum VIII rounded to sub-trapezoidal, posterior margin with paired patch of hairs and with shallow medial emargination, anteromedial arms long and narrow (Fig. 36). Uncus deeply divided posteromedially into digitate lobes that are weakly narrowed apically and covered with strong setae laterally; gnathos approx. as long as uncus, medial sclerite weakly curved, dorsal surface with several folds; tegumen sub-triangular, gradually narrowed distally, anteromedial incision reaching to ~ 1/3 of its length; valva slender, apex weakly broadened; sacculus short, narrow, acute,



Figures 37–39. *Filatima afghana* sp. nov., female genitalia **37** gen. slide 57/22, OB **38** gen. slide 25/18, OB **39** gen. slide 45/17, OB.

inwardly turned, with basal tooth; vinculum with broad and deep U-shaped medial emargination; saccus 2 × longer than broad, sub-rectangular, apex weakly rounded; phallus slightly shorter than tegumen, nearly of equal width, weakly narrowed at base, distal 2/3 with a sclerotised ribbon along the left side, with two small teeth in one specimen and without them in other specimens, vesica with large irregular sclerotised plate, bulbus ejaculatorius long, coiled.

Variation. Left sacculus is broader than the right one in one specimen; the basal tooth of the sacculus among specimens varies in size.

Female genitalia (Figs 37–39). Papillae anales sub-ovate, elongate, setose; apophyses posteriores 1.3–1.5 as long as length of bursae copulatrix; apophyses anteriores shorter than segment VIII, straight; sternum VIII longer than broad, sub-rectangular, weakly narrowed posteriorly, with large, weakly sclerotised posteromedial plate, subgenital plates $1/4$ – $1/3$ width of segment VIII, medial $1/3$ – $2/3$ membranous, mainly covered with fine microtrichia medially and anteriorly, lateral sub-ostial sclerite densely covered with short teeth, elongated, turned inwards, rounded, more strongly sclerotised and edged medially; medial sub-ostial sclerite weakly sclerotised, sub-rectangular to rounded with posteromedial emargination; antrum subquadrate, shorter than apophyses anteriores; ductus bursae short, broad with indistinct transition to corpus bursae, with broad bulla seminalis arising from right side and extending to $1/2$ – $2/3$ length of corpus bursae, with ribbon of long and narrow needle-shaped spines extending from ductus bursae to base of bulla seminalis, ductus seminalis arising from anterior part of bulla seminalis; corpus bursae broadly rounded; signum plate sub-ovate, strongly sclerotised and weakly serrate anteriorly with pair of lateral long, narrow acute sclerites directed anteriorly.

Variation. The shape of the posteromedial plate varies from sub-triangular to sub-rectangular; lateral sub-ostial sclerite varies in width from elongate to broadly rounded, usually with distinct sclerotisation in medial $1/4$, but is uniformly sclerotised in one specimen; apophyses anteriores vary in length from as long as, to shorter than segment VIII.

Biology. The adults have been collected from early May to mid-August at altitudes between 970 and 2350 m.

Distribution. Afghanistan, Pakistan.

Etymology. The specific name reflects the distribution of this new species in Afghanistan.

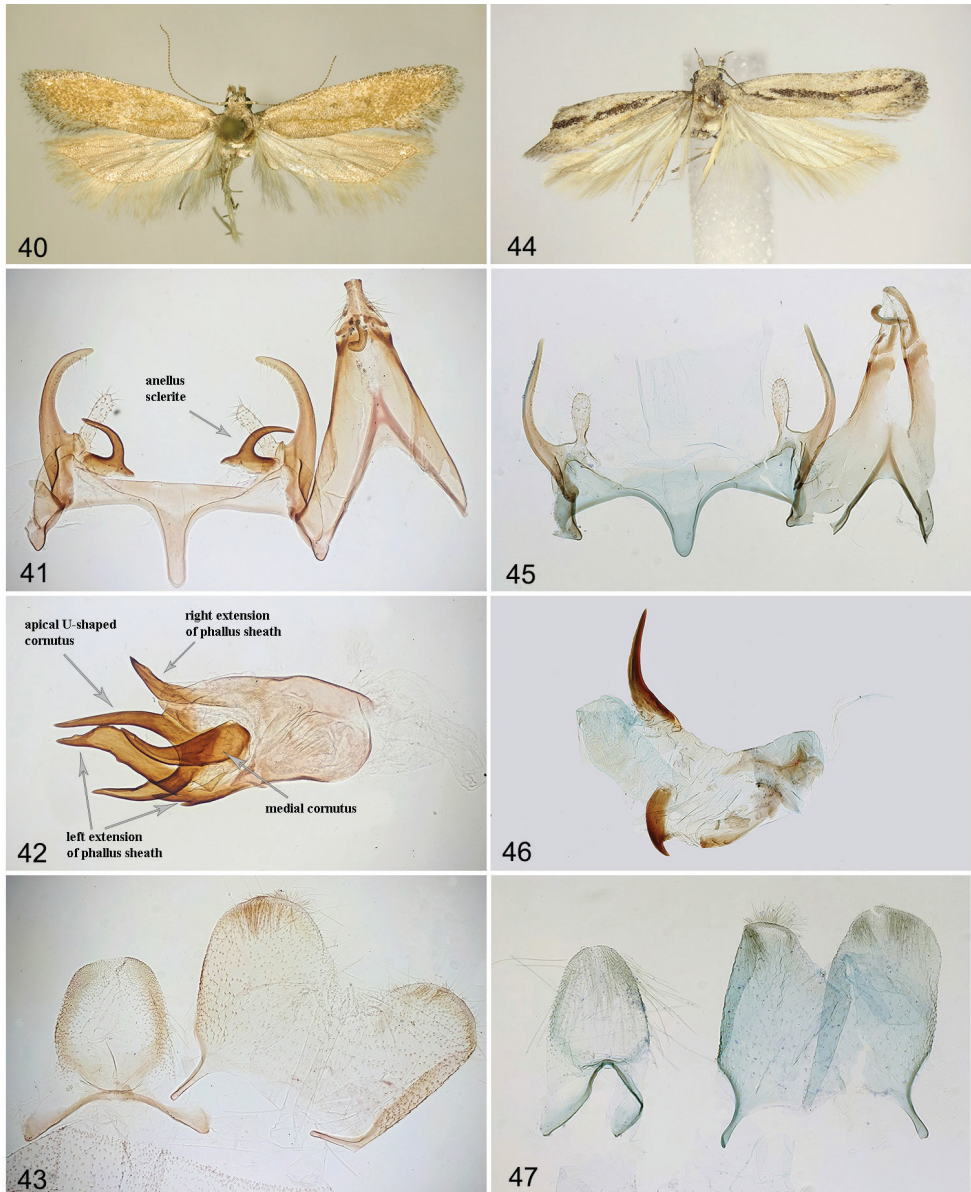
***Filatima karii* sp. nov.**

<http://zoobank.org/5322FBFF-6C65-47A4-9BC8-E64BEAC3C2FD>

Figs 4, 40–43

Material examined. *Holotype* [TAJIKISTAN] • ♂; W-Pamir mts, 37°00'55"N, 72°34'32"E, Pijan/Pamir River by Zugvand village; 2810 m; 25 Jul 2013; [genitalia slide number] 152/16, O. Bidzilya; K. Nupponen & R. Haverinen leg.; NUPP.

Diagnosis. Externally this new species is recognised by the light brown forewing with the costal margin distinctly mottled with black (Fig. 40). *Filatima fontisella* Lvo-vsky & Piskunov, 1989 from Mongolia shares with *Filatima karii* sp. nov. the absence of row of scales on the ventral surface of the male hindwings and somewhat similar forewing pattern. However, in *F. fontisella* forewing is lighter, pale yellow, and the wingspan is smaller (11–15 mm contrary to 17.2 mm in *F. karii* sp. nov.). The male genitalia (Figs 41, 42) resemble those of *F. fontisella*, *F. ukrainica* Piskunov, 1971, and *F. multicornuta*, all with well-developed horn-shaped anellus sclerites. Apical U-shaped (V-shaped in above species) cornutus and very broad left extension of the phallus sheath are characteristic for the new species.



Figures 40–43. *Filatima kari* sp. nov., holotype **40** adult **41** male genitalia, unrolling **42** phallus **43** segment VIII **44–47** *Filatima nigrimediella* Bidz., holotype **44** adult **45** male genitalia, unrolling (gen. slide 109/18, OB) **46** phallus (gen. slide 109/18, OB) **47** segment VIII (gen. slide 109/18, OB).

Description. (Figs 4, 40). Wingspan 17.2 mm. Head covered with pale white, brown-tipped scales, frons white, labial palpus recurved, segment 2 white, dark brown at base, underside with brush of modified white scales and few brown scales at apex, segment 3 slender, 1/3 width and ~ 2/3 length of segment 2, white mixed with light brown, antennal scape white densely mixed with brown, flagellum ringed white and

brown (Fig. 4); thorax and tegulae slightly darker than neck, brown mottled with pale white; forewing light brown, slightly darker in distal 2/3, diffuse dark brown spots in mid-wing at 1/3 and 2/3, fold slightly darker than adjacent area of forewing, costal margin and base with distinct black suffusion, cilia pale white to light brown, with distinct brown tips; hindwing grey in basal half and darker, light brown in distal half, veins distinct, mottled with dark brown.

Male genitalia (Figs 41–43). Tergum VIII egg-shaped, with distinct moderately broad anterolateral arms, anterior margin sclerotised; sternum VIII subtrapezoidal, posterolateral corners rounded, posteromedial emargination broad, anterolateral arms long and narrow (Fig. 43). Uncus basally as broad as long, narrowed to 3/4 length, apically weakly widened, posterior margin straight, laterally covered with strong setae; gnathos approx. length of uncus, apical 1/3 of medial sclerite curved at right angle, weakly broadened; tegumen elongated, sub-triangular, gradually narrowed distally, anteromedial incision reaching to ~ 1/2 of its length; valva moderately broad, gradually tapered to a bluntly pointed apex, gradually curved, extending to apex of gnathos; sacculus membranous, finger-shaped, of even width and apex bluntly rounded, 1/2 length of valva; sclerites of anellus symmetrical, with stout base and long horn-shaped outwardly turned distal sclerite, as long as sacculus; vinculum short, band-shaped, saccus weakly narrowed towards rounded apex, slightly extending beyond anterior projection of pedunculus; phallus slightly shorter than tegumen, weakly narrowed at base, with medial horn-shaped cornutus and apical U-shaped cornutus with its right process slightly longer than left process; additionally, there are two lateral extensions of the phallus sheath: the left one is long and broad with two basal teeth on left side, and the right one is short, narrow; bulbus ejaculatorius short.

Female genitalia. Unknown.

Biology. The holotype was collected in late July at an altitude of c. 2800 m. The collecting site is the edge between a steep rocky slope and riverside sand dunes with plenty of *Salix* (see Bidzilya et al. 2019: 125, fig. 43).

Distribution. Tajikistan.

Etymology. We dedicate this species to the late Kari Nupponen, leading specialist on the Scythrididae, outstanding collector, and a wonderful friend who passed away much too early.

***Filatima multicornuta* Bidzilya & Nupponen, 2018**

Figs 48, 49

Filatima multicornuta Bidzilya & Nupponen, 2018: 395

Material examined. [MONGOLIA] • 1 ♂, 1 ♀; Central aimak, 12 km S von Somon Bajanbaraat; 1380 m; 8 Jun 1967; [genitalia slide number] 214/20♂, 215/20♀, O. Bidzilya; Exp. Dr. Z. Kaszab, 1967, Nr. 776 • 1 ♂, 1 ♀; Bajanchongor aimak, 8 km S von Somon Zinst; 1400 m; 25 Jun 1964; [genitalia slide number] 49/22♂, 50/22♀,



Figures 48–50. *Filatima* spp., female genitalia **48, 49** *Filatima multicornuta* Bidz. & Nupp., Mongolia. **48** Gen. slide 50/22, OB **49** gen. slide 215/20, OB **50** *F. zagulajevi* Anikin & Piskunov, Kazakhstan, gen. slide 15/18, OB.

O. Bidzilya; Exp. Dr. Z. Kaszab, 1964, Nr. 198 • 1 ♀; Gobi Altaj aimak, NW Ecke des Chasat chajrchan ul Gebirge, 2 km NW von Somon Bičigt. 1900 m; 14 Jul 1966; [genitalia slide number] 62/22♀, O. Bidzilya; Exp. Dr. Z. Kaszab, 1966, Nr. 688; all NHMB.

The species has been recently described from four males from Tuva Republic of Russia and Mongolian Altai. Our study of additional material from Mongolia resulted in the discovery of the hitherto unknown female which is described below.

Female genitalia (Figs 48, 49). Papillae anales sub-ovate, densely covered with short setae; apophyses anteriores 4 × as long as apophyses posteriores; segment VIII subrectangular, slightly longer than broad; sternum VIII with posterior margin weakly emarginated, evenly sclerotised, with rounded sclerites covered with minute thorns at base of apophyses anteriores; medial sclerite narrow, cone-shaped, extending to the anterior margin of sternum VIII; ductus bursae short and broad, with indistinct transition to corpus bursae, numerous dense and strong needle-shaped spines do not extend so far anteriorly as on the right side, more delicate and less dense hair-like spines from 1/3 to 1/2 length in left side, several longitudinal overlapping folds extending to 1/4 to 1/2 length into corpus bursae; corpus bursae oval, signum basal plate rounded, covered with short thorns and two anteriorly directed horn-shaped lobes.

Remarks. The female genitalia of *F. multicornuta* (Figs 48, 49) resemble that of *F. zagulajevi* Anikin & Piskunov, 1996 (Fig. 50), but the left side of the ductus bursae is more densely covered with microspines, whereas the right side is less covered with microspines in *F. zagulajevi*. Additionally, the longitudinal folds are longer and the medial sclerite is shorter in *F. zagulajevi* (Fig. 50).

An annotated list of the species of *Filatima* in the Palaearctic region

Filatima algarbiella Corley, 2014

Filatima algarbiella Corley, 2014: 233

Distribution. Portugal (Corley 2014: 233).

Filatima angustipennis Sattler, 1961

Filatima angustipennis Sattler, 1961: 117

Filatima albicostella auct. (nec Clarke 1942); misidentification

Distribution. France (Sattler 1961: 117), Russia: Altai Republic (Bidzilya 2002: 68).

Filatima asiatica Sattler, 1961

Filatima asiatica Sattler, 1961: 119

= *Filatima bidentella* Bidzilya, 1998. Synonymised by Bidzilya and Nupponen (2018: 392)

Distribution. Kyrgyzstan, Mongolia (Sattler 1961; Piskunov 1979), Russia: Tuva, Buryatia, Zabaikalskiy krai (Bidzilya and Budashkin 1998; Bidzilya and Nupponen 2018).

***Filatima djakovica* Anikin & Piskunov, 1996**

Filatima djakovica Anikin & Piskunov, 1996: 173

Distribution. Romania (Rákósy et al. 2003), Ukraine (Bidzilya and Budashkin 2017: 13), Russia: Vladimir and Saratov regions (Anikin and Piskunov 1996; Piskunov and Uskov 2006).

***Filatima fontisella* Lvovsky & Piskunov, 1989**

Filatima fontisella Lvovsky & Piskunov, 1989: 560

Distribution. Mongolia (Lvovsky and Piskunov 1989: 560).

Remarks. As the only Russian record of *Filatima fontisella* (Kostjuk et al. 1994: 10) is based on misidentification of *F. multicornuta*, this species should be removed from the list of the Lepidoptera of Russia.

***Filatima incomptella* (Herrich-Schäffer, 1854)**

[no genus] *incomptella* Herrich-Schäffer, 1853: pl. 71, fig. 536

Gelechia incomptella Herrich-Schäffer, 1854: 162, 178

= *Gelechia turbidella* Nolcken, 1871: 561

Distribution. Europe (Huemer and Karsholt 1999), eastwards to Siberia: Omsk region (Ponomarenko and Knyazev 2020: 281) and Zabaikalskiy krai of Russia.

***Filatima karsholti* Ivinskis & Piskunov, 1989**

Filatima karsholti Ivinskis & Piskunov, 1989: 572

Distribution. Mongolia, China: Xinjiang (Ivinskis and Piskunov 1989: 575), Russia: Buryatia (Bidzilya and Nupponen 2018: 392).

***Filatima kerzhneri* Ivinskis & Piskunov, 1989**

Filatima kerzhneri Ivinskis & Piskunov, 1989: 575

Distribution. Mongolia (Ivinskis and Piskunov 1989: 575).

***Filatima multicornuta* Bidzilya & Nupponen, 2018**

Filatima multicornuta Bidzilya & Nupponen, 2018: 395

Distribution. Mongolia, Russia: Tuva Republic (Bidzilya and Nupponen 2018: 395), Zabaikalskiy krai (new record).

New record. [RUSSIA] • 1 ♂; SE Zabaikalie, Nizhniy Tsasutchei; 4 Aug 1989; [genitalia slide number] 33/17, O. Bidzilya; I. Kostjuk leg.; ZMKU.

***Filatima nigrimediella* Bidzilya, 1998**

Filatima nigrimediella Bidzilya, 1998: 53. In Bidzilya et al. 1998: 53.

Distribution. Russia: Zabaikalskiy krai (Bidzilya et al. 1998: 53).

Remarks. The species is known only from the male holotype collected in Borzja, S of Zabaikalskiy kray of Russia. The original description is accompanied by a black and white photograph of the adult and a drawing of male genitalia in lateral view (Bidzilya et al. 1998, Figs 17, 18). Here we provide colour photographs of the holotype (Fig. 44) and the slide of the unrolled male genitalia (Figs 45–47).

***Filatima pagicola* (Meyrick, 1936)**

Gelechia pagicola Meyrick, 1936: 44

Distribution. China: Taishan (Meyrick 1936: 44).

Remarks. The photograph of the lectotype and its male genitalia are illustrated in Clarke (1969: 96, pl. 48, figs 1–1b).

***Filatima pallipalpella* (Snellen, 1884)**

Gelechia pallipalpella Snellen, 1884: 167

= *Gelechia autocrossa* Meyrick, 1937. In Caradja and Meyrick 1937: 157. Synonymised by Bidzilya and Nupponen (2018: 397)

Distribution. Russia: Lower Volga, southern Ural, Novosibirsk region, Altai, Tuva, South of Krasnoyarskiy krai, Buryatia, Zabaikalskiy krai, Amur region, Primorskiy krai (Ponomarenko 2008, 2016; Junnilainen et al. 2010; Bidzilya and Nupponen 2018: 398), Kyrgyzstan (new record), China: Shandong Province (Caradja and Meyrick 1937: 157).

New record. [KYRGYZSTAN] • 1 ♀; Turkestan mts, valley river Kalay-Makhmud; 1830 m; 10 Jun 2010; [DNA barcode identification number] TLMF Lep 21784; N. Pöll leg.; TLMF.

The new record from Kyrgyzstan is based on molecular evidence with barcodes corresponding to samples from S Ural of Russia.

***Filatima sciocrypta* (Meyrick, 1936)**

Gelechia sciocrypta Meyrick, 1936: 44

= *Gelechia digrapta* Meyrick, 1936: 44. Synonymised by Beccaloni et al. (2003)

= *Gelechia demophila* Meyrick, 1937: 157. In Caradja and Meyrick 1937: 157. Synonymised by Beccaloni et al. (2003)

Distribution. Mongolia (Emelyanov and Piskunov 1982: 393), China: Shandong, Jilin (Meyrick 1936: 44; Caradja and Meyrick 1937: 157); Russia: Buryatia (Bidzilya and Nupponen 2018: 397), Zabaikalskiy krai (Caradja 1938: 92), Amur region (Ponomarenko 2016: 124).

Remarks. The above synonymy is based on NHMUK's card index and its computerised and updated version (Beccaloni et al. 2003), but it has not been formally published. We did not examine type specimens of *G. digrapta* and *G. demophila* and therefore cannot confirm this synonymy.

***Filatima spurcella* (Duponchel, [1843])**

Anacamptis spurcella Duponchel, [1843]: 269.

= *Gelechia fuscantella* Heinemann, 1870: 213

Distribution. Europe, Turkey, Armenia (Sattler 1960: 53; Huemer and Karsholt 1999).

***Filatima tephritidella* (Duponchel, 1844)**

Anacamptis tephritidella Duponchel, 1844: 432

Gelechia tephritidella Herrich-Schäffer, 1854: 162, 178,

[no genus] *tephritidella* Herrich-Schäffer, 1853: pl. 69, figs 517, 518.

Distribution. Europe from France to Lower Volga (Huemer and Karsholt 1999) and western Kazakhstan (Caradja 1920), Omsk region (Ponomarenko and Knyazev 2020: 281) and Tuva Republic of Russia (Bidzilya 2005: 14).

***Filatima textorella* (Chrétien, 1908)**

Gelechia textorella Chrétien, 1908: 59

Distribution. Spain, France (Huemer and Karsholt 1999), North Macedonia (new record), Turkey (new record).

New records. [NORTH MACEDONIA] • 1 ♂; Treskaschluht; 1–5 Jun 1967; [genitalia slide number] 85/18, O. Bidzilya; R. Pinker leg.; SMNK; [TURKEY] • 1 ♂, 1 ♀; Asia min., Anatolien, Kizilcahamam; 925 m; 3 Jun 1970; [genitalia slide number] 78/18♂. O. Bidzilya; AR0277♀, A.L.M. Rutten; M. and W. Glaser leg.; SMNK.

Filatima transsilvanella Kovács & Kovács, 2001

Filatima transsilvanella Kovács & Kovács, 2001: 363

Distribution. Romania (Kovács and Kovács, 2001: 363), Russia (South Ural) (Junnilainen et al. 2010: 38).

Filatima ukrainica Piskunov, 1971

Filatima ukrainica Piskunov, 1971; 1106

Distribution. Ukraine (Piskunov 1971: 1106), Lithuania, Sweden (Ivinskis and Piskunov 1981: 50).

Filatima zagulajevi Anikin & Piskunov, 1996

Fig. 50

Filatima zagulajevi Anikin & Piskunov, 1996: 175

Distribution. Russia: Lower Volga, South Ural (Anikin and Piskunov 1996: 175; Piskunov and Anikin 2005: 51; Junnilainen et al. 2010: 39), Kazakhstan (new record).

New record. [KAZAKHSTAN] • 1 ♀; Sopki Kokshetau near Tersakkan river; 4 Jun 1958; [genitalia slide number] 15/18, O. Bidzilya; M. Falkovitsh leg.; ZIN.

Acknowledgements

The authors thank Robert Trusch, Michael Falkenberg (SMNK), Sabine Gaal-Haszler (NHMV) and Szolt Bálint (NHMB) for assistance during the work with collections under their care. Ole Karsholt (ZMUC) kindly shared records of *F. armata* sp. nov. from the ZMUC collection. We are very thankful to Robert J. Heckford (U.K.) who kindly commented on and improved the English language of the manuscript. Terry Harrison and Jan Šumpich reviewed the manuscript and provided helpful comments

and suggestions. The work was supported by the Ukrainian State Budget Program “Support for the Development of Priority Areas of Scientific Research” (Code: 6541230) (O. Bidzilya).

References

- Anikin VV, Piskunov VI (1996) New species of gelechiid moths from Saratov Province, Russia (Lepidoptera, Gelechiidae). *Zoosystematica Rossica* 4: 171–175.
- Beccaloni G, Scoble M, Kitching I, Simonsen T, Robinson G, Pitkin B, Hine A, Lyal C (2003) The Global Lepidoptera Names Index (LepIndex). <https://www.nhm.ac.uk/our-science/data/lepindex/> [accessed 16 February 2022]
- Bidzilya O (2002) On the distribution of Gelechiid Moths (Lepidoptera: Gelechiidae) in the southern Siberia. *The Kharkov Entomological Society Gazette* 9: 64–72. [in Russian]
- Bidzilya O (2005) On the distribution of Gelechiid Moths (Lepidoptera, Gelechiidae) in Siberia. Contribution 2. *Proceedings of Zoological Museum of Kyiv Taras Shevchenko National University* 3: 7–19. [in Russian]
- Bidzilya OV, Budashkin YuI (1998) New records of Microlepidoptera from the Ukraine. *Journal of Ukrainian Entomological Society* 4(3–4): 3–16. [in Russian]
- Bidzilya O, Budashkin Yu (2017) New records of Lepidoptera from Ukraine and description of a new species of *Caloptilia* Hübner, 1825 (Lepidoptera, Gracillariidae) from the mountains of Crimea. *Nota Lepidopterologica* 40(2): 145–161. <https://doi.org/10.3897/nl.40.13085>
- Bidzilya O, Nupponen K (2018) New species and new records of gelechiid moths (Lepidoptera, Gelechiidae) from southern Siberia. *Zootaxa* 4444(4): 381–408. <https://doi.org/10.11646/zootaxa.4444.4.2>
- Bidzilya O, Budashkin Yu, Kostjuk I (1998) Addition to the fauna of Microlepidoptera of Transbaikalia. *Journal of Ukrainian Entomological Society* 1–2: 33–63. [in Russian]
- Bidzilya O, Huemer P, Nupponen K, Šumpich J (2019) A review of some new or little-known species of the genus *Gnorimoschema* (Lepidoptera, Gelechiidae) from the Palaearctic region. *ZooKeys* 857: 105–138. <https://doi.org/10.3897/zookeys.857.34188>
- Caradja A (1920) Beitrag zur Kenntnis der geographischen Verbreitung der Microlepidopteren des palaearktischen Faunengebietes nebst Beschreibung neuer Formen. III. Teil. *Deutsche entomologische Zeitschrift Iris* 34: 75–179.
- Caradja A (1938) Ueber eine kleine Microlepidopterenausbeute aus Mancinkuo und Transbaikalien. *Deutsche entomologische Zeitschrift Iris* 52(4): 90–92.
- Caradja A, Meyrick E (1937) Materialien zur einer Lepidopterenfauna des Taishanmassivs, Provinz Shantung. *Deutsche entomologische Zeitschrift Iris* 50(4): 145–159.
- Clarke JFG (1942) Notes and new species of Microlepidoptera from Washington State. *Proceedings of the United States National Museum* 92(3149): 267–276. <https://doi.org/10.5479/si.00963801.92-3149.267>
- Clarke JFG (1969) Catalogue of the Type Specimens of Microlepidoptera in the British Museum (Natural History) described by Edward Meyrick. Vol. 7. Gelechiidae (D–Z). Trustees of the British Museum (Natural History), London, 531 pp.

- Corley M (2014) Five new species of Microlepidoptera from Portugal. *Entomologist's Record and Journal of Variation* 126: 229–243.
- Emelyanov IM, Piskunov VI (1982) New data on the fauna of the gelechiid and anarsiid moths (Lepidoptera: Gelechiidae, Anarsiidae) of Mongolia, the USSR and North China. *Nasekomye Mongolii* 8: 366–407. [in Russian]
- Hodges R (1999) Gelechioidea, Gelechiidae (Part), Gelechiinae (Part-*Chionodes*). In: Dominick RB et al. (Eds) *The Moths of America North of Mexico, Fascicle 7*. 6: 1–339. The Wedge Entomological Research Foundation, Washington.
- Huemer P (1988) A taxonomic revision of *Caryocolum* (Lepidoptera: Gelechiidae). *Bulletin of the British Museum of Natural History. Entomology* 57: 439–571.
- Huemer P, Karsholt O (1999) Gelechiidae I (Gelechiinae: Teleiodini, Gelechiini). In: Huemer P, Karsholt O, Lyneborg L (Eds) *Microlepidoptera of Europe*, 3: 1–356. Apollo Books, Stenstrup.
- Huemer P, Karsholt O (2010) Gelechiidae II (Gelechiinae: Gnorimoschemini). In: Huemer P, Karsholt O, Nuss M (Eds) *Microlepidoptera of Europe*, Stenstrup 6: 1–586. <https://doi.org/10.1163/9789004260986>
- Ivinskis PP, Piskunov VI (1981) Review of palearctic species of genus *Filatima* Busck, 1939 and description of new female of species *Filatima ukrainica* Piskunov, 1981, femina nova (Lepidoptera, Gelechiidae) found on Lithuanian coast of the Baltic Sea. *Trudy Akademii Nauk Litovskoi SSR, Series B* 76(4): 47–52. [in Russian]
- Ivinskis PP, Piskunov VI (1989) Two new species of the genus *Filatima* (Lepidoptera, Gelechiidae) from Central Asia. *Nasekomye Mongolii* 10: 572–577. [in Russian]
- Junnilainen J, Karsholt O, Nupponen K, Kaitila J-P, Nupponen T, Olschwang V (2010) The gelechiid fauna of the southern Ural Mountains, part II: list of recorded species with taxonomic notes (Lepidoptera: Gelechiidae). *Zootaxa* 2367(1): 1–68. <https://doi.org/10.11646/zootaxa.2367.1.1>
- Karsholt O, Mutanen M, Lee S, Kaila L (2013) A molecular analysis of the Gelechiidae (Lepidoptera, Gelechioidea) with an interpretative grouping of its taxa. *Systematic Entomology* 38(2): 334–348. <https://doi.org/10.1111/syen.12006>
- Kostjuk IYu, Budashkin YuI, Golovushkin MI (1994) *The Lepidoptera of the Dahursky Nature Reserve (An annotated checklist)*. Kiev, 36 pp. [in Russian]
- Kovács Z, Kovács S (2001) A new species of *Filatima* Busck, 1939 (Lepidoptera, Gelechiidae) from Transylvania, Romania. *Acta Zoologica Academiae Scientiarum Hungaricae* 47(4): 363–370.
- Lee S, Hodges RW, Brown RL (2009) Checklist of Gelechiidae (Lepidoptera) in America North of Mexico. *Zootaxa* 2231(1): 1–39. <https://doi.org/10.11646/zootaxa.2231.1.1>
- Lvovsky AL, Piskunov VI (1989) The gelechiid moths (Lepidoptera, Gelechiidae) of the Transaltai Gobi. *Nasekomye Mongolii* 10: 521–571. [in Russian]
- Meyrick E (1936) *Exotic Microlepidoptera* 5(1–2): 1–64.
- Piskunov VI (1971) New species of Gelechiidae (Lepidoptera) from the USSR. *Zoologicheskii Zhurnal* 50(7): 1104–1107. [in Russian]
- Piskunov VI (1979) On the fauna of the gelechiid moths (Lepidoptera, Gelechiidae) of Mongolia and Tuva. *Nasekomye Mongolii* 6: 394–403. [in Russian]

- Piskunov VI, Anikin VV (2005) Gelechiid Moth (Lepidoptera, Gelechiidae) of arid territory of Lower Volga region. Entomological and Parasitological investigations in Volga Region 4: 50–52. [in Russian]
- Piskunov VI, Uskov MV (2006) Two new species of gelechiid moths (Lepidoptera: Gelechiidae) from the center of European Russia. Eversmannia 5: 3–5. [In Russian]
- Pitkin L (1986) A technique for the preparation of complex male genitalia in Microlepidoptera. Entomologist's Gazette 37: 173–179.
- Ponomarenko MG (2008) Gelechiidae. In: Sinev SYu (Ed.) Katalog Cheshuekrylyh (Lepidoptera) Rossii (Catalogue of the Lepidoptera of Russia). KMK Scientific Press, St.Petersburg-Moscow, 87–106, 327–329. [in Russian]
- Ponomarenko MG (2016) Fam. Gelechiidae. In: Lelej AS (Ed.) Annotated catalogue of the insects of Russian Far East. Vol. 2. Lepidoptera. Dalnauka, Vladivostok, 115–139. [in Russian]
- Ponomarenko MG, Knyazev SA (2020) On the fauna of Gelechiid Moths from the Omsk region. Amurian Zoological Journal 12(3): 275–285. <https://doi.org/10.33910/2686-9519-2020-12-3-275-285> [in Russian]
- Rákósy L, Goia M, Kovács Z (2003) Catalogul Lepidopterelor României. Societatea Lepidopterologică Romană, Cluj-Napoca, 447 pp.
- Sattler K (1960) Generische Gruppierung der europäischen Arten der Sammelgattung *Gelechia* (Lepidoptera, Gelechiidae). Deutsche Entomologische Zeitschrift 7(1–2): 10–118. <https://doi.org/10.1002/mmnd.4800070103>
- Sattler K (1961) Zwei neue Arten der Gattung *Filatima* Busck, 1939 (Lep., Gelech.). Deutsche Entomologische Zeitschrift 8: 117–120. <https://doi.org/10.1002/mmnd.4800080109>
- Sattler K (1968) Die systematische Stellung einiger Gelechiidae. Deutsche entomologische Zeitschrift. Neue Folge 15: 111–131. <https://doi.org/10.1002/mmnd.4810150108>

Two new species of the subgenus *Reticularisus* (Lepidoptera, Limacodidae, *Rhamnosa*) from China, with a checklist of the genus *Rhamnosa* Fixsen, 1887

Jun Wu¹, Ting-Ting Zhao¹, Hui-Lin Han^{1,2,3}

1 School of Forestry, Northeast Forestry University, Harbin, 150040, China **2** Key Laboratory of Sustainable Forest Ecosystem Management, Ministry of Education, Northeast Forestry University, Harbin, 150040, China **3** Northeast Asia Biodiversity Research Center, Northeast Forestry University, Harbin, 150040, China

Corresponding author: Hui-Lin Han (hanhuilin@aliyun.com)

Academic editor: Andrew Mitchell | Received 5 October 2021 | Accepted 31 January 2022 | Published 3 May 2022

<http://zoobank.org/818DEAD3-4D0A-4D62-A990-C3188D8D7CB6>

Citation: Wu J, Zhao T-T, Han H-L (2022) Two new species of the subgenus *Reticularisus* (Lepidoptera, Limacodidae, *Rhamnosa*) from China, with a checklist of the genus *Rhamnosa* Fixsen, 1887. ZooKeys 1099: 111–121. <https://doi.org/10.3897/zookeys.1099.76163>

Abstract

Two new species of the subgenus *Reticularisus* Wu, Wu & Han, 2022 of the genus *Rhamnosa* Fixsen, 1887, *Rhamnosa (Reticularisus) chenjunii* **sp. nov.** and *Rh. (R.) mangshanensis* **sp. nov.**, are described from the provinces of Hunan and Guangdong, China. The adults and genital structures of the new species and similar examined species are illustrated. A checklist of the genus is provided.

Keywords

Guangdong, Hunan, slug caterpillar moths, taxonomy, Zygaenoidea

Introduction

The genus *Rhamnosa* Fixsen, 1887 was erected based on the type species *Rh. angulata* Fixsen, 1887 from “Korea”. Since then, approximately ten new species have been described and reported (Fixsen 1887; Hering 1931, 1933; Matsumura 1931; Okano and

Pak 1964; Wu 2008; Wu and Fang 2009). Solovyev and Witt (2009) divided *Rhamnosa* into two subgenera, *Rhamnosa* Fixsen, 1887 and *Caniodes* Matsumura, 1927, based on the external features and the male genitalia. Later, Solovyev and Dubatolov (2015) clarified the exact taxonomic position of some species and provided a distribution map for *Rh. angulata* Fixsen, 1887. Solovyev (2017) established a third subgenus, *Rhamnopsis* Matsumura, 1931, for the endemic species *Rh. arizanella* (Matsumura, 1931) from Taiwan. However, *Rh. arizanella* was misplaced in the subgenus *Rhamnosa* by Wu et al. (2022), which is corrected in this paper. A fourth subgenus, *Reticularisus* Wu, Wu & Han, 2022, was established based on overall appearance and male genitalic characters. This subgenus contains two species: *Rh. (R.) henanensis* Wu, 2008 and *Rh. (R.) shierbeihoua* Wu, Wu & Han, 2022 (Wu et al. 2022). To date, the genus included nine described species belonging to four subgenera, all of which have been recorded in China.

In this study, two new species of the subgenus *Reticularisus*, *Rh. (R.) chenjuni* sp. nov. and *Rh. (R.) mangshanensis* sp. nov., collected from the Hunan and Guangdong provinces of China, are described.

Materials and methods

The specimens were collected with a 220V/450W mercury vapour lamp and DC black light lamps at Mangshan National Nature Reserve and Nanling National Forest Park, respectively in the Hunan and Guangdong provinces of China. Standard methods for dissection and preparation of the genitalia slides were used (Kononenko and Han 2007). The specimens were photographed using a Nikon D700 camera, whereas the genitalia slides were photographed with an Olympus photo microscope and processed using the Helicon Focus software and Adobe Photoshop CS6. All type materials of the new species are deposited in the collection of the Northeast Forestry University (NEFU), Harbin, China. Material from the National Zoological Museum of China, Institute of Zoology, Chinese Academy of Sciences, Beijing, China (IZCAS) was also examined in this study.

Taxonomic account

Genus *Rhamnosa* Fixsen, 1887

Rhamnosa Fixsen, 1887: 339. Type species: *Rhamnosa angulata* Fixsen, 1887, by monotypy. Type locality: “Korea”.

Caniodes Matsumura, 1927: 91. Type species: *Caniodes takamukui* Matsumura, 1927. Type locality: “Formosa” (Horisha).

Rhamnopsis Matsumura, 1931: 101. Type species: *Rhamnopsis arizanella* Matsumura, 1931. Type locality: “Formosa” (Arisan).

Subgenus *Reticularisus* Wu, Wu & Han, 2022

Reticularisus Wu, Wu & Han, 2022: 138. Type species: *Rhamnosa henanensis* Wu, 2008, by original designation. Type locality: Henan Province, China.

Notes. The subgenus is characterized by the forewing being pale yellow in ground colour and covered with reddish-brown scales. The antemedial and postmedial lines are entire, not parallel, straight or slightly curved, darkish, running from the wing margin near the apex to the inner margin. The venation of the forewing is usually of an obvious dark brownish red colour. The species are not sexually dimorphic; the females are usually slightly larger, with filiform or slightly bipectinated antennae.

The male genitalia are diagnostic: apical part of juxta with massive numbers of tiny spines; basal part flat, with a pair of lateral processes that can be strongly sclerotized or not; saccus visible or simply present; valva without basal processes; aedeagus slender and always more or less spiral-shaped near the coecum.

***Rhamnosa (Reticularisus) chenjuni* sp. nov.**

<http://zoobank.org/DF51CFAB-D023-45C3-8B51-A0EF7CB0D55F>

Figs 1, 2, 7, 11

Holotype. ♂, CHINA, Hunan Province, Chenzhou City, Yizhang County, Mangshan National Nature Reserve, Jiangjunzhai scenic spot, 30.VII–7.VIII.2021, leg. J. Wu and Q. Lin, genit. prep. WuJ-583-1 (NEFU).

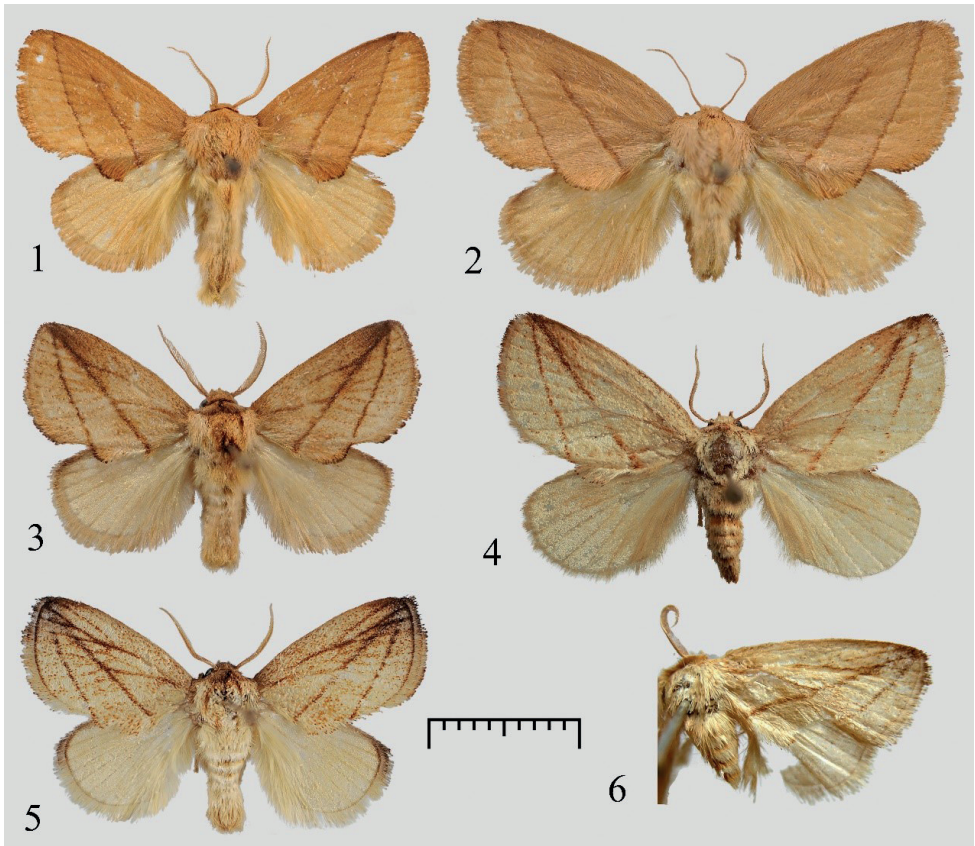
Paratypes. 17♂, 4♀, same date as for holotype, genit. prep. WuJ-582-1, WuJ-584-2, WuJ-585-2 (NEFU). 2♂, CHINA, Guangdong Province, Shaoguan City, Ruyuan County, Nanling National Forest Park, 24–27.V.2021, leg. MR. Li and G. Fu, genit. prep. WuJ-594-1, WuJ-595-1 (NEFU).

Diagnosis. The new species *Rh. chenjuni* sp. nov. (Figs 1, 2) can be distinguished from the other three species (Figs 3–6) in the subgenus *Reticularisus* by the forewing patterns. The antemedial line of the forewing is barely visible in the region near the apex and does not intersect with the subterminal line, but in *Rh. mangshanensis* sp. nov. (Figs 3, 4), *Rh. shierbeihoua* (Fig. 5), and *Rh. henanensis* (Fig. 6), the antemedial lines are entire and intersect with the subterminal lines at the wing margin near the apex.

In the male genitalia, *Rh. chenjuni* sp. nov. (Fig. 7) is most similar to the other new species *Rh. mangshanensis* sp. nov. (Fig. 8), but the diagnostic features are the short and stout gnathos, the lateral processes of the juxta strongly sclerotized and gradually diverging into 3–7 long, acute spines, and the saccus is small and triangular rather than tongue-shaped. However, in *Rh. mangshanensis* sp. nov. the gnathos is slender and curved at the middle; the lateral processes of the juxta bear a strongly sclerotized, long, hook-shaped process, and the saccus is tongue-shaped. *Rh. chenjuni* sp. nov. differs from *Rh. shierbeihoua* (Fig. 9) and *Rh. henanensis* (Fig. 10) by the following characteristics of the male genitalia: the sacculus of the valva is wavy;

the juxta bears a pair of lateral processes that are strongly sclerotized and gradually diverging into several long spines; the saccus is visible, small, triangular. However, in *Rh. shierbeihoua*, the sacculus of the valva is smoothly arc-curved, the lateral processes of juxta are short, not sclerotized, covered with massive numbers of spinules, and the saccus is not visible. In *Rh. henanensis*, the sacculus of the valva is straight, the juxta bears a pair of sawblade-shaped and strongly sclerotized lateral processes, and the saccus is short and broad.

In the female genitalia, *Rh. chenjuni* sp. nov. (Fig. 11) differs from *Rh. mangshanensis* sp. nov. (Fig. 12) by its strongly swollen genital chamber, highly modified lamella postvaginalis, less spiraled ductus bursae, larger corpus bursae, and the upper position of the signum.



Figures 1–6. Adults of *Rhamnosa (Reticularis)* spp. **1** *Rh. chenjuni* sp. nov., male, holotype (NEFU) **2** *Rh. chenjuni* sp. nov., female, paratype (NEFU) **3** *Rh. mangshanensis* sp. nov., male, holotype (NEFU) **4** *Rh. mangshanensis* sp. nov., female, paratype (NEFU) **5** *Rh. shierbeihoua* Wu, Wu & Han, 2022, male, holotype, Guizhou, China (NEFU) **6** *Rh. henanensis* Wu, 2008, male, holotype, Henan, China (IZCAS). Scale bar: 1 cm.

Description. Adult (Figs 1, 2). Forewing length 11–13 mm, wingspan 23–29 mm in male (13–15 mm and 29–34 mm in female). Head brown; labial palpus short, brown; antennae bipectinated almost to the apex in male, filiform in female. Forewing ground colour ochreous to pale brown, with two distinct, slightly sinuous, dark brown antemedial and subterminal lines running from costal margin near apex, and reaching inner margin at ca. $1/3$ and $2/3$ distance from the wing base, respectively; antemedial line barely visible near apical region; a conspicuous dentiform tuft located at middle of inner margin; fringe ochreous with black terminally. Hindwing pale yellow, mixed with a little brown. Scales on legs ochreous to pale yellow. Abdomen pale yellow.

Male genitalia (Fig. 7). Uncus triangular, with a strongly sclerotized apical spur. Gnathos hook-shaped, slightly thinner terminally. Valva of almost equal width, upper half part covered with dense hairs; sacculus obviously waved; cucullus broad and rounded. Juxta flattened, rounded, slightly divided apically; lateral process plate-shaped, bearing a strongly sclerotized process gradually diverging into 3–7 (normally of 5) long, acute spines. Saccus visible, as a small triangle. Aedeagus slender, slightly spiral-shaped near coecum; cornuti of vesica not obvious.

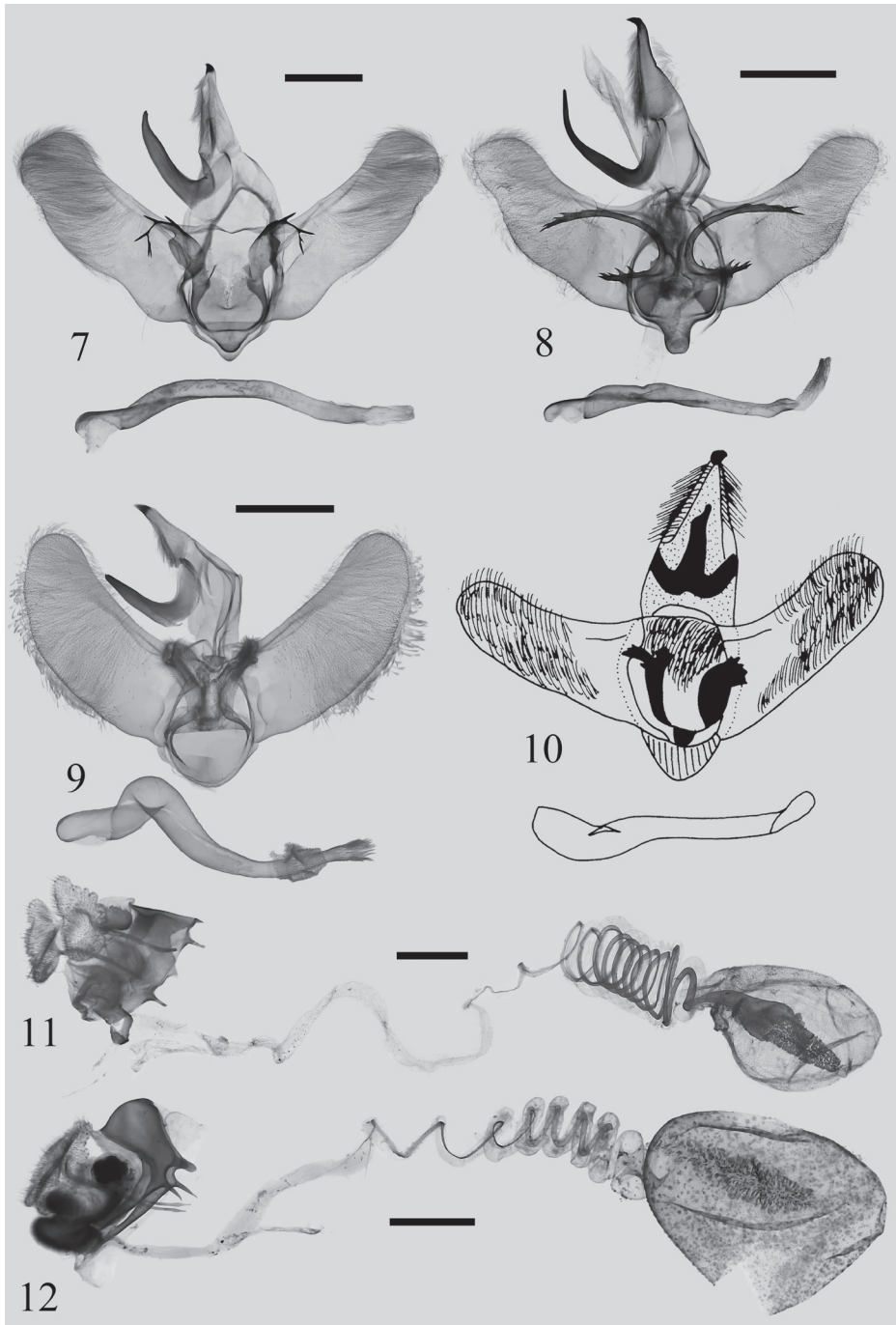
Female genitalia (Fig. 11). Papillae anales ear-shaped, covered with dense setae on surface, margins with a dorsal and ventral lobe and several deep clefts in the middle. Postvaginal plate strongly sclerotized, nearly square. Anterior apophysis short; posterior apophysis long and slender, ca. $4\times$ length of anterior apophysis. Ostium bursae strongly sclerotized. Ductus bursae very long, strongly spiral-shaped in basal part. Corpus bursae pear-shaped, covered with dense spines on the outside and with a spindle-shaped signum that is strongly sclerotized and almost as long as corpus bursae.

Distribution (Fig. 13). China (Hunan: Mangshan; Guangdong: Nanling).

Etymology. The species name is dedicated to Mr. Jun Chen, who works in the Mangshan State-owned Forestry Administration in Hunan Province, China. He was of great assistance to us when we were collecting in Mangshan National Nature Reserve.

Remarks. This new species differs clearly in appearance from the other three species in the subgenus *Reticularisus*, mainly in having antemedial line not visible near the apical region and forewing lacking distinctive marks other than the antemedial and submarginal lines. It shares some similarities with *Rb. (Rhamnosa) hatita* (Druce, 1896); however, because it highly matches the characters of the subgenus *Reticularisus* for the male genitalia, i.e., valva without a basal process, juxta with a pair of distinct lateral processes, saccus visible, and aedeagus spiraled near coecum, it is provisionally placed in this subgenus.

These moths fly from late May to August. The specimens were collected by 220V/450W mercury light and DC black light at 570–1,265 m a.s.l.; the collecting site in Hunan province is located close to mixed coniferous and broad-leaved forests (Figs 14, 16).



Figures 7–12. Genitalia of *Rhamnosa (Reticularis)* spp. **7** *Rb. chenjunii* sp. nov., male, holotype (NEFU) **8** *Rb. mangshanensis* sp. nov., male, holotype (NEFU) **9** *Rb. shierbeihoua* Wu, Wu & Han, 2022, male, holotype, genit. slide WuJ-301-1 (NEFU) **10** *Rb. henanensis* Wu, 2008, male, holotype (IZCAS) **11** *Rb. chenjunii* sp. nov., female, paratype, genit. slide WuJ-585-2 (NEFU) **12** *Rb. mangshanensis* sp. nov., female, paratype, genit. slide WuJ-593-2 (NEFU). Scale bars: 1 mm.

***Rhamnosa (Reticularisus) mangshanensis* sp. nov.**

<http://zoobank.org/72F98AFB-557A-49B0-BB6A-68FAB1D4009F>

Figs 3, 4, 8, 12

Holotype. ♂, CHINA, Hunan Province, Chenzhou City, Yizhang County, Mangshan National Nature Reserve, Jiangjunzhai scenic spot, 30.VII–7.VIII.2021, leg. J. Wu and Q. Lin, genit. prep. WuJ-581-1 (NEFU).

Paratypes. 27♂, same date as for holotype, genit. prep. WuJ-579-1, WuJ-580-1 (NEFU); 1♂, 1♀, CHINA, Guangdong Province, Shaoguan City, Ruyuan County, Nanling National Forest Park, 24–27.V.2021, leg. MR. Li and G. Fu, genit. prep. WuJ-592-1, WuJ-593-2 (NEFU).

Diagnosis. Three of the species in the subgenus *Reticularisus*, *Rh. mangshanensis* sp. nov. (Figs 3, 4), *Rhamnosa. shierbeihoua* (Fig. 5), and *Rh. henanensis* (Fig. 6), are very similar in appearance. *Rh. mangshanensis* sp. nov. can be distinguished from *Rh. shierbeihoua* by the point of emergence of the two oblique antemedial and subterminal lines (running from the costal margin near the apex in *Rh. mangshanensis* sp. nov. but from the outer margin near the apex in *Rh. shierbeihoua*), and by the ground colour of the body (pale brownish-yellow in *Rh. mangshanensis* sp. nov. but pale yellow in *Rh. shierbeihoua*). However, it is hard to distinguish it from the *Rh. henanensis* only by its external appearance.

The male genitalia of *Rh. mangshanensis* sp. nov. (Fig. 8) are clearly distinguishable from those of *Rh. shierbeihoua* (Fig. 9) and *Rh. henanensis* (Fig. 10). The gnathos of *Rh. mangshanensis* sp. nov. is slender and up-curved at an obtuse angle at the middle, the sacculus of the valva is distinctly waved, and the lateral processes of the juxta are strongly sclerotized with a long, slender, hook-shaped, basally serrated and terminally forked process. In *Rh. shierbeihoua* (Fig. 9) and *Rh. henanensis* (Fig. 10) the gnathos are shorter and thicker, the sacculi are straight or smoothly arc-curved, the lateral processes of the juxta are short, nearly plate-shaped, without a long slender process at apex. The differences in external appearance and genitalia between *Rh. mangshanensis* sp. nov. and *Rh. chenjuni* sp. nov. are listed under the latter species.

Description. Adult (Figs 3, 4). Forewing length 11–12 mm, wingspan 24–27 mm in male (14 mm and 29 mm in the single studied female). Head dark brown; labial palpus short, dark brown; male antennae bipectinated almost to apex, female antennae also bipectinated but extremely thinner than male's. Thorax brownish yellow; patagium reddish-brown; tegula brownish-yellow. Forewing ground colour pale brownish-yellow; costal margin dark brown to black near apex; two distinct, oblique, dark brown antemedial and subterminal lines running from costal margin near apex to inner margin: antemedial line straight, reaching to ca. 1/3 from wing base, subterminal line slightly curved towards outer margin, reaching to ca. 2/3 from wing base; a mixed brownish-yellow and dark brown dentiform tuft is located between these two lines along the inner margin; venation visible in forewing, brown, veins at margins of cell dark brown; fringe dark brown to black. Hindwing pale yellow; fringe dark brown at apex, remainder pale yellow. Scales on legs brown to pale yellow. Abdomen brownish-yellow.

Male genitalia (Fig. 8). Uncus triangular, elongated, with a strongly sclerotized apical spur. Gnathos slender, hook-shaped, up-curved at an obtuse angle at middle. Valva broad at base; sacculus obviously waved; cucullus slightly narrower, rounded. Juxta highly modified, covered with massive numbers of tiny spines in upper part; basal part with a pair of strongly sclerotized, long, slender, hook-shaped lateral processes, with a row of teeth at base and terminally forked. Vinculum narrow. Saccus strongly sclerotized, tongue-shaped. Aedeagus slender, slightly spiral-shaped near coecum, sclerotized at apex; vesica with dense, tiny cornuti.

Female genitalia (Fig. 12). Papillae anales ear-shaped, covered with dense setae on surface, margins with several small clefts. Anterior apophysis short but robust, pointed apically, with an obvious tongue-shaped process next to it; posterior apophysis long and slender, slightly enlarged subapically, ca. 4.5× length of anterior apophysis. Genital chamber strongly sclerotized and obviously swollen, with a pair of rounded processes below it. Lamella postvaginalis highly modified, oval-shaped, densely covered with short hairs, with a pair of small hairy processes. Ductus bursae long, membranous, thick and strongly spiral-shaped at base. Corpus bursae large, oval-shaped, densely covered with tiny sclerotized flecks, with a spindle-shaped, strongly sclerotized, erect signum situated in upper 2/3.

Distribution (Fig. 13). China (Hunan: Mangshan; Guangdong: Nanling).

Etymology. The new species is named after its type locality, the Mangshan National Nature Reserve of Hunan Province, China.

Remarks. These moths fly from late May to August. The specimens were collected by 220V/450W mercury light and DC black light at 570–1,265 m a.s.l.; the collecting site in Hunan province is close to mixed coniferous and broad-leaved forests (Figs 15, 16).

Checklist of species of the genus *Rhamnosa* Fixsen, 1887

Subgenus *Rhamnosa* Fixsen, 1887

Rh. (R.) angulata Fixsen, 1887

Rh. (R.) hatita (Druce, 1896)

= *Rh. angulate kwangtungensis* Hering, 1931

= *Rh. (R.) kwangtungensis* Hering, 1931

Rh. (R.) dentifera Hering & Hopp, 1927

Rh. (R.) convergens Hering, 1931

Subgenus *Caniodes* Matsumura, 1927

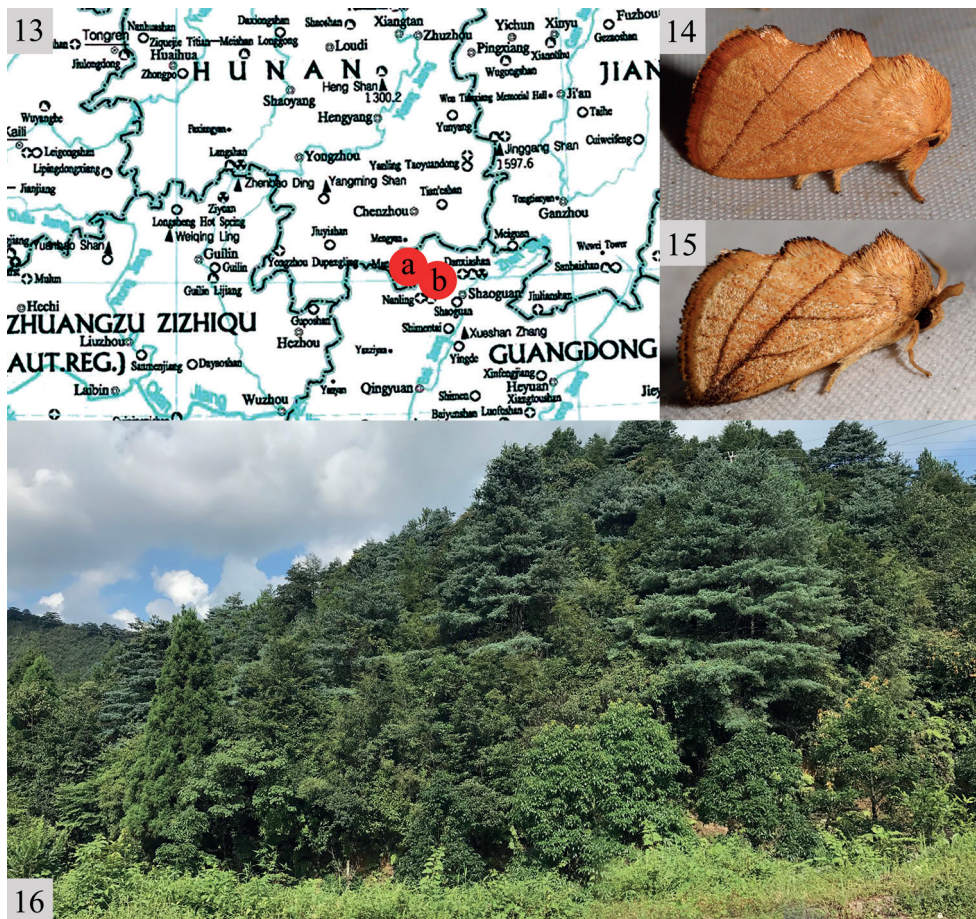
Rh. (C.) uniformis (Swinhoe, 1895)

= *Cania notodonta* Hampson, 1897

= *Caniodes takamukui* Matsumura, 1927

= *Rh. uniformis rufina* Hering, 1931

Rh. (C.) uniformoides Wu & Fang, 2009

Subgenus *Rhamnopsis* Matsumura, 1931*Rh. (R.) arizanella* (Matsumura, 1931)= *Rhamnopsis arizanella* Matsumura, 1931= *Rh. arizanella* (Matsumura, 1931)**Subgenus *Reticularisus* Wu, Wu & Han, 2022***Rh. (R.) henanensis* Wu, 2008*Rh. (R.) chenjunii* sp. nov.*Rh. (R.) mangshanensis* sp. nov.*Rh. (R.) shierbeihoua* Wu, Wu & Han, 2022

Figures 13–16. 13 collecting sites of the two new species: Hunan Province, Mangshan National Nature Reserve (red dot a); Guangdong Province, Nanling National Forest Park (red dot b) 14, 15 adult male, living habitus: 14 *Rh. chenjunii* sp. nov. 15 *Rh. mangshanensis* sp. nov. 16 the biotope of these two new species in Hunan is close to a mixed coniferous and broad-leaved forest.

Discussion

The genus *Rhamnosa* includes four subgenera with a total of eleven species, all 11 species are recorded in China based on the literature. The subgenus *Reticularisus* was established for its unique characteristics of the forewing and male genitalia. In the four known species of the subgenus, the antemedial and subterminal lines of the forewing always intersect near the apex (the antemedial line of *Rh. (R.) chenjuni* sp. nov. is not visible anteriorly so the two lines do not intersect, but the two lines would cross if both visible), and the aedeagus is always more or less spiral-shaped near the coecum, so these two characters may be considered as apomorphies of the subgenus.

Acknowledgements

The present study was supported by the National Natural Science Foundation of China (No. 31872261) and the Fundamental Research Funds for the Central Universities (No. 2572021DJ08, 2572019CP11). We sincerely thank Mr. Jun Chen, who works at the Mangshan State-owned Forestry Administration in Hunan Province, for his great assistance during collecting in Mangshan National Nature Reserve; and the colleagues from our laboratory for collecting a part of the material of these two new species.

References

- Fixsen C (1887) Lepidoptera aus Korea. In: Romanoff NM (Ed.) Mémoires sur les lépidoptères, Tom III. St. Pétersbourg, Imprimerie de M. M. Stassuléwitch, 233–356. [pl. 15]
- Hering M (1931) Limacodidae (Cochliopodidae). In: Seitz A (Ed.) Die Gross-Schmetterlinge der Erde. Vol. 10. Alfred Kerner Verlag, Stuttgart, 665–728.
- Hering M (1933) Familie: Limacodidae (Cochliopodidae). In: Seitz A (Ed.) Die Gross-Schmetterlinge der Erde. Supplement 2. Die Palaearktischen Spinner und Schwärmer. Alfred Kernen Verlag, Stuttgart, 201–209.
- Kononenko VS, Han HL (2007) Atlas Genitalia of Noctuidae in Korea (Lepidoptera). In: Park K-T (Ed.) Insects of Korea (Series 11). Junhaeng-Sa, Seoul, 464 pp.
- Matsumura S (1927) New species and subspecies of moths from the Japanese Empire. The journal of the College of Agriculture, Tohoku Imperial University, Sapporo, Japan 19(1): 1–91.
- Matsumura S (1931) Descriptions of some new genera and species from Japan, with a list of species of the family Cochlidionidae. Insecta Matsumurana 5(3): 101–116.
- Okano M, Pak SW (1964) A revision of the Korean species of the family Heterogeneidae (Lepidoptera). Annual report of the College of Liberal Arts. University of Wate 22: 1–10.
- Solovyev AV (2017) Limacodid moths (Lepidoptera, Limacodidae) of Taiwan, with descriptions of six new species. Entomological Review 97(8): 1140–1148. <https://doi.org/10.1134/S0013873817080140>

- Solovyev AV, Dubatolov VV (2015) *Rhamnosa angulata* Fixsen, 1887 (Lepidoptera, Limacodidae) – a new record of slug moths for the Russian fauna, with a review of species recorded near the Russian border. *Evrziatskii Entomologicheskii Zhurnal* 14(1): 63–69. [in Russian with English summary]
- Solovyev AV, Witt ThJ (2009) The Limacodidae of Vietnam. *Entomofauna* (Supplement 16): 33–229.
- Wu CS (2008) A new species of the genus *Rhamnosa* Fixsen from Henan Province (Lepidoptera: Limacodidae). In: Shen XC, Lu CT (Eds) *The fauna and taxonomy of insects in Henan*, vol. 6: *Insects of Baotianman National Nature Reserve*, China Agricultural Science and Technology Press, Beijing, 7–8. [in Chinese]
- Wu CS, Fang CL (2009) A review of *Rhamnosa* from China (Lepidoptera: Limacodidae). *Oriental Insects* 43(1): 253–259. <https://doi.org/10.1080/00305316.2009.10417586>
- Wu J, Wu CS, Han HL (2022) *Reticularisus* Wu, Wu & Han, a new subgenus of the genus *Rhamnosa* Fixsen, 1887 from China, with description of a new species (Lepidoptera: Limacodidae). *SHILAP Revista de Lepidopterologia* 50(197): 137–144.

A new cryptic species in the *Theلودerma rhododiscus* complex (Anura, Rhacophoridae) from China–Vietnam border regions

Lingyun Du^{1,2*}, Jian Wang^{3,4*}, Shuo Liu⁵, Guohua Yu^{1,2}

1 Key Laboratory of Ecology of Rare and Endangered Species and Environmental Protection (Guangxi Normal University), Ministry of Education, Guilin 541004, China **2** Guangxi Key Laboratory of Rare and Endangered Animal Ecology, College of Life Science, Guangxi Normal University, Guilin 541004, China **3** Ministry of Education Key Laboratory for Ecology of Tropical Islands & Key Laboratory of Tropical Animal and Plant Ecology of Hainan Province, College of Life Sciences, Hainan Normal University, Haikou 571158, China **4** College of Biological and Agricultural Sciences, Honghe University, Mengzi 661199, China **5** Kunming Natural History Museum of Zoology, Kunming Institute of Zoology, Chinese Academy of Sciences, Kunming 650223, China

Corresponding authors: Guohua Yu (yugh2018@126.com), Shuo Liu (liushuo@mail.kiz.ac.cn)

Academic editor: Angelica Crottini | Received 11 January 2022 | Accepted 24 March 2022 | Published 3 May 2022

<http://zoobank.org/5C7E35BD-A831-4403-9831-7FFAC17DA0A7>

Citation: Du L, Wang J, Liu S, Yu G (2022) A new cryptic species in the *Theلودerma rhododiscus* complex (Anura, Rhacophoridae) from China–Vietnam border regions. ZooKeys 1099: 123–138. <https://doi.org/10.3897/zookeys.1099.80390>

Abstract

We describe a new species of *Theلودerma* from southern Yunnan, China and northern Vietnam based on morphological and molecular evidence. *Theلودerma hekouense* sp. nov., which had been recorded as *T. rhododiscus*, is the sister to *T. rhododiscus*. The new species differs genetically from *T. rhododiscus* by 4.2% and 10.7% in 16S rRNA and COI genes, respectively, and it can be morphologically distinguished from *T. rhododiscus* by having more densely spaced white warts on the dorsal surface, red subarticular tubercles, red metacarpal tubercles, a red metatarsal tubercle, and black dorsal and ventral surfaces in preservative. Currently the new species is only known from the China–Vietnam border regions of Yunnan and Ha Giang, while *T. rhododiscus* has a wide distributional range in China including Guangxi, Guangdong, Hunan, Fujian, Jiangxi, and presumably Guizhou and eastern Yunnan. Including the new species, there are currently 10 *Theلودerma* species in China and seven *Theلودerma* species in Yunnan, where more species will probably be found.

Keywords

16S rRNA, COI, southern Yunnan, *Theلودerma hekouense* sp. nov.

* These authors contributed equally to this work.

Introduction

Theلودerma Tschudi, a genus of the family Rhacophoridae, occurs in southern and eastern areas of Asia and currently contains 26 species (Frost 2021), of which nine are recognized from China and seven are known from Yunnan including *T. albopunctatum* (Liu & Hu), *T. baibungense* (Jiang, Fei & Huang), *T. bicolor* (Bourret), *T. gordonii* Taylor, *T. moloch* (Annandale), *T. pyaukkya* Dever, and *T. rhododiscus* (Liu & Hu) (Du et al. 2020).

Theلودerma rhododiscus was originally described from Mt Dayao, Guangxi, China in 1962 (Liu and Hu 1962; Fig. 1) and now is widely recorded from Fujian, Jiangxi, Hunan, Guangdong, Yunnan (Fei et al. 2012; Hou et al. 2017a, 2017b; Zeng et al. 2017), and northern Vietnam (Bain and Nguyen 2004). It was characterized by fingers and toes with orange-red disks, dorsal surface tea-brown, and a dorsum covered with white tubercles interweaved as a network (Liu and Hu 1962).

Numerous studies have shown that widely recorded amphibian species might actually be composed of multiple cryptic species (e.g., Lyu et al. 2019; Yu et al. 2019a, 2019b). Although Zeng et al. (2017) confirmed that the records of *T. rhododiscus* from Guangdong (Mt Nankun) and Jiangxi (Mts Jiulian and Sanbai) are conspecific with *T. rhododiscus* from the type locality based on morphological and molecular evidence, records of *T. rhododiscus* from other places need further confirmation from both morphological and molecular perspectives. Our earlier phylogenetic analysis of *Theلودerma* (Hou et al. 2017b) showed that the clade consisting of populations from Yunnan and northern Vietnam is separated from the clade consisting of the topotypes with a relative large genetic divergence, which indicates that more studies are needed to test whether the records of *T. rhododiscus* from Yunnan and Vietnam belong to *T. rhododiscus* or not.

In this study, we compared the *T. rhododiscus* specimens from Yunnan with the topotypes of this species from both morphological and molecular perspectives. Our results supported that the records of *T. rhododiscus* from Yunnan and northern Vietnam warrant distinct taxonomic recognition. Additionally, we confirmed two new distribution sites of *T. rhododiscus* in northwestern (Longlin County) and northern Guangxi (Huanjiang County).

Materials and methods

Sampling

Specimens were collected by Guohua Yu during fieldwork in Jinxiu and Longlin counties, Guangxi, China in April and June of 2020, by Jian Wang during fieldwork in Hekou County, Yunnan, China in May and September 2020 and 2021, and by Shuo Liu during field surveys in Huanjiang County, Guangxi in September 2019. Specimens were fixed and then stored in 75% ethanol. Liver tissues were preserved in 99% ethanol. All specimens were deposited at Guangxi Normal University (GXNU).

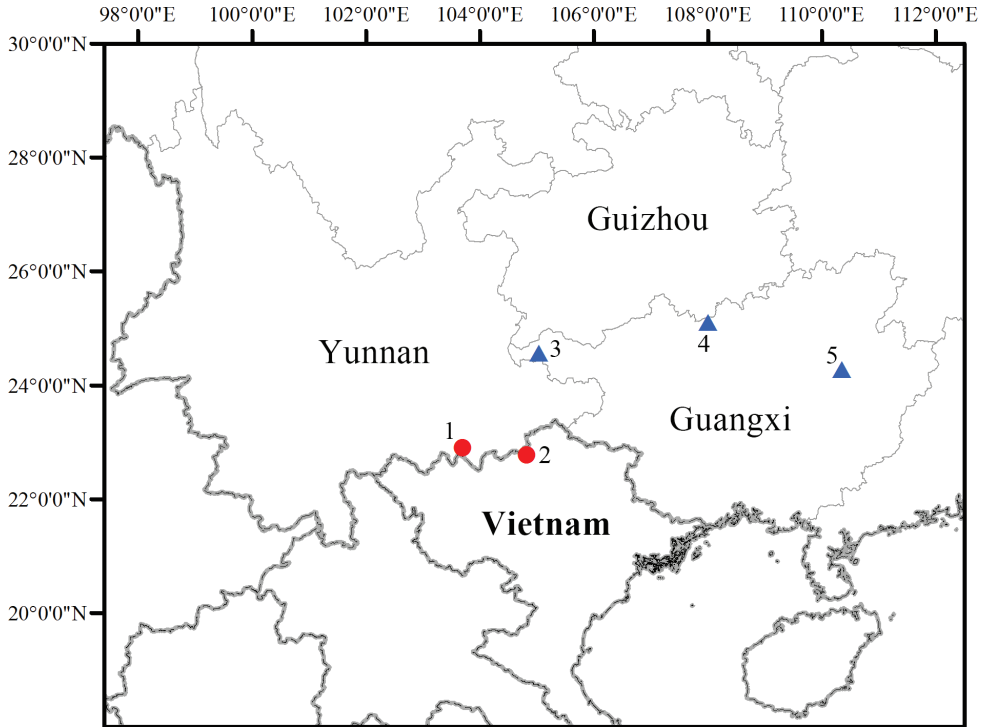


Figure 1. Map showing the collection sites of *T. hekouense* sp. nov. (circle) and *T. rhododiscus* (triangle) in this study **1** Hekou (type locality of the new species) **2** Ha Giang **3** Longlin **4** Huanjiang **5** Jinxiu (type locality of *T. rhododiscus*)

Morphology

Morphometric data were taken using digital calipers to the nearest 0.1 mm. Morphological terminology follows Yu et al. (2019a). Measurements include: snout-vent length (SVL, from tip of snout to vent); head length (HL, from tip of snout to rear of jaws); head width (HW, width of head at its widest point); snout length (SL, from tip of snout to anterior border of eye); internarial distance (IND, distance between nares); interorbital distance (IOD, minimum distance between upper eyelids); upper eyelid width (UEW, maximum width of upper eyelid); eye diameter (ED, diameter of exposed portion of eyeball); tympanum diameter (TD, the greater of tympanum vertical and horizontal diameters); forearm and hand length (FHL, from elbow to tip of third finger); tibia length (TL, distance from knee to heel); foot length (FL, from proximal end of inner metatarsal tubercle to tip of fourth toe); length of foot and tarsus (TFL, from tibiotarsal joint to tip of fourth toe). Comparative morphological data of other *Theلودerma* species were taken from their original descriptions or redescrptions (Taylor 1962; Stuart and Heatwole 2004; Orlov and Ho 2005; Orlov et al. 2006; McLeod and Ahmad 2007; Rowley et al. 2011; Poyarkov et al. 2015, 2018; Nguyen et al. 2016; Sivongxay et al. 2016; Dever 2017; Du et al. 2020).

Molecular phylogenetic analyses

Total genomic DNA was extracted from liver tissues. Tissue samples were digested using proteinase K, and subsequently purified following a standard phenol/chloroform isolation and ethanol precipitation. Sequences of 16S rRNA (16S) and cytochrome oxidase subunit I (COI) genes were amplified using the primers and experimental protocols of Du et al. (2020). Sequencing was conducted directly using the corresponding PCR primers. All new sequences were deposited in GenBank under accession numbers OL843957–OL843967 and OL843972–OL843982 (Table 1). Available homologous sequences of members of *Theloderma* were obtained from GenBank (Table 1). *Buergeria oxycephala*, *Liuxialus hainanus*, *Gracixalus jinxiuensis*, and *Nyxtixalus pictus* were selected as hierarchical outgroups according to Yu et al. (2009) and Du et al. (2020).

Sequences were aligned using MUSCLE with the default parameters in MEGA v. 7 (Kumar et al. 2016). Uncorrected pairwise distances between species were calculated in MEGA v. 7. The best substitution model was selected using the Akaike Information Criterion (AIC) in jMODELTEST v. 2.1.10 (Darriba et al. 2012). Bayesian inferences were performed in MRBAYES v. 3.2.6 (Ronquist et al. 2012) under the selected substitution model (GTR + I + G). Two runs were performed simultaneously with four Markov chains starting from random tree. The chains were run for 3,000,000 generations and sampled every 100 generations. The first 25% of the sampled trees were discarded as burn-in after the standard

Table 1. Samples used in molecular analyses of this study.

Species	Voucher number	Locality	16s	COI
<i>Buergeria oxycephala</i>	MVZ 230425	Hainan, China	KU244359	KU244459
<i>Liuxialus hainanus</i>	LJT V15	Hainan, China	KC465826	–
<i>Gracixalus jinxiuensis</i>	KIZ 061210YP	Guangxi, China	EU215525	–
<i>Nyxtixalus pictus</i>	KUHE 53517	Malaysia	LC012863	–
<i>Theloderma albopunctatum</i>	VNMN JR2887	Vinh Phuc, Vietnam	KU244375	KU244431
<i>Theloderma laeve</i>	NAP01644	Lam Dong, Vietnam	KT461907	–
<i>Theloderma leporosum</i>	LJT W46	Malaysia	KC465841	–
<i>Theloderma palliatum</i>	NAP02516	Lam Dong, Vietnam	KT461903	–
<i>Theloderma vietnamense</i>	AMS R174047	Mondol Kiri, Cambodia	JN688171	KU244460
<i>Theloderma stellatum</i>	Stel1	Chanthaburi, Thailand	KT461918	–
<i>Theloderma truongsongense</i>	VNMN 4402	Khanh Hoa, Vietnam	LC012847	–
<i>Theloderma ryabovi</i>	VNMN 3924	Kon Tum, Vietnam	LC012860	–
<i>Theloderma phrynoderma</i>	CAS247910	Myanmar	KJ128283	KU244449
<i>Theloderma nebulosum</i>	ROM 39588	Kon Tum, Vietnam	KT461887	–
<i>Theloderma lycin</i>	MVZ 9458	Indonesia	KU244368	KU244447
<i>Theloderma lateriticum</i>	VNMN 1216	Bac Giang, Vietnam	LC012851	–
<i>Theloderma lacustrinum</i>	NCSM 84683	Vientiane, Laos	KX095246	–
<i>Theloderma horridum</i>	KUHE 52582	Negeri Sembilan, Malaysia	LC012861	–
<i>Theloderma gordoni</i>	MVZ 226469	Vinh Phuc, Vietnam	KU244363	KU244451
<i>Theloderma corticale</i>	MVZ 223905	Vinh Phuc, Vietnam	KU244364	KU244452
<i>Theloderma auratum</i>	ZMMU A5828	Gia Lai, Vietnam	MG917767	–

Species	Voucher number	Locality	16s	COI
<i>Theلودerma annae</i>	NAP05558	Hoa Binh, Vietnam	MG917766	–
<i>Theلودerma asperum</i>	ZRC1.1.9321	Malaysia	GQ204725	–
<i>Theلودerma baibungense</i>	YPX31940	Motuo, Tibet, China	KU981089	–
<i>Theلودerma bicolor</i>	LC1	Lvchun, Yunnan, China	KY495632	–
<i>Theلودerma moloch</i>	GXNU YU000115	Yingjiang, Yunnan, China	MT509809	–
<i>Theلودerma pyaukkya</i>	GXNU YU000116	Yingjiang, Yunnan, China	MT509810	MT522176
<i>Theلودerma petilum</i>	HNUE MNA2012.0001	Dien Bien, Vietnam	KJ802925	–
<i>Theلودerma rhododiscus</i>	CIB GX200807017	Jinxiu, Guangxi, China	LC012842	–
<i>Theلودerma rhododiscus</i>	KIZ060821063	Jinxiu, Guangxi, China	EF564533	–
<i>Theلودerma rhododiscus</i>	KIZ060821170	Jinxiu, Guangxi, China	EF564534	–
<i>Theلودerma rhododiscus</i>	SCUM 061102L	Jinxiu, Guangxi, China	EU215530	–
<i>Theلودerma rhododiscus</i>	CIB GX200807048	Jinxiu, Guangxi, China	KJ802921	–
<i>Theلودerma rhododiscus</i>	GXNU YU000069	Jinxiu, Guangxi, China	OL843957	OL843972
<i>Theلودerma rhododiscus</i>	GXNU YU000070	Jinxiu, Guangxi, China	OL843958	OL843973
<i>Theلودerma rhododiscus</i>	GXNU YU000309	Huanjiang, Guangxi, China	OL843959	OL843974
<i>Theلودerma rhododiscus</i>	GXNU YU000318	Longlin, Guangxi, China	OL843960	OL843975
<i>Theلودerma rhododiscus</i>	GXNU YU000319	Longlin, Guangxi, China	OL843961	OL843976
<i>Theلودerma rhododiscus</i>	C051	Jinxiu, Guangxi, China	–	KP996753
<i>Theلودerma rhododiscus</i>	C089	Jinxiu, Guangxi, China	–	KP996786
<i>Theلودerma rhododiscus</i>	C090	Jinxiu, Guangxi, China	–	KP996787
<i>Theلودerma hekouense</i> sp. nov.	GXNU YU000397	Hekou, Yunnan, China	OL843962	OL843977
<i>Theلودerma hekouense</i> sp. nov.	GXNU YU000398	Hekou, Yunnan, China	OL843963	OL843978
<i>Theلودerma hekouense</i> sp. nov.	GXNU YU000412	Hekou, Yunnan, China	OL843964	OL843979
<i>Theلودerma hekouense</i> sp. nov.	GXNU YU000413	Hekou, Yunnan, China	OL843965	OL843980
<i>Theلودerma hekouense</i> sp. nov.	GXNU YU000495	Hekou, Yunnan, China	OL843966	OL843981
<i>Theلودerma hekouense</i> sp. nov.	GXNU YU000496	Hekou, Yunnan, China	OL843967	OL843982
<i>Theلودerma hekouense</i> sp. nov.	AMNH A163893	Vi Xuyen, Ha Giang, Vietnam	DQ283393	–
<i>Theلودerma hekouense</i> sp. nov.	HHU-WJHK01	Hekou, Yunnan, China	KY495639	–
<i>Theلودerma hekouense</i> sp. nov.	HHU-WJHK02	Hekou, Yunnan, China	KY495640	–

deviation of split frequencies of the two runs was less than a value of 0.01, and then the remaining trees were used to create a consensus tree and to estimate Bayesian posterior probabilities (BPPs).

Results

The obtained sequence alignments of the 16S and COI genes were 784 bp and 561 bp, respectively. Our phylogenetic analysis strongly supported that specimens from Yunnan and Vietnam form a clade (clade A), which is the sister to the clade consisting of topotypes and other specimens from Guangxi (clade B; Figs 2, 3). The genetic divergence between these two clades is 4.2% and 10.7% in 16S and COI genes, respectively.

The specimens from Hekou, Yunnan, China can be morphologically distinguished from topotypes of *T. rhododiscus* by a series of characters: i.e., red subarticular tubercles, red metacarpal tubercles, a red metatarsal tubercle, and denser white warts on dorsal surface. Therefore, based on the molecular and morphological evidence, we consider the Hekou specimens to represent a cryptic species and describe this species below.

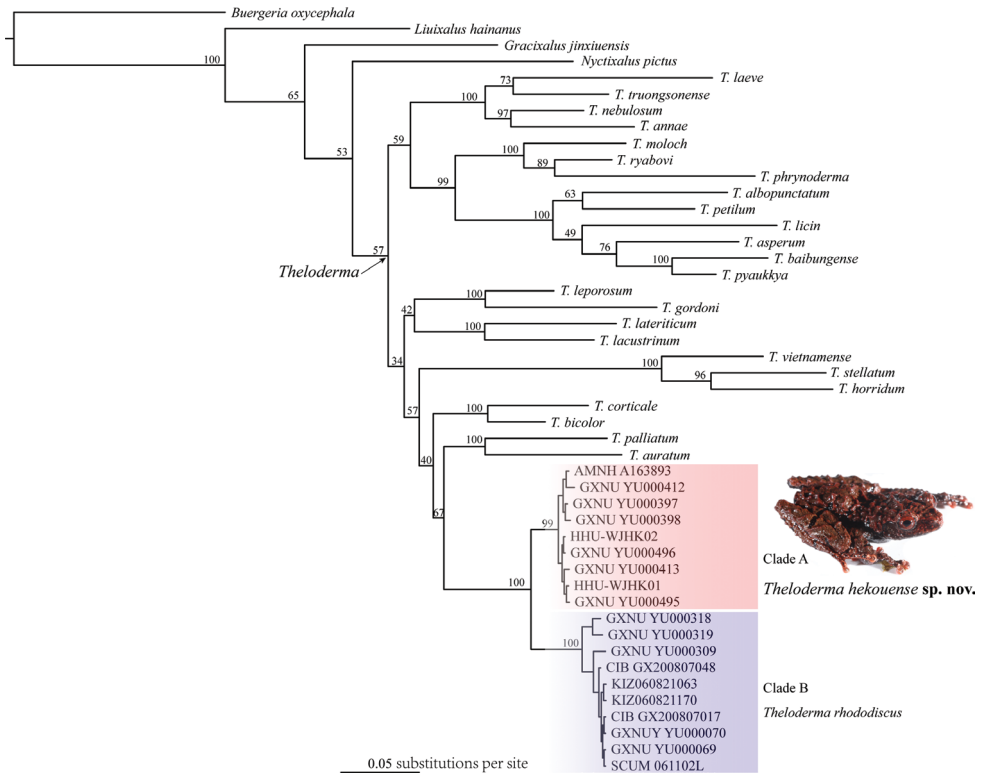


Figure 2. Bayesian phylogram of *Theloderma* inferred from 784 bp of 16S rRNA gene. The values above the branches are Bayesian posterior probabilities.

Theloderma hekouense sp. nov.

<http://zoobank.org/65A68280-DECC-4559-BB78-1FBA7F82474B>

Figs 4, 5A–C

Holotype. GXNU YU000496, adult male, collected on 9 September 2021 by Jian Wang from Hekou, Yunnan, China (22°54'N, 103°42'E, 2109 m a.s.l.; Fig. 1).

Paratypes. GXNU YU000397 and GXNU YU000398, two adult males, collected from the type locality by Jian Wang on 1 May 2021; GXNU YU000413 and GXNU YU000495, two adult males collected from the type locality by Jian Wang on 28 May 2020 and 9 September 2021, respectively; GXNU YU000412, one adult female, collected from the type locality by Jian Wang on 28 May 2020.

Etymology. The specific epithet is named after the type locality, Hekou County, Yunnan, China. We suggested “Hekou Bug-eyed frog” for the common English name and 河口棱皮树蛙 (Hé Kǒu Léng Pí Shù Wā) for the common Chinese name.

Diagnosis. The new species was assigned to genus *Theloderma* by its phylogenetic position and the following morphological characters: distinct tympanum, terminal phalanx with Y-shaped distal end, intercalary cartilage between terminal and penultimate

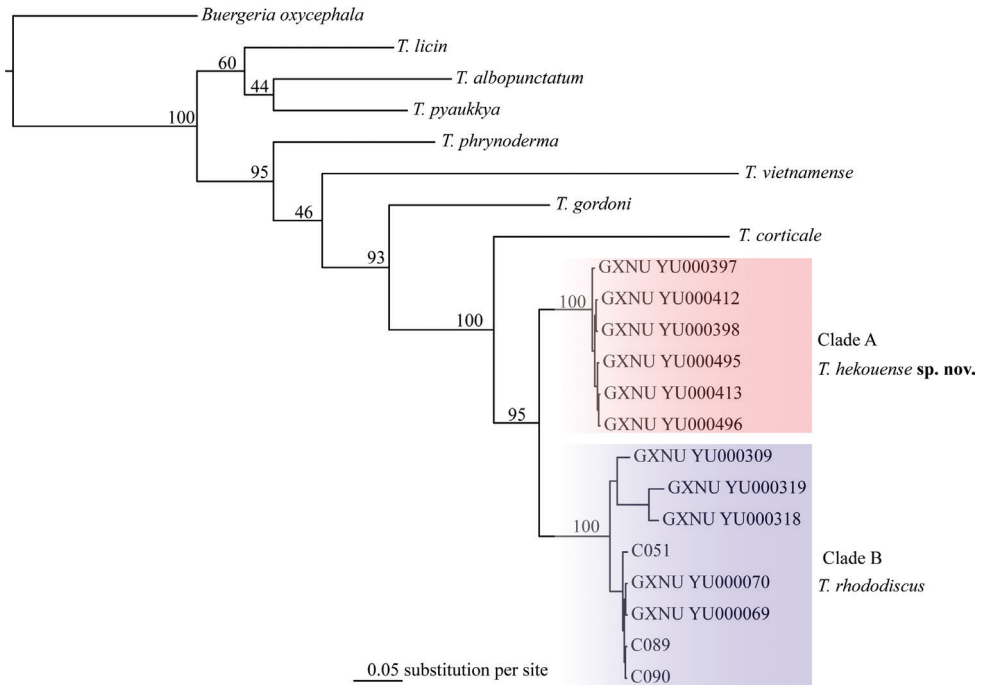


Figure 3. Bayesian phylogram of *Theلودerma* inferred from 561 bp of COI gene. The values above the branches are Bayesian posterior probabilities.

phalanges of digits, tips of digits expanded into large discs bearing circummarginal grooves, head skin not co-ossified to skull (Poyarkov et al. 2018). *Theلودerma hekouense* sp. nov. can be distinguished from *T. rhododiscus* and other congeners by having a combination of the following characters: 1) small body size; 2) dorsal surface coarsely rough with large ridges and tubercles; 3) dense warts on dorsal surface; 4) absence of white markings on dorsal surface; 5) iris uniformly reddish brown; 6) discs, metacarpal tubercles, metatarsal tubercles, and subarticular tubercles red; 7) webbing between fingers, vocal sac, and vomerine teeth absent.

Description of holotype. Adult male (SVL 25.7 mm; Table 2); head width (HW 8.5 mm) nearly equal to head length (HL 8.9 mm); snout slopes upward towards the tip, slightly protruding beyond lower jaw in ventral view; canthus rostralis distinct; loreal region sloping; nostrils oval, lateral, nearer tip of snout; interorbital distance (IOD 3.0 mm) greater than internarial distance (IND 2.4 mm) and upper eyelid width (UEW 2.6 mm); pineal spot absent; pupil oval, horizontal; tympanum distinct (TD 2.2 mm), rounded, greater than half eye diameter (ED 3.1 mm); supratympanic fold indistinct; vomerine teeth absent; choanae oval; tongue cordiform, wide deeply notched posteriorly; no vocal sac.

Forelimbs moderately robust; relative length of fingers I<II<IV<III; all fingertips expanded into discs with circummarginal grooves, relative width of finger disks



Figure 4. Views of holotype of *Theloderma bekouense* sp. nov. (GXNU YU000496) in life.

I<II<IV<III; nuptial pad present on base of finger I; webbing between fingers absent; subarticular tubercles prominent and rounded, formula 1, 1, 2, 2; supernumerary tubercle prominent; two metacarpal tubercles, the outer divided into two.

Hindlimbs long; tibiotarsal articulation reaching tip of snout when hindlimb stretched alongside of body; heels overlapping when legs positioned at right angles to body; tarsal glands absent; relative length of toes I<II<III=V<IV; toe I with preaxial dermal fringe and toe V with postaxial dermal fringe; all toe tips expanded into discs with circummarginal grooves; toes webbed, webbing formula I2-2II1.5–3III2-3IV3-1.75V; subarticular tubercles prominent and rounded, formula 1,1,2,3,2; inner metatarsal tubercle prominent, light red; outer metatarsal tubercle absent.

Dorsolateral fold absent; dorsal surface very rough with prominent irregular ridges, conical tubercles, and dense white small warts on dorsum, top of head, upper eyelids, and dorsal of limbs; head side and body flank rough, scattered with warts; no warts on tympanum; dorsal skin of digits relatively smooth, scattered with white warts; white tubercles and warts around vent; chest, belly, body flank, and ventral surface of forearm and thigh coarsely granular, more so on venter; white tubercles and warts scattered on venter of tarsus and feet.

Coloration in life. Dorsal surface tea-brown with black spots between the nostrils and eyes, between eyes, and on dorsum and dorsal surface of limbs; head side almost uniformly tea-brown, with few white dots on tympanum region; body flank tea-brown, scattered with black spots enclosed by white stripes; a large black spot on sacral area extended to dorsum and connected with the black band on thigh when thigh adhered to body; ventral surface brownish black with white spots on chin and white marbled network on belly and limbs; dorsal and ventral surfaces of discs orange-red; subarticular



Figure 5. *Theلودerma hekouense* sp. nov. and *T. rhododiscus* **A–C** dorsal and ventral views of *Theلودerma hekouense* sp. nov. **A, B** holotype (GXNU YU000496) in preservative **C** paratype (GXNU YU000495) in life **D–F** *T. rhododiscus* **D, E** topotype (GXNU YU000069) in preservative **F** topotype (GXNU YU000417) in life.

tubercles, metacarpal tubercles, and metatarsal tubercle semitransparent with light red; nuptial pad greyish white; toe webbing orange-red mottled with dark; iris red-brown.

Coloration in preservative. Dorsal surface faded to brownish black with black spots, pattern as in life; tubercles and warts white; ventral surface brownish black with white spots and white marbled network; discs, subarticular tubercles, metacarpal tubercles, and metatarsal tubercles faded to white (Fig. 5A, B).

Morphological variation. The new species is sexually dimorphic in that the female has no nuptial pad. Black spots on dorsal surface varied among individuals in that 1) GXNU YU000398 and YU000495 have no distinct black spots between snout and eyes, 2) GXNU YU000398 and YU000413 have only one large black spot on dorsum whereas other types have two or more, and 3) GXNU YU000397 has two large black spots between eyes whereas other types have only one.

Distribution. In addition to the type locality, Hekou, Yunnan, China, the new species also occurs in Ha Giang, northern Vietnam (Bain and Nguyen 2004) because our molecular analyses revealed that the samples from Ha Giang also belong to the clade of the new species. The new species inhabits shrubs and prefers to breed in water-filled tree hollows. All specimens from Yunnan were found in an artificial breeding trap constructed using water bottles for surveillance of amphibian diversity (Fig. 6).

Comparisons. Orlov et al. (2006) identified three groups in *Theلودerma* based on SVL, including small (28–35 mm), medium-sized (40–45 mm), and large (48–75 mm).

Table 2. Measurements (in mm) of *Theلودerma hekouense* sp. nov. from the type locality (holotype is marked with asterisk).

Character	GXNU YU000397	GXNU YU000398	GXNU YU000412	GXNU YU000413	GXNU YU000495	GXNU YU000496*
Sex	M	M	F	M	M	M
SVL	25.9	27.2	26.8	25.9	26.2	25.7
HL	8.9	9.0	8.9	8.8	8.9	8.9
HW	8.6	9.0	9.1	8.7	8.5	8.5
SL	3.7	3.8	3.8	3.6	3.6	3.5
IND	2.4	2.5	2.4	2.4	2.3	2.4
IOD	2.9	2.9	3.0	3.0	2.8	3.0
UEW	2.3	2.5	2.7	2.4	2.4	2.6
ED	3.2	3.1	3.3	3.2	3.2	3.1
TD	2.2	2.2	2.3	2.1	2.1	2.2
DNE	2.4	2.5	2.5	2.3	2.2	2.2
FHL	13.7	14.2	14.5	13.5	14.1	13.3
TL	13.9	14.2	14.9	14.0	14.9	13.9
TFL	19.8	20.3	21.2	19.4	20.3	18.9
FL	12.8	13.2	13.9	12.8	13.7	12.3



Figure 6. Habitat of *Theلودerma hekouense* sp. nov. **A** habitat at the type locality **B** an individual found in a water bucket that was set up in the field as potential breeding site of treefrog preferred breeding in water-filled tree holes by the authors for amphibian monitoring.

Here the new species (adult SVL 25.7–27.2 mm) is referred to the small group, and therefore can be easily distinguished from members of the other two groups including: *T. bicolor*, *T. corticale* (male SVL 61 mm, $n = 1$), *T. gordonii* (male SVL 36.4–46.7 mm), *T. horridum* (SVL 37.1–48.7 mm, $n = 4$), *T. leporosum* (SVL 62.6 mm, $n = 1$), *T. moloch*

(SVL 39.6–46.3 mm in two females and SVL 40.2 mm in one male), *T. nagalandense* (male SVL 52.8 mm, $n = 1$), *T. phrynoderma* (SVL 41.4–44.6 mm), and *T. ryabovi* (male SVL 43.8 mm, $n = 1$).

A morphological comparison between small-bodied *Theلودerma* species is summarized in Table 3. The new species can be distinguished from its sister-species *T. rhododiscus*, with which it was previously confused, by the denser white warts on dorsal surface (vs relatively sparse), red subarticular tubercles (vs white), red metacarpal tubercles (vs white), a red metatarsal tubercle (vs white), and dorsal and ventral surfaces blackish in preservative (vs tea-brown) (Fig. 4).

Theلودerma hekouense sp. nov. is distinguishable from *T. annae*, *T. auratum*, *T. laeve*, *T. lacustrinum*, *T. lateriticum*, *T. licin*, *T. nebulosum*, *T. palliatum*, *T. petilum*, and *T. truongsongense* by having the dorsal surface coarsely roughened with large ridges and tubercles (vs smooth or weakly rugose with small asperities), and from *T. albopunctatum*, *T. asperum*, *T. baibungense*, *T. pyaukkya*, *T. stellatum*, and *T. vietnamense* by absence of white markings on the dorsal surface (vs present).

The new species further differs from *T. annae*, *T. auratum*, *T. lacustrinum*, *T. laeve*, *T. nebulosum*, *T. palliatum*, *T. petilum*, *T. stellatum*, *T. truongsongense*, and *T. vietnamense* by the uniformly reddish-brown iris (vs lacking red colouration or bicoloured); from *T. albopunctatum*, *T. licin*, *T. stellatum*, and *T. vietnamense* by lacking webbing between the fingers (vs present); from *T. albopunctatum*, *T. asperum*, *T. baibungense*, *T. licin*, *T. pyaukkya*, and *T. vietnamense* by lacking a vocal sac (vs present); from *T. petilum* by lacking vomerine teeth (vs present); from *T. annae*, *T. albopunctatum*, *T. asperum*, *T. auratum*, *T. baibungense*, *T. lacustrinum*, *T. lateriticum*, *T. laeve*, *T. licin*, *T. nebulosum*, *T. palliatum*, *T. petilum*, *T. pyaukkya*, *T. stellatum*, *T. truongsongense*, and *T. vietnamense* by having both dorsal and ventral surfaces of the discs reddish brown (vs lacking red colouration or red only on the dorsal surface); and from all small-bodied congeners in having red metacarpal, metatarsal, and subarticular tubercles (vs lacking red colouration).

Discussion

Theلودerma rhododiscus was thought to have a broad distribution ranging from eastern China to southwestern China and northern Vietnam (Zeng et al. 2017). Although previous molecular studies have revealed relatively large genetic divergence between samples from the type locality and limited samples from Yunnan and Vietnam (e.g., Poyarkov et al. 2015; Hou et al. 2017b), the taxonomic status of *T. rhododiscus* from the western part of its distribution (Yunnan and Vietnam) has never been doubted in previous publications. In this study, our molecular data and morphological comparison supports that the taxon known as *T. rhododiscus* from Yunnan, China and adjacent northern Vietnam should be considered representing a sibling species of *T. rhododiscus*, from which the new species differs morphologically by denser white warts on the dorsal surface and red subarticular, metacarpal, and metatarsal tubercles, and genetically by 4.2% and 10.7% divergence in 16S rRNA and COI genes, respectively.

Table 3. Morphological comparison of members of *Thelodermia* with small size (SVL < 35 mm). “?” means unknown.

Species	Iris color	Finger webbing	Color of discs	Dorsal colour	Ventral colour	Vomerine teeth	Vocal sac	Dorsal skin	Metacarpal, metatarsal, and subarticular tubercles
<i>T. hebouense</i> sp. nov.	red brown	absent	both dorsal and ventral surfaces orange red	tea-brown with no white markings	brownish black with white marbled network	absent	absent	coarsely rough with large asperities	red
<i>T. annae</i>	greyish green	absent	both dorsal and ventral surfaces greyish white	greyish green	greyish white	absent	absent	smooth	gray
<i>T. albopunctatum</i>	red brown	present	both dorsal and ventral surfaces brown	brown with white markings	dark olive with white stripes	absent	present	smooth with small asperities	greyish white
<i>T. asperum</i>	reddish brown	absent	both dorsal and ventral surfaces brown	dark grey-brown with white markings	marbled black and bluish grey/white	absent	present	rough with large asperities	?
<i>T. auratum</i>	golden above and black below	absent	dorsal surface dark brown and ventral surface grey	golden yellow	greyish blue with brown blotches	absent	absent	smooth	gray
<i>T. baibungense</i>	red brown	absent	dorsal surface black brown and ventral surface grey	brown with white markings	black with white stripes	absent	present	smooth with small asperities	white
<i>T. lacustrinum</i>	uniformly bronze	absent	dorsal and ventral surfaces bronze	light brown	uniformly gray	absent	?	smooth with small asperities	gray
<i>T. lateriticum</i>	deep brick-red	absent	both dorsal and ventral surfaces grey	brick-red	grey-brown with white spots	absent	absent	granular with small bumps	gray-brown
<i>T. laeae</i>	grey above and dark brown below	absent	both dorsal and ventral surfaces grey	beige with thin light middorsal stripe	uniformly violet-grey	absent	absent	smooth	gray
<i>T. licin</i>	red	present	dorsal surface black-brown	pale whitish brown to light brown	white with brown reticulation	absent	present	nearly smooth with fine asperities	?
<i>T. nebulosum</i>	pale gold above and reddish brown below	absent	both dorsal and ventral surfaces brown	brown with dark patterning	dark brownish black with pale blue/white marbling	absent	?	nearly smooth with very sparsely distributed minute asperities	brown
<i>T. palliatum</i>	pale dark above and dark red below	absent	both dorsal and ventral surface brown to greyish brown	pale to medium brown with dark brown blotches	dark warm brown with pale bluish white marbling	absent	absent	weakly rugose with sparsely scattered minute asperities	faint white
<i>T. petilum</i>	reddish brown above and grey below	absent	dorsal surface lavender and ventral surface creamy-white	light brown with dark brown reticulations	creamy white	present	?	nearly smooth with small, white asperities	creamy white
<i>T. pyaulbeya</i>	uniformly red	absent	dorsally red and ventrally brown	brown with white markings	brown with cream marbling	absent	present	rough with fine asperities	grayish white
<i>T. rhododiscus</i>	uniformly reddish brown	absent	both dorsal and ventral surface red	tea-brown with black blotches	brownish black with gray-white network	absent	absent	rough with large asperities	white

Species	Iris color	Finger webbing	Color of discs	Dorsal colour	Ventral colour	Vomerine teeth	Vocal sac	Dorsal skin	Metacarpal, metatarsal, and subarticular tubercles
<i>T. stellatum</i>	dark gold with black	present	dorsal surface reddish and ventral surface grey	brown with white markings	cream with purplish-brown flecks or spots	absent	absent	rough with small or large asperities	flesh-white
<i>T. truongoanense</i>	golden yellow above and black below	absent	dorsal surface beige to black brown and ventral surface	yellow-goldish with dark brown	dark gray with black speckles	absent	?	smooth with small asperities	gray
<i>T. vietnamense</i>	golden-brownish	present	dorsally reddish and ventrally grey	brown with white markings	dark brown to blackish with slight whitish to bluish reticulations	absent	present	rough with large ridges and warts	whitish to bluish

With the exclusion of Yunnan and northern Vietnam from the geographic range of *T. rhododiscus*, the range of *T. rhododiscus* should be revised to include Guangxi, Guangdong, Hunan, Fujian, and Jiangxi. In Guangxi, *T. rhododiscus* was previously known from three areas including Jinxiu (Dayao Mt National Natural Reserve), Longsheng (Huaping National Natural Reserve), and Nanning (Daming Mt National Natural Reserve) (Zeng et al. 2017). In this study, we found two new occurrences of *T. rhododiscus* in northern and northwestern Guangxi, including Longlin and Huanjiang counties. The former is adjacent to southwestern Guizhou and eastern Yunnan and the latter is adjacent to southern Guizhou. Therefore, it can be expected that *T. rhododiscus* will be found from Guizhou and eastern Yunnan in the future.

Yunnan is the region richest in species of bug-eyed frogs in China. With the addition of *T. hekouense* sp. nov., there are now 10 *Theلودerma* species in China and seven of them are distributed in Yunnan including *T. albopunctatum*, *T. baibungense*, *T. bicolor*, *T. gordonii*, *T. moloch*, *T. pyaukkya*, and *T. hekouense* sp. nov. Most of these species were recorded from there recently (e.g., Hou et al. 2017b; Qi et al. 2018; Du et al. 2020), indicating that species diversity of *Theلودerma* in Yunnan was obviously underestimated probably owing to that *Theلودerma* species are not easy to be found because of their preference of breeding in water-filled tree hollows. Taxonomic progress of amphibians from Yunnan in recent years (e.g., Yuan et al. 2018; Yu et al. 2019a, 2019b; Du et al. 2020; Jiang et al. 2020) reflects that amphibian diversity in Yunnan remains to be poorly known. Beside *T. rhododiscus* mentioned above, we expect that more *Theلودerma* species known from adjacent regions will be found from southern Yunnan, China (e.g., *T. corticale*, *T. lateriticum*, and *T. petilum*).

Acknowledgements

We thank our colleagues from Daweishan National Nature Reserve for their assistance during the fieldwork. This work was supported by grants from the National Natural Science Foundation of China (32060114), Key Laboratory of Ecology of Rare and Endangered Species and Environmental Protection (Guangxi Normal University), Ministry of Education (ERESEP2020Z22), and Guangxi Key Laboratory of Rare and Endangered Animal Ecology, Guangxi Normal University (19-A-01-06).

References

- Bain RH, Nguyen TQ (2004) Herpetofauna diversity of Ha Giang Province in northeastern Vietnam, with descriptions of two new species. *American Museum Novitates* 3453: 1–42. [https://doi.org/10.1206/0003-0082\(2004\)453<0001:HDOHGP>2.0.CO;2](https://doi.org/10.1206/0003-0082(2004)453<0001:HDOHGP>2.0.CO;2)
- Darriba D, Taboada GL, Doallo R, Posada D (2012) jModelTest 2: More models, new heuristics and parallel computing. *Nature Methods* 9(8): 772–772. <https://doi.org/10.1038/nmeth.2109>

- Dever JA (2017) A new cryptic species of the *Theلودerma asperum* complex (Anura: Rhacophoridae) from Myanmar. *Journal of Herpetology* 51(3): 425–436. <https://doi.org/10.1670/17-026>
- Du LN, Liu S, Hou M, Yu GH (2020) First record of *Theلودerma pyaukkya* Dever, 2017 (Anura: Rhacophoridae) in China, with range extension of *Theلودerma moloch* (Annan-dale, 1912) to Yunnan. *Zoological Research* 41(5): 576–580. <https://doi.org/10.24272/j.issn.2095-8137.2020.083>
- Fei L, Ye CY, Jiang JP (2012) *Colored Atlas of Chinese Amphibians and Their Distributions*. Sichuan Publishing Group Sichuan Publishing House of Science and Technology, Chengdu.
- Frost DR (2021) *Amphibian species of the world: an online reference*. Version 6.1 (2021-12-2). American Museum of Natural History, New York. <http://research.amnh.org/herpetology/amphibia/index.html/>
- Hou YM, Zhang MF, Chen J, Chen DS, Hu F, Wang B (2017a) New record of *Theلودerma rhododiscus* from Hunan, China. *Sichuan Journal of Zoology* 36(6): 718–719.
- Hou M, Yu GH, Chen HM, Liao CL, Zhang L, Chen J, Li PP, Orlov NL (2017b) The taxonomic status and distribution range of six *Theلودerma* species (Anura: Rhacophoridae) with a new record in China. *Russian Journal of Herpetology* 24(2): 99–127. <https://doi.org/10.30906/1026-2296-2019-24-2-99-127>
- Jiang K, Ren J, Wang J, Guo J, Wang Z, Liu Y, Jiang D, Li J (2020) Taxonomic revision of *Raorchestes menglaensis* (Kou, 1990) (Amphibia: Anura), with descriptions of two new species from Yunnan, China. *Asian Herpetological Research* 11: 263–281. <https://doi.org/10.16373/j.cnki.ahr.200018>
- Kumar S, Stecher G, Tamura K (2016) MEGA7: Molecular Evolutionary Genetics Analysis version 7.0 for bigger datasets. *Molecular Biology and Evolution* 33(7): 1870–1874. <https://doi.org/10.1093/molbev/msw054>
- Liu C, Hu S (1962) A herpetological report of Kwangsi. *Acta Zoologica Sinica* 14(Supplement): 73–104.
- Lyu ZT, Huang LS, Wang J, Li YQ, Chen HH, Qi S, Wang YY (2019) Description of two cryptic species of the *Amolops ricketti* group (Anura, Ranidae) from southeastern China. *ZooKeys* 812: 133–156. <https://doi.org/10.3897/zookeys.812.29956>
- McLeod DS, Ahmad N (2007) A new species of *Theلودerma* (Anura: Rhacophoridae) from southern Thailand and peninsular Malaysia. *Russian Journal of Herpetology* 14: 65–72.
- Nguyen TQ, Pham CT, Nguyen TT, Ngo HN, Ziegler T (2016) A new species of *Theلودerma* (Amphibia: Anura: Rhacophoridae) from Vietnam. *Zootaxa* 4168(1): 171–186. <https://doi.org/10.11646/zootaxa.4168.1.10>
- Orlov NL, Ho TC (2005) A new species of *Philautus* from Vietnam (Anura: Rhacophoridae). *Russian Journal of Herpetology* 12: 135–142.
- Orlov NL, Dutta SK, Ghate HV, Kent Y (2006) New species of *Theلودerma* from Kon Tum Province (Vietnam) and Nagaland State (India) (Anura: Rhacophoridae). *Russian Journal of Herpetology* 13: 165–175.
- Poyarkov NA, Orlov NL, Moiseeva AV, Pawangkhanant P, Ruangsawan T, Vassilieva AB, Galoyan EA, Nguyen TT, Gogoleva SI (2015) Sorting out Moss Frogs: mtDNA data on taxonomic diversity and phylogenetic relationships of the Indochinese species of the

- genus *Theلودerma* (Anura, Rhacophoridae). Russian Journal of Herpetology 22: 241–280. https://doi.org/10.30906/1026-2296_2015_2204-0241
- Poyarkov NA, Kropachev II, Gogoleva SI, Orlov NL (2018) A new species of the genus *Theلودerma* Tschudi, 1838 (Amphibia: Anura: Rhacophoridae) from Tay Nguyen Plateau, central Vietnam. Zoological Research 39: 158–184.
- Qi S, Yu GH, Lei B, Fan Y, Zhang DL, Dong ZW, Li PP, Orlov NL, Hou M (2018) First record of *Theلودerma gordonii* Taylor, 1962 from Yunnan Province, China. Russian Journal of Herpetology 25: 43–55. <https://doi.org/10.30906/1026-2296-2019-25-1-43-55>
- Ronquist F, Teslenko M, van der Mark P, Ayres DL, Darling A, Höhna S, Larget B, Liu L, Suchard MA, Huelsenbeck JP (2012) MrBayes 3.2: Efficient Bayesian phylogenetic inference and model choice across a large model space. Systematic Biology 61(3): 539–542. <https://doi.org/10.1093/sysbio/sys029>
- Rowley JLL, Le DTTT, Hoang HD, Dau QV, Cao TT (2011) Two new species of *Theلودerma* (Anura: Rhacophoridae) from Vietnam. Zootaxa 3098(1): 1–20. <https://doi.org/10.11646/zootaxa.3098.1.1>
- Sivongxay N, Davankham M, Phimmachak S, Phoumixay K, Stuart BL (2016) A new small-sized *Theلودerma* (Anura: Rhacophoridae) from Laos. Zootaxa 4147(4): 433–442. <https://doi.org/10.11646/zootaxa.4147.4.5>
- Stuart BL, Heatwole HF (2004) A new *Philautus* (Amphibia: Rhacophoridae) from northern Laos. Asiatic Herpetological Research 10: 17–21.
- Taylor EH (1962) The amphibian fauna of Thailand. The University of Kansas Science Bulletin 43: 265–599. <https://doi.org/10.5962/bhl.part.13347>
- Yu GH, Rao DQ, Zhang MG, Yang JX (2009) Re-examination of the phylogeny of Rhacophoridae (Anura) based on mitochondrial and nuclear DNA. Molecular Phylogenetics and Evolution 50(3): 571–579. <https://doi.org/10.1016/j.ympev.2008.11.023>
- Yu GH, Hui H, Hou M, Wu ZJ, Rao DQ, Yang JX (2019a) A new species of *Zhangixalus* (Anura: Rhacophoridae), previously confused with *Zhangixalus smaragdinus* (Blyth, 1852). Zootaxa 4711(2): 275–292. <https://doi.org/10.11646/zootaxa.4711.2.3>
- Yu GH, Hui H, Wang J, Rao DQ, Wu ZJ, Yang JX (2019b) A new species of *Gracixalus* (Anura, Rhacophoridae) from Yunnan, China. ZooKeys 851: 91–111. <https://doi.org/10.3897/zookeys.851.32157>
- Yuan Z, Jin J, Li J, Btuart BL, Wu J (2018) A new species of cascade frog (Amphibia: Ranidae) in the *Amolops monticola* group from China. Zootaxa 4415(3): 498–512. <https://doi.org/10.11646/zootaxa.4415.3.5>
- Zeng ZC, Zhang CY, Yuan Y, Lü ZT, Wang J, Wang YY (2017) The new record of red-disked small treefrog (*Theلودerma rhododiscus*) and its expansion of the distribution. Chinese Journal of Zoology 52(2): 235–243.

Thailandorchestia rhizophila sp. nov., a new genus and species of driftwood hopper (Crustacea, Amphipoda, Protorcheștiidae) from Thailand

Koraon Wongkamhaeng¹, Pongrat Dumrongrojwattana²,
Ratchaneewarn Sumitrakij³, Tosaphol Saetung Keetapithchayakul¹

1 Department of Zoology, Faculty of Science, Kasetsart University, Bangkok, 10900, Thailand **2** Department of Biology, Faculty of Science, Burapha University, Bangsaen, Chonburi, 20130, Thailand **3** National science museum, Khlong Ha, Khlong Luang District, Pathum Thani, 12120, Thailand

Corresponding author: Koraon Wongkamhaeng (Koraon@gmail.com)

Academic editor: Rachael Peart | Received 1 March 2022 | Accepted 5 April 2022 | Published 4 May 2022

<http://zoobank.org/7F832E2C-76D9-4CC9-BD40-0E074B0D37BB>

Citation: Wongkamhaeng K, Dumrongrojwattana P, Sumitrakij R, Keetapithchayakul TS (2022) *Thailandorchestia rhizophila* sp. nov., a new genus and species of driftwood hopper (Crustacea, Amphipoda, Protorcheștiidae) from Thailand. ZooKeys 1099: 139–153. <https://doi.org/10.3897/zookeys.1099.82949>

Abstract

During a scientific survey, a new genus of driftwood hopper was found in mangrove roots in Ko Kut District, Trat Province, Thailand. We placed this new genus, *Thailandorchestia* **gen. nov.**, within the family Protorcheștiidae. The new genus can be distinguished from the remaining genera by uropod 1 outer ramus with robust setae, uropod 2 outer ramus without robust setae, and pereopod 7 basis without a posterodistal lobe. The type species of *Thailandorchestia* **gen. nov.**, *Thailandorchestia rhizophila* **sp. nov.**, is described herein, and an updated key to the genera of the family Protorcheștiidae is provided.

Keywords

Description, Ko Kut District, marsh hopper, Talitroidea, *Thailandorchestia* gen. nov.

Introduction

The family Protorcheștiidae is a mascupod family established by Myers and Lowry (2020) and contains 24 species belonging to six genera, namely *Cochinorchestia* Lowry & Peart, 2010, *Eorchestia* Bousfield, 1984, *Microrchestia* Bousfield, 1984, *Neorchestia* Friend, 1987, and *Protorchestia* Bousfield, 1982. All of them are classified as a post-

Gondwanaland group (Myers and Lowry 2020). Each genus is distributed in different areas of the world, with *Cochinorchestia* located in southern India and Mozambique on the western coast of Africa (Lowry and Peart 2010; Lowry and Springthorpe 2015), *Eorchestia* in South Africa (Richardson 1993), and *Microchestia*, *Neorchestia*, and *Protochestia* in Australia (Bousfield 1984; Friend 1987; Richardson 1996). All members of this group are marsh hoppers who occupy mangrove forests, except *Neorchestia*, which are forest hoppers. They all have some primitive characteristics, including: 1) maxilliped palp article 2 without a distomedial lobe; 2) article 4 small, distinct and gnathopod 2 subchelate; 3) pereopods 3–7 simplidactylate; and 4) pereopod 4 dactylus basidactylate.

Herein, we describe a 4-dentate noncuspidactylate palustral amphipod with basis of pereopod 7 without a posterodistal lobe as a new genus and species of the family Protorchestiidae. The new species was discovered in mangrove roots (*Rhizophora* sp.) and rotting logs in Ko Kut District, Trat Province, Thailand.

Materials and methods

Amphipods were collected from driftwood, rotting logs and mangrove roots (*Rhizophora* sp.) in a mangrove forest near Ao Phrao, Ko Kut District, Trat Province, Thailand (11°35'40.2"N, 102°33'52.6"E) (Fig. 1). The mangrove forest is located near a small creek 50 meters from the beach. Twelve rotting logs were broken apart and 15–30

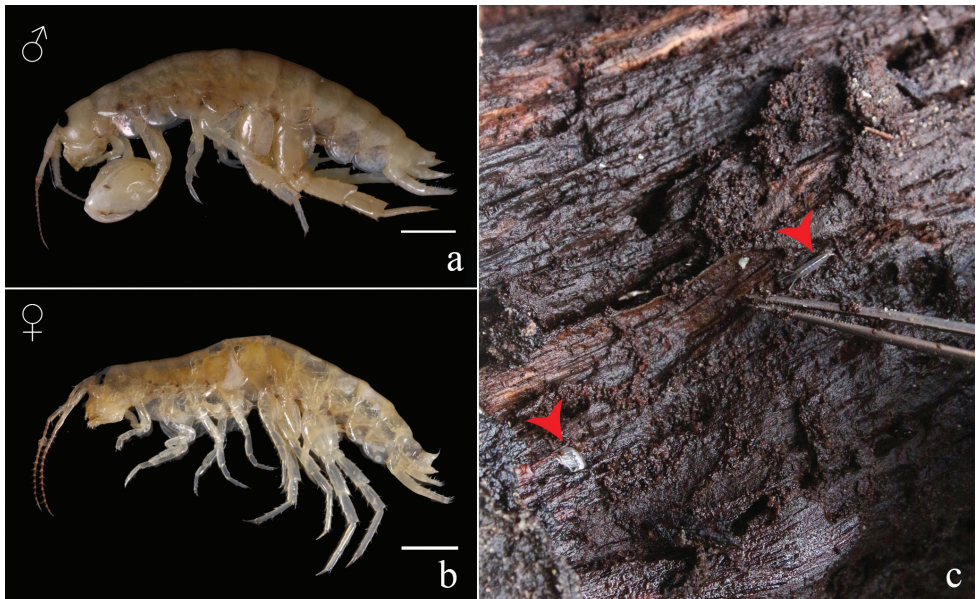


Figure 1. *Thailandorchestia rhizophila* sp. nov. **a** holotype, male, 8.04 mm, THNHM-Iv- 18760 **b** allotype, female, 7.80 mm, THNHM-IV- 18961 **c** rotting mangrove log, habitat of *Thailandorchestia rhizophila* sp. nov.

amphipod individuals were found inside each log (see Suppl. material 1). The amphipod specimens were sorted and fixed in 70% ethanol. The specimens were transferred from ethanol onto a glycerol slide for morphological study in the laboratory. Drawings were made using a drawing tube attached to an Olympus CH30 light microscope. The pencil drawings were scanned and digitally inked using a WACOM bamboo CTH-970 graphics board in Adobe Illustrator CC 2017, following the method described in Coleman (2003). Setae and mouthparts were following Zimmer et al. (2009). Abbreviations used in the text are as follows: A, antenna; G, gnathopod; UL, labrum; LL, labium; MD, mandible; MX, maxilla; MP, maxilliped; P, pereopod; p, palp; pl, pleopod; T, telson; U, uropod; L, left; R, right. Institutional abbreviations: THNHM, Thailand Natural History Museum, Bangkok, Thailand.

Results

Systematics

Order Amphipoda Latreille, 1816

Suborder Senticaudata Lowry & Myers, 2013

Family Protorchestiidae Myers & Lowry, 2020

Genus *Thailandorchestia* gen. nov.

<http://zoobank.org/9DDD49ED-997C-430E-B06A-2586B8DB34EE>

Type species. *Thailandorchestia rhizophila* sp. nov., here designated.

Diagnosis. Protorchestiidae with *maxilliped* palp article 2 distomedial lobe absent. *Mandible* left lacinia mobilis 4-dentate. *Gnathopod 2* coxal gill simple. *Pereopod 4* carpus significantly shorter than carpus of pereopod 3. *Pereopods 6–7* sexually dimorphic (male merus and carpus incrassate). *Pereopod 7* posterodistal lobe absent. *Uropod 1* peduncle distolateral robust setae present, very large (1/3–1/2 length of outer ramus); inner ramus linear, not modified; outer ramus with marginal robust setae. *Uropod 2* outer ramus without marginal robust setae. *Uropod 3* peduncle with 2 robust setae; ramus shorter than peduncle, linear (narrowing). *Telson* apically incised, with 2 robust setae per lobe.

Etymology. The generic name, *Thailandorchestia* gen. nov., is derived from “Thailand” in combination with the *Orchestia* stem.

Type locality. Mangrove forest near Ban Ao Prao Beach (11°35'40.2"N, 102°33'52.6"E), Trat Province, Thailand.

Ecological type. Driftwood hoppers (virtually confined to rotting driftwood where they live in galleries, consuming rotting driftwood and reproducing with relatively small broods).

Remarks. The new genus clearly belongs to Protorchestiidae due to the presence of: 1) maxilliped palp article 2 without distomedial lobe; 2) article 4 small, distinct; 3) gnathopod 2 subchelate; 4) pereopods 3–7 simplidactylate; 5) pereopod 4 dactylus basidactylate; and 6) telson with apical robust setae only or with apical and marginal robust setae, with 1–6 robust setae per lobe.

The new genus is closely related to *Microrchestia* in having: 1) left mandible lacinia mobilis 4-dentate; 2) carpus of pereopod 3 subequal to those of pereopod 4; and 3) pereopods 6 and 7 sexually dimorphic. However, the current genus differs from *Microrchestia* from Australia by having: 1) maxilliped palp article 2 distomedial lobe absent (vs. well developed); 2) pereopod 7 posterodistal lobe absent (vs. present), and 3) U1 outer ramus with marginal robust setae (vs. without marginal robust setae) (Table 1).

Table 1. Comparison of diagnostic characteristics in different protorcheistiid genera.

Genus	MP palp article 2 distomedial lobe	LMD lacinia mobilis	G1 sexual dimorphism	Carsi of P4:P3	P6–7 sexual dimorphism	P7 posterodistal lobe	U1 outer ramus	U2 outer ramus marginal setae	U3 robust setae on peduncle	U3 ramus	Number of setae per telsonic lobe
<i>Carpentaria</i>	well developed	4-dentate	absent, palm obtuse	subequal	absent	present	linear without marginal setae	present	1–4	bud-like	3–6
<i>Cochinorchestia</i>	present	4-dentate	absent, palm transverse	longer	unknown	present	spoon-shape with marginal setae	absent	1	linear	2
<i>Eorchestia</i>	absent	4-dentate	absent, palm transverse	longer	absent	present	linear without marginal setae	absent	3	linear	1–2
<i>Microrchestia</i>	well developed	4-dentate	present, palm transverse	longer	present	present	linear without marginal setae	absent	2	linear	2
<i>Neorchestia</i>	absent	5-dentate	absent, palm transverse	longer	unknown	present	linear without marginal setae	absent	2	linear	1
<i>Protorchestia</i>	absent	5-dentate	absent, palm transverse	subequal	absent	present	linear without marginal setae	absent	3	linear	2
<i>Thailandorchestia</i> gen. nov.	absent	4-dentate	present, palm transverse	longer	present	absent	linear with marginal setae	absent	2	linear	2

Only one protocheistiid amphipod had been previously reported from Thailand. Bussarawich (1985) studied the diversity of amphipods in the mangrove forest and reported *Microchestia* sp., a member of the family Protorcheistiidae. Later, Lowry and Springthorpe (2015) revised the genus *Cochinorchestia* Lowry & Peart, 2010. Although the *Microrchestia* sp. from Thailand was also mentioned as a *Cochinorchestia* sp. based on the illustration of the previous publication, some details such as the maxilliped and gnathopods 1 and 2 remain unclear. The specimens from the report of Bussarawich (1985) presumed lost, which makes the *Cochinorchestia* sp. in this report still tentative.

The new genus is similar to *Cochinorchestia* from China in having: 1) left mandible lacinia mobilis 4-dentate; 2) carpus of pereopod 3 longer than that of pereopod 4; and 3) uropod 1 outer ramus with marginal setae. However, the current genus differs from *Cochinorchestia* in having: 1) pereopod 7 without a posterodistal lobe (vs. pereopod 7 with a posterodistal lobe); 2) uropod 1 outer ramus linear (vs. spoon-shaped) and uropod 3 peduncle with 2 robust setae (vs. with 3 robust setae); and 3) uropod 2 outer ramus without robust setae (vs. with marginal robust setae in 1 row).

The new genus is identifiable using the following key to genera of Protorcheistiidae.

Key to genera of Protorchestiidae

- 1 Uropod 3 peduncle with 4 robust setae..... *Carpentaria*
 – Uropod 3 peduncle with less than 4 robust setae..... 2
 2 Uropod 3 peduncle with 3 robust setae..... 3
 – Uropod 3 peduncle with less than 3 robust setae..... 4
 3 Maxilliped palp article 2 distomedial lobe absent; mandible left lacinia mobilis 4-dentate; pereopod 4 carpus shorter than carpus of pereopod 3 *Eorchestia*
 – Maxilliped palp article 2 distomedial lobe present; mandible left lacinia mobilis 5-dentate; pereopod 4 carpus subequal to carpus of pereopod 3 ... *Protorchestia*
 4 Uropod 3 peduncle with 1 robust seta *Cochinorchestia*
 – Uropod 3 peduncle with 2 robust setae..... 5
 5 Mandible left lacinia mobilis 5-dentate *Neorchestia*
 – Mandible left lacinia mobilis 4-dentate 6
 6 Uropod 1 outer ramus without marginal robust setae; basis of pereopod 7 with a posterodistal lobe *Microrchestia*
 – Uropod 1 outer ramus with marginal robust setae; basis of pereopod 7 without a posterodistal lobe *Thailandorchestia* gen. nov.

Thailandorchestia rhizophila sp. nov.

<http://zoobank.org/BDA296BD-ED94-4AEA-AF3E-B6894581D459>

Diagnosis. As for the genus unless otherwise stated. *Antenna 1* long, reaching from midpoint to end of article 5 of antenna 2 peduncle. *Eye* medium (1/5–1/3 of head length). *Gnathopod 1* not sexually dimorphic, palm transverse, dactylus shorter than palm. *Gnathopod 2* sexually dimorphic (male subchelate, female mitten-shaped). *Pleopod 1* outer ramus subequal in length to peduncle. *Pleopod 3* outer ramus longer than peduncle.

Material examined. *Holotype*, male, 8.04 mm, THNHM-Iv- 18760; allotype, female, 7.80 mm, THNHM-IV- 18961; *Paratypes*, 2 males, 1 non-gravid female, and 2 gravid females, THNHM- Iv 18761. All collected from the type locality on 4 May 2019, KW and PD leg.

Ecology. Driftwood hoppers, living inside rotten logs and mangrove roots in the softest part under the bark. The mangrove forest is located near a small creek 50 meters from the beach. The sediment in the forest is muddy sand mixed with leaf litter.

Type locality. Mangrove forest near Ban Ao Prao Beach (11°35'40.2"N, 102°33'52.6"E), Ko Kut District, Trat Province, Thailand.

Etymology. The specific epithet refers to the habitat of this amphipod, which is also found inside mangrove roots.

Description of male holotype. (THNHM-Iv- 18760, Figs 2–5).

Head. *Eye* medium (1/5–1/3 head length). *Antenna 1* (Fig. 2A1) long, reaching from midpoint to end of article 5 of antenna 2 peduncle. *Antenna 2* (Fig. 2A2) peduncular articles slender, article 5 longer than article 4. *Upper lip* (Fig. 3UL)

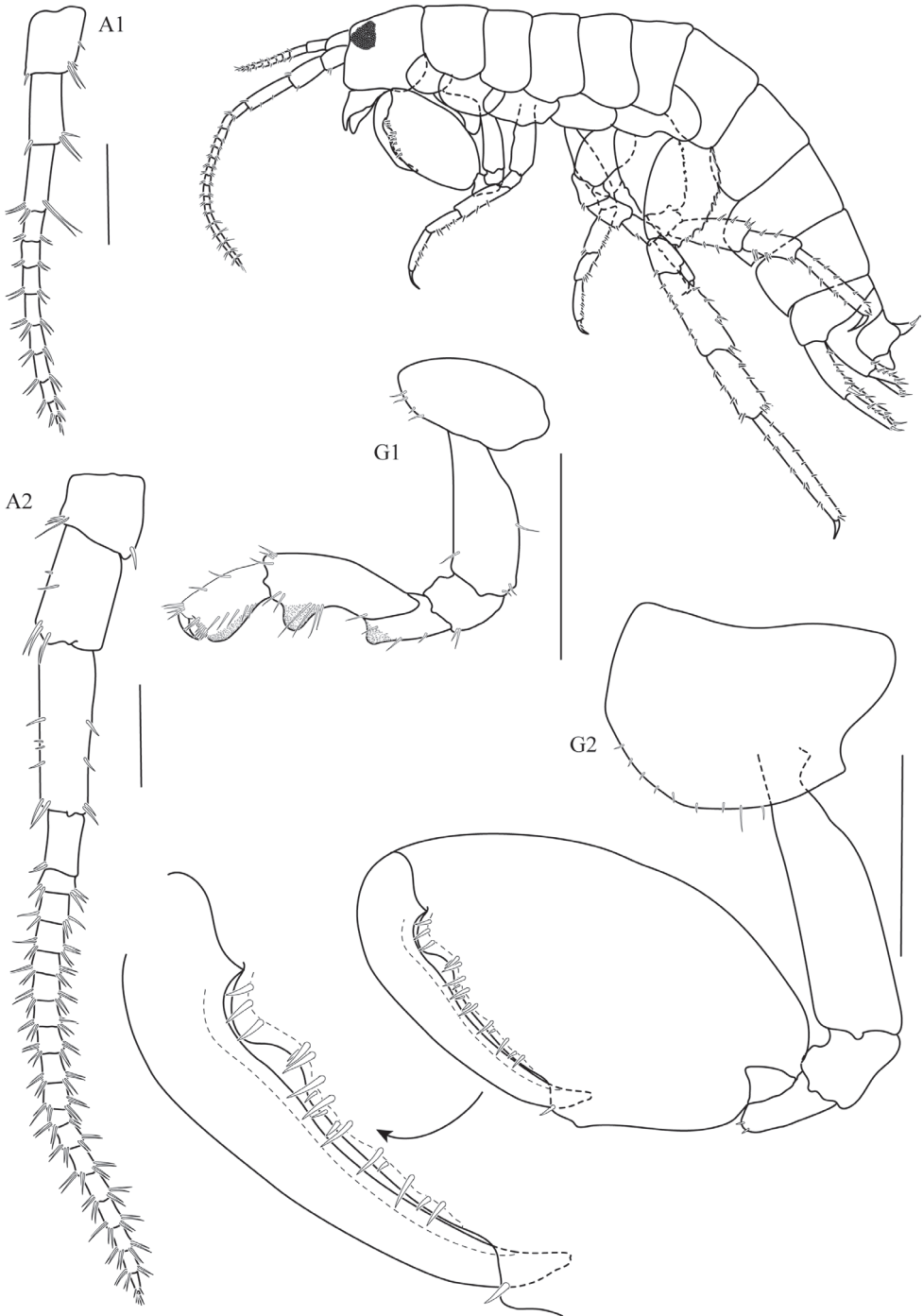


Figure 2. *Thailandorchestia rhizophila* sp. nov. holotype, male, 8.04 mm, THNHM-Iv- 18760. Scale bars: 1 mm.

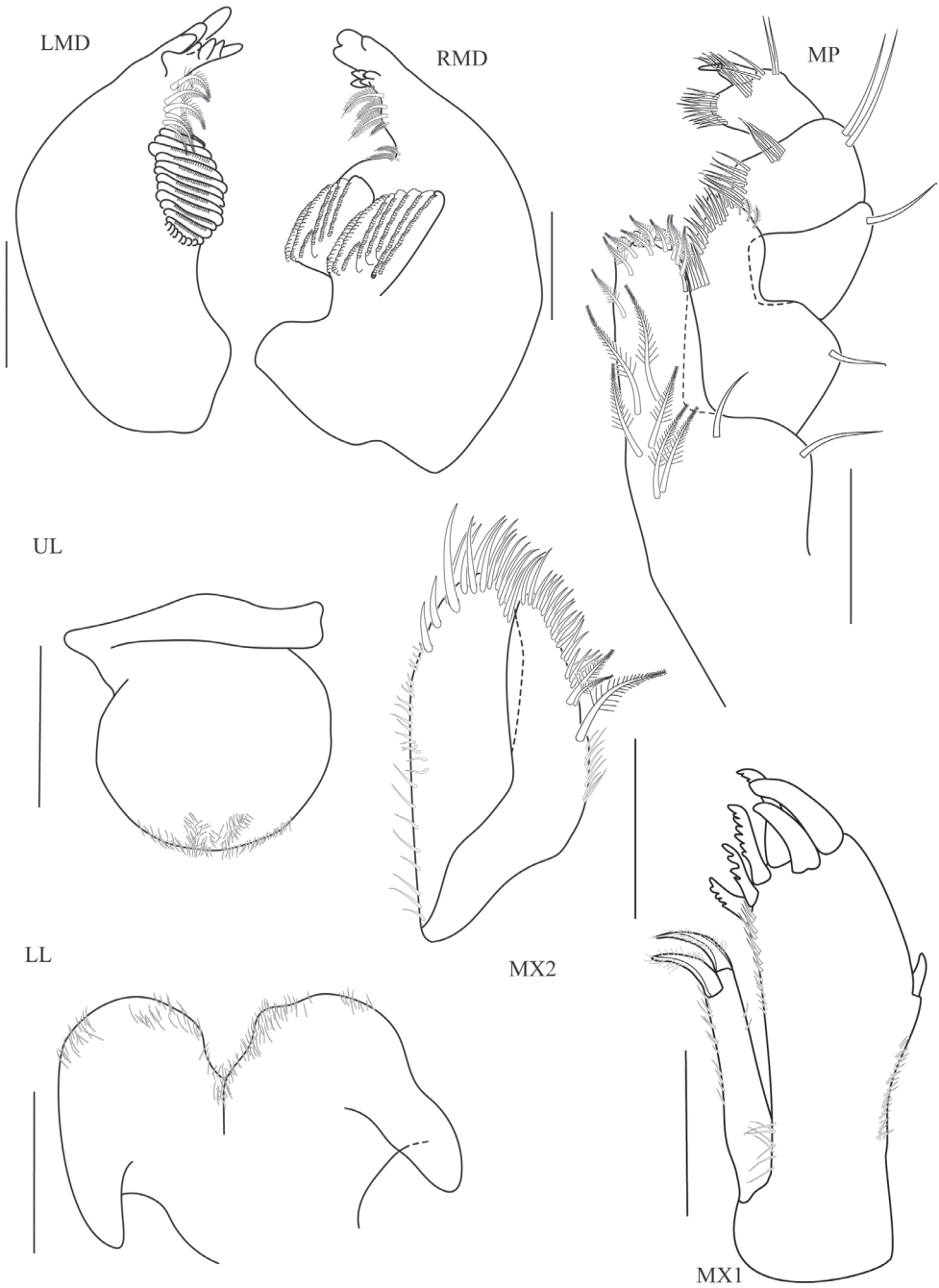


Figure 3. *Thailandorchestia rhizophila* sp. nov. holotype, male, 8.04 mm, THNHM-Iv- 18760. Scale bars: 0.2 mm.

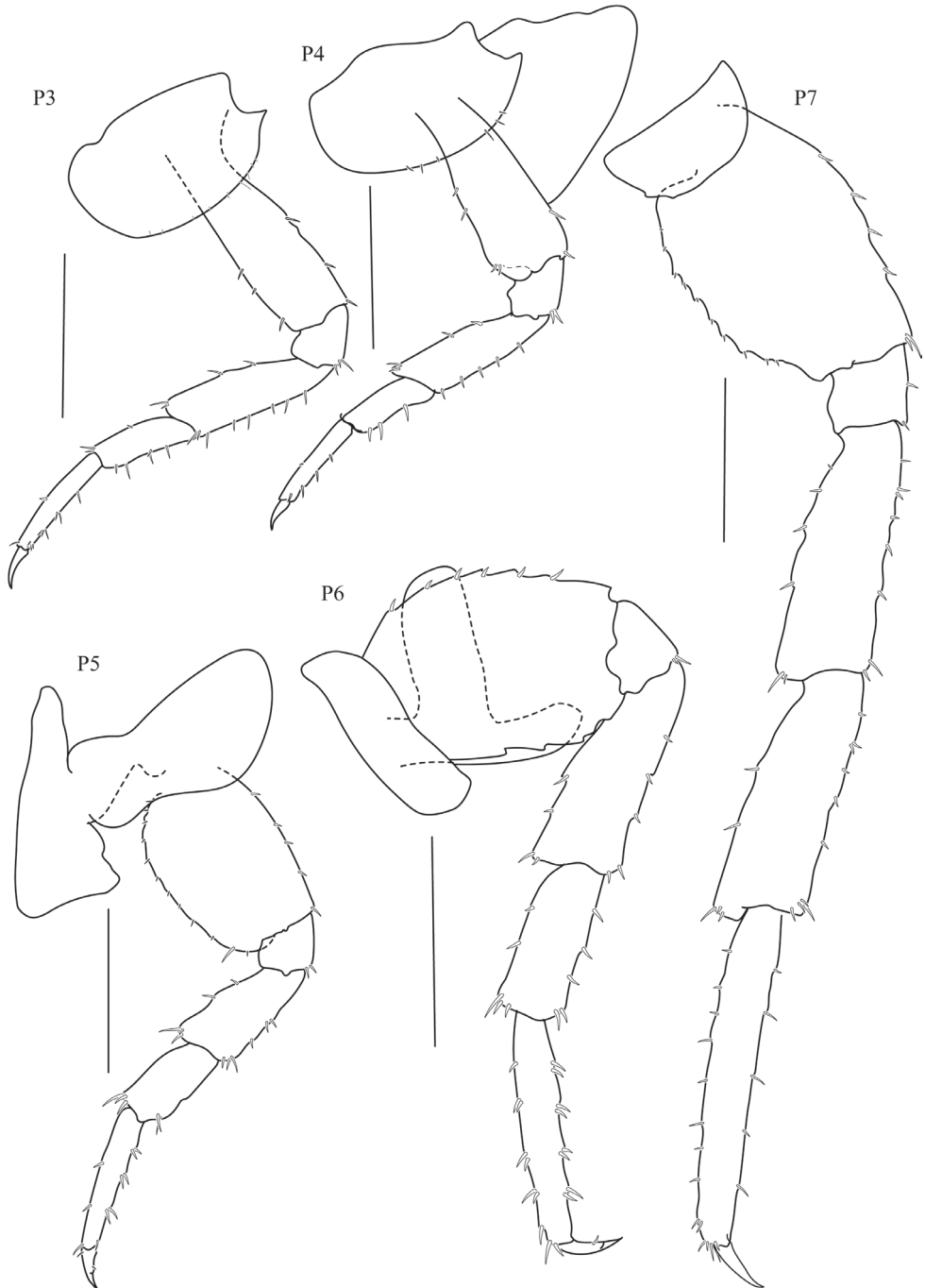


Figure 4. *Thailandorchestia rhizophila* sp. nov. holotype, male, 8.04 mm, THNHM-Iv- 18760. Scale bars: 1 mm.

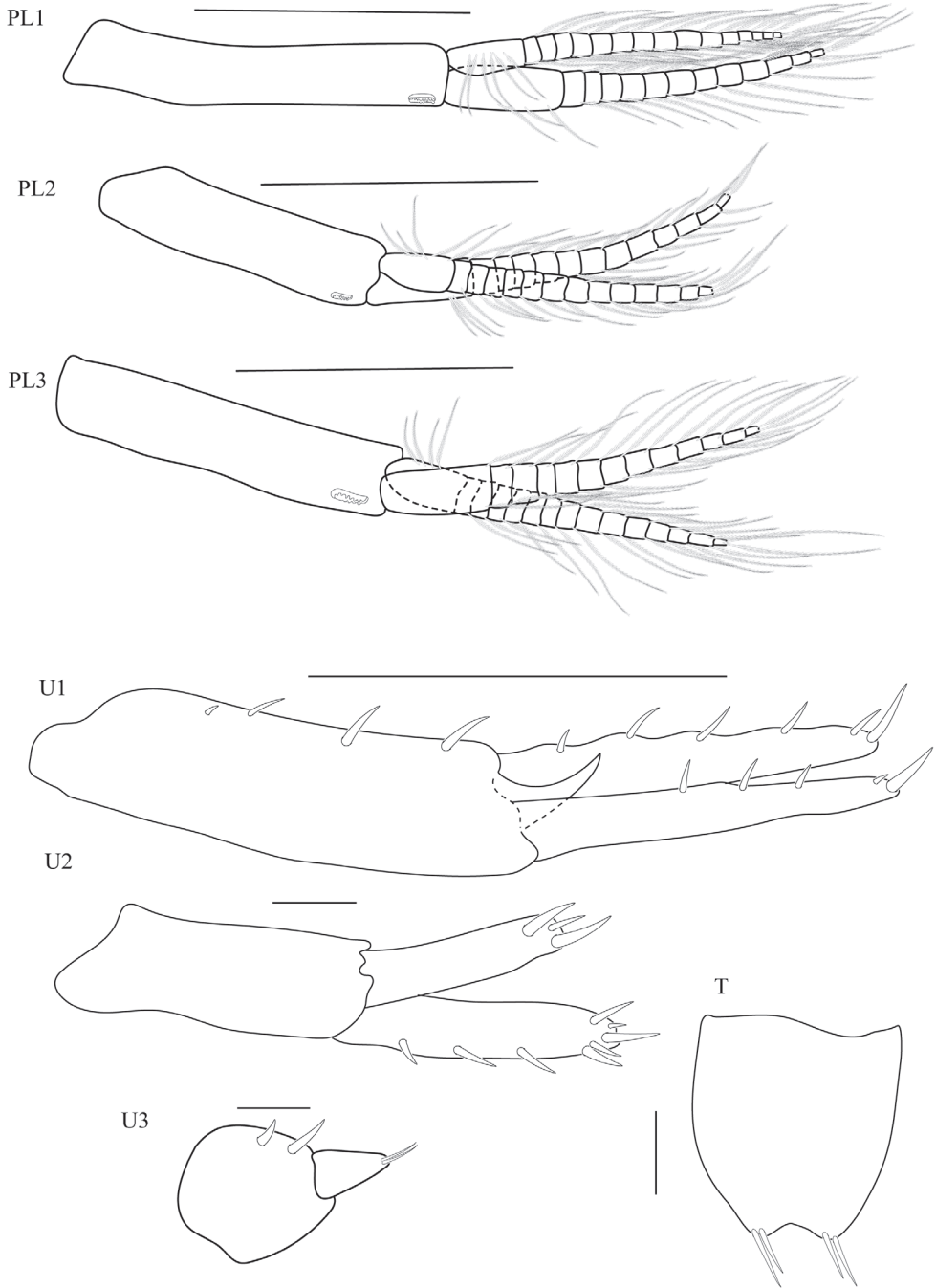


Figure 5. *Thailandorchestia rhizophila* sp. nov. holotype, male, 8.04 mm, THNHM-Iv- 18760. Scale bars (U1–U3, T): 0.1 mm; (PL1–PL3): 0.5 mm.

without robust setae. **Mandible** (Fig. 3LMD) left lacinia mobilis 4-dentate. **Maxilla 1** (Fig. 3MX1) with small palp, 1-articulate. **Maxilliped** (Fig. 3MP) palp article 2 distomedial lobe absent; article 4 small, well defined.

Pereon. Gnathopod 1 (Fig. 2G1) sexually dimorphic; subchelate; coxa 1 smaller than coxa 2; posterior margins of merus, carpus, and propodus each with lobe covered in palmate setae, palmate lobes present; propodus shorter than carpus, subrectangular; palm transverse. **Gnathopod 2** (Fig. 2G2) sexually dimorphic; subchelate; coxal gill simple (or slightly lobate); basis slender; carpus triangular, reduced (enclosed by the merus and propodus), posterior lobe absent, not projecting between merus and propodus; 1.8× as long as wide; palm acute, weakly toothed, with a subquadrate protuberance near dactylar ring, lined with robust setae, posterodistal corner with socket; dactylus subequal in length to palm. **Pereopod 3–4** (Fig. 4P3–P4) coxae wider than deep. **Pereopods 3–7** (Fig. 4P3–P7) simplidactylate. **Pereopod 4** (Fig. 4P4) subequal or slightly shorter than pereopod 3; carpus similar in length to pereopod 3 carpus; dactylus similar to pereopod 3 dactylus. **Pereopod 5** propodus distinctly longer than carpus. **Pereopod 6** (Fig. 4P6) slightly sexually dimorphic; shorter than pereopod 7; coxa posterior lobe inner view posteroventral corner rounded, posterior margin oblique with respect to ventral margin, posterior lobe without a ridge, posterior lobe without marginal setae; coxal gill lobate. **Pereopod 7** (Fig. 4P7) sexually dimorphic (merus and carpus broadly incrassate); basis lateral sulcus absent, posterodistal lobe absent; distal articles (merus and carpus) expanded; merus posterior margin expanded distally, subtriangular.

Pleon. Pleopods all well developed. **Pleopod 1** (Fig. 5PL1) peduncle without marginal setae; biramous, outer ramus subequal in length to peduncle; inner ramus with 17 articles, outer ramus with 13 articles. **Pleopod 2** (Fig. 5PL2) peduncle without marginal setae; biramous, outer ramus subequal in length to peduncle; inner ramus with 15 articles, outer ramus with 14 articles. **Pleopod 3** (Fig. 5PL3) peduncle without marginal setae; biramous, outer ramus subequal in length to peduncle; inner ramus with 15 articles, outer ramus with 13 articles. **Uropod 1** (Fig. 5U1) peduncle with 4 robust setae, distolateral robust seta present, large (1/4 length of outer ramus), with simple tip; inner ramus subequal in length to outer ramus, inner ramus with marginal robust setae; outer ramus with 3 marginal robust setae. **Uropod 2** (Fig. 5U2) inner ramus subequal in length to outer ramus, with marginal robust setae, with 3 lateral robust setae; outer ramus without marginal robust setae. **Uropod 3** (Fig. 5U2) peduncle with 2 robust setae; ramus shorter than peduncle, ramus triangular, with 2 apical setae. **Telson** (Fig. 5T) longer than broad, apically incised, dorsal midline vestigial or absent, with apical robust setae only and 2 robust setae per lobe.

Description of female allotype. (THNHM-Iv- 18761, Figs 6–7)

Pereon. Gnathopod 1 (Fig. 6G1) propodus narrower than that of male; dactylus subequal to palm. **Gnathopod 2** (Fig. 6G2) mitten-shaped; basis slightly expanded; posterior margins of merus, carpus, and propodus each with lobe covered in palmate setae; carpus well developed (not enclosed by merus and propodus), posterior lobe present, projecting between merus and propodus; propodus length twice as long as wide; palm obtuse, smooth, without a protuberance or shelf near dactylar hinge, posterodistal corner

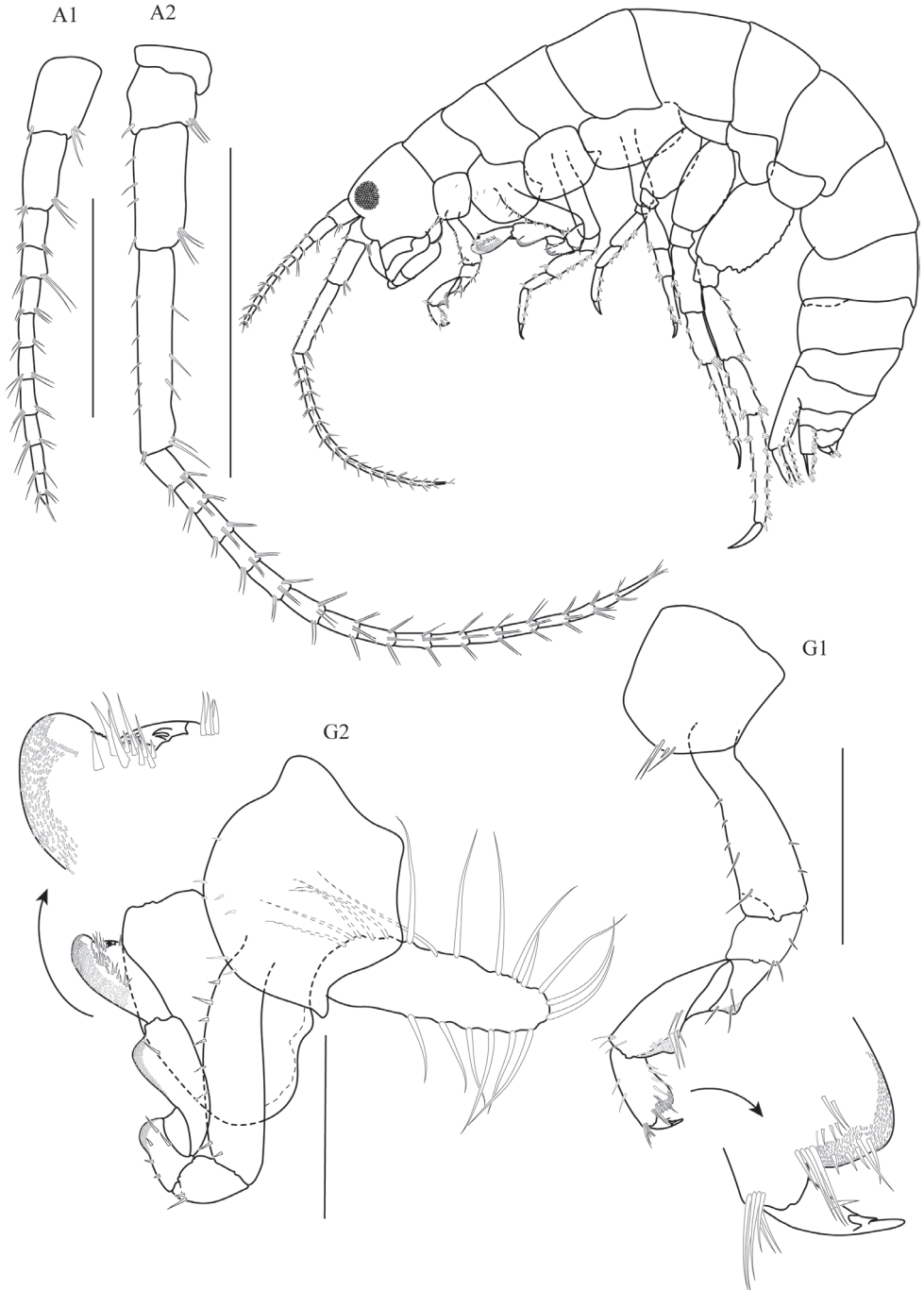


Figure 6. *Thailandorchestia rhizophila* sp. nov. allotype, female, 7.80 mm, THNHM-Iv- 18761. Scale bars: 1 mm.

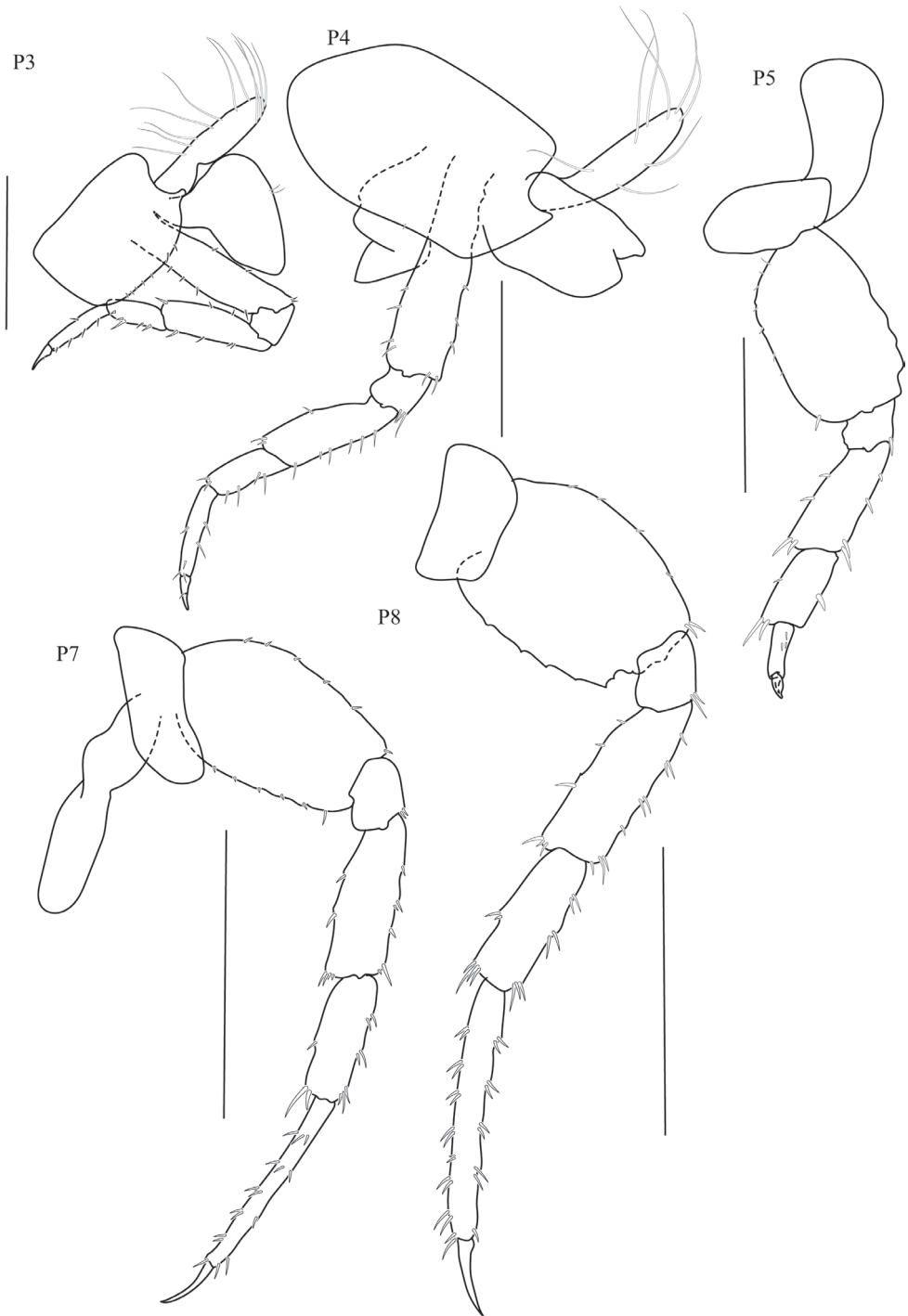


Figure 7. *Thailandorchestia rhizophila* sp. nov. allotype, female, 7.80 mm, THNHM-Iv- 18761. Scale bars: 1 mm.

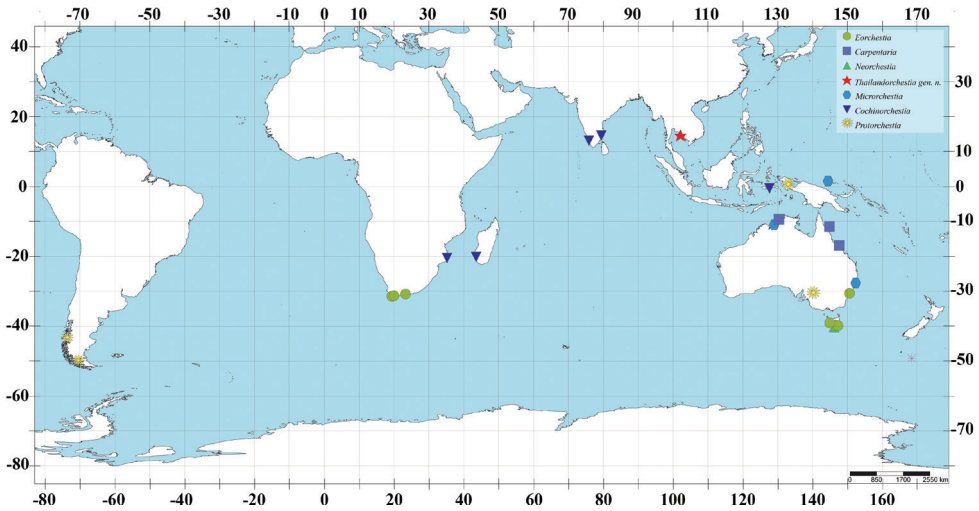


Figure 8. Map showing distribution of genera in the family Protorcheistiidae.

naked; dactylus shorter than palm; gill lobate. **Pereopod 5** (Fig. 7P5) propodus shorter than carpus. Distal articles (merus and carpus) slender. **Preopods 6–7** (Fig. 7P6–7) sexually dimorphic (merus and carpus not broadly incrassate). **Oostegites** long (length greater than 2× width), longer than wide, weakly setose, setae with simple, smooth tips.

Habitat. Mangrove wood, inside roots and rotting logs.

Distribution. Thailand, Ko Kut District, Inner Gulf of Thailand.

Discussion

Most species of Protorcheistiidae are known to be semiaquatic marsh hoppers that inhabit salt marshes and mangrove swamps (Myers and Lowry 2020), except for *Neorchestia*, which has adapted to life on land (Friend 1987). Protochestiid amphipods were previously reported to live in hard substrates (rock) and soft substrates (sand, mangrove debris, and wet forest soil) (Myers and Lowry 2020). Surprisingly, *Thailandorchestia* gen. nov. specimens live in galleries inside the mangrove roots, where gravid females are also found, implying that these amphipods reproduce inside the roots. According to this ecology, these amphipods should be classified as driftwood hoppers. This is the second genus reported as a driftwood hopper; a previous driftwood hopper report is of the genus *Macarorchestia* in the northeast Atlantic and Mediterranean coastal regions (Wildish 2014). Based on these observations, the adaptations observed in *Thailandorchestia rhizophila* sp. nov. are akin to those in *Macarorchestia* in having: 1) reduced pleopod and oostegites; 2) fewer ova per brood (5–6 individuals); 3) small eyes; and 4) lack of dorsal pigment (Wildish 2017). Another behavior found in the present study was negative phototaxis, whereby *T. rhizophila* sp. nov. specimens escaped deeper inside the wood upon its splitting.

According to the recent checklist of the amphipods of Southeast Asia (Azman et al. 2022), a total of 25 species of Talitroidea amphipods have been reported, with four species

(16%) occurring in Thailand. From that, *Thailandorchestia rhizophila* sp. nov. is the only one species has been reported from mangrove forest while consider the area of mangrove forest in Thailand covers 2,300 square kilometres (Pumijumnong 2014). Further intensive study of mangrove amphipods, especially in the marsh hopper group, is required.

Acknowledgements

This study is a part of the research project “Diversity of amphipods along coastal area of Koh Kut, Trat Province” under the Plant Genetic Conservation Project under the Royal initiative of Her Royal Highness Princess Maha Chakri Sirindhorn. This work was financially supported by the Office of the Ministry of Higher Education, Science, Research and Innovation of Thailand and the Thailand Science Research and Innovation, Higher Education, Science, Research and Innovation of Thailand through the Kasetsart University Reinventing University Program 2021 and grants from the Kasetsart University Research and Development Institute (KURDI), Kasetsart University, Bangkok, Thailand. In addition, we are grateful to the Department of Zoology, Faculty of Science, Kasetsart University for the laboratory facilities.

References

- Azman AR, Sivajothy K, Shafie BB, Ja'afar N, Wongkamhaeng K, Bussarawit S, Alip AE, Lee YL, Metillo EB, Won MEQ (2022) The amphipod (Crustacea: Peracarida) of the South-east Asia and the neighbouring waters: an updated checklist with new records of endemic species. *Research Bulletin - Phuket Marine Biological Center* 79(1): 42–84.
- Bousfield EL (1982) The amphipod superfamily Talitroidea in the northeastern Pacific region. Family Talitridae. Systematics and distributional ecology. *National Museum of Natural Science, Publications in Biological Oceanography*, 11, [i–vii] 73 pp.
- Bousfield EL (1984) Recent advances in the Systematics and Biogeography of Landhoppers (Amphipoda: Talitridae) of the Indo-Pacific Region. *Bishop Museum Special Publications* 72: 169–205.
- Bussarawich S (1985) Amphipod Mangroves Thailand. In: NRCT (Ed.) *Fifth Seminar on Mangrove Ecosystems*, Phuket, Thailand, 17 pp.
- Coleman C (2003) “Digital inking”: How to make perfect line drawings on computers. *Organisms, Diversity & Evolution* 3(4): 1–14. <https://doi.org/10.1078/1439-6092-00081>
- Friend JA (1987) Terrestrial Amphipods (Amphipoda: Talitridae) of Tasmania: Systematics and Zoogeography. *Records of the Australian Museum* 7: 1–85. <https://doi.org/10.3853/rj.0812-7387.7.1987.97>
- Latreille PA (1816) *Nouveau Dictionnaire d'histoire naturelle, appliquée aux arts, à l'Agriculture, à l'Economie rurale et domestique, à la Médecine, etc. Par une Société de Naturalistes et d'Agriculteurs. Nouvelle Édition. Paris*. 1: 467–469.
- Lowry JK, Peart R (2010) The genus *Microrchestia* (Amphipoda: Talitridae) in eastern Australia. *Zootaxa* 2349(1): 23–38. <https://doi.org/10.11646/zootaxa.2349.1.2>

- Lowry JK, Springthorpe RT (2015) Coastal Talitridae (Amphipoda: Talitroidea) from north-western Australia to Darwin with a revision of the genus *Cochinorchestia* Lowry & Peart, 2010. *Zootaxa* 3985(2): 151–202. <https://doi.org/10.11646/zootaxa.3985.2.1>
- Myers AA, Lowry JK (2020) A phylogeny and classification of the Talitroidea (Amphipoda, Senticaudata) based on interpretation of morphological synapomorphies and homoplasies. *Zootaxa* 4778(2): 281–310. <https://doi.org/10.11646/zootaxa.4778.2.3>
- Pumijumnong N (2014) Mangrove Forests in Thailand. In: Faridah-Hanum I, Latiff A, Hakeem K, Ozturk M (Eds) *Mangrove Ecosystems of Asia*. Springer, New York, NY, New York, 60–79. https://doi.org/10.1007/978-1-4614-8582-7_4
- Richardson AMM (1993) Tasmanian intertidal Talitridae (Crustacea: Amphipoda). Palustral talitrids: two new species of *Eorchestia* Bousfield, 1984. *Journal of Natural History* 27(2): 267–284. <https://doi.org/10.1080/00222939300770131>
- Richardson AMM (1996) *Protorchestia lakei*, new species (Amphipoda: Talitridae), from Maatsuyker Island, Tasmania, with a key to the genus and notes on the diversity of Tasmanian Talitridae. *Journal of Crustacean Biology* 16(3): 574–583. <https://doi.org/10.2307/1548749>
- Wildish DJ (2014) New genus and two new species of driftwood hoppers (Crustacea, Amphipoda, Talitridae) from northeast Atlantic and Mediterranean coastal regions. *Zoosystematics and Evolution* 90(2): 133–146. <https://doi.org/10.3897/zse.90.8410>
- Wildish DJ (2017) Evolutionary ecology of driftwood talitrids: A review. *Zoosystematics and Evolution* 93(2): 353–361. <https://doi.org/10.3897/zse.93.12582>
- Zimmer A, Araujo PB, Bond-Buckup G (2009) Diversity and arrangement of the cuticular structures of *Hyaella* (Crustacea: Amphipoda: Dogielinotidae) and their use in taxonomy. *Zoologia* 26(1): 127–142. <https://doi.org/10.1590/S1984-46702009000100019>

Supplementary material I

Video of living *Thailandorchestia rhizophila*

Authors: Koraon Wongkamhaeng, Pongrat Dumrongrojwattana, Ratchaneewarn Sumitrakij, Tosaphol Saetung Keetapithchayakul

Data type: Mp4 file.

Explanation note: Video of living *Thailandorchestia rhizophila* inside the rotting branch and their food item.

Copyright notice: This dataset is made available under the Open Database License (<http://opendatacommons.org/licenses/odbl/1.0/>). The Open Database License (ODbL) is a license agreement intended to allow users to freely share, modify, and use this Dataset while maintaining this same freedom for others, provided that the original source and author(s) are credited.

Link: <https://doi.org/10.3897/zookeys.1099.82949.suppl1>

Review of *Ophioplinthaca* Verrill, 1899 (Echinodermata, Ophiuroidea, Ophiacanthidae), description of new species in *Ophioplinthaca* and *Ophiophthalmus*, and new records from the Northwest Pacific and the South China Sea

Hasitha Nethupul^{1,2}, Sabine Stöhr³, Haibin Zhang¹

1 Institute of Deep-sea Science and Engineering, Chinese Academy of Sciences, CAS, 57200 Sanya, China

2 University of Chinese Academy of Sciences, Beijing 100039, China **3** Swedish Museum of Natural History, Dept of Zoology, Box 50007, 10405 Stockholm, Sweden

Corresponding author: Haibin Zhang (hzhang@idsse.ac.cn)

Academic editor: A. Martynov | Received 13 October 2021 | Accepted 18 February 2022 | Published 11 May 2022

<http://zoobank.org/A963E7C7-F1BF-4BF2-BB4F-A0CD5D319691>

Citation: Nethupul H, Stöhr S, Zhang H (2022) Review of *Ophioplinthaca* Verrill, 1899 (Echinodermata, Ophiuroidea, Ophiacanthidae), description of new species in *Ophioplinthaca* and *Ophiophthalmus*, and new records from the Northwest Pacific and the South China Sea. ZooKeys 1099: 155–202. <https://doi.org/10.3897/zookeys.1099.76479>

Abstract

The ophiuroid genus *Ophioplinthaca* is well characterized by the deep incisions in the disc. Prior to this study, it contained 32 accepted species, but species limits and geographic distributions were not well understood. The manned submersible vehicle ‘Shenhaiyongshi’ was used to collect ophiuroid specimens from the deep-sea seamounts and cold seeps in the South China Sea and Northwest Pacific at 602–3600 m depth, during 2018 to 2020. The genus *Ophioplinthaca* was reviewed using both morphological data and a phylogenetic analysis, based on COI sequences. The taxonomic status of the genus *Ophiophthalmus* Matsumoto, 1917, a junior homonym of *Ophiophthalmus* Fitzinger, 1843 (a reptile) was clarified by proving prevailing usage of the ophiuroid name. A total of eight species were identified, including two new species, described as *Ophioplinthaca brachispina* sp. nov. and *Ophiophthalmus serratus* sp. nov., and two new records. The new species are characterized by unique features of the arm skeletons. Tabular keys to all *Ophioplinthaca* and *Ophiophthalmus* species are provided. Interspecific and intraspecific genetic distance of *Ophioplinthaca* species ranged from 2.32% to 19.72%, and from 0.26% to 0.90%, respectively. The data suggest that species of the genus *Ophioplinthaca* are more widely spread around the Northwest Pacific region deep-sea seamounts than previously known.

Keywords

COI, cold seep, molecular phylogeny, morphology, seamounts, SEM, taxonomy

Introduction

The ophiuroid family Ophiacanthidae Ljungman, 1867 is one of the largest and diverse families in the order Ophiacanthida, containing 239 accepted species within 15 genera to date (Paterson 1985; Martynov 2010a; Martynov et al. 2015; Stöhr et al. 2021). In the present study, we focused on the genera *Ophioplinthaca* Verrill, 1899 and *Ophiophthalmus* Matsumoto, 1917. *Ophioplinthaca* can easily be distinguished from other genera by deep incisions in the disc that create distally enlarged wedge-shaped lobes (Verrill 1899; O'Hara and Stöhr 2006). A total of 32 accepted species are included in the genus *Ophioplinthaca*, and most of them have been recorded from the Indo-Pacific Ocean (OBIS 2021; Stöhr et al. 2021). Recent studies suggested *Ophioplinthaca* species were dominant megafauna on seamounts from the Northwest Pacific region (Cho and Shank 2010; Chen et al. 2021a; Na et al. 2021). However, species diversity and geography of *Ophioplinthaca* species are still not fully understood due to limited collecting efforts in this area (Cho and Shank 2010; Yesson et al. 2011; Chen et al. 2021a, b; Na et al. 2021). Previous morphological studies reported that *Ophioplinthaca* species were difficult to separate due to complex intraspecific morphological variation (O'Hara and Stöhr 2006; Chen et al. 2021a, b; Na et al. 2021).

The genus *Ophiophthalmus* was created by Matsumoto (1917) to accommodate particular species that at the time were placed in the genera *Ophiomitra*, *Ophiomitrella*, and *Ophiacantha*, but currently only four species are included in this genus. Paterson (1985) considered *Ophiophthalmus* as an invalid junior homonym of a reptilian genus described by Fitzinger (1843), without proposing a replacement name. Therefore, the taxonomic status of *Ophiophthalmus* will be clarified herein.

This study covers deep waters around the Northwest Pacific region near southwest Guam Island, and in the South China Sea (Xisha Islands and Haima cold seep). Here, we present an account of the ophiuroid species collected. Our goal is to present a diagnosis of the morphological features of these species, combined with molecular details, to complement the limited original descriptions and the lack of figures in the literature. We present comprehensive tabular keys for all species within the genera *Ophioplinthaca* and *Ophiophthalmus*. Two new species, one in *Ophioplinthaca* and one in *Ophiophthalmus*, are described, and six species of *Ophioplinthaca* are redescribed, including two new records from the Northwest Pacific region, all richly illustrated. These species live on seamounts and cold seeps, and this study adds to the known diversity in these unique habitats to better understand ophiuroid distribution and biogeography.

Materials and methods

Sample collecting

The manned submersible vehicle ‘Shenhaiyongshi’ was used to collect samples for this study on a seamount near Xisha Islands and on the Haima cold seep in the South China Sea, as well as on a seamount southwest of Guam Island (Fig. 1). Most of the specimens were frozen without preservation fluid, then transported to the Institute of Deep-sea Science and Engineering, Chinese Academy of Sciences (CAS), Sanya,

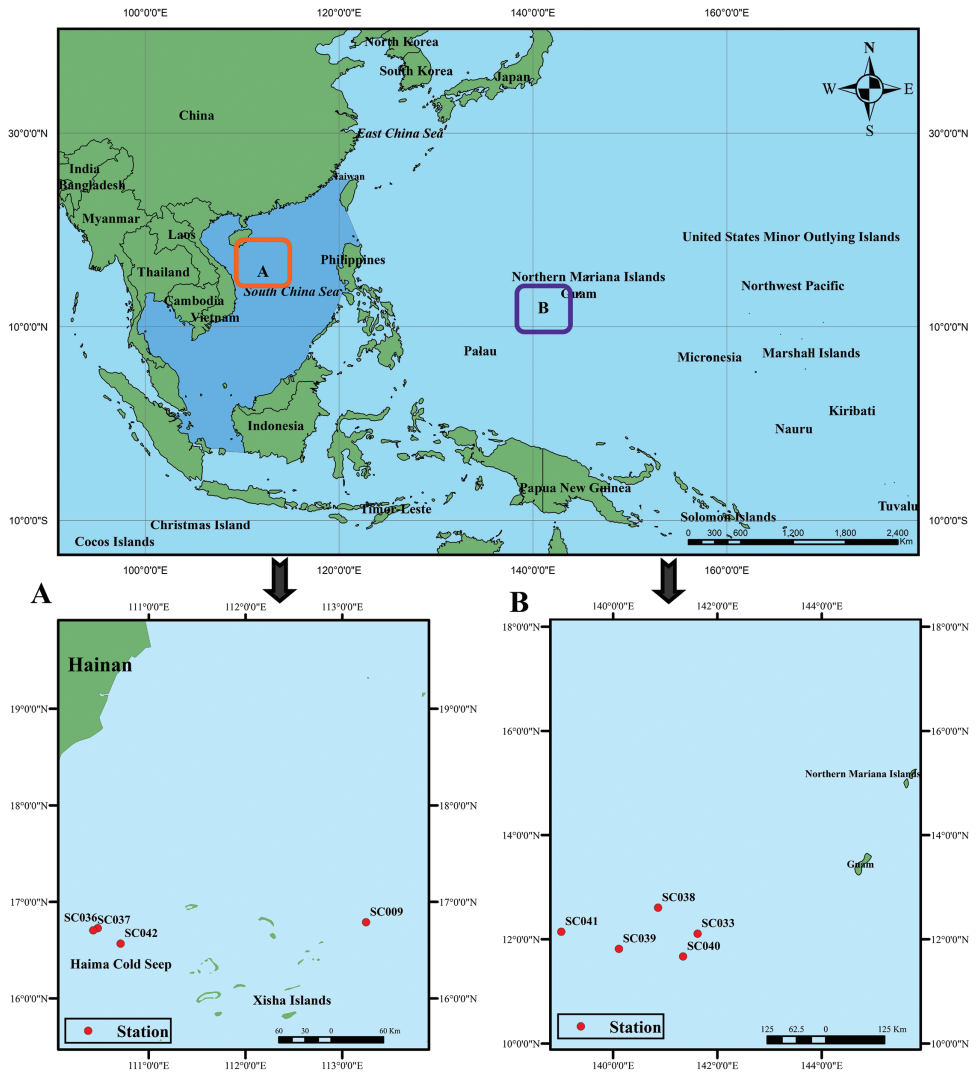


Figure 1. Collecting stations in this study **A** South China Sea (Xisha Islands and Haima cold seep) **B** Northwest Pacific region (Southwest of Guam island). Source: International Hydrographic Organization and Sieger 2012.

China, for further analysis. The samples were sorted and the species identified using available literature (Thomson 1877; Lyman 1878, 1882, 1883; Koehler 1904, 1922, 1930, 1897; H. L. Clark 1900, 1911, 1915, 1939; Matsumoto 1917; A. H. Clark 1949; Mortensen 1933; John and A. M. Clark 1954; Cherbonnier and Sibuet 1972; Guille 1981; O'Hara and Stöhr 2006; Chen et al. 2021a, b; Na et al. 2021) and by molecular analysis.

Morphological analysis

Specimens were photographed through a dissecting stereo microscope (OLYMPUS SZX7) to identify external morphological characters. Arm skeletons were photographed by a scanning electron microscope (SEM) Phenom ProX. Arm skeletal elements were prepared by dissolving the soft tissue in undiluted NaOCl. The excess NaOCl in skeletal elements (ossicles) was removed by repeated flushing with distilled water. After drying, the ossicles were mounted on a stub, using ethanol dissolvable carbon tapes. Holotypes, paratypes and all other newly recorded specimens were deposited at the Institute of Deep-sea Science and Engineering (CAS), Sanya, China. The terms used to describe ophiuroids follow previous authors (Martynov 2010a, b; Stöhr 2011, 2012; O'Hara et al. 2017; Hendler 2018; Stöhr and O'Hara 2021).

Type material and one other specimen of *Ophioplinthaca lithosora* (H. L. Clark, 1911) were examined from digital photographs.

Molecular analysis

DNA of identified specimens was extracted by using the TIANamp Marine Animals DNA kit (TianGen, Beijing) following the manufacturer's protocol. We sequenced cytochrome c oxidase I (COI) partial genes for phylogenetic analysis by amplifying COI_{ceF} (5'-ACTGCCACGCCCTAGTAATGATATTTTTTTATGGTNATGCC-3') and COI_{ceR} (5'-TCGTGTGTCTACGTCCATTCCTACTGTRAACATRTG-3') COI primer set, with an initial denaturation at 95 °C for 3 min, followed by 40 cycles of denaturation at 94 °C for 45 s, annealing temperature at 51 °C to 55 °C for 70 s, and extension at 72 °C for 80 s; and a final extension at 72 °C for 5 min as a suitable PCR cycle (Hoareau and Boissin 2010). Total PCR mixture was 50 µL volume, containing 25 µL Premix Taq with 1.25 U Taq, 0.4 mM of each dNTP and 4 mM Mg²⁺ (Ex Taq version, Takara, Dalian, China), 0.5 µM each of the primers and approximately 100 ng template DNA. PCR product quality was determined by electrophoresis using a 1.0% agarose gel and the NanoDrop 1000 (Thermo Scientific, Waltham, MA, USA). PCR products were sequenced in both directions on ABI3730 DNA Analyzer, and all new sequences were deposited at NCBI GenBank.

We constructed a maximum likelihood (ML) phylogenetic tree to represent the family Ophiacanthidae by adding ten species from our collection and an additional 11 sequences from NCBI GenBank (Table 1). As outgroup we used *Ophiomyxa brevirima* H. L. Clark, 1915 and *Ophiomyxa anisacantha* H. L. Clark, 1911. All sequences were

Table 1. Localities, voucher information, and GenBank accession numbers for all specimens used in this study.

Species	Locality	Voucher number	COI
<i>Ophioplinthaca</i> sp.	Mariana Trench: Southwest of Guam island	IDSSE-EEB-SW0108	OK043831
<i>Ophioplinthaca defensor</i>	Mariana Trench: Southwest of Guam island	IDSSE-EEB-SW0112	OK043836
<i>Ophioplinthaca defensor</i>	Northwest Pacific Ocean: Caiwei Guyot	RSIO410611	MT025778
<i>Ophioplinthaca athena</i>	Mariana Trench: Southwest of Guam island	IDSSE-EEB-SW0110	OK043833
<i>Ophioplinthaca</i> sp.	Northwest Pacific Ocean: St. RC-ROV08	RSIO56058	MW284981
<i>Ophioplinthaca</i> cf. <i>lithosora</i>	South China Sea: Xisha islands	IDSSE-EEB-SW0111	OK043834
<i>Ophioplinthaca globata</i>	Papua New Guinea	MNHN BP32	KU895134
<i>Ophioplinthaca semele</i>	Northwest Pacific Ocean: St. RC-ROV08	RSIO56057	MW284980
<i>Ophioplinthaca semele</i>	Mariana Trench: Southwest of Guam island	IDSSE-EEB-SW0113	OK043835
<i>Ophioplinthaca plicata</i>	Australia: Tasman Sea	MV F144758	EU869989
<i>Ophioplinthaca plicata</i>	New Zealand	MV F188868	KU895133
<i>Ophioplinthaca grandisquama</i>	Northwest Pacific Ocean: St. RC-ROV05	RSIO56060	MW284982
<i>Ophioplinthaca amezianae</i>	Mariana Trench: Southwest of Guam island	IDSSE-EEB-SW0109	OK043832
<i>Ophioplinthaca brachispina</i> sp. nov.	Mariana Trench: Southwest of Guam island	IDSSE-EEB-SW0106	OK043829
<i>Ophioplinthaca brachispina</i> sp. nov.	Mariana Trench: Southwest of Guam island	IDSSE-EEB-SW0107	OK043830
<i>Ophiophthalmus cataleimmoidus</i>	Canada: British Columbia, Kyoquot Sound	RBCM EC00208	HM542946
<i>Ophiophthalmus normani</i>	Canada: British Columbia, Kyoquot Sound	RBCM EC00186	HM542947
<i>Ophiophthalmus serratus</i> sp. nov.	South China Sea: Haima cold seep	IDSSE-EEB-SW0136	OK043837
<i>Ophiophthalmus serratus</i> sp. nov.	South China Sea: Haima cold seep	IDSSE-EEB-SW0137	OK043838
<i>Ophiomyxa brevirima</i>	New Zealand	MVF95868	KU895170
<i>Ophiomyxa anisacantha</i>	Japan: Sagami Sea	NSMT E-6269	AB758822

aligned using the Clustal W algorithm in MEGA X. The best-fit substitution model of the COI gene in the ML trees was T92 + G + I model (Tamura 3-parameter model + Gamma distributed with invariant sites), and estimated by the “Find Best DNA/Protein Models” Option of MEGA X. A phylogenetic tree was reconstructed for the partial COI gene by using the maximum likelihood bootstrap method. The ML analysis was run with MEGA X, and ML trees were constructed, including 1,000 bootstrap replicates (Kimura 1980; Thompson et al. 1994; Kumar et al. 2016, 2018). The genetic distances with standard error of specimen groups were analyzed according to the Kimura 2-parameter model with performing 1,000 bootstrap replications (Kimura 1980).

The following abbreviations are used in the text, tables, and figures:

ars	arm spine;
as	adoral shield;
ASE	arm segment;
ass	adoral shield spine;
COI	Cytochrome C oxidase subunit 1;
D	dorsal;
DAP/dap	dorsal arm plate;
DAS/das	dorsal arm spines;
de	depression;
dist	distal;
dl	dorsal lobe;
ds	disc spine;
dsc	disc scale;

gra	granules;
gs	genital slit;
IDSSE	Institute of Deep-sea Science and Engineering;
j	jaw;
lac	lateral ambulacral canal;
lap	lateral arm plate;
LOP	lateral oral papillae;
m	madreporite;
ML	Maximum Likelihood;
mo	muscle opening;
msv	manned submersible vehicle;
no	nerve opening;
NSMT	National Science Museum, Tokyo;
os	oral shield;
pb	podial basin;
prox	proximal;
ri	ridge;
RS/rs	radial shield;
th	thorns;
TS/ts	tentacle scale;
v	ventral;
VAP/vap	ventral arm plate;
VAS/vas	ventral arm spines;
vl	ventral lobe;
VMT	ventralmost tooth;
vs	volute-shape;
USNM	United States National Museum, Smithsonian Institution.

Results

Seven species of *Ophioplinthaca* were identified, among them one new to science, and all are described below. One specimen was identified as belonging to *Ophiophthalmus* and is described as a new species. One unidentified specimen of *Ophioplinthaca* is described, but not assigned to a name pending further investigations of variability within the genus. A tabular key to all species of *Ophioplinthaca* is provided in Table 3, to the species in *Ophiophthalmus* in Table 4.

Molecular phylogenetic analysis

A total of 21 COI sequences trimmed to 581 bp were obtained after removing ambiguous aligned sites and successfully reconstructing a genera *Ophioplinthaca* and *Ophiophthalmus* ML tree (Fig. 2).

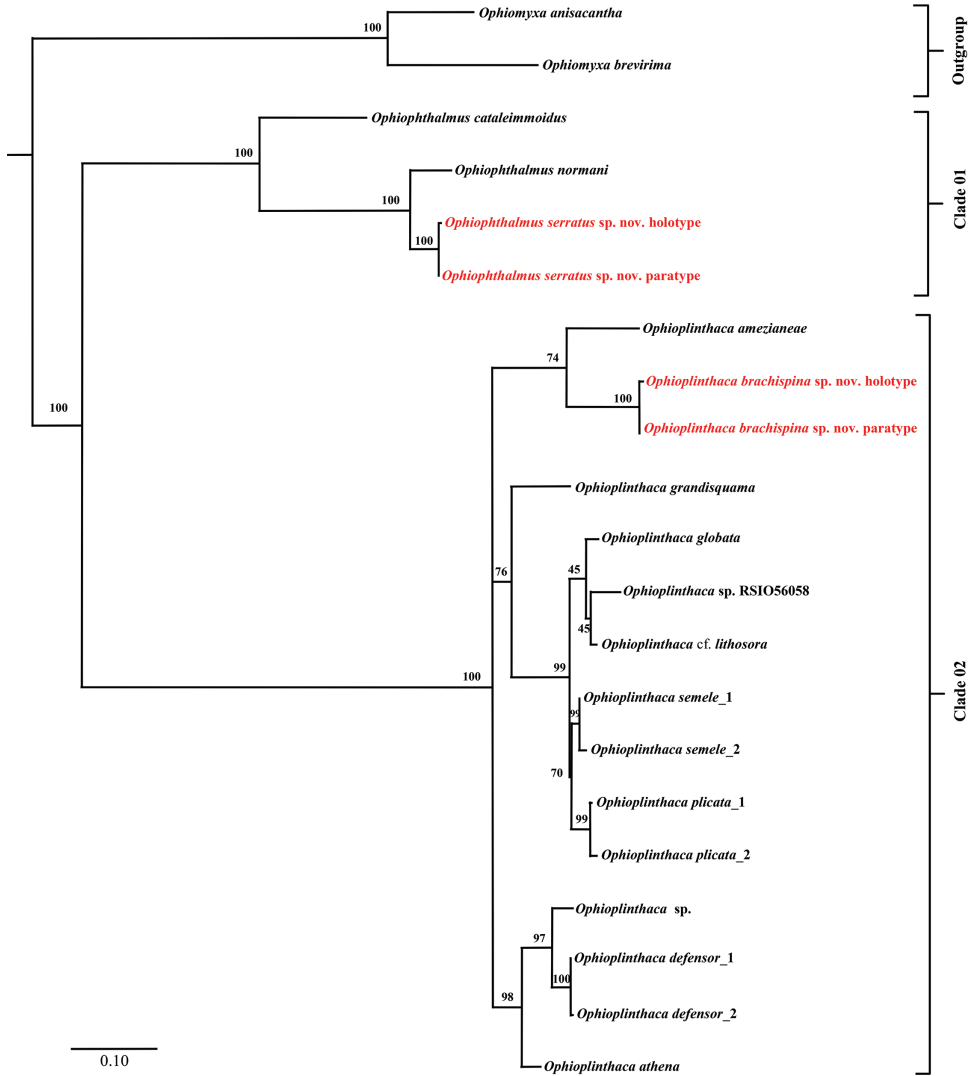


Figure 2. Maximum likelihood (ML) tree of *Ophioplinthaca* and *Ophiophthalmus*, based on partial COI sequences (bootstrap support values were generated with rapid bootstrapping algorithm for 1,000 replicates; red = new species).

Two main clades were detected within the ML Tree (clade 01: genus *Ophiophthalmus*); clade 02: genus *Ophioplinthaca*). Average mean genetic distance of Ophiacanthidae was $21.74 \pm 2.79\%$ SE (19 specimens), and maximum value between two genera was $46.09 \pm 4.81\%$ SE. Overall average mean genetic distance of COI within *Ophioplinthaca* was $11.85 \pm 1.70\%$ SE (15 specimens). Interspecies and intraspecies genetic distance range among *Ophioplinthaca* species were 2.32–19.72% and 0.26–0.9% respectively. Overall average mean genetic distance of COI among *Ophiophthalmus* was

Table 2. *Ophioblattacea* and *Ophioblattinus*, pairwise distance values based on 581 bp mitochondrial COI sequences, calculated using the Kimura 2-parameter method with 1,000 bootstrap replicates (values in blue color represent Standard Error).

No.	Species	1	2	3	4	5	6	7	8	9	10	11	12	13	14	15	16	17	18	19	20	21
1	<i>Ophioblattacea</i> sp.		0.90%	1.15%	1.16%	2.13%	1.64%	1.86%	1.92%	1.59%	1.91%	1.60%	2.01%	1.97%	2.02%	2.02%	3.60%	3.80%	3.12%	3.11%	3.47%	3.54%
2	<i>Ophioblattacea defensor_1</i>	4.27%		0.26%	1.17%	2.11%	1.63%	1.81%	1.97%	1.60%	1.89%	1.60%	1.68%	1.94%	1.85%	1.89%	3.70%	3.97%	3.24%	3.23%	3.37%	3.52%
3	<i>Ophioblattacea defensor_2</i>	4.34%	0.26%		1.45%	2.26%	2.04%	2.39%	1.95%	1.95%	1.97%	2.01%	1.81%	2.41%	2.36%	2.43%	4.25%	4.70%	4.68%	4.64%	4.76%	4.75%
4	<i>Ophioblattacea abnana</i>	6.73%	7.09%	7.20%		1.94%	1.54%	1.76%	1.71%	1.50%	1.70%	1.55%	1.84%	1.78%	1.81%	1.86%	3.69%	3.85%	3.28%	3.27%	3.40%	3.51%
5	<i>Ophioblattacea</i> sp. RSIO56058	15.13%	15.34%	15.59%	12.50%		1.01%	1.41%	1.29%	1.22%	1.39%	1.36%	1.98%	2.23%	2.16%	2.21%	3.90%	4.33%	4.70%	4.68%	4.54%	4.32%
6	<i>Ophioblattacea</i> cf. <i>libinona</i>	13.34%	13.29%	13.89%	11.47%	4.17%		0.73%	1.03%	0.85%	1.04%	0.95%	1.84%	1.92%	1.84%	1.88%	3.86%	4.33%	3.64%	3.66%	3.60%	3.66%
7	<i>Ophioblattacea globata</i>	13.06%	12.20%	11.77%	11.16%	5.21%	2.32%		1.31%	0.96%	1.33%	1.20%	2.04%	2.15%	2.02%	2.07%	4.28%	4.69%	3.63%	3.62%	3.95%	4.04%
8	<i>Ophioblattacea senale_1</i>	12.97%	13.81%	13.24%	10.28%	5.81%	4.15%	4.43%		0.43%	1.01%	1.11%	1.80%	2.48%	2.34%	2.40%	4.25%	4.56%	4.80%	4.81%	4.74%	4.52%
9	<i>Ophioblattacea senale_2</i>	13.15%	13.32%	13.26%	11.26%	5.48%	3.92%	4.00%	0.76%		0.88%	0.80%	1.74%	1.98%	1.82%	1.86%	3.97%	4.29%	3.47%	3.47%	3.47%	3.58%
10	<i>Ophioblattacea plicata_1</i>	13.88%	13.80%	13.57%	11.40%	6.76%	4.39%	5.08%	3.87%	3.20%		0.45%	1.72%	2.44%	2.25%	2.28%	4.12%	4.38%	4.74%	4.77%	4.15%	4.06%
11	<i>Ophioblattacea plicata_2</i>	13.34%	13.51%	14.18%	12.05%	6.74%	5.01%	5.95%	4.67%	3.54%	0.90%		1.79%	2.04%	1.91%	1.94%	4.12%	4.48%	3.68%	3.69%	3.31%	3.48%
12	<i>Ophioblattacea gaudisiquama</i>	13.96%	10.46%	10.79%	11.62%	13.89%	12.14%	10.26%	11.43%	11.27%	11.25%	12.08%		2.50%	2.31%	2.36%	4.22%	4.33%	4.47%	4.44%	4.35%	4.48%
13	<i>Ophioblattacea amezanace</i>	16.84%	15.90%	15.96%	14.17%	16.99%	16.45%	16.04%	18.62%	17.81%	19.72%	18.21%	19.37%		1.70%	1.68%	3.59%	3.78%	3.16%	3.14%	3.59%	3.58%
14	<i>Ophioblattacea brachispina</i> sp. nov. holotype	17.35%	15.96%	17.44%	14.76%	15.80%	15.35%	15.43%	16.97%	15.37%	17.66%	16.40%	18.83%	12.66%		0.25%	3.96%	4.15%	3.38%	3.35%	3.80%	3.98%
15	<i>Ophioblattacea brachispina</i> sp. nov. paratype	17.68%	16.25%	17.80%	15.03%	16.13%	15.42%	15.53%	17.32%	15.45%	17.68%	16.27%	19.17%	12.46%	0.35%		3.91%	4.10%	3.36%	3.33%	3.86%	4.03%
16	<i>Ophioblattinus catalimmoides</i>	35.83%	36.53%	39.34%	35.96%	38.04%	39.02%	34.92%	41.28%	39.91%	41.56%	41.75%	41.45%	35.60%	39.28%	39.24%		2.52%	2.54%	2.56%	3.96%	3.56%
17	<i>Ophioblattinus normani</i>	37.88%	40.61%	44.94%	37.99%	41.88%	43.15%	37.96%	43.18%	42.77%	43.61%	45.13%	43.34%	37.52%	40.43%	40.38%	21.20%		1.37%	1.34%	3.62%	3.51%
18	<i>Ophioblattinus serratus</i> sp. nov. holotype	35.25%	36.45%	44.60%	35.71%	45.98%	41.04%	34.51%	45.59%	39.18%	47.62%	41.61%	45.15%	34.14%	36.18%	36.04%	20.86%	7.31%		0.24%	2.99%	3.13%
19	<i>Ophioblattinus serratus</i> sp. nov. paratype	34.95%	36.15%	44.08%	35.41%	45.50%	41.04%	34.51%	46.09%	39.18%	48.09%	41.61%	44.68%	33.56%	35.58%	35.43%	21.17%	7.06%	0.35%		3.00%	3.15%
20	<i>Ophiomyza brevitarsis</i>	41.60%	40.93%	47.22%	41.42%	45.76%	41.96%	39.47%	47.33%	40.93%	43.09%	38.75%	44.10%	41.77%	45.04%	45.07%	39.60%	38.90%	35.26%	35.54%		2.05%
21	<i>Ophiomyza anisacantha</i>	41.81%	41.07%	46.86%	40.25%	43.58%	40.99%	38.67%	44.39%	40.64%	41.50%	39.95%	44.05%	41.43%	45.62%	46.31%	35.76%	35.91%	35.47%	35.77%	17.85%	

12.99 ± 1.76% SE (4 specimens), and interspecies genetic distance ranged between 7.06–21.20% (Table 2).

The new species, described morphologically below, were confirmed by the molecular analysis as separate from all other sequenced species (Fig. 2) and species identified by morphological characters were confirmed by the COI analysis.

Taxonomic account

Superorder Ophintegrida O'Hara, Hugall, Thuy, Stöhr and Martynov, 2017

Order Ophiacanthida O'Hara, Hugall, Thuy, Stöhr and Martynov, 2017

Suborder Ophiacanthina O'Hara, Hugall, Thuy, Stöhr and Martynov, 2017

Family Ophiacanthidae Ljungman, 1867

Genus *Ophioplinthaca* Verrill, 1899

***Ophioplinthaca brachispina* sp. nov.**

<http://zoobank.org/B225308A-59B8-431C-B9AF-1E4F729878D2>

Figs 3–5

Material examined. Holotype. NORTHWEST PACIFIC • 1 specimen; near Mariana Trench, Southwest of Guam Island, seamount; 11°49.09'N, 140°6.93'E; depth 2713 m; 23 October 2019; Collecting event: stn. SC039; Shenhaiyongshi msv leg; preserved in -80 °C; GenBank: OK043829; IDSSE-EEB-SW0106. **Paratype.** NORTHWEST PACIFIC • 1 specimen; same data as for holotype; GenBank: OK043830; IDSSE-EEB-SW0107.

Diagnosis. Disc sub-circular and deeply incised interradially to nearly 1/4 disc radius (Fig. 3A). Disc scales irregular, variable in size, bearing disc spines in center of disc (Fig. 3C). Radial shields completely separated by large single disc scale (Fig. 3G). Oral shield as wide as long, pentagonal with pointed proximal end, curved lateral margins along adoral shields, truncated distal edge with straight to slightly angular lateral margins (Fig. 3H). Surface of arm plates along entire arm rough with small spines (Fig. 3K–M).

Holotype description. Disc diameter 12 mm, arm base width 3 mm (Fig. 3).

Disc. Disc sub-circular and deeply incised interradially to more than 1/3 disc diameter, creating five wedge-shaped lobes over each arm base in contrast to sunken center and interradii of disc (Fig. 3A, B). Disc scales irregular, variable in size, compact, and overlapping in center of disc (Fig. 3C). Most central disc scales bear disc spines/stumps (Fig. D–F). Disc scales increasingly enlarged from disc center to periphery, interradially and between radial shields (Fig. 3D–F). Disc spines in disc center 0.2 to 0.3 mm high, cylindrical to conical, pointed thorny or bifurcated tip. Disc spines at distal end of wedge-shaped lobes 0.1–0.2 mm high, conical, thorny, with pointed tip (Fig. 3D–F). Radial shields large, naked, roughly triangular, ~ 1/3 disc diameter in length, twice as long as wide, triangular proximal end, and smooth, truncated or slightly convex distal end. Radial shields on three of five lobes proximally separated,

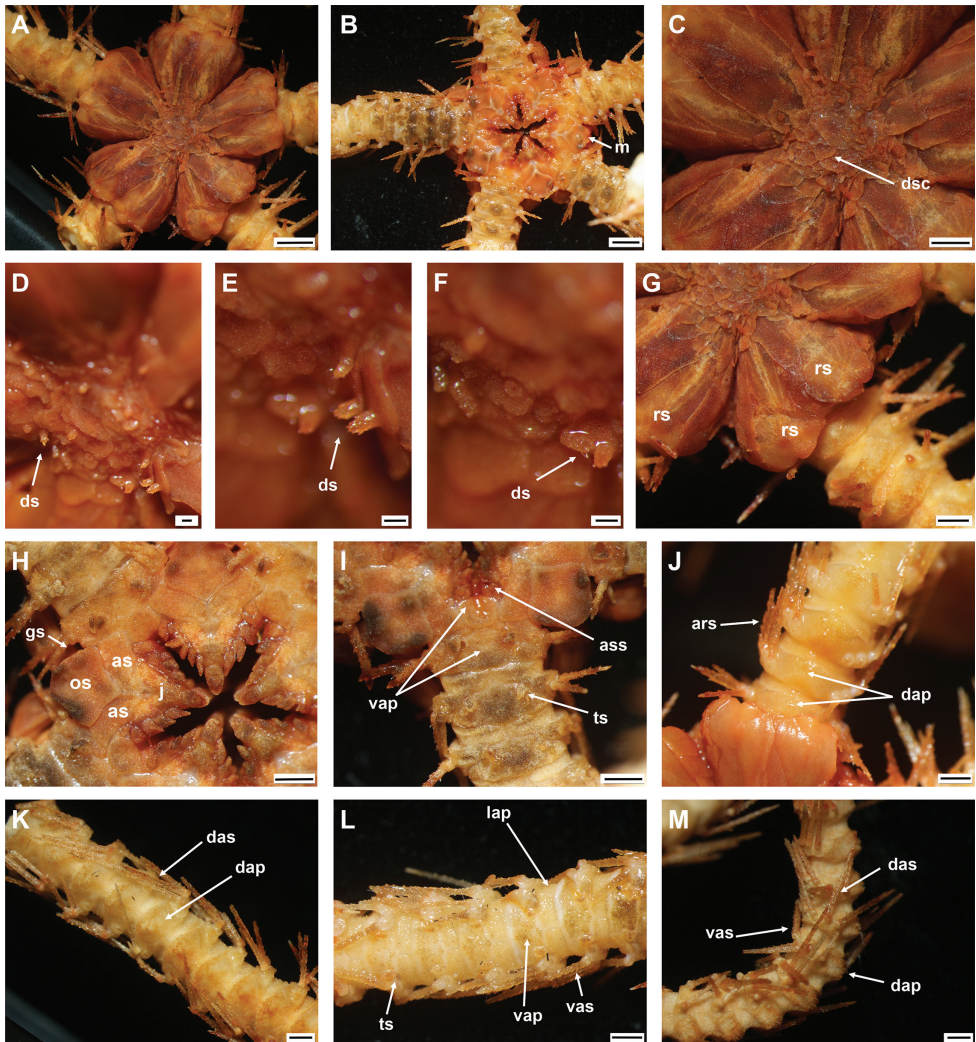


Figure 3. *Ophioplinthaca brachispina* sp. nov., holotype (IDSSE-EEB-SW0106) **A** dorsal disc **B** ventral disc **C** center of the disc **D–F** disc spines **G** radial shield **H** oral frame **I** ventral side of the arm base **J** dorsal side of the arm base **K** dorsal arm **L** ventral arm **M** lateral arm. Abbreviations: **ars** arm spine, **as** adoral shield, **ass** adoral shield spine, **dap** dorsal arm plate, **das** dorsal arm spine, **dp** disc plate, **gs** genital slit, **j** jaw, **lap** lateral arm plate, **m** madreporite, **os** oral shield, **rs** radial shield, **ts** tentacle scale, **vap** ventral arm plate, **vas** ventral arm spine. Scale bars: 2 mm (**A, B**); 1 mm (**C, G–M**); 200 μ m (**D–F**).

but distal ends connected. Radial shields on other two lobes completely separated by large single disc scale (Fig. 3A, G). Ventral disc covered by smaller scales than those on radial shields, and overlapped without bearing spines (Fig. 3B). Genital slits conspicuous and extending from oral shield to periphery of disc (Fig. 3H). Oral shield as wide as long, pentagonal with pointed proximal end, curved lateral margins along adoral shields, truncated distal edge with straight to slightly angular lateral margins (Fig. 3H).

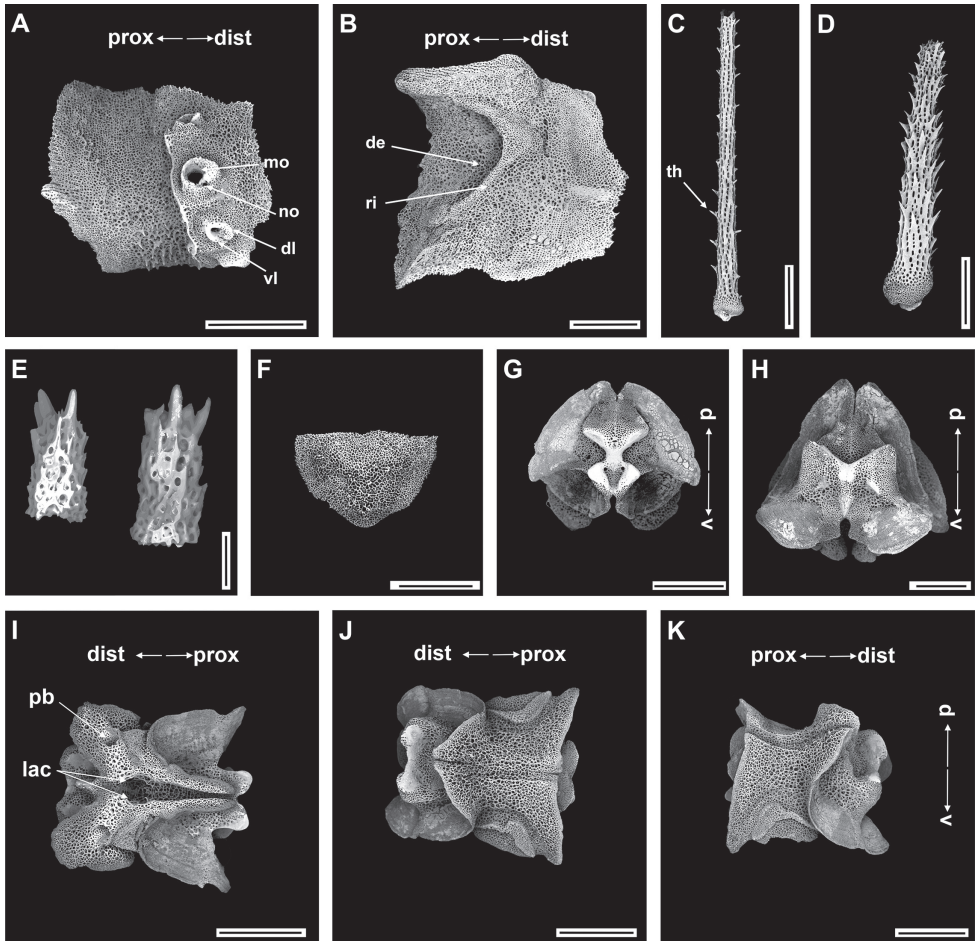


Figure 4. *Ophioplinthaca brachispina* sp. nov., paratype (IDSSE-EEB-SW0107) **A, B** lateral arm plate **C** dorsal arm spine **D** ventral arm spine **E** disc spine **F** dorsal arm plate **G–K** vertebrae **G** proximal view **H** distal view **I** ventral view, **J** dorsal view, **K** lateral view. Abbreviations: **d** dorsal, **de** depression, **dist** distal, **dl** dorsal lobe, **lac** lateral ambulacral canals, **mo** muscle opening, **no** nerve opening, **pb** podial basin, **prox** proximal, **ri** ridge, **th** thorns, **v** ventral, **vl** ventral lobe. Scale bars: 800 μm (**A, C, F–G, I–K**); 500 μm (**B, E, H**); 100 μm (**D**).

Madreporite similar to other oral shields, but with hydropore at lateral edge (Fig. 3B). Adoral shield $2.5 \times$ as long as wide, with straight or slightly curved lateral margin, but near first ventral arm plate straight, and pair of shields proximally connected (Fig. 3H). Adoral shields enclose proximal edges of oral shield, and slightly separate oral shield from arm by connecting to lateral arm plate of first arm segment (Fig. 3H, I). Jaw triangular, large, and longer than wide, bearing one slightly blunt, wide, and large ventralmost tooth and three or four spiniform lateral oral papillae (Fig. 3H). Proximalmost one or two lateral oral papillae spine-like pointed, rugose, and distalmost lateral oral papillae with shorter and rounded base with more or less pointed tip (Fig. 3H).

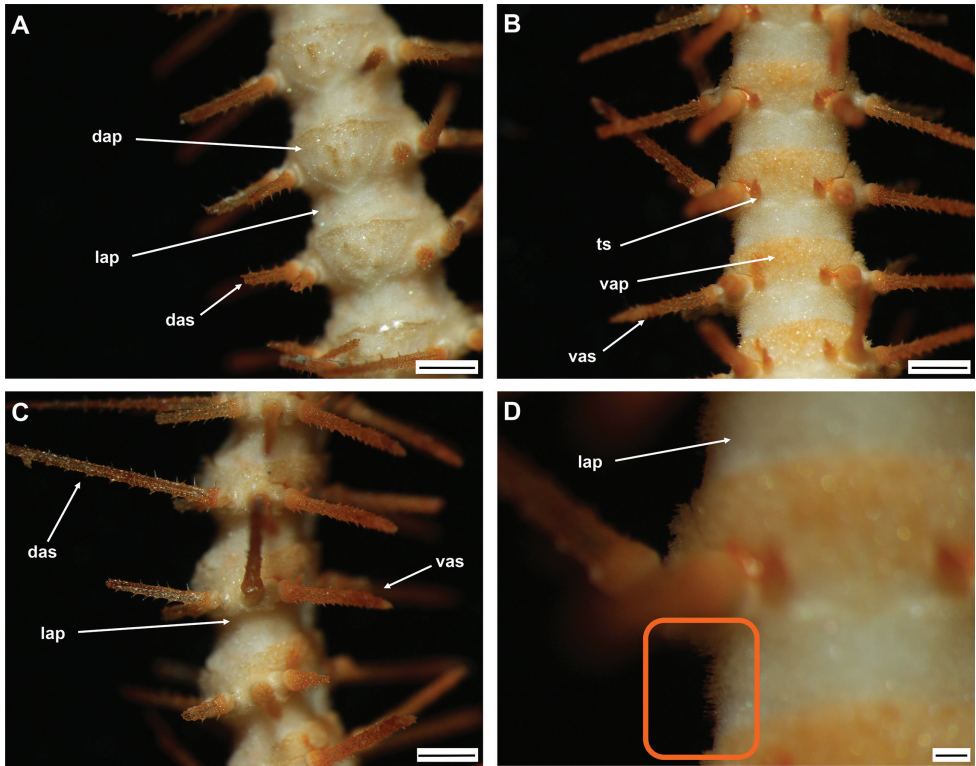


Figure 5. *Ophioplinthaca brachispina* sp. nov., paratype (IDSSE-EEB-SW0107) **A** dorsal arm **B** ventral arm **C** lateral arm **D** lateral arm plate (small thorns on the lateral arm plate surface shown in the orange rectangle). Abbreviations: **dap** dorsal arm plate, **das** dorsal arm spine, **lap** lateral arm plate, **ts** tentacle scale, **vap** ventral arm plate, **vas** ventral arm spine. Scale bars: 1 mm (**A–C**); 200 μ m (**D**).

One adoral shield spine, situated at lateral margin of adoral shield in mouth angle, slightly similar to distalmost lateral oral papilla, but with blunt tip (Fig. 3I). Cluster of small granules visible between distal end of jaw and proximal end of first ventral arm plate (Fig. 3I). Usually, cluster of granules covered by adoral shield spine (Fig. 3H).

Arms. Five moniliform arms with rough plates. Dorsal arm plates longer than wide, slightly separated, straight to slightly convex distal end, triangular proximal end, with curved lateral margins on first few proximal arm segments, but as long as wide, fan-shaped, and widely separated on middle to distal half of arm (Fig. 3J, K). Dorsal arm plate with dense rough surface and short spines (Fig. 3K, M). First ventral arm plate rectangular to slightly trapezoid, as wide as long, straight proximal end, and distal end without rough surface (Fig. 3I). Second ventral arm plate trapezoid to slightly pentagonal, as wide as long, triangular proximal end, straight distal end, concave and diverging lateral edges, and contiguous with first ventral arm plate (Fig. 3I). The following ventral arm plates two or three times as wide as long, with obtuse proximal end, slightly wavy proximolateral margins, curved lateral angles, straight distal end, and widely separated (Fig. 3L). All ventral arm plates except first one with dense rough

surface (Fig. 3I, L). Lateral arm plates meeting above and below, with dense rough surface and short spines (Fig. 3K–M). Up to five arm spines (Fig. 3M). Three or two dorsal arm spines, three arm segments in length, thorny, lateral margins with row of tall sharp thorns, apex truncated or bluntly rounded (Fig. 3K–M). Two ventral arm spines, one to two arm segments in length, pointed, thorny, rugose. Proximal arm segments bear five arm spines, distalwards decreasing to four beyond middle section of the arm (Fig. 3K–M). First tentacle pore covered by two oval, rough tentacle scales (Fig. 3I). The following tentacle pore covered by scale half as long as ventral arm plate, blunt to pointed tip with thorny surface (Fig. 3L). Tentacle scales on middle to distal half of arm decreasing in size, small, more pointed, leaf-like, with thorns.

Color. In live specimen, orange-brown disc, and arm spines, but arms pale brown (Fig. 3).

Ossicle morphology of paratype. Arm spine articulations well developed and placed at slight angle to distal edge of lateral arm plate (Fig. 4A). Volute-shaped perforated lobe forms dorsal and distal part of articulation, but reduced in dorsalmost one (Fig. 4A). Arm spine articulating structures with large muscle opening and small nerve opening in second articulation, decreasing significantly in size ventralwards (Fig. 3A). Ventral half of lateral arm plate surface covered by conspicuous thorns, inner side with depression, a continuous ridge, and a prominent knob close to ventral edge forming vertebral articulations, shaped like a broad, nose-shaped beak (Fig. 4A, B). Dorsal arm spine laterally compressed, thorny, and several longitudinal rows of perforations with widely spaced tall thorns (Fig. 4C). Entire ventral arm spine surface covered with slightly longer thorns, with blunt apex (Fig. 4D). Disc spines 0.2–0.3 mm high, cylindrical, pointed thorny or bifurcated tip (Fig. 4E). Dorsal arm plate triangular, as long as wide, with rugose surface (Fig. 4F). Vertebrae with streptospondylous articulating structures, short, broad podial basin at proximal end and narrow small distal end (Fig. 4G–K). Dorsal end of vertebrae distally triangular and proximally flattened with longitudinal groove along midline (Fig. 4J). Ventral side of vertebrae with broad ambulacral groove (Fig. 4I–K).

Paratype variations. One specimen from same location as holotype, but badly damaged due to rough handling. Therefore, only small disc part with arms present. Possibly smaller than holotype according to size of arms (arm base width 1.5–2 mm). Arm characters similar to holotype, but spines slightly thinner, and denser compared to holotype (Fig. 5A–D).

Distribution. 2713 m depth, Northwest Pacific, near Mariana trench, Southwest of Guam Island.

Etymology. Species name derived from a combination of two Latin words, *brachium* (arm), *spina* (spine) referring to the unique rough arm surface with spines.

Remarks. Deep interradiar incisions into the disc, which are lined distally by enlarged disc scales are the main delimiting character of the genus *Ophioplinthaca* from other genera within the family Ophiacanthidae. *Ophioplinthaca brachispina* sp. nov. showed similar morphological characters to many other *Ophioplinthaca* species. However, *O. brachispina* sp. nov. can easily be distinguished from congeners by the rough

thorny surface on the arm plates and additionally by the number of arm spines, disc spines, and tentacle scale (Table 3). *Ophioplinthaca brachispina* sp. nov. is the only *Ophioplinthaca* species with a rough surface with thorns on the whole arm.

Some species share morphological characters with the new species. *Ophioplinthaca globata* Koehler, 1922 is similar to *O. brachispina* sp. nov. by having similar disc spine shape, arm spine shape, radial shields separated proximally and connected distally, number of lateral oral papillae, and separated ventral and dorsal arm plates, but differs by number of arm spines (up to six), the disc spines being scattered across the disc, radial shields separated by disc scales, characters of the oral shield, and a smooth surface on the arm plates along the entire arm. *Ophioplinthaca hastata* Koehler, 1922 is similar to *O. brachispina* sp. nov. by having a slightly similar shape of the disc spines, separated dorsal and ventral arm plates, and similar tentacle scales on the distal end of the arm, but differs by number of arm spines (up to seven) and shape of dorsal arm spines, size of radial shields, characters of oral parts, and smooth arm surface. *Ophioplinthaca athena* A.H. Clark, 1949 is similar to *O. brachispina* sp. nov. by having similar disc spines with thorny tip, similar number of arm spines, separated radial shields, number of lateral oral papillae, but differs by large radial shields, thorny and leaf-like tentacle scales, separated dorsal and ventral arm plates. *Ophioplinthaca amezianeeae* O'Hara & Stöhr, 2006 is similar to *O. brachispina* sp. nov. by having similar thorny tentacle scales, separated radial shields, separated dorsal and ventral arm plates, number of lateral oral papillae, but differs by number of arm spines, tall and thorny disc spines, and spiniform lateral oral papillae. *Ophioplinthaca bythiaspis* (H. L. Clark, 1911) is similar to *O. brachispina* sp. nov. by having separated radial shields and number of lateral oral papillae, but differs by oval tentacle scales, conical disc spines, number of arm spines and contiguous dorsal arm plates. *Ophioplinthaca grenadensis* John & A. M. Clark, 1954 is similar to *O. brachispina* sp. nov. by having similar number of arm spines, separated radial shields, number of lateral oral papillae, and separated arm plates but differs by leaf-like thornless tentacle scales, long and thick disc spines. *Ophioplinthaca plicata* (Lyman, 1878) is similar to *O. brachispina* sp. nov. by having similar disc and arm spines, and number of lateral oral papillae, but differs by continues dorsal arm plates, pointed tentacle scale with rounded base, and contiguous radial shields. *Ophioplinthaca rudis* (Koehler, 1897) is similar to *O. brachispina* sp. nov. by having similar thorny leaf-like tentacle scales, similar number of arm spines, separated radial shields, separated dorsal and ventral arm plates, but differs by number of lateral oral papillae, tall and thorny disc spines, and spiniform lateral oral papillae.

One of the most distinguishing characters to delimit the new species from almost all species in the genus *Ophioplinthaca* is the presence of spines with rough surface on lateral, ventral, and dorsal arm plates. The paratype (relatively smaller than the holotype) has thinner and denser spines on the arm. Although, some *Ophioplinthaca* species have a rough surface on dorsal arm plates or the distal margin covered with minute spines (*Ophioplinthaca plicata* and *Ophioplinthaca incisa*; (O'Hara 2010), this is the first record of a species with spines on the entire arm in the genus *Ophioplinthaca*.

Table 3. Tabular key to all species of the genus *Ophioplinthaca*. Abbreviations: ASE arm segment, ASS Adoral shield spine, DAP dorsal arm plate, DAS dorsal arm spines, L length, LOP lateral oral papillae, VAP ventral arm plate, VAS ventral arm spines, VMT ventralmost tooth, W width.

Species	No. of arm spines	Radial shields	Oral frame	Tentacle scale	Dorsal arm plate (DAP), and ventral arm plate (VAP)	Arm spine shape and length	Disc spines	References
<i>Ophioplinthaca abscondis</i> Cherbonnier & Sibuet, 1972	up to 7	separated proximally but connected at distal ends	4–5 LOP, spiniform, 1 VMT	1 st pore 2, then 1, elongated, blunt	VAP-separated, DAP 1–3 have few spines and contiguous then separated	thorny surface	long, conical	Cherbonnier and Sibuet (1972)
<i>Ophioplinthaca amezianae</i> O'Hara & Stöhr, 2006	up to 10	separated, L = 2W	up to 4–5 LOP; spiniform, 1 VMT	1 st pore 2–3, 2 nd pore 1–2, then 1, spiniform with rounded base, tapering sharply or tip covered in irregular thorns	separated	covered with conspicuous thorns	long, rounded base, with spinelets on lateral surface	O'Hara and Stöhr (2006), this study
<i>Ophioplinthaca arborea</i> A.H. Clark, 1949	up to 5	separated proximally, connected at distal ends, L = 4W	4 LOP; pointed, flattened; larger, equal in size, 1 VMT	1 st pore 2, then 1, oval, pointed; beyond 3 rd pore slender spiniform	VAP on 1 st ASE contiguous with next, then separated, DAP contiguous (terminal portion slightly separated)	1 st DAS smooth, 2 × ASE length; 2 nd DAS, 4 × ASE length; shorter thorny VAS	elongated with thorny tip, at periphery with smooth tip	A. H. Clark (1949), this study
<i>Ophioplinthaca brachipina</i> sp. nov.	up to 5	separated by large single disc scale or connect at distal ends	4 LOP; pointed, distal one with wider flat edge, 1 VMT, ASS covered by cluster of granules	1 st pore 2, half as long as VAP; terminally spiniferous, oval on base of arm, then slightly pointed along arm	DAP and VAP separated, thorny surface	DAS with distal lateral thorns; VAS ≈ 1–2 × ASE length, pointed, thorny, rugose	bifid or thorny pointed tip, cylindrical	this study
<i>Ophioplinthaca bythiopsis</i> (H. L. Clark, 1911)	up to 6	separated, L = 4W	4–5 LOP; equal in height, distally slightly wider, 1 VMT	oval to bottle-shaped, as long as VAP	VAP separated beyond 3 ASE	DAS smooth, VAS with thorny surface	conical or more rounded with thorns at tip	H. L. Clark (1911, 1915), O'Hara and Stöhr (2006)
<i>Ophioplinthaca carolinus</i> (Lyman, 1878)	up to 6	separated	4–5 LOP; first 3–4 conical, blunt tip, distalwards flat, spearhead-shaped, small, pointed, 1 VMT; curved adoral shield	strongly thorny; after 1 st pore, with 1 or 2 lateral thorns	VAP separated, DAP on 1–3 × ASE contiguous, then separated	stout, cylindrical, glassy, blunt, very thorny	short, stout stump with thorny tip	Lyman (1878)
<i>Ophioplinthaca cheylis</i> (C. W. Thomson, 1877)	up to 6	separated, deep sunken	5 LOP; first 3–4 conical, blunt tip, 1 VMT	large and flat	VAP and DAP separated	cylindrical, glassy, blunt, very thorny	cylindrical, thorny or smooth, thorny tip, spines dense in disc center.	C. W. Thomson (1877)
<i>Ophioplinthaca citata</i> Koehler, 1904	up to 9	separated L = 3–4W	3–4 LOP blunt, distal one has wider flat edge, 1 VMT	oval to elliptical	DAP contiguous, except first few ASE, VAP contiguous	DAS ≈ 4 × ASE length, VAS short, thorny, hollow	cylindrical, terminal crown of thorns	Koehler (1904), O'Hara and Stöhr (2006)
<i>Ophioplinthaca clohilde</i> A.H. Clark, 1949	up to 7 at arm base then 5	contiguous, ovoid; about half as long as broad	4 LOP; pointed, flattened, large, 1 VMT of equal size	1 st pore 2, then 1, leaf-like to narrow, sharply pointed with numerous spinelets at tip	VAP separated after 2 ASE, DAP separated	DAS ≈ 4 × ASE length, DAS and VAS with thorny surface, DAS longest	in disc center cylindrical base ending in 2–3 sub-crowns, at periphery short, stout with irregular crown of a dozen or more thorns	A. H. Clark (1949)

Species	No. of arm spines	Radial shields	Oral frame	Tentacle scale	Dorsal arm plate (DAP), and ventral arm plate (VAP)	Arm spine shape and length	Disc spines	References
<i>Ophioplathaca codonomorpha</i> (H. L. Clark, 1911)	up to 8 4 then up to 5 or 7	widely separated, small, convex proximally, as wide as long	3 LOP, 1 VMT	1 st pore 2, oval, conspicuously large, then oval with pointed tip	VAP at 1 st to 2 nd ASE contiguous then separated, DAP barely contiguous	1–3 DAS smooth or thorny; VAS also smooth	minute rough granules	H. L. Clark (1911)
<i>Ophioplathaca crassa</i> H. L. Clark, 1939	basally 4 then up to 5 or 7	distally connected, small, as wide as long, convex proximally	3 LOP; narrow, elongated, pointed, distalwards short and wide, 1 large VMT	1 st pore 2–3, blunt, 1 mm long and wide, very thick, somewhat triangular, then less stout, slender pointed	VAP, DAP in first 1–2 ASE contiguous, then separated	short, stout, but fragile, thorny spines, DAS = 2 × ASE length	low cylindrical tube	H. L. Clark (1939)
<i>Ophioplathaca defensor</i> Koehler, 1930	up to 7 at arm base	separated proximally, connected distally	4 LOP, 1 VMT	1 st pore 1, long, and leaf-like then narrower with pointed tip	DAP and VAP contiguous	thorny surface, conspicuous thorns on DAS; DAS = 3 × ASE, VAS = 1 × ASE length	cylindrical with thorn at tip	Koehler (1930), Na et al. (2021), this study
<i>Ophioplathaca dipsacos</i> (Lyman, 1878)	up to 6	separated proximally, connected distally	4–5 LOP; pointed, flattened, ill-defined distalwards, 1 VMT	large, pointed with 1 or 2 microscopic thorns	VAP and DAP separated	long, slender; DAS 5–7 × ASE length, with conspicuous thorns, VAS 1½–2 × ASE length with thorny surface	short, stout, with thorny tip, at periphery smooth	Lyman (1878)
<i>Ophioplathaca globata</i> Koehler, 1922	up to 6	separated proximally, connected distally	3–4 LOP, blunt, distal one has wider flat edge, 1 VMT, ASS covered by small granules	1 st pore 2–3, as long as VAP terminally spiniferous in larger specimen	DAP and VAP separated	thorny surface	cylindrical, bifid or tip mostly with 3 thorns	Koehler (1922, 1930), O'Hara and Stöhr (2006)
<i>Ophioplathaca gandsiqumua</i> Chen, Na, & Zhang, 2021a	up to 7	contiguous, L = 1.5W	up to 3–4 LOP, spiniform, 1 or 2 VMT	1 st pore 1–2, only 1 in following ASE, long, thorny with thick base, tapering into blunt point	DAP contiguous, VAP separated	DAS thin with distal lateral thorns, up to 3 × ASE length; VAS short, blunt, and finely rugose	stout, tall, bearing numerous distinct thorns laterally or at tip, some bifurcated into two prongs with thorny tips	Chen et al. (2021a)
<i>Ophioplathaca grenadensis</i> John and A. M. Clark, 1954	up to 5	separated oval proximally	up to 5 LOP; spiniform, 1 VMT	leaf-like, then slightly elongated with pointed tip along arm	DAP in first 1–2 ASE contiguous, then separated, VAP separated	flattened, covered by glassy spines	long, thick spinelets with rough thorny lateral surface in disc center, at periphery shorter	John and A. M. Clark (1954)
<i>Ophioplathaca hastata</i> Koehler, 1922	up to 7	contiguous, L = 1.5W	4–5 LOP; spiniform to club-shaped, distal ones largest, sometimes small granules present on distal edge of jaw, 1 VMT, 1 or 2 ASS	1 st pore 2, then 1, clavate, terminally spiniferous, longer than VAP	separated	smooth, DAS = 3 × ASE length	numerous thorns at cylindrical tip	Koehler (1922), O'Hara and Stöhr (2006)
<i>Ophioplathaca incisa</i> (Lyman, 1883)	up to 5	small, separated proximally, connected distally	4–5 LOP; spiniform., distal ones wide, flat, 1 VMT, 1 or 2 ASS	1 st pore 3, then 1	VAP separated	smooth, DAS = 3 × ASE, VAS = 1 × ASE length	cylindrical with thorny tip or thorny surface laterally, at disc periphery smooth	Lyman (1883)

Species	No. of arm spines	Radial shields	Oral frame	Tentacle scale	Dorsal arm plate (DAP), and ventral arm plate (VAP)	Arm spine shape and length	Disc spines	References
<i>Ophioplinthaca laudator</i> Koehler, 1930	up to 7	small, separated proximally, connected distally	4 LOP, sometimes irregularly arranged, elongated, pointed but distalmost one flat and wide, 1 VMT	—	VAP separated beyond 2 nd ASE, DAP separated	DAS thorny, VAS smooth, DAS = 2 × ASE, VAS = 1½–2 × ASE length	cylindrical with 2–3 thorns at tip or lateral thorns, at disc periphery smooth, conical	Koehler (1930)
<i>Ophioplinthaca lithosora</i> (H. L. Clark, 1911)	up to 6 or 7	long, narrow, separated	10–15 LOP including small granules at distal edge of jaw	1 st pore 3, 2 nd pore 2, then one, large, pointed tip	VAP separated, tetragonal	first 1–2 DAS, smooth, 3 × ASE length, with thorny tip, 3 thorny VAS	cylindrical, bifid or mostly with 3 thorns at tip or with lateral thorns	H. L. Clark (1911), this study
<i>Ophioplinthaca manillae</i> Guille, 1981	up to 6	as wide as long, contiguous	3 LOP; 1 VMT, rough edges, large, pointed, small granules at distal edge of jaw	oval, large, rough edges	DAP on first 1–2 ASE contiguous, then separated, VAP separated	DAS = 3 × ASE, VAS = 1 × ASE length, thorny	bifid or mostly with 3 divided thorns at tip, central spines longer than peripheral ones	Guille (1981)
<i>Ophioplinthaca minanda</i> Koehler, 1904	up to 5 or 6	separated proximally, connected distally	3 LOP; 1 large VMT	triangular	DAP and VAP contiguous	both DAS and VAS small, thorny, rugose and same length	cylindrical with thorny circular tip	Koehler (1904)
<i>Ophioplinthaca monitor</i> Koehler, 1930	up to 7 or 8	separated	4 LOP, 1 VMT, distalmost one smaller	1 st pore 2, then 1, oval to rounded proximally and pointed distally	DAP on first 2 ASE contiguous, then separated, fan-shaped	DAS with conspicuously sparse thorny surface, VAS thorny	granules with thorny tip	Koehler (1930), O'Hara and Stöhr (2006)
<i>Ophioplinthaca papillosa</i> H. L. Clark, 1939	up to 7	separated, narrow	3–4 LOP; narrow, subequal, long, pointed, 1 VMT	flat, moderately, large, pointed	separated	rough surface, DAS ≈ 3 × ASE, VAS ≈ 1 × ASE length	in disc center with long tip dividing into 2–3 thorns, at periphery with spinous tip	H. L. Clark (1939)
<i>Ophioplinthaca plicata</i> (Lyman, 1878)	up to 8	contiguous, L = 2–2.5W	3–5 LOP; 1–3 VMT, spiniform	1 st pore 2–3, curved inward, pointed round tip	DAP contiguous, VAP separated	thorny surface	conical, cylindrical, finely rugose or rarely with few longer thorns	Lyman (1878, 1882), Koehler (1904), O'Hara and Stöhr (2006)
<i>Ophioplinthaca pulchra</i> Koehler, 1904	up to 7	separated proximally, connected distally	4 LOP; 1 VMT	leaf-like	first two VAP contiguous, then separated, DAP contiguous	thorny, rugose surface, uppermost DAS longest	cylindrical with thorny tip in center, at periphery smaller and conical	Koehler (1904, 1922), O'Hara and Stöhr (2006)
<i>Ophioplinthaca rufis</i> (Koehler, 1897)	up to 5	completely separated or distally connected	5–6 LOP; spiniform, 1 VMT	leaf-like	DAP contiguous or separated, VAP widely separated	finely thorny	long spines with smooth surface	Koehler (1897), O'Hara and Stöhr (2006)
<i>Ophioplinthaca sarsii</i> (Lyman, 1878)	up to 8	separated	3 LOP small, pointed, 1 VMT	flat, tapering, jagged	DAP, VAP separated	stout, cylindrical, glassy, blunt, very thorny	smooth cylindrical	Lyman (1878)
<i>Ophioplinthaca senale</i> (A.H. Clark, 1949)	up to 7	separated proximally, connected in distally, L ≈ 2½–3W	5 LOP; pointed, flared, ill-defined, 1 VMT	1 st pore 3 or rarely 5, 2 nd pore 2–3, 3 rd pore 2, then one, large, pointed tip	VAP in first 1–2 ASE contiguous, then separated, DAP separated	long, slender, DAS with conspicuous thorns, VAS thorny surface	short, stout, with thorny tip, or 3 thorns, at periphery smooth spines without thorns	A. H. Clark (1949), Chen et al. (2021a), this study

Species	No. of arm spines	Radial shields	Oral frame	Tentacle scale	Dorsal arm plate (DAP), and ventral arm plate (VAP)	Arm spine shape and length	Disc spines	References
<i>Ophioplathaca senadia</i> Mortensen, 1933	up to 4	separated proximally, connected distally	3 LOP, 1 VMT	small, leaf-like	separated, small	small, thick base	irregular scales with conical tubercles	Mortensen (1933)
<i>Ophioplathaca spinissima</i> H. L. Clark, 1900	up to 9	separated proximally, connected in distally, longer than wide	up to 5–7 LOP, spiniform, 1 VMT	1 st pore one or divided into two, then more pointed distalwards along arm	DAP widely separated	thorny surface	spine with thorny tip, or 3 thorns, at periphery smooth spines without thorns, tip relatively flat with thorns	H. L. Clark (1900)
<i>Ophioplathaca</i> sp.	up to 6	contiguous, distally convex, proximally triangular L = 2W	4–5 LOP, pointed, elongated, slightly flattened distal end, 1 VMT large, slightly longer than LOP	1 st pore 1–2, then 1, leaf-like, but along arm narrower, thorny, pointed; as long as VAP	both VAP and DAP widely separated	DAS has conspicuous lateral thorns; VAS with thorny surface	disc center: conical or short cylindrical spines, when cylindrical with two sub-cylindrical with two sub-thorns; at periphery smooth, conical or short, cylindrical, finely rugose to smooth	this study
<i>Ophioplathaca tyloia</i> H. L. Clark, 1939	up to 6	separated proximally, connected distally	4 LOP; narrow, equal, long, pointed, 1 VMT	very thick, heavy, smooth but increasingly flatter along arm, smaller, very thorny	first and second DAP contiguous, then separated, VAP separated	thorny spine; DAS with conspicuous thorns, DAS ≈ 3 × ASE, VAS = 1 × ASE length	smooth, rounded spine	H. L. Clark (1939)
<i>Ophioplathaca webri</i> (Koehler, 1904)	up to 7	separated proximally, connected distally	4 LOP; narrow, equal, long, pointed, 1 large VMT	1 st pore 2–3, then 1, elongated	DAP and VAP contiguous	—	—	Koehler (1904)

***Ophioplinthaca* sp.**

Figs 6, 7

Material examined. NORTHWEST PACIFIC • 1 specimen; near Mariana Trench, Southwest of Guam Island, seamount; 12°36.44'N, 140°51.73'E; depth 2779 m; 23 September 2019; Collecting event: stn. SC038; Shenhaiyongshi msv leg; preserved in -80 °C; GenBank: OK043831; IDSSE-EEB-SW0108.

Description. Disc diameter 9 mm, arm base width 2 mm (Fig. 6).

Disc. Disc sub-pentagonal, incised interradially to nearly 1/5 disc radius, creating five wedge-shaped lobes over each arm base in contrast to sunken center and interradii of disc (Fig. 6A, B). Disc scales polygonal to rounded, somewhat similar in size, overlapping at center (Fig. 6C). Most disc scales bear one or two spines (Fig. 6C). Disc spines at center 0.25–0.3 mm high, smooth, or finely rugose, cylindrical single base with two or three sub-thorns, which bend into opposite directions (Fig. 6D, E). Some disc spines at center 0.2–0.3 mm high, smooth, or finely rugose, cylindrical with large, blunt tip (Fig. 6D, E). Disc spines around radial shields and periphery of disc 0.2 mm high, smooth, or finely rugose cylindrical, with blunt rounded tip (Fig. 6E–G). Disc scales interradially slightly increasing in size distalwards, and between radial shields, with one to four spines (Fig. 6G, H). Radial shields naked, $\sim 1/4$ disc diameter in length, 1.5–2 \times as long as wide, with acute proximal end, and wide, slightly convex distal end (Fig. 6G). Radial shields connected, but at proximal end separated by disc scales, and surrounded by disc spines (Fig. 6G). Ventral disc covered by small disc scales similar to interradii dorsal scales, bearing spines similar to periphery of disc (Fig. 6H–J). Genital slits conspicuous and extending from oral shield to periphery of disc (Fig. 6H–J). Madreporite arrowhead-shaped, as wide as long, pentagonal with pointed proximal end, lobed distal edge with thickened lateral margins (Fig. 6B). Oral shields twice as wide as long, diamond-shaped with obtuse proximal end, concave lateral margins along the adoral shields, distal edge with central lobe (Fig. 6I). Adoral shield 3 \times as long as wide, slightly curved, proximal edge concave, distal edge convex, but near first ventral arm plate straight, and pair of shields proximally connected (Fig. 6I). Adoral shields enclose proximal edges of oral shield, and partly separate oral shield from arm by connecting to lateral arm plate of first arm segment (Fig. 6I, J). Jaw large, triangular, longer than wide (Fig. 6I). One slightly pointed, and large ventralmost tooth, longer and thicker than the four to five long, spiniform lateral oral papillae (Fig. 6I). One round, scale-like small adoral shield spine located at lateral margin of adoral shield at edge of second tentacle pore, in some jaw angles (Fig. 6I).

Arms. Five slightly moniliform arms, with smooth plates. Dorsal arm plates fan-shaped, as long as wide, widely separated, with convex distal edge, triangular proximal edge, straight lateral margins. Proximal edge of dorsal arm plate changes from obtuse to sharp triangular along arm (Fig. 6K). First ventral arm plate square to slightly trapezoid, as wide as long, with straight proximal and distal ends. Second and third ventral arm plate trapezoid, twice as wide as long, with straight proximal edge, slightly wavy distal edges, concave and diverging lateral edges (Fig. 6J). Second ventral arm

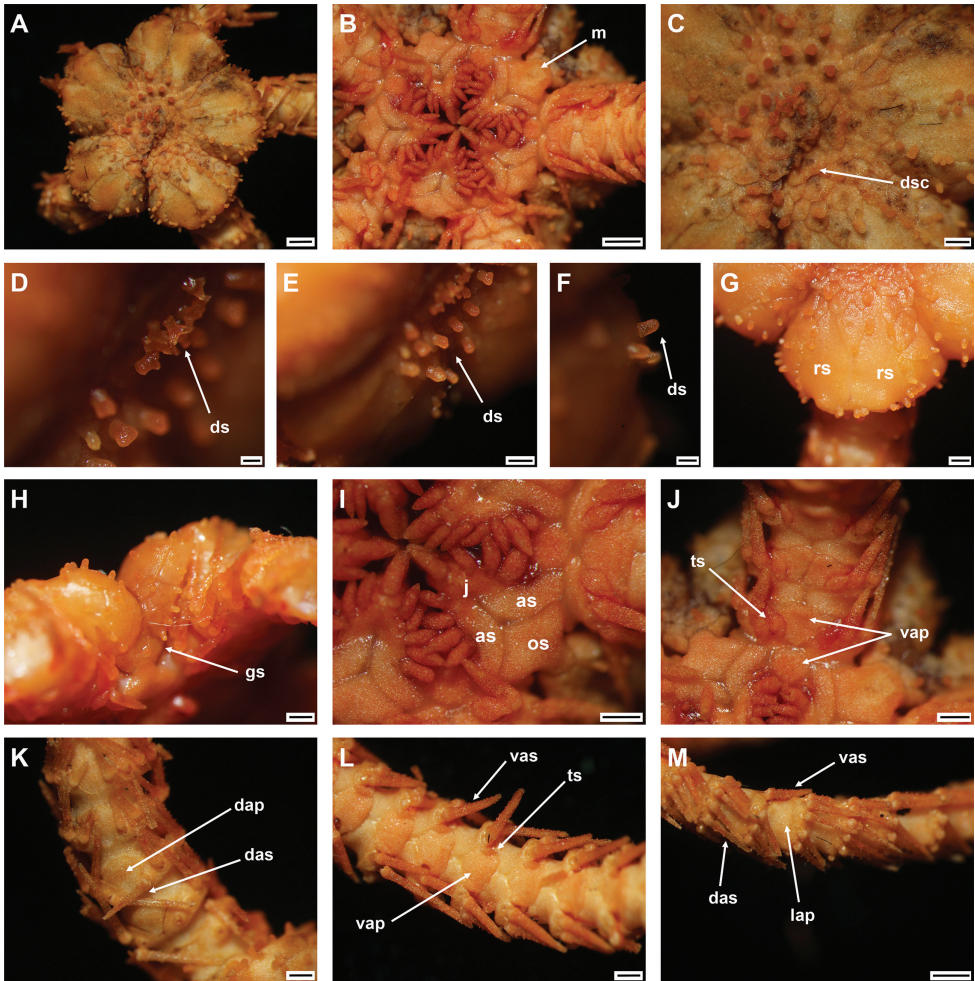


Figure 6. *Ophioplinthaca* sp. (IDSSE-EEB-SW0108) **A** dorsal disc **B** ventral disc **C** center of the disc **D–F** disc spines **G** radial shield **H** lateral disc **I** oral frame **J** ventral side of the arm base **K** dorsal arm **L** ventral arm **M** lateral arm. Abbreviations: **as** adoral shield, **dap** dorsal arm plate, **das** dorsal arm spine, **dp** disc plate, **gs** genital slit, **j** jaw, **lap** lateral arm plate, **m** madreporite, **os** oral shield, **rs** radial shield, **ts** tentacle scale, **vap** ventral arm plate, **vas** ventral arm spine. Scale bars: 1 mm (**A, B, M**); 500 μ m (**C, E, G–L**); 200 μ m (**D, F**).

plate contiguous with first ventral arm plate; following ventral arm plates as wide as long, pentagonal, with blunt to pointed proximal end, straight proximolateral margins, slightly curved lateral angles, straight to slightly curved inwards at distal end, and widely separated (Fig. 6J, L). Lateral arm plates meeting above and below (Fig. 6K–M). Up to six arm spines: three dorsal arm spines, two and a half arm segments in length, thorny or rarely smooth, lateral margins with scattered sharp thorns, apex pointed (Fig. 6M); three ventral arm spines, one to one and a half arm segments in length, pointed, and thorny or rough surface (Fig. 6K–M). First tentacle pore covered with one or two leaf-like, pointed tentacle scales (Fig. 6J). Following tenta-

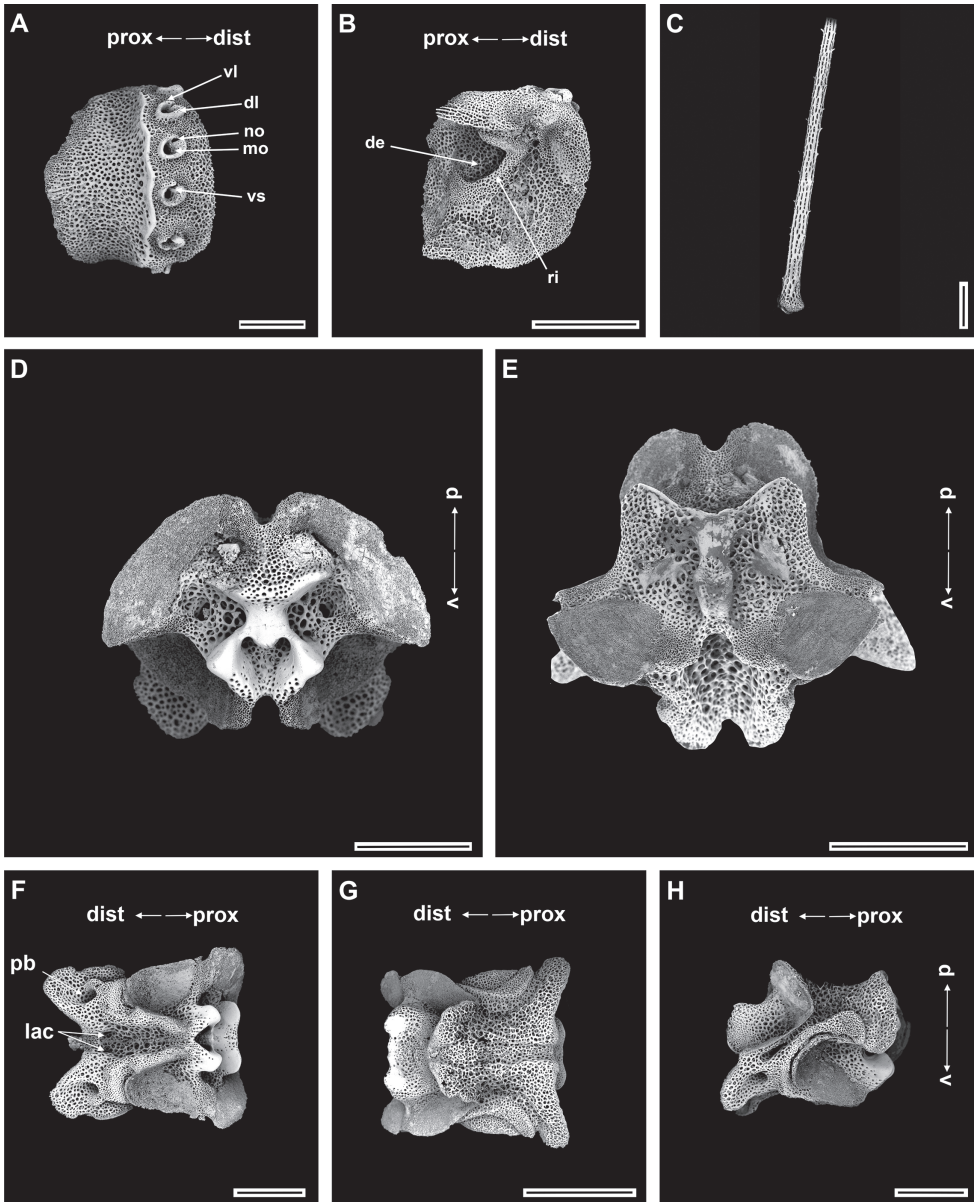


Figure 7. *Ophioplinthaca* sp. (IDSSE-EEB-SW0108) **A, B** lateral arm plate **C** dorsal arm spine **D–H** vertebrae **D** proximal view **E** distal view **F** ventral view **G** dorsal view **H** lateral view. Abbreviations: **d** dorsal, **de** depression, **dist** distal, **dl** dorsal lobe, **lac** lateral ambulacral canals, **mo** muscle opening, **no** nerve opening, **pb** podial basin, **prox** proximal, **ri** ridge, **th** thorns, **v** ventral, **vl** ventral lobe, **vs** volute-shape. Scale bars: 800 μ m (**B**); 500 μ m (**A, C–H**).

cle pores covered with one tentacle scale, as long as ventral arm plate, leaf-like, with thorny pointed tip (Fig. 6L).

Color. In live specimen, pale orange-brown (Fig. 6).

Ossicle morphology. Arm spine articulations well developed, six in number, placed at slight angle to distal edge of lateral arm plate. A volute-shaped perforated lobe forms dorsal and distal parts of articulation (Fig. 7A). Arm spine articulation with large muscle opening and small nerve opening (Fig. 7A). Inner half of lateral arm plate with continuous ridge and prominent knob close to ventral edge forming vertebral articulation, shaped like a deep, nose-shaped beak (Fig. 7B). Dorsal arm spine thorny, with several longitudinal rows of perforations with widely spaced small thorns (Fig. 7C). Vertebrae with streptospondylous articulation, short, broad podial basin, and narrow small distal end (Fig. 7D–H). Dorsal end of vertebrae distally triangular and proximally flattened with longitudinal groove along midline (Fig. 7G). Ventral end of vertebrae with broad ambulacral groove, with lateral ambulacral canals (Fig. 7F, H).

Distribution. 2779 m depth, Northwest Pacific, near Mariana trench, Southwest of Guam Island.

Remarks. *Ophioplinthaca* sp. shares morphological characters with many other *Ophioplinthaca* species, but can easily be delimited by the number of arm spines, disc spine shape, radial shields, and tentacle scale characters (Table 3). One of the distinguishing characters of this species is its smooth sub-thorny disc spines. According to the literature, only three *Ophioplinthaca* species have disc spines with sub-thorns on a single base (*Ophioplinthaca clothilde* A.H. Clark, 1949, *Ophioplinthaca grandisquama* Chen, Na & Zhang, 2021a, and *Ophioplinthaca manillae* Guille, 1981), but the disc spines are covered with numerous spinules in these species.

The most similar species to *Ophioplinthaca* sp. is *Ophioplinthaca clothilde* sharing contiguous radial shields, similar number of arm spines (up to seven), number and shape of lateral oral papillae, similar tentacle scale, and separated ventral and dorsal arm plates, but differs in longer dorsal arm spines (up to four arm segments), disc spines with single cylindrical base ending in two or three crowns, or a stout disc spine with irregular crown of a dozen or more spinules, more or less ovoid radial shields with convex proximal side, slightly contiguous dorsal arm plates on proximal arm segments, and equal size of ventralmost tooth and lateral oral papillae. We refrain from naming our specimen, as these differences may suggest an undescribed species or fall within the insufficiently known variability of *O. clothilde*. This question may be answered, when more specimens have been collected, and molecular data are needed for *O. clothilde*.

Ophioplinthaca globata is similar to *Ophioplinthaca* sp. by having a similar number of arm spines (up to six), number of lateral oral papillae, and separated ventral and dorsal arm plate and shape, but differs by thorny disc spine and spine shape, separated radial shields and their shape, and tentacle scale longer than ventral arm plate. *Ophioplinthaca laudator* Koehler, 1930 shares with *Ophioplinthaca* sp. almost the same number of arm spines (up to seven), by size of radial shields, number and shape of lateral oral papillae, and separated dorsal and ventral arm plates, but differs in thorny disc spines, with two to three thorns or sub-thorns on their lateral surface, separated radial shields, and smooth arm spines. *Ophioplinthaca grandisquama* is similar to *Ophioplinthaca* sp. by having contiguous radial shields, closer number of arm spines (up to seven), and by the shape of arm and disc spines, but differs by tall (0.8 mm in high) long, thorny disc spines with two or three thorny sub-crowns, blunt

tentacle scale, and contiguous ventral and dorsal arm plates. *Ophioplinthaca manillae* Guille, 1981 is similar to *Ophioplinthaca* sp. by having similar number and shape of arm spines, contiguous radial shields, shape of lateral oral papillae, and separated dorsal and ventral arm plates, but differs in an oval tentacle scale, and in height and shape of disc spines.

Ophioplinthaca amezianeae O'Hara & Stöhr, 2006

Figs 8, 9

Ophioplinthaca amezianeae O'Hara & Stöhr, 2006: 77–78, fig. 9D–G.

Material examined. NORTHWEST PACIFIC • 1 specimen; near Mariana Trench, Southwest of Guam Island, seamount; 11°40.33'N, 141°20.57'E; depth 3600 m; 27 November 2020; Collecting event: stn. SC040; Shenhaiyongshi msv leg; preserved in -80 °C; GenBank: OK043832; IDSSE-EEB-SW0109.

Description. Disc diameter 11.5 mm, arm base width 2.5 mm (Fig. 8).

Disc. Sub-pentagonal and incised interradially to 1/8 disc radius, creating five wedge-shaped lobes over each arm base in contrast to sunken center and interradii of disc (Fig. 8A, B). Disc scales variable in size, overlapping, dense at center, and some scales bear spines (Fig. 8C). Scales increase in size distalwards from disc center to distal end of radial shields interradially (Fig. 8C–G). Disc spines at disc center 0.7–0.9 mm high, thick, with cylindrical to rounded base, tapering to a sharp point, or terminating in usually one or two small thorns, with additional irregular flanged thorns arising from lateral margins along the spine (Fig. 8D, E). Disc spines on disc periphery and around radial shields, slightly smaller than center spines (0.5–0.7 mm in height), cylindrical, finely rugose, with thorny blunt tip (Fig. 8F, G). Radial shields large, twice as long as wide, with acute proximal end, much wider convex distal end, and completely separated by disc scales (Fig. 8H). Ventral disc covered by smaller scales compared to dorsal scales and overlapped, without or rarely bearing spines (Fig. 8B, I). Genital slits conspicuous and extending from oral shield to periphery of disc (Fig. 8I). Madreporite arrowhead-shaped, as wide as long, triangular with pointed proximal end, convex distal edge with thickened lateral margins (Fig. 8I). Oral shield arrowhead-shaped, as wide as long, triangular with pointed proximal end, slightly concave lateral margins along adoral shields, lobed distal edge with rounded lateral margins (Fig. 8I). Adoral shield 3 × as long as wide, with straight lateral margin, and pair of shields proximally connected (Fig. 8I). Jaw longer than wide, and oral plates concealed by adoral shields (Fig. 8I). Jaw bearing one large, pointed ventralmost tooth with three pointed, rod-like lateral oral papillae, shorter than ventralmost tooth, finely rugose, with wide, rounded base, and pointed tip (Fig. 8I). One small, oval adoral shield spine at lateral margin of adoral shield at edge of second tentacle pore (Fig. 8I).

Arms. Five slightly moniliform arms, with smooth plates. Dorsal arm plates fan-to bell-shaped, with truncated proximal end on first dorsal arm plate, but following

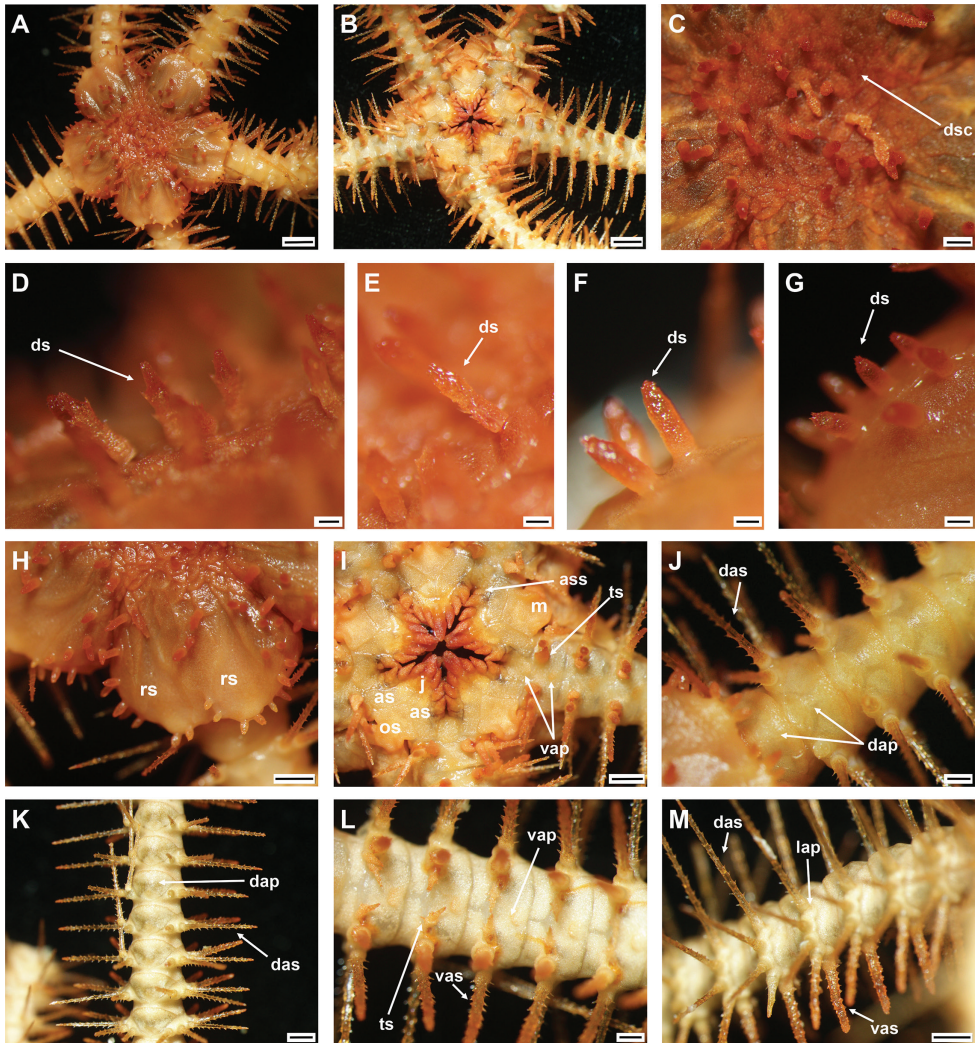


Figure 8. *Ophioplinthaca amezianee* O'Hara & Stöhr, 2006 (IDSSE-EEB-SW0109) **A** dorsal disc **B** ventral disc **C** center of the disc **D–G** disc spines **H** radial shield **I** oral frame **J** dorsal side of the arm base **K** dorsal arm **L** ventral arm, **M** lateral arm. Abbreviations: **as** adoral shield, **ass** adoral shield spine, **dap** dorsal arm plate, **das** dorsal arm spine, **dp** disc plate, **gs** genital slit, **j** jaw, **lap** lateral arm plate, **m** madreporite, **os** oral shield, **rs** radial shield, **ts** tentacle scale, **vap** ventral arm plate, **vas** ventral arm spine. Scale bars: 2 mm (**A, B**); 1 mm (**H, I, K, M**); 500 μ m (**C, J, L**); 200 μ m (**D–G**).

plates with obtuse proximal end, straight to slightly convex proximolateral margins, and convex distal margin (Fig. 8J, K). Dorsal arm plates at proximal end barely separated, but distally widely separated (Fig. 8J, K). First ventral arm plate trapezoid, as wide as long, with sunken proximal end, distally connected to second ventral arm plate (Fig. 8I). Following ventral arm plates twice as wide as long, with obtuse proximal end, straight proximolateral margins, straight lateral angles, straight to slightly wavy distal end, and widely separated (Fig. 8L). Lateral arm plates meeting above and below. Up

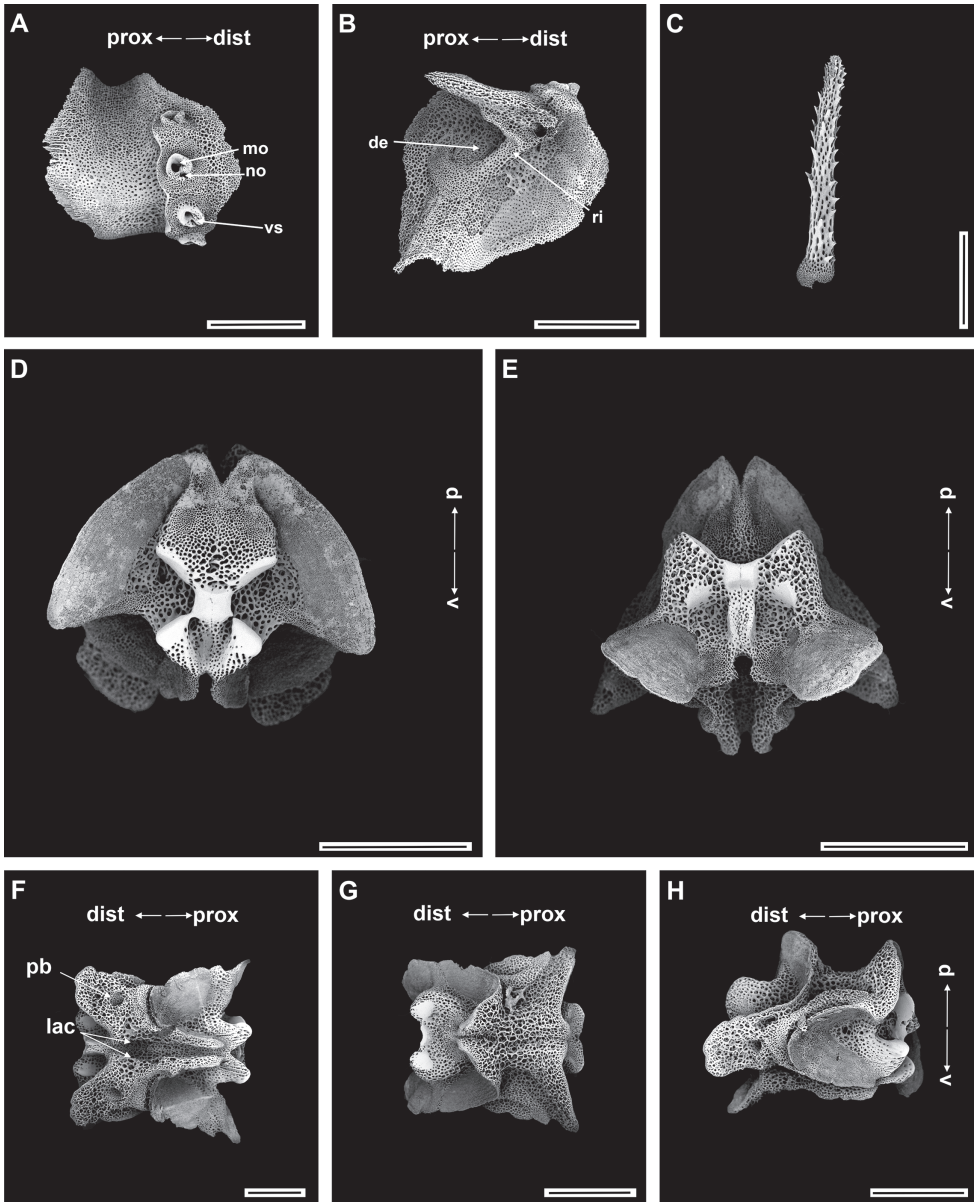


Figure 9. *Ophioplinthaca amezianeae* O'Hara & Stöhr, 2006 (IDSSE-EEB-SW0109) **A, B** lateral arm plate **C** ventral arm spine **D–H** vertebrae **D** proximal view **E** distal view **F** ventral view **G** dorsal view **H** lateral view. Abbreviations: **d** dorsal, **de** depression, **dist** distal, **lac** lateral ambulacral canals, **mo** muscle opening, **no** nerve opening, **pb** podial basin, **prox** proximal, **ri** ridge, **th** thorns, **v** ventral, **vs** volute-shape. Scale bars: 800 μ m (**A–E, G, H**); 500 μ m (**F**).

to five arm spines: two dorsal spines, three arm segments in length, slender, thorny, laterally compressed with row of tall sharp thorns (Fig. 8J–M); two ventral spines, two arm segments in length, thick, with blunt tip, rugose, and thorny surface (Fig. 8J, K). First tentacle pore covered by one or two tentacle scales with rounded base and pointed

tip (Fig. 8I). Following tentacle scales with rounded base, spiniform, pointed tip and covered in irregular thorns, mostly on middle to distal half of arm (Fig. 8L).

Color. In live specimen, orange-brown dorsal disc, pale color on arms and ventral disc, arm spines orange, and disc spines red (Fig. 8).

Ossicle morphology. Arm spine articulations well developed, four in number, and placed at slight angle to distal edge of lateral arm plate. Volute-shaped perforated lobe forms dorsal and distal part of articulation (Fig. 9A); large muscle opening, small nerve opening (Fig. 9A). Proximal half of lateral arm plate internal surface with continuous ridge and prominent knob close to ventral edge forming vertebral articulation, shaped like a broad, nose-shaped beak (Fig. 9B). Ventral arm spine thorny, with blunt apex, several longitudinal rows of perforations and small thorns (Fig. 9C). Vertebrae with streptospondylous articulation, short, broad podial basin at proximal end, and narrow small distal end (Fig. 9D–H). Dorsal end of vertebrae distally triangular and proximally flattened with longitudinal groove along midline (Fig. 9D, E). Ventral end of vertebrae with broad ambulacral groove with lateral ambulacral canals (Fig. 9F–H).

Distribution. 1618–3600 m depth, Southwest of Guam Island, Northwest Pacific, New Caledonia, New Zealand.

Remarks. *Ophioplinthaca amezianeae* was described by O’Hara and Stöhr (2006), and recorded from deep waters in the South Pacific region. It can easily be delimited from most species in the genus *Ophioplinthaca* by disc spine, radial shield, and tentacle scale characters (Table 3).

Ophioplinthaca amezianeae from the present study is similar to the holotype description, but it differs slightly in the disc spine shape and number of arm spines on the lateral arm plate. However, the number of arm spines differs between individuals (6–10 arm spines) according to the description of paratype variations of *O. amezianeae* (O’Hara and Stöhr 2006). The disc spines of our specimen are slightly thicker than in the holotype, but their shape and irregular flanged thorns arising from lateral margins along the spine are similar to the holotype description. The holotype is significantly larger than our specimen (14.5 mm disc diameter), and *Ophioplinthaca* species usually show high intraspecific morphological variation. Therefore, a slight difference in disc spine thickness can be considered as intraspecific morphological variation within *O. amezianeae*.

***Ophioplinthaca athena* A. H Clark, 1949**

Figs 10, 11

Ophioplinthaca athena A. H Clark, 1949: 23–24, fig. 9; Chen et al. 2021b: 60–61, fig. 3.

Material examined. NORTHWEST PACIFIC • 1 specimen; near Mariana Trench, Southwest of Guam Island, seamount; 12°8.83’N, 139°0.37’E; depth 1987 m; 27 November 2020; Collecting event: stn. SC041; Shenhaiyongshi msv leg; preserved in -80 °C; GenBank: OK043833; IDSSE-EEB-SW0110.

Description. Disc diameter 12.5 mm, arm base width 1.5 mm (Fig. 9).

Disc. Sub-circular and incised interradially, creating five wedge-shaped lobes over each arm base in contrast to sunken center and interradial of disc (Fig. 10A, B). Disc scales small, irregular, overlapping, and some scales bear more than one stump (Fig. 10C–F). Scales increase in size distalwards from disc center to periphery interradially (Fig. 10D–F). Disc stumps in disc center with cylindrical base and few radiating spinules at truncated tip (Fig. 10D–F). Spines at disc periphery and around radial shields, slightly smaller, less cylindrical, more conical, smooth, with pointed tip (Fig. 10D, E). Radial shields large, 3 × as long as wide, acute proximal end, much wider and slightly convex distal end, pairs separated along proximal half, and barely connected distally (Fig. 10F). Ventral disc covered by small, overlapping disc scales without or rarely bearing conical granules (Fig. 10B, G). Genital slits conspicuous and extending from oral shield to periphery of disc (Fig. 10G). Madreporite arrowhead-shaped, as wide as long, triangular with pointed proximal end, lobed distal edge with thickened lateral margins. Other oral shields widely triangular, twice as wide as long, wide proximal angle, distal edge folded ventralwards with minute central lobe, and lateral angle connected to first lateral arm plate (Fig. 10H). Adoral shield 2 × as long as wide, with concave proximolateral margin, pair of shields proximally connected, and connected to first lateral and ventral arm plates (Fig. 10H). Jaw longer than wide, bearing one slightly blunt, flat, elongated, and large ventralmost tooth and four elongated, spiniform lateral oral papillae (Fig. 10H). Lateral oral papillae, finely rugose, equal in height to ventralmost tooth, with pointed tip (Fig. 10H). One small scale-like rounded adoral shield spine at lateral margin of adoral shield at edge of second tentacle pore (Fig. 10I).

Arms. Five slightly moniliform arms, with smooth plates. Dorsal arm plates twice as long as wide, with truncated proximal end in first dorsal arm plate (Fig. 10J), but following plates with triangular proximal end, slightly curved proximolateral margins, and convex to slightly wavy distal margins covered with minute spines (Fig. 10J, K). Dorsal arm plates at proximal to middle arm segments barely separated, but distally widely separated (Fig. 10J, K). First ventral arm plate trapezoid, as wide as long, with sunken proximal end, and distal end connected to second ventral arm plate (Fig. 10I). Following ventral arm plates twice as wide as long, with obtuse proximally, straight proximolateral margins, curved lateral angles, straight to slightly wavy distal end, distal margins covered with minute spines, and widely separated (Fig. 10L). Lateral arm plates meeting above and below (Fig. 10K–M). Up to five arm spines. Proximal arm segment bearing two dorsal and three ventral arm spines (Fig. 10M). Dorsalmost arm spines at proximal end two to two and a half arm segments in length, smooth or with few thorns at lateral edge (Fig. 10M). Next dorsal arm spine much longer, nearly four arm segments in length, smooth or with thorns at lateral margin (Fig. 10M). Ventral arm spines short, less conspicuous thorns, more rugose surface (Fig. 10L, M). First tentacle pore covered with two leaf-like tentacle scales with pointed tip (Fig. 10H, I). Following pores covered with leaf-like pointed tentacle scale with rounded base and tip covered in micro spinules (Fig. 10L).

Color. In live specimen, orange-brown dorsal disc, light color in arms and ventral disc, arm spines orange, disc spines and papillae red (Fig. 10).

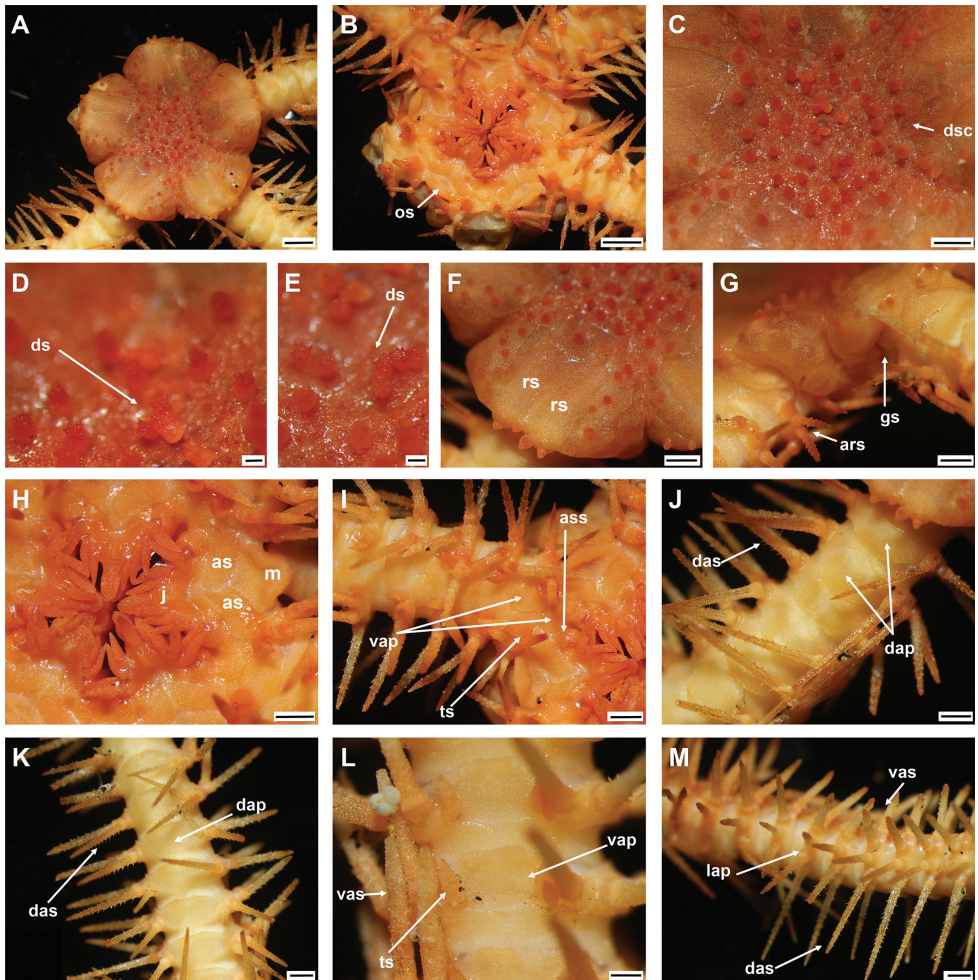


Figure 10. *Ophioplinthaca athena* A. H. Clark, 1949 (IDSSE-EEB-SW0110) **A** dorsal disc **B** ventral disc **C** center of the disc **D–E** disc spines **F** radial shield **G** lateral disc **H** oral frame **I** ventral side of the arm base **J** dorsal side of the arm base **K** dorsal arm **L** ventral arm **M** lateral arm. Abbreviations: **as** adoral shield, **ass** adoral shield spine, **dap** dorsal arm plate, **das** dorsal arm spine, **dp** disc plate, **gs** genital slit, **j** jaw, **lap** lateral arm plate, **m** madreporite, **os** oral shield, **rs** radial shield, **ts** tentacle scale, **vap** ventral arm plate, **vas** ventral arm spine. Scale bars: 2 mm (**A, B**); 1 mm (**C, F–K, M**); 500 μ m (**L**); 200 μ m (**D, E**).

Ossicle morphology. Arm spine articulations well developed, four in number, and placed at slight angle to distal edge of lateral arm plate. Volute-shaped perforated lobe forms dorsal and distal part of articulation, with large muscle opening and small nerve opening (Fig. 11A). Distal half of inner side of lateral arm plate with group of small, irregular perforations parallel to row of spine articulations; a continuous ridge and a prominent knob close to ventral edge form vertebral articulation, shaped like a broad, nose-shaped beak (Fig. 11B). Dorsal arm spine thorny, with several longitudinal rows of perforations and widely spaced tall thorns (Fig. 11C). Dorsal arm plate triangular

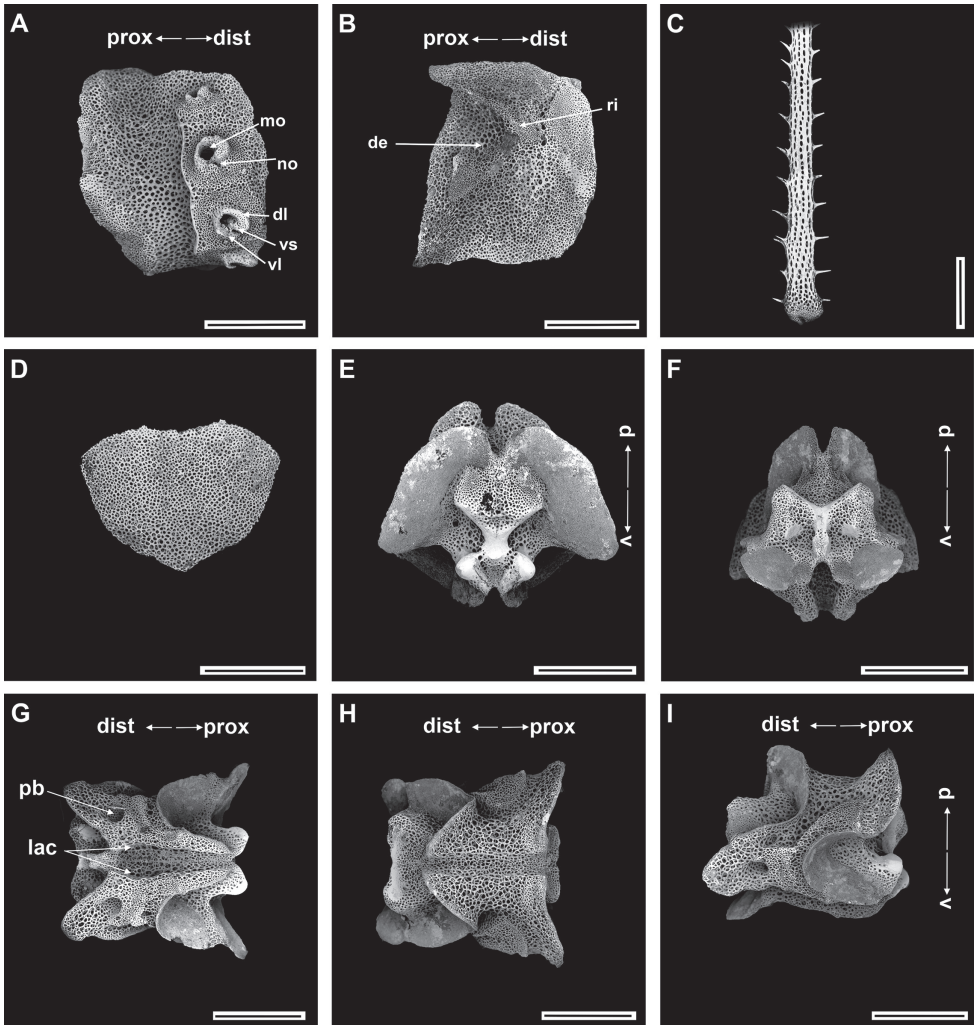


Figure 11. *Ophioplinthaca athena* A. H. Clark, 1949 (IDSSE-EEB-SW0110) **A, B** lateral arm plate **C** dorsal arm spine **D** dorsal arm plate **E–I** vertebrae **E** proximal view **F** distal view **G** ventral view **H** dorsal view **I** lateral view. Abbreviations: **d** dorsal, **de** depression, **dist** distal, **dl** dorsal lobe, **lac** lateral ambulacral canals, **mo** muscle opening, **no** nerve opening, **pb** podial basin, **prox** proximal, **ri** ridge, **th** thorns, **v** ventral, **vl** ventral lobe, **vs** volute-shape. Scale bars: 800 μm (**A–I**).

with smooth surface (Fig. 11D). Vertebrae with streptospondylous articulation, short, broad podial basin at proximal end and narrow small distal end (Fig. 11E–I). Dorsal end of vertebrae distally triangular and proximally flattened with longitudinal groove along midline (Fig. 11E, F). Ventral end of vertebrae with broad ambulacral groove and lateral ambulacral canals (Fig. 11G–I).

Distribution. 1866–2157 m depth, Southwest of Guam Island, Northwest Pacific, Kupuai, Hawaii Islands.

Remarks. *Ophioplinthaca athena* was described by A. H. Clark (1949), and recorded from deep waters in the Hawaiian Islands. *Ophioplinthaca athena* resembles *O. papillosa*, *O. globata*, *O. hastata*, *O. plicata*, *O. carduus*, *O. semele*, *O. clothilde*, and *O. dipsacos* in disc spine characters, but differs in arm spine, oral frame, and radial shield characters (Table 3).

Ophioplinthaca athena from the present study is similar to the holotype description, but it differs slightly by separated dorsal arm plates and the shape of the dorsal arm spines, although the latter varies within our individual. Therefore, the shape of the arm spines is not a suitable morphological character to delimit *O. athena*. The description of the holotype mentioned that dorsal arm plates were contiguous, but in our specimen, they are just separated along the arm, and there are no paratypes of *O. athena*. Therefore, this difference may be related to the size of the specimen (holotype 14.5 mm disc diameter; A. H. Clark 1949), and these small morphological differences can be considered as intraspecific variation within *O. athena*.

***Ophioplinthaca* cf. *lithosora* (H. L. Clark, 1911)**

Figs 12, 13

Ophiocamax lithosora H. L. Clark, 1911: 191–193, fig. 89.

Ophiomitra lithosora: Matsumoto 1917: 131.

Material examined. CHINA • 1 specimen; South China Sea, near Xisha Islands archipelago, seamount; 16°47.79'N, 113°15.04'E; depth 602 m; 31 March 2020; Collecting event: stn. SC009; Shenhaiyongshi msv leg; preserved in -80 °C; GenBank: OK043834 IDSSE-EEB-SW0111.

Comparative material. JAPAN • **Holotype** specimen; East China Sea, Osumi Islands, Kuchnioerabu Island; 30°22'N, 129°08.5'E; depth 660 m; 13 Aug 1906; Collecting event: stn. 4918; R/V Abatross, North Pacific Expedition leg; preserved dry; USNM 25622. • 1 **paratype** specimen; North Pacific Ocean, Wakayama, Honshu Island, Shiono Misaki; 33°25.17'N, 135°37.33'E; depth 446–463 m; 29 Aug 1906; Collecting event: stn. 4967; R/V Abatross, North Pacific Expedition leg.; preserved dry; USNM 26220. • 1 specimen; S off Daiozaki, Kumanonada; 34°05.12'N, 136°51.24'E to 34°05.05'N, 136°50.5'E; depth 475–494 m; 25 May 1994; Collecting event: stn. KN25; R/V Tansei-Marui KT-94-07 leg.; gear 3 m ORE beam trawl; preserved in ethanol; NSMT E-7943.

Description. Disc diameter 20 mm, arm base width 4.5 mm (Fig. 12).

Disc. Sub-pentagonal and incised interradially, creating five wedge-shaped lobes over each arm base in contrast to sunken center and interradii of disc (Fig. 12A, B). Disc scales small, irregular, overlapping, some scales bear more than one low stout spine, these spread across entire disc except radial shields (Fig. 12C). Spines in disc center, 0.9–1.4 mm high, thick, with cylindrical to rounded base, tapering to sharp point, with truncated or pointed tip, and additional irregular flanged thorns arising from lateral margins along spine. Proximal end of disc spines, 0.8–0.9 mm high, thick, base cylindrical, with thorny pointed tip (Fig. 12D–G). Peripheral disc spines decreas-

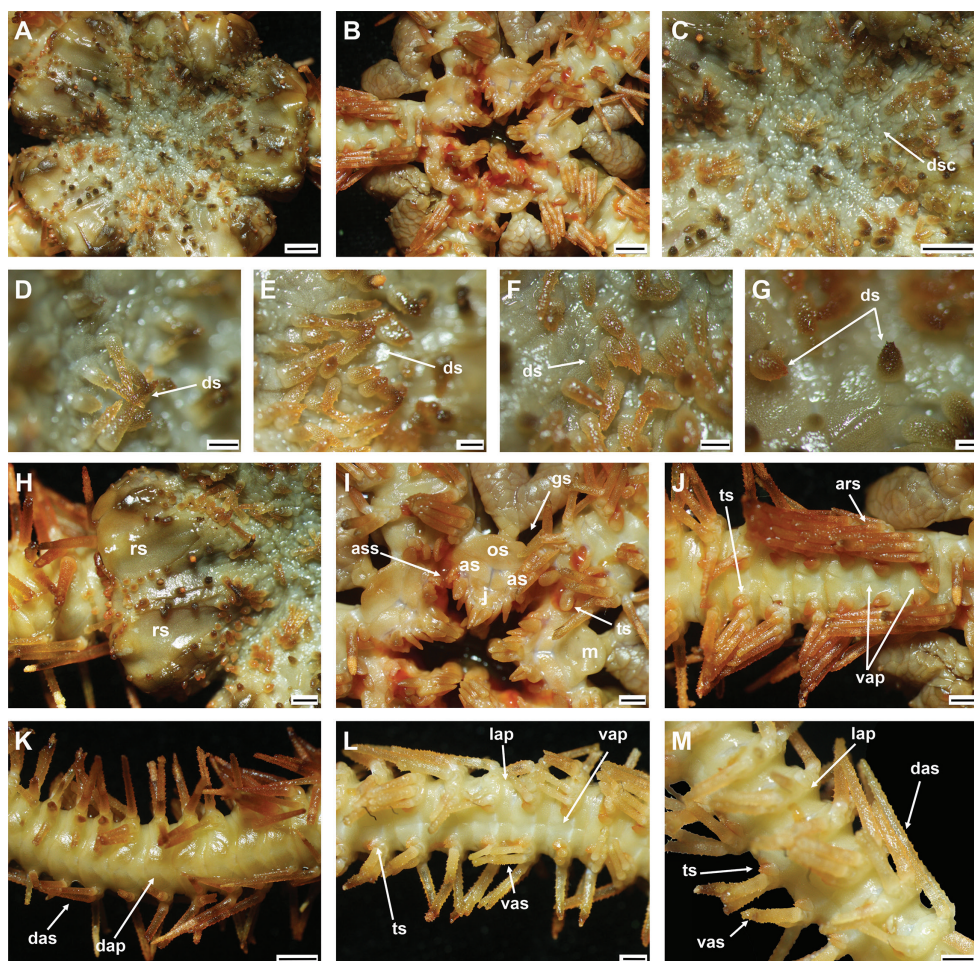


Figure 12. *Ophioplinthaca* cf. *lithosora* (H. L. Clark, 1911) (IDSSE-EEB-SW0111) **A** dorsal disc **B** ventral disc **C** center of the disc **D–G** disc spines **H** radial shield **I** oral frame **J** ventral side of the arm base **K** dorsal arm **L** ventral arm, **M** lateral arm. Abbreviations: **ars** arm spine, **as** adoral shield, **ass** adoral shield spine, **dap** dorsal arm plate, **das** dorsal arm spine, **dp** disc plate, **gs** genital slit, **j** jaw, **lap** lateral arm plate, **m** madreporite, **os** oral shield, **rs** radial shield, **ts** tentacle scale, **vap** ventral arm plate, **vas** ventral arm spine. Scale bars: 2 mm (**A–C, K**); 1 mm (**H–J, L, M**); 500 μ m (**D, E**); 200 μ m (**F, G**).

ing in size, conical, with smooth or slightly thorny pointed tip (Fig. 12F, G). Radial shields large, $2 \times$ as long as wide, acute proximal end, much wider convex distal end, completely separated (Fig. 12H). Ventral disc covered by small, overlapping disc scales without spines (Fig. 12B, I). Genital slits conspicuous and extending from oral shield to periphery of disc (Fig. 12B, I). Oral shield wide fan-shaped, $2 \times$ as wide as long, with rounded proximal end, concave lateral margins, convex to wavy distal edge, and lateral angle connected to first lateral arm plate (Fig. 12I). Madreporite as long as wide, proximal end with wide angle. Distal edge strongly convex (Fig. 12I). Adoral shield $2 \times$ as long as wide, with straight lateral margin, pair of shields proximally connected

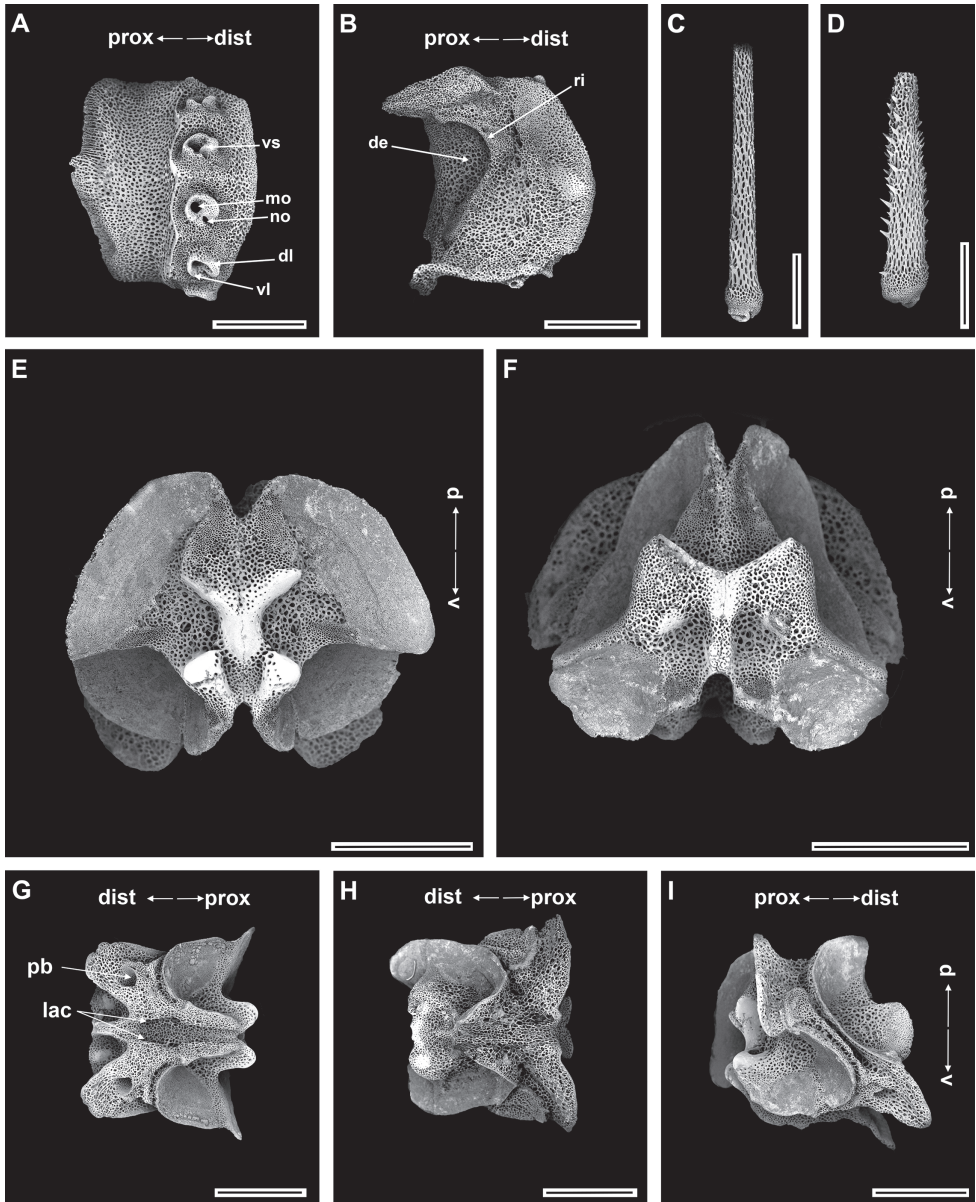


Figure 13. *Ophioplinthaca* cf. *lithosora* (H. L. Clark, 1911) (IDSSE-EEB-SW0111) **A, B** lateral arm plate **C** dorsal arm spine **D** ventral arm spine **E–I** vertebrae **E** proximal view **F** distal view **G** ventral view **H** dorsal view **I** lateral view. Abbreviations: **d** dorsal, **de** depression, **dist** distal, **dl** dorsal lobe, **lac** lateral ambulacral canals, **mo** muscle opening, **no** nerve opening, **pb** podial basin, **prox** proximal, **ri** ridge, **th** thorns, **v** ventral, **vl** ventral lobe. Scale bars: 800 μ m (**A–I**).

(Fig. 12I). Adoral shields connected to first lateral and ventral arm plates (Fig. 12I). Jaw longer than wide, bearing four to five elongated, pointed leaf-like lateral oral papillae, cluster of up to three pointed tooth papillae, and small, 4–6 granules covered by

adoral shield spines in some jaw slits (Fig. 12I). Two adoral shield spines, one larger, oval, scale-like flat, other one smaller, situated at lateral margin of adoral shield at second tentacle pore (Fig. 12I).

Arms. Dorsal arm plates pentagonal, wider than long, with truncated proximal end, weakly convex proximolateral margins, straight lateral margins, and convex to slightly wavy distal margins, on proximal to middle arm segments contiguous, but distally separated (Fig. 12K). First ventral arm plate nearly square, connected to second ventral arm plate (Fig. 12J). Following ventral arm plates twice as wide as long, with obtuse proximal end, straight proximolateral margins, slightly concave lateral edges, straight distal edge, and widely separated (Fig. 12L). Lateral arm plates meeting only below (Fig. 12K–M). Up to seven arm spines, three dorsal and four ventral; dorsal arm spines two to three arm segments in length, thick, with smooth or rugose surface and lateral thorns; ventral arm spines shorter, two arm segments in length, smooth, or slightly rugose, thick, with pointed tip (Fig. 12L). First tentacle pore covered by two or three thickened, oval, blunt tentacle scales (Fig. 12J). Subsequent seven to eight tentacle pores covered by single similar oval scale (Fig. 12J). Further tentacle pores covered by one small scale, with rounded base and spinules at tip (Fig. 12L).

Color. In live specimen, orange-brown dorsal disc, pale color in arms and ventral disc, arm spines orange, disc spines and papillae red (Fig. 12).

Ossicle morphology. Arm spine articulations well developed, five in number, and placed at slight angle to distal edge of lateral arm plate. Volute-shaped perforated lobe forms dorsal and distal part of articulation, with large muscle opening and small nerve opening, and decreasing in size ventralwards (Fig. 13A). Distal half of inner side of lateral arm plate with group of small, irregular perforations parallel to row of spine articulations; a continuous ridge and a prominent knob close to ventral edge form vertebral articulation, shaped like a broad, nose-shaped beak (Fig. 13B). Dorsal arm spine thorny, with several longitudinal rows of perforations and widely spaced small thorns (Fig. 13C). Ventral arm spine short, rough, thorny surface with truncated apex (Fig. 13D). Vertebrae with streptospondylous articulation, short, broad podial basin at proximal end and narrow small distal end (Fig. 13E–I). Dorsal end of vertebrae distally acute and proximally flattened with longitudinal groove along midline (Fig. 13E, F). Ventral end of vertebrae with broad ambulacral groove and lateral ambulacral canals (Fig. 13G–I).

Distribution. 462–663 m depth, South China Sea, East China Sea, Japan Sea.

Remarks. *Ophioplinthaca lithosora* was described by H. L. Clark (1911) in the genus *Ophiocamax* Lyman, 1878, and is currently accepted in *Ophioplinthaca* (Stöhr et al. 2021). However, we could not find the taxonomic act that transferred it to *Ophioplinthaca* and assume that this decision may never have been formalized in a publication. We agree that it belongs in this genus on account of its deeply incised disc. Matsumoto (1917) considered *O. lithosora* in *Ophiomitra* Lyman, 1869, despite noticing the incised disc and enlarged marginal disc scales. These genera and *Ophiocamax* share indeed many other characters, but by molecular data they have not been found to be closely related and at least *Ophiomitra* may be polyphyletic (Christodoulou et al. 2019). *Ophioplinthaca lithosora* was previously recorded from the East China Sea and

Japan Sea. It is easily recognized within the genus *Ophioplinthaca* by radial shield, oral frame, and tentacle scale characters (Table 3).

Ophioplinthaca cf. *lithosora* from the present study concurs with the holotype description in most respects, but it differs slightly by having contiguous dorsal arm plates, long spines in the center of the disc and few granules in the mouth angle at only some jaws. These granules are present at the second tentacle pore at the adoral shield at all jaw angles in the holotype, paratype and an additional specimen, all of which we examined from digital photographs. They are more obvious than in any other species of *Ophioplinthaca* and H. L. Clark (1911) included them in the series of oral papillae, which explains his high number of up to 15 lateral papillae at a single jaw edge. They may perhaps form a funnel around the tube foot. None of these specimens has long disc spines. However, the information about morphological variations within *O. lithosora* is still incomplete (H. L. Clark 1911), because it appears to be a rare species of which only few specimens are known. Therefore, these small morphological changes may represent intraspecific variation between *O. lithosora* specimens. We still cautiously refrain from fully associating our specimen with this species, due to the small differences between species in *Ophioplinthaca*.

***Ophioplinthaca semele* (A. H Clark, 1949)**

Fig. 14

Ophiomitra semele A. H Clark, 1949: 20–23, fig. 8a, b.

Ophioplinthaca semele: O'Hara and Stöhr 2006: 76; Chen et al. 2021a: 14–18, fig. 6–8.

Material examined. NORTHWEST PACIFIC • 1 specimen; near Mariana Trench, Southeast of Guam Island, seamount, 12°6.67'N, 141°37.27'E; depth 1160 m; 03 September 2019; Collecting event: stn. SC033; Shenhaiyongshi msv leg; preserved in -80 °C; GenBank: OK043835, IDSSE-EEB-SW0113.

Distribution. 537–1987 m depth, southwest of Guam Island, Northwest Pacific, Hawaii Islands.

Remarks. *Ophioplinthaca semele* was first described by A. H Clark (1949) in the genus *Ophiomitra*, then redescribed by Chen et al. (2021a), and that recent study included rich morphological information. *Ophioplinthaca semele* from the present study concurs largely with the holotype description and Chen et al. (2021a), but it differs slightly in the disc stumps at the periphery of the disc. According to the holotype description, the disc stumps had a thorny tip or three thorns in the disc center, but at the periphery these stumps were smooth. Our specimen has a crown of somewhat longer thorns, both in the center and periphery of the disc (Fig. 14A–H). *Ophioplinthaca dipsacos* (Lyman, 1878) is one of the species that most closely resemble *Ophioplinthaca semele* by having a similar number and shape of arm spines, radial shield characters, number of lateral oral papillae, similar disc spines, and separated dorsal and ventral

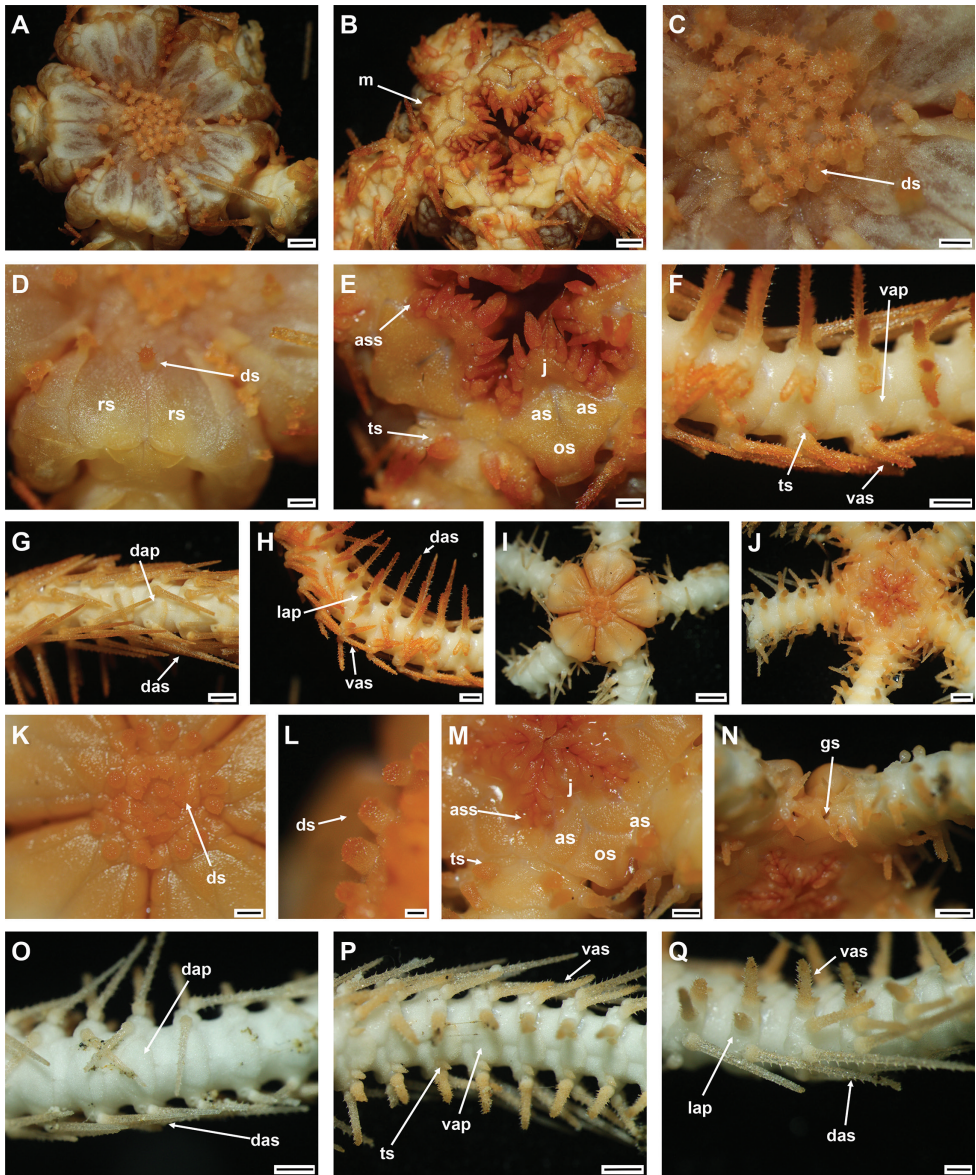


Figure 14. *Ophioplinthaca semele* (A. H Clark, 1949) (IDSSE-EEB-SW0113: **A–H**) **A** dorsal disc **B** ventral disc **C** center of the disc **D** radial shield **E** oral frame **F** ventral arm **G** dorsal arm **H** lateral arm; *Ophioplinthaca defensor* Koehler, 1930 (IDSSE-EEB-SW0112: **I–Q**) **I** dorsal disc **J** ventral disc **K** center of the disc **L** disc spine **M** oral frame **N** lateral disc **O** dorsal arm **P** ventral arm **Q** lateral arm. Abbreviations: **as** adoral shield, **dap** dorsal arm plate, **das** dorsal arm spine, **gs** genital slit, **j** jaw, **lap** lateral arm plate, **m** madreporite, **os** oral shield, **rs** radial shield, **ts** tentacle scale, **vap** ventral arm plate, **vas** ventral arm spine. Scale bars: 2 mm (**I**); 1 mm (**A, B, F–H, J, N–P**); 500 μ m (**C–E, K, M, Q**); 200 μ m (**L**).

arm plates, but it differs in the number of tentacle scales at the first to third tentacle pore, and in the shape of the tentacle scale (Table 3). Moreover, *O. dipsacos* was recorded from the Gulf of Mexico, far from the known distribution of *O. semele* (Lyman, 1878). *Ophioplinthaca globata*, *O. lithosora*, *O. citata*, and *O. clothilde* show a similar shape of the disc spines, but differ in size and other morphological characters (Table 3). Therefore, variations within species from our collection can be considered as intraspecific variation, rather than species delimiting characters.

***Ophioplinthaca defensor* Koehler, 1930**

Fig. 14

Ophioplinthaca defensor Koehler, 1930: 84–86, pl. 9, figs 1, 2; Na et al. 2021: 3–6, figs 2, 4.

Material examined. NORTHWEST PACIFIC • 1 specimen; near Mariana Trench, Southwest of Guam Island, seamount; 12°8.83'N, 139°0.37'E; depth 1987 m; 27 November 2020; Collecting event: stn. SC041; Shenhaiyongshi msv leg; preserved in -80°C; GenBank: OK043836; IDSSE-EEB-SW0112.

Distribution. 385–2000 m depth, Southwest of Guam Island, Caiwei Guyot, Weijia Guyot, Batiza Guyot, Northwest Pacific, New Caledonia, New Zealand, Tasman Sea.

Remarks. *Ophioplinthaca defensor* was first described by Koehler (1930) based on a single specimen. However, Na et al. (2021) provided rich details of morphological variation from juvenile to adult *O. defensor*, and the specimen from our collection concurs with their intraspecific morphological variations (Fig. 14I–Q).

Genus *Ophiophthalmus* Matsumoto, 1917

Type species. *Ophiacantha cataleimmoidea* H. L. Clark, 1911

Included species:

Ophiophthalmus normani (Lyman, 1879)

Ophiophthalmus relictus (Koehler, 1904)

Ophiophthalmus hylacanthus (H. L. Clark, 1911)

Diagnosis. Adapted from Matsumoto (1917), H. L. Clark (1911), Lyman (1879), Paterson (1985), and Koehler (1904, 1922). Disc rounded to sub-pentagonal, and covered by irregular overlapping disc scales with sparse to coarse minute granules. Radial shields ovoid, naked, and widely separated by disc scales with granules. Three or four spiniform lateral oral papillae, with one ventralmost tooth at jaw apex. Dorsal arm plates contiguous at arm base then separated. Ventral arm plates pentagonal to trapezoidal, and separated. Four to seven arm spines at each lateral arm plate. Arm spines smooth to rugose, one to three arm segments in length, thick, with blunt tip. Mostly single, large, flat, oval tentacle scale.

Distribution and habitat. 100–2194 m depth, North Pacific, Australia, New Zealand, Papua New Guinea, South Africa. Substrate of mud, fine grey sand, Foraminifera, and small stones (Olbers et al. 2019).

Remarks. *Ophiophthalmus* was created by Matsumoto (1917) for species, which at the time were included in the genera *Ophiomitra*, *Ophiomitrella*, and *Ophiacantha*. However, Paterson (1985) noted that the ophiuroid genus *Ophiophthalmus* is a junior homonym of a reptilian genus described by Fitzinger (1843). Some later works (Olbers et al. 2019; Okanishi et al. 2021) used the name *Ophiophthalmus* in quotation marks, indicating its invalid status, while other works (Suppl. material 1) seem to have been oblivious to the issue, causing confusion and taxonomic instability. Article 23.9.1 of the International Code of Zoological Nomenclature (International Commission of Nomenclature 2000), states that “prevailing usage of a name must be maintained when the senior homonym has been used as a taxon’s presumed valid name, in at least 25 works, published by at least ten authors in the immediately preceding 50 years and encompassing a span of not less than ten years”. In the present case, the 50-year period extends from 1971 to 2021 and 25 publications by more than ten authors have been found in this period (Suppl. material 1).

Both names are available, because they have been published with either a description or mention of a type species, and they satisfy articles 10, 11, and 12 of the Code. Fitzinger (1843) proposed the reptile’s name *Ophiophthalmus* as a replacement name for *Lialis* Gray, 1834 with the same type species *L. burtonis* Gray, 1835, immediately making *Ophiophthalmus* Fitzinger, 1843 a junior synonym of *Lialis* (Shea 2021). Fitzinger’s contemporary colleagues and later researchers rejected his proposed name change, and *Ophiophthalmus* was thus never used for a reptile and cannot be used in the future, because it lacks a type species separate from *Lialis*. Instead, prevailing usage of the name *Ophiophthalmus* Matsumoto, 1917 has been shown here and it must be maintained.

Ophiophthalmus belongs to one of the largest and diverse ophiuroid families, Ophiacanthidae in the order Ophiacanthida, and is delineated from most other genera by having minute granular coverage of the disc, smooth and somewhat finely serrated arm spines, ovoid radial shields, and by characters of the arm plates (Koehler 1904, 1922; H. L. Clark 1911; Matsumoto 1917; Paterson 1985; Liao 2004; Martynov et al. 2015; Olbers et al. 2019). Currently, *Ophiophthalmus* includes four species: *O. cataleimmoidus*, *O. hylacanthus*, *O. normani*, and *O. relictus*. The genus *Ophiomitra* is closely resembles *Ophiophthalmus* by having ovoid, separated radial shields, and smooth, long arm spines, but differs in a thorny tip on granules or stumps, 10–16 oral papillae at the jaw, up to nine arm spines (Lyman 1869; Lütken and Mortensen 1899; H. L. Clark 1911; Matsumoto 1917; Koehler 1922; Olbers et al. 2019). Matsumoto (1917b) suggested that contiguous dorsal arm plates on the arm base, and the proximal arm spines not arranged in a fan shape can be used to distinguish *Ophiophthalmus* from *Ophiomitrella*, whereas Koehler (1922) distinguished these from each other by naked radial shields and overlapping disc scales, but Paterson (1985) observed that these characters are not consistent among all species within these genera. However, H. L. Clark

(1911) mentioned that *Ophiophthalmus* species were remarkably consistent in some specific characters (he examined more than 4,000 specimens). Recent molecular studies suggested that *Ophiomitrella* may be polyphyletic in the family Ophiacanthidae, and species from this genus need to be revised (Christodoulou et al. 2019).

***Ophiophthalmus serratus* sp. nov.**

<http://zoobank.org/D2B3B231-FCA7-49F9-9696-328B7DD742D5>

Figs 15, 16

Material examined. Holotype. CHINA • 1 specimen; South China Sea, Haima cold seep; 16°42.45'N, 110°25.68'E; depth 1378 m; 05 February 2021; Collecting event: stn. SC036; Shenhaiyongshi msv leg; preserved in 95% ethanol; GenBank: OK043837; IDSSE-EEB-SW0136. **Paratypes.** CHINA • 5 specimens; South China Sea, Haima cold seep; 16°42.45'N, 110°25.68'E; depth 1378 m; 05 February 2021; Collecting event: stn. SC036; Shenhaiyongshi msv leg; preserved in 95% ethanol; GenBank: OK043838; IDSSE-EEB-SW0137 to IDSSE-EEB-SW0141. • 9 specimens; South China Sea, Haima cold seep; 16°44.02'N, 110°27.61'E; depth 1388 m; 01 May 2018; Collecting event: stn. SC036; Shenhaiyongshi msv leg; preserved in 95% ethanol; IDSSE-EEB-SW0114 to IDSSE-EEB-SW0122. • 13 specimens; South China Sea, Haima cold seep; 16°43.75'N, 110°28.34'E; depth 1378 m; 05 February 2021; Collecting event: stn. SC037; Shenhaiyongshi msv leg; preserved in 95% ethanol; IDSSE-EEB-SW0123 to IDSSE-EEB-SW0135. • 2 specimens; South China Sea, Haima cold seep; 16°34.13'N, 110°42.55'E; depth 1408 m; 07 February 2021; Collecting event: stn. SC042; Shenhaiyongshi msv leg; preserved in 95% ethanol; IDSSE-EEB-SW0142, IDSSE-EEB-SW0143.

Diagnosis. Disc circular to sub-pentagonal, covered by dense smooth granules. Radial shields ovoid, naked, and widely separated (Fig. 15A). One pointed ventralmost tooth and three slightly smaller, spiniform, finely rugose, pointed lateral oral papillae (Fig. 15E). Dorsal arm plates triangular to fan-shaped, contiguous on proximal part of arm, then separated. Five finely serrated, arm spines with blunt tip, and one slightly elongated, blunt tipped tentacle scale (Fig. 15F–I).

Holotype description. Disc diameter 9.5 mm, arm base width 1.65 mm, and arm length 45–50 mm (Fig. 15).

Disc. Disc circular to sub-pentagonal, raised above arm base, and covered by overlapping irregular scales, bearing rounded to cylindrical stumps with blunt tip, and smooth granules (Fig. 15A–C). Granules densely covering the surface, except radial shields, and small area in the center of the disc (Fig. 15C, D). Radial shields, ovoid, small, slightly longer than wide, naked, and widely separated (Fig. 15D). Distal edge of dorsal arm plate on arm base covered by row of few small granules, but only on two arms (Fig. 15F). Ventral disc also covered by overlapping scales with granules, but fewer granules near oral shields (Fig. 15E). Genital slits large, conspicuous, and extending from oral shield to periphery of disc (Fig. 15E). Oral shield triangular, twice as wide

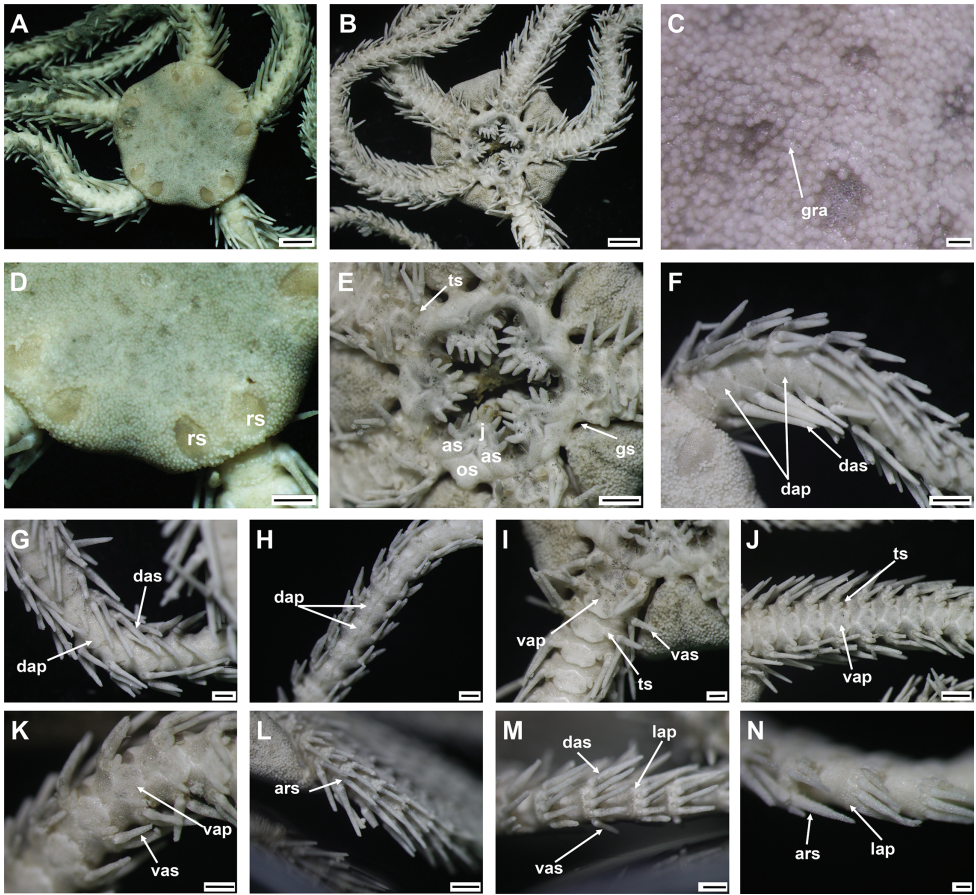


Figure 15. *Ophioplinthacus serratus* sp. nov., holotype (IDSSE-EEB-SW0136) **A** dorsal disc **B** ventral disc **C** center of the disc **D** radial shield **E** oral frame dorsal side of the arm base **G** dorsal arm (proximal half) **H** dorsal arm (distal half) **I** ventral side of the arm base **J** ventral arm (proximal half) **K** ventral arm (distal half) **L** lateral arm base **M** lateral arm (proximal half) **N** lateral arm (distal half). Abbreviations: **ars** arm spine, **as** adoral shield, **dap** dorsal arm plate, **das** dorsal arm spine, **gra** granules, **gs** genital slit, **j** jaw, **lap** lateral arm plate, **os** oral shield, **rs** radial shield, **ts** tentacle scale, **vap** ventral arm plate, **vas** ventral arm spine. Scale bars: 2 mm (**A, B**); 1 mm (**D–F, J, L**); 500 μ m (**C, G–I, K, M**); 200 μ m (**N**).

as long (madreporite almost as long as wide), distal end with median lobe, proximal edges straight to slightly concave, and lateral angle connected to first lateral arm plate (Fig. 15E). Adoral shields 3 \times as long as wide, with straight lateral margins, and pair of shields barely connected proximally (Fig. 15E). Adoral shields connected to first lateral and ventral arm plates (Fig. 15E). Jaw large, as wide as long, with one pointed ventralmost tooth and three elongated, separated, pointed, finely rugose lateral oral papillae, slightly smaller than ventralmost tooth (Fig. 15E).

Arms. Dorsal arm plates triangular to fan-shaped, twice as wide as long, distal edge slightly convex, contiguous at proximal end of arm, then separated (Fig. 15F–H).

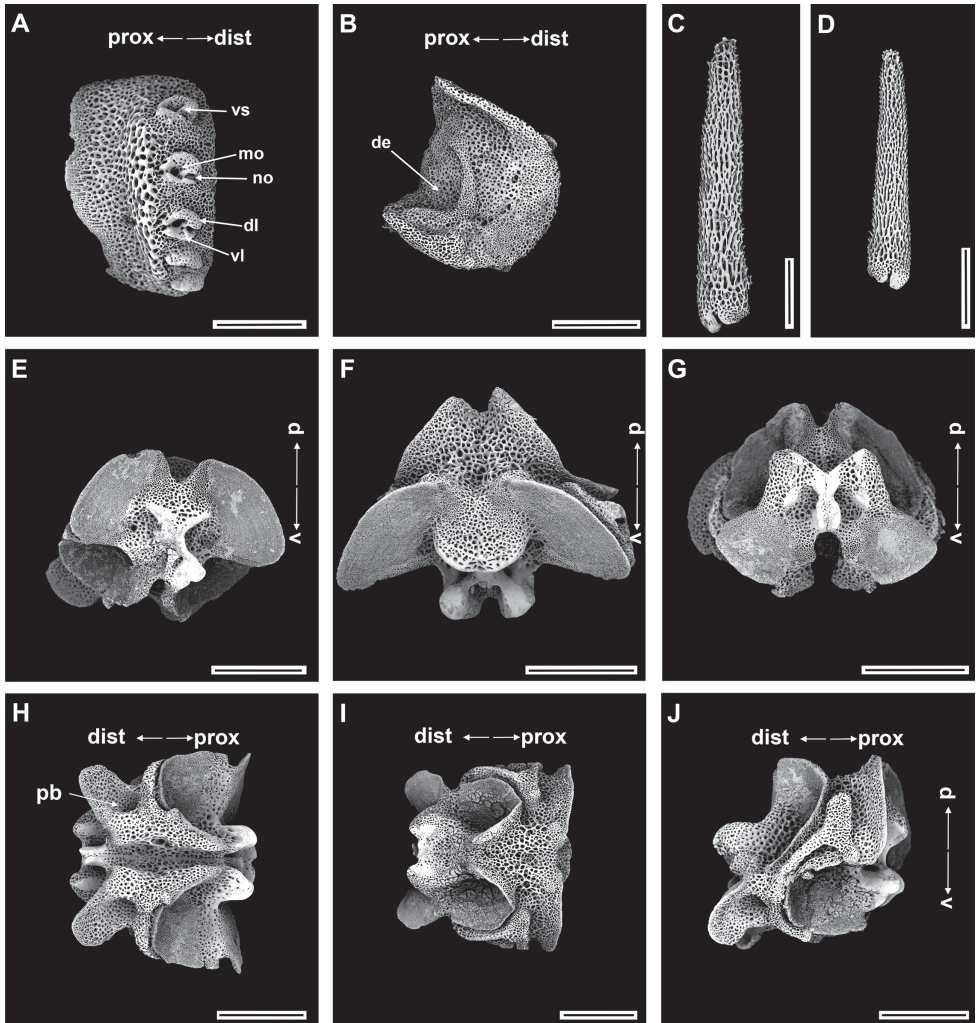


Figure 16. *Ophiophthalmus serratus* sp. nov., paratype (IDSSE-EEB-SW0137) **A, B** lateral arm plate **C** dorsal arm spine **D** ventral arm spine **E–J** vertebrae **E–F** proximal view **G** distal view **H** ventral view **I** dorsal view **J** lateral view. Abbreviations: **d** dorsal, **de** depression, **dist** distal, **dl** dorsal lobe, **lac** lateral ambulacral canals, **mo** muscle opening, **no** nerve opening, **pb** podial basin, **prox** proximal, **v** ventral, **vl** ventral lobe. Scale bars: 500 μ m (**A–C, E–J**); 300 μ m (**D**).

Ventral arm plate on first arm segment small, triangular, pointed distally, and slightly curved inwards proximally (Fig. 15I). Second to third ventral arm plates slightly pentagonal, wider than long, straight proximal margins, and obtuse or wavy distal edge (Fig. 15I). Following plates, as wide as long, straight lateral and proximal margins, and straight to wavy distal edge (Fig. 15J). Ventral arm plates separated along arm, including first plate (Fig. 15I–K). Lateral arm plates meeting below and above, except on dorsal arm base (Fig. 15G–N). Five finely serrated arm spines, with blunt tip in proximal

to middle regions of arm, then reduced to four at distal half of arm (Fig. 15H, K, N). Dorsal arm spines one and a half to two arm segments in length (Fig. 15F, L, M). Ventral arm spines shorter, one or one and a half arm segments in length (Fig. 15J, L, M). Dorsalmost arm spine longest, next two arm spines slightly shorter, but both similar in length, and last two ventral arm spines shortest, also equal in length (Fig. 15L, M). Arm spines increasingly finely serrated to thorny, and shorter at distal end of arm (Fig. 15K, N). One slightly elongated, blunt tipped tentacle scale, nearly as long as ventral arm plate (Fig. 15I, J).

Color. In ethanol, whole specimen pale brown-white. (Fig. 15).

Ossicle morphology of paratype. IDSSE-EEB-SW0137: Arm spine articulations well developed, five in number, and placed at slight angle to distal edge of lateral arm plate. Volute-shaped perforated lobe forms dorsal and distal part of articulation, but turns into two unequal subparallel curved lobes ventralwards; large muscle opening and small nerve opening (Fig. 16A). Proximal half of inner side of lateral arm plate with depression (Fig. 16B). Arm spines thorny, finely serrated with blunt apex (Fig. 16C, D). Vertebrae with streptospondylous articulation, short, broad podial basin at proximal end (Fig. 16E–J). Dorsal side of vertebrae distally triangular and proximally flattened with shallow longitudinal groove along midline (Fig. 16E–G). Ventral end of vertebrae with broad ambulacral groove with pair of lateral ambulacral canals, oral bridge absent (Fig. 16H–J).

Paratype variations. Here, we examined 29 paratypes, ranging in disc diameter from 4 mm to 17 mm, and found only few notable variations among them. Large specimens had five arm spines at proximal to middle regions of the arm, then reduced to four arm spines at distal end, but small specimens showed five arm spines only at arm base, then reduced to four along the distal half of the arm. However, the finely serrated surface of the arm spine was similar in both small and large specimens. The number of lateral oral papillae differed from three to four, but most specimens had three papillae. Most specimens had dense granular coverage of the disc except larger specimens (16–17 mm). Color ranges from creamy white to dark among specimens from our collection. The above mentioned variations depend mainly on the size of the disc, and specimens with similar disc diameter showed similar morphological characters.

Distribution. 1378–1408 m in depth, Haima cold seep, South China Sea.

Etymology. The species name was derived from the Latin word *serratus* (saw like, serrate), alluding to the surface of the arm spine.

Remarks. All specimens of *Ophiophthalmus serratus* sp. nov. were collected from a methane cold seep in the South China Sea. *Ophiophthalmus serratus* sp. nov. showed similar morphological characters to three congeners, except *O. hylacanthus*. *Ophiophthalmus normani* resembles *O. serratus* sp. nov. in having similar radial shield and arm plate characters, and granule coverage on the disc, but differs in number of arm spines (up to four), peg-like lateral oral papillae, smooth and slender arm spines, spaced granular coverage, arrangement of arm spines at lateral arm plate, and large oval tentacle scales (Lyman 1879; H. L. Clark 1911; Koehler 1922; Liao 2004). *Ophiophthalmus cataleimmoidus* is similar to *O. serratus* sp. nov. by having similar radial shield

Table 4. Tabular key to all species of the genus *Ophiophthalmus*. Abbreviations: **ASE** arm segment, **DAP** dorsal arm plate, **DAS** dorsal arm spines, **LOP** lateral oral papillae, **RS** radial shield, **TS** tentacle scale, **VAP** ventral arm plate, **VAS** ventral arm spines, **VMT** ventralmost papillae.

Species	No. of arm spines	Radial shield	Oral frame	Tentacle scale	Dorsal arm plate (DAP) and Ventral arm plate (VAP)	Arm spine shape and length	Disc spine or granular	References
<i>Ophiophthalmus catalaenimoides</i> (H. L. Clark, 1911)	up to 7	small, ovoid, naked, as long as wide, widely separated	3–4 LOP; 1 VMT equal of size	one, large, flat, rounded, and distinctly curved outward	1 st VAP rounded triangular shape, then wider than long, hexagonal or pentagonal, separated DAP wider than long, triangular shape with distal curve, first few DAP with single row of rounded grain in distal margin, contiguous only in proximal half	smooth, slender, tapering spine, next to uppermost DAS longest, 3 × ASE length	more or less sparsely with coarse, rounded granules	H. L. Clark (1911), Liao (2004)
<i>Ophiophthalmus hylacanthus</i> (H. L. Clark, 1911)	up to 8	small, ovoid, naked, widely separated	3 LOP; 1 VMT; LOP smaller than VMT	one, large, flat, rounded, but become narrow and pointed along the arm	VAP wider than long, hexagonal or pentagonal, separated DAP wider than long, triangular shape with distal curve, first few DAP with rounded grain in distal margin, contiguous only at arm base	second or third form upper DAS longest more than 2 × ASE length, uppermost DAS and lowermost VAS smooth, intermediate ones with slightly rough tip	stout, pointed, rough spine, scattered coarse granules among spine near RS	H. L. Clark (1911)
<i>Ophiophthalmus normani</i> (Lyman, 1879)	up to 4	small, ovoid, naked, as long as wide, widely separated	3 LOP; widely spaced, cylindrical, tapering, peg-like, 1 VMT	one, large and oval	1 st VAP rounded triangular shape, then wider than long, separated DAP as wide as long, distal curve, 1–4 DAP with single row of rounded grain in distal margin, contiguous only in proximal half	smooth, slender, blunt, and tapering spine, lowest VAS ≈ 1 × ASE, upper DAS 1–1½ × ASE length	rounded granules or short stump, sparsely spread on the disc	Lyman (1879), H. L. Clark (1911), Koehler (1922), Liao (2004)
<i>Ophiophthalmus retatus</i> (Koehler, 1904)	up to 6	ovoid, naked, distal end well rounded, widely separated	3–4 LOP; Conical to pointed tip, 1 VMT	one, pointed	1 st VAP rounded triangular shape, then wider than long, hexagonal or pentagonal, separated DAP wider than long, triangular shape with distal curve, DAP with rounded grain in distal margin and surface, contiguous only in proximal half	short, stout, longest one nearly 1 × ASE length, VAS quite rough near tip	dense, smooth or sometime rough minute granules	Koehler (1904), H. L. Clark (1911)
<i>Ophiophthalmus serratus</i> sp. nov.	up to 5	ovoid, naked, widely separated	3–4 LOP; rugose, pointed tip, 1 VMT	one, slightly elongated blunt tipped, as long as VAP	1 st VAP rounded triangular shape, then slightly pentagonal, separated DAP twice as wide as long, triangular shape with distal curve, first DAP has few rounded grains in distal margin (only 2 or 3 arms), contiguous only in arm base then separated	finely serratus, blunt tip; DAS ≈ 1½–2 × ASE length, dorsalmost longest, next two similar in length, VAS shorter, 1–1½ × ASE length, rough and shorter at distal end of the arm	dense, rounded to cylindrical stumps-like smooth granules, except radial shield and small area at center of disc	this study

and arm plate characters, and granular coverage on the disc, but differs in number of arm spines (up to six or seven), smooth arm spines, and shape of the tentacle scales (H. L. Clark 1911; Liao 2004). *Ophiophthalmus relictus* is similar to *O. serratus* sp. nov. by having similar radial shield and arm plate characters, and granular coverage on the disc, but differs in pointed to conical granules, six rough, short, and stout arm spines, and pointed tentacle scales (Koehler 1904; H. L. Clark 1911). *Ophiophthalmus hylacanthus* is similar to *O. serratus* sp. nov. by having similar radial shield and oral frame characters, but differs significantly by rough spines on the disc, up to eight arm spines, short genital slits, and narrow, pointed tentacle scales (H. L. Clark, 1911).

Discussion

The molecular phylogenetic analysis of the family Ophiacanthidae concurs with previous molecular studies (Christodoulou et al. 2019; O'Hara et al. 2019). In this study, we prepared a molecular phylogenetic tree of two clades that belong to the genera *Ophioplinthaca* and *Ophiophthalmus* in the family Ophiacanthidae (Fig. 2). Previous molecular studies suggested an intraspecific genetic distance of nearly 2.2% among ophiuroids, and the family Ophiacanthidae had slightly higher intraspecific and interspecific genetic distance values (Boissin et al. 2017; Christodoulou et al. 2019; O'Hara et al. 2019). However, our study showed somewhat lower genetic distance values among *Ophioplinthaca* species, probably because most of the species analyzed here live in the same biogeographic region (Northwest Pacific: *Ophioplinthaca defensor*: 0.26%; *Ophioplinthaca semele*: 0.76%; Table 2). The phylogenetic reconstruction showed that *Ophioplinthaca* cf. *lithosora* clustered with *O. globata*, whereas *O. semele* clustered with *O. plicata*, together forming sister clades among *Ophioplinthaca* species. Other sister clades were formed by *O. brachispina* sp. nov. with *O. amezianae*, and *Ophioplinthaca* sp. with *O. defensor* and *O. athena* (Fig. 2). *Ophioplinthaca* species can easily be delimited from other genera within Ophiacanthidae due to unique morphological characters, but showed highly variable, complex, and mixed morphological differences among them. Therefore, size and shape of the radial shields, and the form of the disc stumps/spines have been suggested as primary characters to delimit species of *Ophioplinthaca* (O'Hara and Stöhr 2006). *Ophioplinthaca* species from the present study were collected from the Northwest Pacific region near the Marina Trench, southwest of Guam Island, except *Ophioplinthaca* cf. *lithosora*, which was collected from a South China Sea seamount. The present study and recent studies done in the Northwest Pacific region suggest higher *Ophioplinthaca* species diversity from deep seamounts than previously known, and it may increase with future expeditions to this area (Chen et al. 2021a; Na et al. 2021).

The species in the genus *Ophiophthalmus* share many morphological features, and the main distinguishing characters were number and shape of arm spines and maximum size. However, they have high genetic distance variations between them. As an example, the main morphological difference between *Ophiophthalmus cataleimoidus* and *O. normani* were number of arm spines, and lateral oral papillae (Koehler 1904, 1922; H.

L. Clark 1911; Matsumoto 1917; Paterson 1985; Liao 2004; Olbers et al. 2019), but they had a 21.20% high genetic distance between them. *Ophiophthalmus* species were previously recorded in the North to South Pacific Ocean, Australia, and Indonesian waters, but *Ophiophthalmus serratus* sp. nov. was the first record from the South China Sea.

Acknowledgements

The authors want to thank the crews of the vessel ‘Tansuo’ 1 and the pilots of the HOV ‘Shenhaiyongshi’. The authors also thank the members of the marine ecology and evolutionary biology laboratory at the Institute of Deep-sea Science and Engineering, CAS for their help in sample collection and analysis. Many thanks to Hou Xue and Zhi Zheng for their help in acquiring SEM images of specimens. We are grateful to C. Mah (USNM) for taking photos of the type specimens of *O. lithosora* and to T. Fujita (NSMT) for taking photos of a non-type specimen of *O. lithosora*, and making these available to us. Many thanks also to the reviewers and the editor Alexander Martynov, who helped to improve the manuscript and proposed validity of the ophiuroid genus *Ophiophthalmus*. This work was supported by the Major scientific and technological projects of Hainan Province (ZDKJ2019011), the National Key Research and Development Program of China (2016YFC0304905, 2018YFC0309804), and Strategic Priority Research Program of the Chinese Academy of Sciences (XDA22040502).

References

- Boissin E, Hoareau TB, Paulay G, Bruggemann JH (2017) DNA barcoding of reef brittle stars (Ophiuroidea, Echinodermata) from the southwestern Indian Ocean evolutionary hot spot of biodiversity. *Ecology and Evolution* 7(24): 11197–11203. <https://doi.org/10.1002/ece3.3554>
- Chen W, Na J, Zhang D (2021a) Description of three species of ophioplutacids, including a new species, from a deep seamount in the Northwest Pacific Ocean. *PeerJ*. <https://doi.org/10.7717/peerj.11566>
- Chen W, Na J, Shen C, Zhang R, Lu B, Cheng H, Wang C, Zhang D (2021b) Ophiuroid fauna of cobalt-rich crust seamounts in the Northwest Pacific Ocean. *Acta Oceanologica Sinica* 40: 55–78. <https://doi.org/10.1007/s13131-021-1887-y>
- Cherbonnier G, Sibuet M (1972) Résultats Scientifique de la campagne Noratlante: Astérides et Ophiures. *Bulletin du Museum National d’Histoire Naturel Paris 3^e série. Zoologie* 102(76): 1333–1394. <https://biodiversitylibrary.org/page/56310281>
- Cho W, Shank TM (2010) Incongruent patterns of genetic connectivity among four ophiuroid species with differing coral host specificity on North Atlantic seamounts. *Marine Ecology (Berlin)* 31: 121–143. <https://doi.org/10.1111/j.1439-0485.2010.00395.x>
- Christodoulou M, O’Hara TD, Hugall AF, Arbizu PM (2019) Dark Ophiuroid Biodiversity in a Prospective Abyssal Mine Field. *Current Biology* 29(22): 3909–3912. <https://doi.org/10.1016/j.cub.2019.09.012>

- Clark HL (1900) The Echinoderms of Porto Rico. Bulletin of the U.S. Fisheries Commission 20: 233–263. <https://www.biodiversitylibrary.org/page/53676098>
- Clark HL (1911) North Pacific Ophiurans in the collection of the United States National Museum. Smithsonian Institution United States National Museum Bulletin 75: 1–302. <https://doi.org/10.5962/bhl.title.32556>
- Clark HL (1915) Catalogue of recent Ophiurans, based on the collection of the Museum of Comparative Zoology. Memoirs of the Museum of comparative Zoology at Harvard College 25: 164–376. <https://doi.org/10.5962/bhl.title.48598>
- Clark HL (1939) Ophiuroidea. Scientific Reports from the John Murray Exp. 1933–34(6): 29–136.
- Clark AH (1949) Ophiuroidea of the Hawaiian Islands. Bulletin of the Bernice P. Bishop Museum 195: 3–133.
- Fitzinger L (1843) Systema Reptilium. In: Fasciculus primus: Amblyglossae. Vindobonae: Braumüller und Seidel, 106.
- Guille A (1981) 91 Mémoires du Muséum national d'Histoire naturelle Echinodermes: Ophiurides. du Muséum national: Forest J (Ed.) Résultats des campagnes MUSORSTOM: 1. Philippines (18–28 Mars 1976). Résultats, 413–456.
- Hendler G (2018) Armed to the teeth: A new paradigm for the buccal skeleton of brittle stars (Echinodermata: Ophiuroidea). Contributions in Science 526: 189–311. <https://doi.org/10.5962/p.324539>
- Hoareau TB, Boissin E (2010) Design of phylum-specific hybrid primers for DNA barcoding: Addressing the need for efficient COI amplification in the Echinodermata. Molecular Ecology Resources 10(6): 960–967. <https://doi.org/10.1111/j.1755-0998.2010.02848.x>
- International Commission of Nomenclature (2000) International Code of Zoological Nomenclature. 4th edn. The International Trust for Zoological Nomenclature 1999, London.
- International Hydrographic Organization [IHO], Sieger R (2012) Names of oceans and seas as digitized table. Alfred Wegener Institute, Helmholtz Centre for Polar and Marine Research, Bremerhaven. <https://doi.org/10.1594/PANGAEA.777976>
- John DD, Clark AM (1954) The “Rosaura” expedition. 3. The Echinodermata. Bulletin of the British Museum (Natural History). Zoology (Jena, Germany) 2: 139–162. <https://doi.org/10.5962/p.314149>
- Kimura M (1980) A simple method for estimating evolutionary rates of base substitutions through comparative studies of nucleotide sequences. Journal of Molecular Evolution 16(2): 111–120. <https://doi.org/10.1007/BF01731581>
- Koehler R (1897) Echinodermes recueillis par “l’Investigator” dans l’Océan Indien. I. Les Ophiures de mer profonde. Annales des Sciences Naturelles Zoologie 8: 277–372. <https://biodiversitylibrary.org/page/35663130>
- Koehler R (1904) Ophiures de l’expédition du Siboga. Part 1. Ophiures de mer profonde. Weber, Siboga Expeditie. MEJ Brill, Leiden 45a: 1–176. <https://doi.org/10.5962/bhl.title.11682>
- Koehler R (1922) Ophiurans of the Philippine seas and adjacent waters. Bulletin of the American Museum of Natural History 5: 1–480. <https://www.biodiversitylibrary.org/item/77301>
- Koehler R (1930) Ophiures recueillies par le Docteur Th. Mortensen dans les Mers d’Australie et dans l’Archipel Malais. Papers from Dr. Th. Mortensen’s Pacific Expedition 1914–1916. LIV. Videnskabelige Meddelelser fra Dansk naturhistorisk Forening 89: 1–295.

- Kumar S, Stecher G, Tamura K (2016) MEGA7: Molecular Evolutionary Genetics Analysis Version 7.0 for Bigger Datasets. *Molecular Biology and Evolution* 33(7): 1870–1874. <https://doi.org/10.1093/molbev/msw054>
- Kumar S, Stecher G, Li M, Knyaz C, Tamura K (2018) MEGA X: Molecular evolutionary genetics analysis across computing platforms. *Molecular Biology and Evolution* 35(6): 1547–1549. <https://doi.org/10.1093/molbev/msy096>
- Liao Y (2004) Echinodermata: Ophiuroidea. *Fauna Sinica. Zoology of China Invertebrates* 40: 1–305. [pls I–VI]
- Ljungman A (1867) Ophiuroidea viventia huc usque cognita enumerat. Öfversigt af Kgl. Vetenskaps-Akademiens Förhandlingar 1866 23: 303–336. <https://www.biodiversitylibrary.org/page/32287761>
- Lütken CF, Mortensen T (1899) Reports on an exploration off the west coasts of Mexico, Central and Southern America and off the Galapagos Islands. XXV. The Ophiuridae. *Memoirs of the Museum of Comparative Zoology* 23: 97–208. <https://www.biodiversitylibrary.org/page/28891692>
- Lyman T (1869) Preliminary report on the Ophiuridae and Astrophytidae dredged in deep water between Cuba and Florida Reef. *Bulletin of the Museum of Comparative Zoology* 1: 309–354. <https://biodiversitylibrary.org/page/6587804>
- Lyman T (1878) Ophiuridae and Astrophytidae of the “Challenger” expedition. Part I. 5: *Bulletin of the Museum of Comparative Zoology at Harvard College, Cambridge, Mass.* 65–168.
- Lyman T (1879) Ophiuridae and Astrophytidae of the “Challenger” expedition. Part II. *Bulletin of the Museum of Comparative Zoology at Harvard College, Cambridge, Mass.* 6: 17–83. <https://www.biodiversitylibrary.org/page/31068674#page/27/mode/1up>
- Lyman T (1882) *Bulletin of the Museum of Comparative Zoology at Harvard College, Cambridge, Mass. Ophiuroidea. Scientific Reports. Results of the voyage of the H.M.S. “Challenger”, Cambridge, Mass.* 388 pp.
- Lyman T (1883) Reports on the results of dredging, under the supervision of Alexander Agassiz, in the Caribbean Sea (1878–79), and on the east coast of the United States, during the summer of 1880, by the U.S. coast survey steamer “Blake”, commander J.R. Bartlett, U.S. *Bulletin of the Museum of Comparative Zoology at Harvard* 10: 227–287. <https://www.biodiversitylibrary.org/page/4211367>
- Martynov AV (2010a) Reassessment of the classification of the Ophiuroidea (Echinodermata), based on morphological characters. I. General character evaluation and delineation of the families Ophiomyxidae and Ophiacanthidae. *Zootaxa* 2697(1): 1–54. <https://doi.org/10.11646/zootaxa.2697.1.1>
- Martynov AV (2010b) Structure of the arm spine articulation ridges as a basis for taxonomy of Ophiuroidea (a preliminary report). In: Harris L (Ed.) *Proceedings of the Twelfth International Echinoderm Conference, Durham, NH, 6–12 August 2006.* Balkema, Rotterdam, 233–239. <https://doi.org/10.1201/9780203869543-c37>
- Martynov AV, Ishida Y, Irimura S, Tajiri R, O’Hara T, Fujita T (2015) When ontogeny matters: A new Japanese species of brittle star illustrates the importance of considering both adult and juvenile characters in taxonomic practice. *PLoS ONE* 10(10): e0139463. <https://doi.org/10.1371/journal.pone.0139463>

- Matsumoto H (1917) A monograph of Japanese Ophiuroidea, arranged according to a new classification. *Journal of the College of Science, Imperial University, Tokyo* 38: 1–408. <https://www.biodiversitylibrary.org/page/7145928#page/5/mode/1up>
- Mortensen T (1933) Echinoderms of South Africa (Asteroidea and Ophiuroidea) Papers from Dr. Th. Mortensen's Pacific Expedition 1914–16. *Videnskabelige Meddelelser fra Dansk naturhistorisk Forening* 93 65: 215–400.
- Na J, Chen W, Zhang D, Zhang R, Lu B, Shen C, Zhou Y, Wang C (2021) Morphological description and population structure of an ophiuroid species from cobalt-rich crust seamounts in the Northwest Pacific: Implications for marine protection under deep-sea mining. *Acta Oceanologica Sinica* 40(12): 1–11. <https://doi.org/10.1007/s13131-020-1666-1>
- O'Hara TD (2010) Ophiuroids from deep-sea southern Australia. Museum Victoria. Version: 1.0. <http://www.museumvictoria.com.au/stars> [January 15, 2022]
- O'Hara TD, Stöhr S (2006) Deep water Ophiuroidea (Echinodermata) of New Caledonia: Ophiacanthidae and Hemieuryalidae. In: Richer de Forges B et al. (Eds) *Tropical Deep-sea Benthos* 24. *Mémoires du Muséum national d'Histoire naturelle* (1993), 33–141. <http://cat.inist.fr/?aModele=afficheN&cpsidt=18965845>
- O'Hara TD, Hugall AF, Thuy B, Stöhr S, Martynov AV (2017) Restructuring higher taxonomy using broad-scale phylogenomics: The living Ophiuroidea. *Molecular Phylogenetics and Evolution* 107: 415–430. <https://doi.org/10.1016/j.ympev.2016.12.006>
- O'Hara TD, Hugall AF, Woolley SNC, Bribiesca-Contreras G, Bax NJ (2019) Contrasting processes drive ophiuroid phylodiversity across shallow and deep seafloors. *Nature* 565(7741): 636–639. <https://doi.org/10.1038/s41586-019-0886-z>
- OBIS (2021) Ocean Biodiversity Information System. Intergovernmental Oceanographic Commission of UNESCO. www.obis.org [accessed 15 January 2022]
- Okanishi M, Matsuo T, Fujita T (2021) A new species of the genus *Ophiomonas* Djakonov (Echinodermata: Ophiuroidea: Amphilepididae) from the deep-sea of Japan. *Zoological Studies (Taipei, Taiwan)* 60: 1–13. <https://doi.org/10.6620/ZS.2021.60-59>
- Olbers JM, Griffiths CL, O'Hara TD, Samyn Y (2019) Field guide to the brittle and basket stars (Echinodermata: Ophiuroidea) of South Africa. *Abc Taxa* 19: 1–354. http://www.abctaxa.be/volumes/volume_19_fieldguide-brittle-and-basket-stars
- Paterson GLJ (1985) The deep-sea Ophiuroidea of the North Atlantic Ocean. *Bulletin of the British Museum (Natural History). Historical Series* 49: 1–162. <http://biodiversitylibrary.org/page/2273511> [Natural History]
- Shea GM (2021) Nomenclature of supra-generic units within the Family Scincidae (Squamata). *Zootaxa* 5067(3): 301–351. <https://doi.org/10.11646/zootaxa.5067.3.1>
- Stöhr S (2011) New records and new species of Ophiuroidea (Echinodermata) from Lifou, Loyalty Islands, New Caledonia. *Zootaxa* 50(1): 1–50. <https://doi.org/10.11646/zootaxa.3089.1.1>
- Stöhr S (2012) Ophiuroid (Echinodermata) systematics – Where do we come from, where do we stand and where should we go? *Zoosymposia* 7(1): 147–162. <https://doi.org/10.11646/zoosymposia.7.1.14>
- Stöhr S, O'Hara TD (2021) Deep-sea Ophiuroidea (Echinodermata) from the Danish Galathea II Expedition, 1950–52, with taxonomic revisions. *Zootaxa* 4963(3): 505–529. <https://doi.org/10.11646/zootaxa.4963.3.6>

- Stöhr S, O'Hara T, Thuy B [Eds] (2021) The World Ophiuroidea Database. <https://doi.org/https://doi.org/10.14284/358>
- Thompson JD, Higgins DG, Gibson TJ (1994) CLUSTALW: Improving the sensitivity of progressive multiple sequence alignment through sequence weighting, position-specific gap penalties and weight matrix choice. *Nucleic Acids Research* 22(22): 4673–4680. <https://doi.org/10.1093/nar/22.22.4673>
- Thomson CW (1877) The voyage of the “Challenger.” The Atlantic; a preliminary account of the general results of the exploring voyage of H.M.S. “Challenger” during the year 1873 and the early part of the year 1876, vol. 1: [xxix +] 424 pp. Macmillan and Co., London. <https://doi.org/10.5962/bhl.title.79255>
- Verrill AE (1899) Report on the Ophiuroidea collected by the Bahama expedition in 1893. *Bulletin from the Laboratories of Natural History of the State University of Iowa* 5: 1–86.
- Yesson C, Clark MR, Taylor ML, Rogers AD (2011) The global distribution of seamounts based on 30 arc seconds bathymetry data. *Deep-sea Research. Part I, Oceanographic Research Papers* 58(4): 442–453. <https://doi.org/10.1016/j.dsr.2011.02.004>

Supplementary material I

List of 36 references that use the name *Ophiophthalmus* as a valid ophiuroid genus name between 1971 and 2021

Authors: Hasitha Nethupul, Sabine Stöhr, Haibin Zhang

Data type: Docx file

Explanation note: List of 36 references that use the name *Ophiophthalmus* as a valid ophiuroid genus name between 1971 and 2021. We included the reference as evidence of prevailing usage of the name (*Ophiophthalmus*).

Copyright notice: This dataset is made available under the Open Database License (<http://opendatacommons.org/licenses/odbl/1.0/>). The Open Database License (ODbL) is a license agreement intended to allow users to freely share, modify, and use this Dataset while maintaining this same freedom for others, provided that the original source and author(s) are credited.

Link: <https://doi.org/10.3897/zookeys.1099.76479.suppl1>